

AD 684718

*Handwritten mark: a large circle with a vertical line through it, and some scribbles above and below.*

DDC  
RECEIVED  
APR 9 1969  
RECEIVED  
*Z B*

A Report On . . .  
**SOUNDING ROCKET VIBRATION AND  
DYNAMIC ANALYSES**  
Report No. 9013TR-1

Reproduced by the  
**CLEARINGHOUSE**  
for Federal Scientific & Technical  
Information Springfield Va. 22151



**SPACE DIVISION**

SOUNDING ROCKET VIBRATION  
AND  
DYNAMIC ANALYSES

Prepared by  
The Technical Staff  
Aerojet-General Corporation  
Space Division  
9200 East Flair Drive  
El Monte, California

Contract No. AF19<sup>628</sup>(~~268~~)-4333

Project No. 7657

Report No. 9013TR-1

This document has been approved for public release and sale;  
its distribution is unlimited.

September 30, 1968

Prepared for  
Air Force Cambridge Research Laboratories  
Office of Aerospace Research  
United States Air Force  
Bedford, Massachusetts

# CONTENTS

|  | <u>Page</u> |
|--|-------------|
| SECTION I - NIRO VIBRATION DATA .....                          | 1-1         |
| 1.1 Introduction .....   | 1-1         |
| 1.2 Determination of Power Spectral Density .....              | 1-1         |
| 1.3 Determination of Harmonic Content .....                    | 1-2         |
| SECTION II - IROQUOIS JOINT ANALYSIS .....                     | 2-1         |
| 2.1 Introduction .....   | 2-1         |
| 2.2 Discussion .....   | 2-2         |
| 2.3 Recommendations .....                                      | 2-3         |
| SECTION III - NIRO LONGITUDINAL VIBRATION ANALYSIS .....       | 3-1         |
| 3.1 Introduction .....   | 3-1         |
| 3.1.1 Purpose of the Analysis .....                            | 3-1         |
| 3.1.2 Brief Summary of Results .....                           | 3-1         |
| 3.2 Discussion .....   | 3-1         |
| 3.2.1 Brazil Flights AG 7. 314 and AG 7. 316 .....             | 3-1         |
| 3.2.2 Lumped Parameter Analysis .....                          | 3-10        |
| 3.2.3 Structural Longitudinal Vibration Stability Limits ..... | 3-24        |
| 3.3 Conclusions .....  | 3-29        |
| 3.4 Recommendations .....                                      | 3-30        |
| SECTION IV - NIRO MARS PLATFORM ANALYSIS .....                 | 4-1         |
| 4.1 Introduction .....   | 4-1         |
| 4.2 Results and Recommendations .....                          | 4-1         |
| 4.3 Discussion .....   | 4-2         |
| 4.3.1 The Defining Equations .....                             | 4-2         |
| 4.4 Computer Program .....                                     | 4-8         |
| 4.5 References .....   | 4-11        |
| APPENDIX A - SIMPLIFIED VIBRATION ANALYSIS METHODS             |             |
| APPENDIX B - LISTING OF MARS PLATFORM PROGRAM                  |             |
| APPENDIX C - NIRO JOINT STUDY DATA SHEETS AND PRINTOUT         |             |

## ILLUSTRATIONS

### Figure

- 1-1 NIRO Brazil Flight AG 7.314, Nike Burn - PSD
- 1-2 NIRO Brazil Flight AG 7.316, Nike Burn - PSD
- 1-3 NIRO Brazil Flight AG 7.314, 2nd Burn End - Harmonic
- 1-4 NIRO Brazil Flight AG 7.316, 2nd Burn End - Harmonic
- 1-5 NIRO Brazil Flight AG 7.314, Longitudinal  $G_{RMS}$  vs Time
- 1-6 NIRO Brazil Flight AG 7.316, Longitudinal  $G_{RMS}$  vs Time
  
- 3-1 NIRO Configuration
- 3-2 NIRO Brazil Payload, 7.314 (Not to Scale)
- 3-3 NIRO Payload Weight Distribution, Brazil Flight Number 7.314
- 3-4 NIRO Payload Extensional Stiffness (AE), Cantilevered Payload Only, Brazil Flight Number 7.314
- 3-5 NIRO Payload Weight Distribution, Brazil Flight Number 7.314, (Less Internally Cantilevered Payload)
- 3-6 NIRO Payload Extensional Stiffness (AE) (Less Internally Cantilevered Payload) Brazil Flight Number 7.314
- 3-7 NIRO Sustainer Mass Distribution
- 3-8 NIRO Sustainer Extensional Stiffness (AE)
- 3-9 NIRO Sustainer Chamber Pressure vs Time
- 3-10 NIRO Lumped Mass and Stiffness Representation, Brazil Flight 7.314, Payload Branched at Midpoint (As Actually Flown)
- 3-11 NIRO Lumped Mass and Stiffness Representation Payload Branched at Base
- 3-12 NIRO Lumped Mass and Stiffness Representation Payload Branched at Quarter Point
- 3-13 NIRO Lumped Mass and Stiffness Representation Payload Branched at Front
- 3-14 NIRO Lumped Mass and Stiffness Representation Acoustic Branch of Sustainer
- 3-15 NIRO First Longitudinal Mode Uniformly Distributed Mass and Stiffness Payload Attached at Base



## ILLUSTRATIONS (Continued)

### Figure

- 3-16 NIRO Second Longitudinal Mode Uniformly Distributed Mass and Stiffness Payload Attached at Base
- 3-17 NIRO Third Longitudinal Mode Uniformly Distributed Mass and Stiffness Payload Attached at Base
- 3-18 NIRO First Longitudinal Mode, Brazil Flight 7.314 Payload
- 3-19 NIRO Second Longitudinal Mode, Brazil Flight 7.314 Payload
- 3-20 NIRO Third Longitudinal Mode, Brazil Flight 7.314 Payload
- 3-21 NIRO First Longitudinal Mode, Brazil Flight 7.314
- 3-22 NIRO Second Longitudinal Mode, Brazil Flight 7.314
- 3-23 NIRO Third Longitudinal Mode, Brazil Flight 7.314
- 3-24 NIRO Fourth Longitudinal Mode, Brazil Flight 7.314
- 3-25 NIRO Fifth Longitudinal Mode, Brazil Flight 7.314
- 3-26 NIRO First Longitudinal Mode, Flight 7.314 Payload
- 3-27 NIRO Second Longitudinal Mode, Flight 7.314 Payload
- 3-28 NIRO Third Longitudinal Mode, Flight 7.314 Payload
- 3-29 NIRO First Longitudinal Mode, Flight 7.314 Payload
- 3-30 NIRO Second Longitudinal Mode, Flight 7.314 Payload
- 3-31 NIRO Third Longitudinal Mode, Flight 7.314 Payload
- 3-32 NIRO Variation of Longitudinal First Mode Natural Frequency with Payload Attach Point
- 3-33 NIRO Longitudinal Modal Frequencies vs Time
- 3-34 NIRO Longitudinal Modal Frequencies vs Time
- 3-35 NIRO First Longitudinal Structural Frequency vs Time for Various Payload Longeron Stiffnesses (AE)
- 3-36 NIRO First Longitudinal Structural Frequency vs Time for Various Payload Longeron Stiffnesses (AE)
- 3-37 NIRO Structural Stability Limits for Motor Excited Longitudinal Vibrations, Payload Attached at Base
- 3-38 NIRO Brazil Flight AG 7.314, Longitudinal  $G_{RMS}$  vs Time

## ILLUSTRATIONS (Continued)

### Figure

- 3-39 NIRO Brazil Flight AG 7.316, Longitudinal  $G_{RMS}$  vs Time
- 3-40 NIRO Brazil Flight AG 7.314, Harmonic Analysis of Longitudinal Vibration Data Just Prior to Sustainer Burnout
- 3-41 NIRO Brazil Flight AG 7.316, Harmonic Analysis of Longitudinal Vibration Data Just Prior to Sustainer Burnout
- 3-42 NIRO Brazil Flight AG 7.314, Power Spectral Density of Longitudinal Vibrations at Staging
- 3-43 NIRO Brazil Flight AG 7.314, Power Spectral Density of Longitudinal Vibrations at Staging
- 3-44 NIRO Brazil Flight AG 7.316, Power Spectral Density of Longitudinal Vibrations Just After Staging
- 3-45 NIRO Brazil Flight AG 7.316, Power Spectral Density of Longitudinal Vibrations Just After Staging
- 4-1 AF7-387 Pitch and Yaw Responses
- 4-2 AF7-387 Roll Responses

## FOREWORD

This task report is submitted in fulfillment of the data requirements under Item 10, Contract AF19(628)-4333. The letter reports required under Item 10 for the tasks listed below are incorporated herein for convenience and report continuity. Letter reports and data for tasks other than those delineated below have been previously submitted. This report represents the final document to be submitted under this contract.

The data submitted herein reflect summation of the work performed under the following contract work statement items.

Item 3 - Supply sensors calibration and support to measure in-flight the vibration environment on three each sounding rockets. Reduce the data obtained from these sensors using power spectral and harmonic analysis methods.

Item 7 - Investigate the Iroquois motor-payload joint under the influence of all known forces to establish the effects of variation, fit, and attachment parameters on rotation of the joint. The rotation will be checked three times in a typical flight: (1) Nike burnout, (2) Iroquois ignition, and (3) Iroquois burnout. The analysis will require the determination of the maximum allowable screw torque in order that bending moment where the joint slippage begins may be computed.

Item 8 - Estimate the axial mode natural frequencies of the as signed NIRO payload-rocket configuration at both second-stage ignition and burn-out times. Develop a chart or nomogram indicating payload deck shelf, breathing mode frequency as a function of shelf thickness, diameter and total weight carried.

Item 9 - Reduce and analyze MARS platform data from selected NIRO flights in order to establish vehicle dynamic characteristics.

The four sections of this report reflect the results of the studies mentioned above. In the case of Item 3, all specified work had been performed and previously submitted with the exception of the reduction of the

data from two flights. Therefore, the section relating to Item 3 merely comprises the data from the two previously missing flights. Each of the subsequent sections is mutually independent but are combined here for convenience.

Section I  
NIRO VIBRATION DATA

1.1 INTRODUCTION

This section contains data reduced from the accelerometers carried on NIRO flights AG 7.314 and AG 7.316. Included are harmonic analysis, power spectral density (PSD) plots and root mean square acceleration (GRMS) plots. The description of the technique involve in reducing these data is given hereafter.

This section presents only the data reduced from the two NIRO flights. Discussions and analysis of these data are contained in Section III of this report.

1.2 DETERMINATION OF POWER SPECTRAL DENSITY

The Power Spectral Density (PSD) of the vibration was determined by the procedure outlined below. The vibration data were recovered from the flight-data magnetic tape with standard IRIG FM-FM telemetry discrimination equipment. A 1050 Hz 6th order low-pass filter was used to minimize aliasing. The digitizer input to a Varian Data Machines 6201 computer was used to digitize a 1.84 second sample of the vibration data at a 5000 sample/second rate during the boost phase of the flight. The digitized data was then recorded on a computer magnetic tape.

The digitized sample was processed with an IBM 360-65 computer to produce the PSD. The sample was first filtered with a digital filter that simulates a 2nd order RC filter with a 12 Hz breakpoint frequency. A 3rd order least-square polynomial fit was determined, and this polynomial was then removed from the data to eliminate offset and drifts during the sample period. The discrete Fourier transform of a selected 1.64 second sample of the data was calculated using the Cooley-Tukey fast Fourier transform method. The square of the transform was determined. The auto correlation function was determined by inverse transformation. A Parzen data window was applied to

this function to achieve spectral smoothing. A Fourier transform was applied to the result to yield the PSD of the vibration data. The PSD was plotted by creating a special 'plot' magnetic tape which was used to operate a Cal Comp Model 565 digital incremental plotter.

### 1.3 DETERMINATION OF HARMONIC CONTENT

The harmonic content of the vibration was determined by the procedure outlined below. The vibration data was recovered from the flight-data magnetic tape with standard IRIG FM-FM telemetry discrimination equipment. A 1050 Hz 6th order low pass filter was used to minimize aliasing. The digitizer input to a Varian Data Machines 620i computer was used to digitize a 1.84 second sample of the vibration data at a 5000 sample/second rate during the boost phase of the flight. The digitized data was then recorded on a computer magnetic tape.

The digitized sample was processed with an IBM 360-65 computer to determine the harmonic content. A 1.64 second sample was selected and the static component was removed. The Cooley-Tukey fast Fourier transform was used to determine the magnitudes of sine and cosine components. The absolute magnitude was determined and plotted by creating a special 'plot' magnetic tape which was used to operate a Cal Comp 565 digital incremental plotter.



AG7.314 NIKE BURN

PSD

Figure  
NIRC  
Brazil Flight  
Nike Burn -

$\sigma^2/\text{cps}$

H

FREQUENCY -

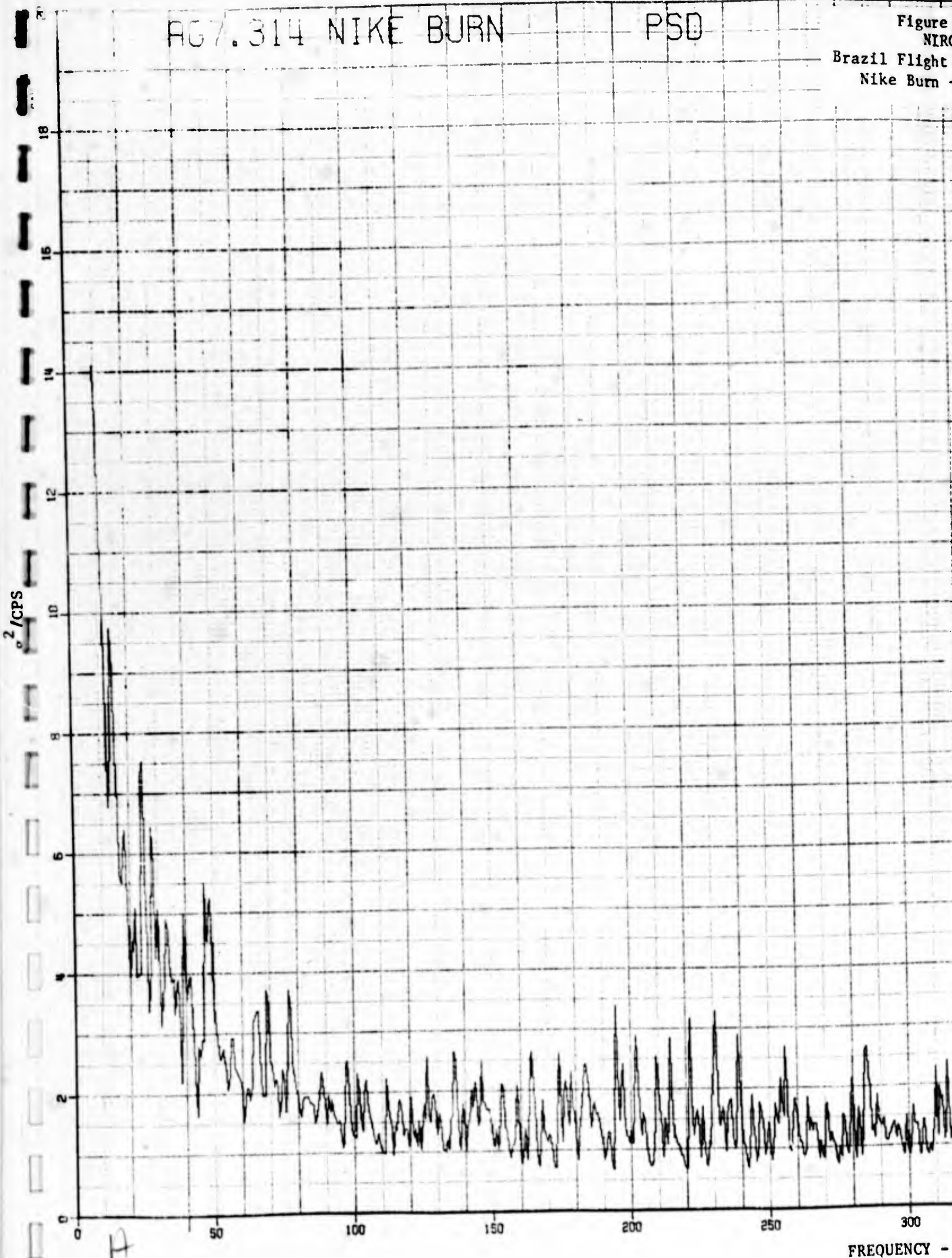
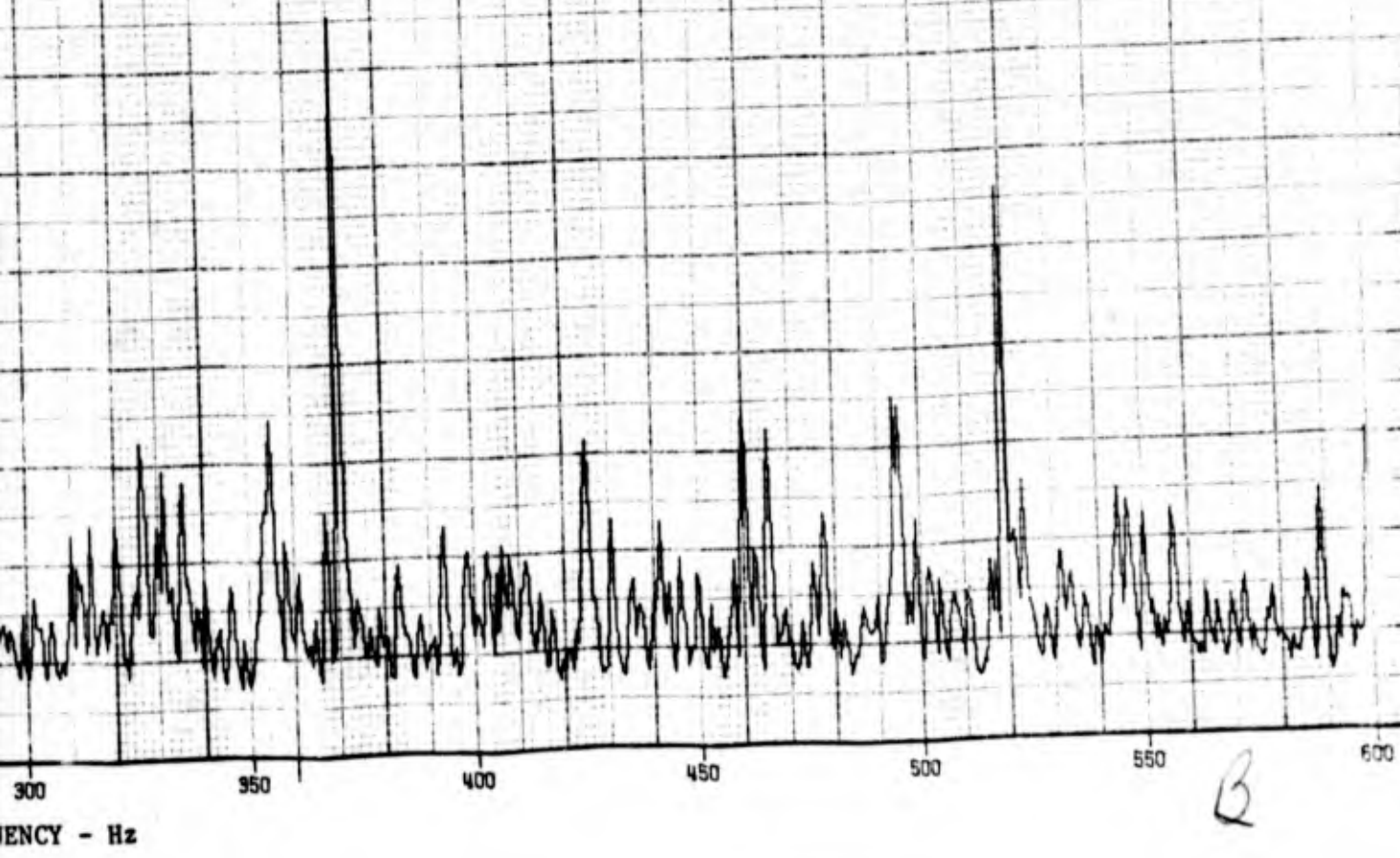


Figure 1-1  
NIRO  
Flight AG 7.314  
Burn - PSD



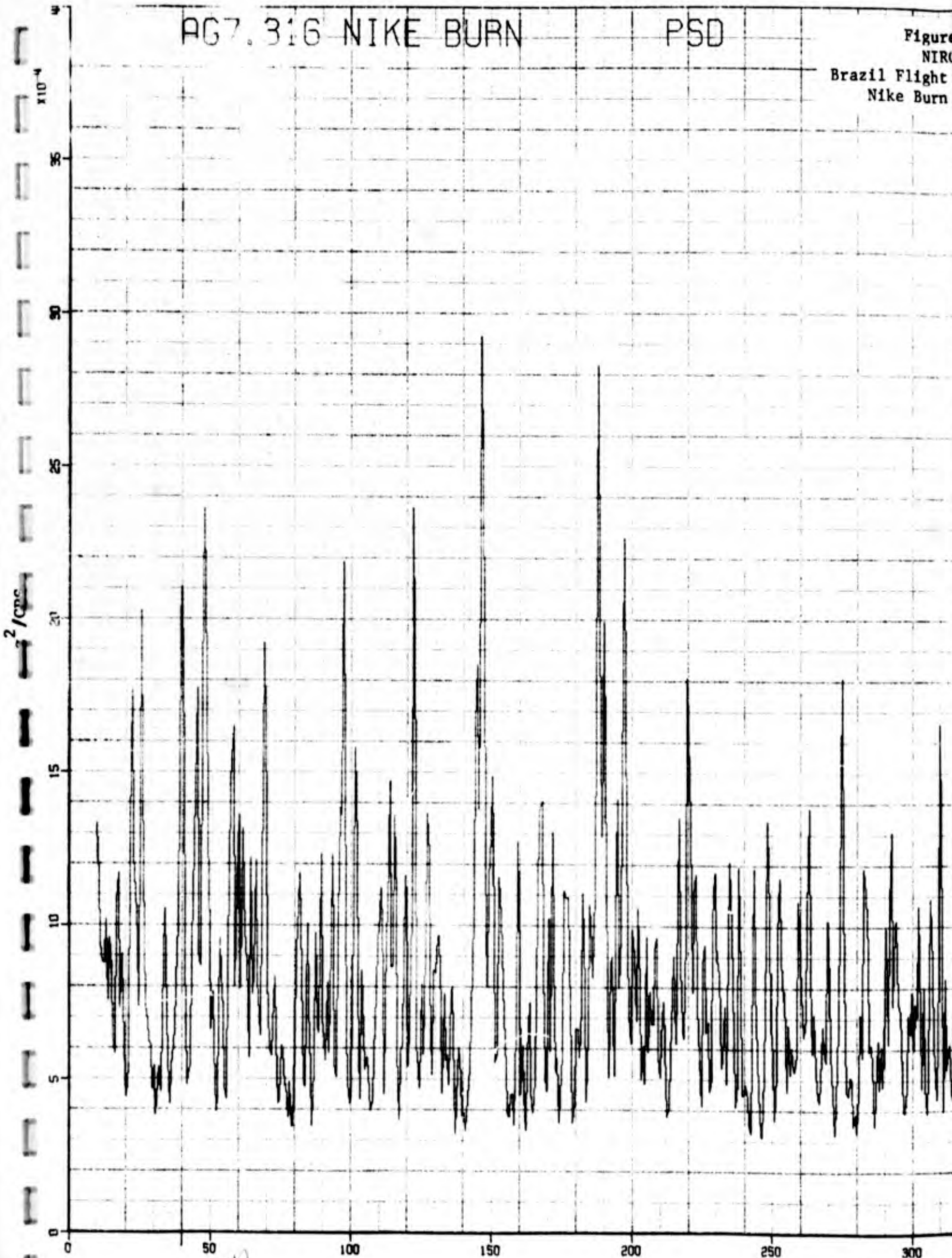
B



AG7.316 NIKE BURN

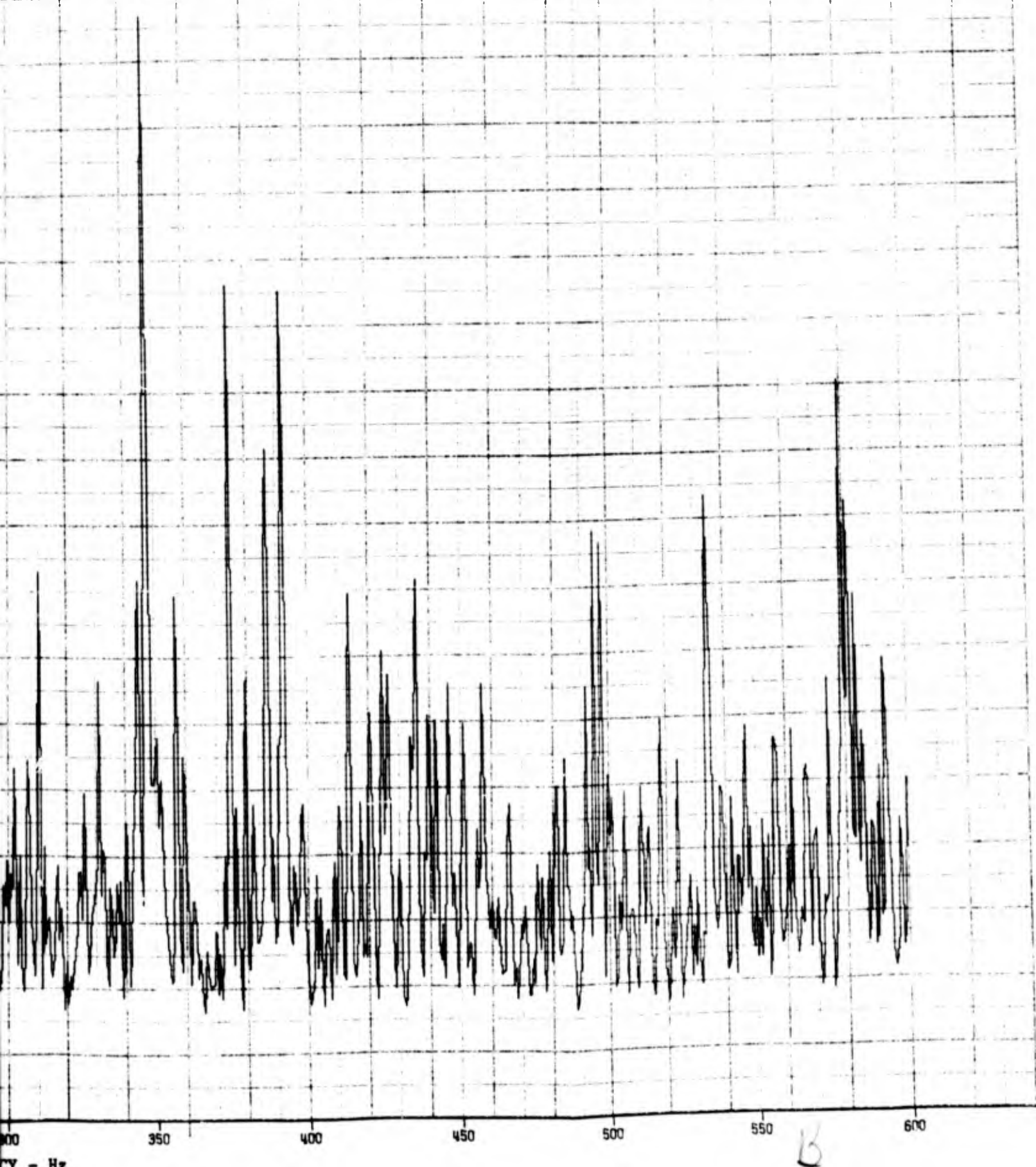
PSD

Figure  
NIR  
Brazil Flight  
Nike Burn



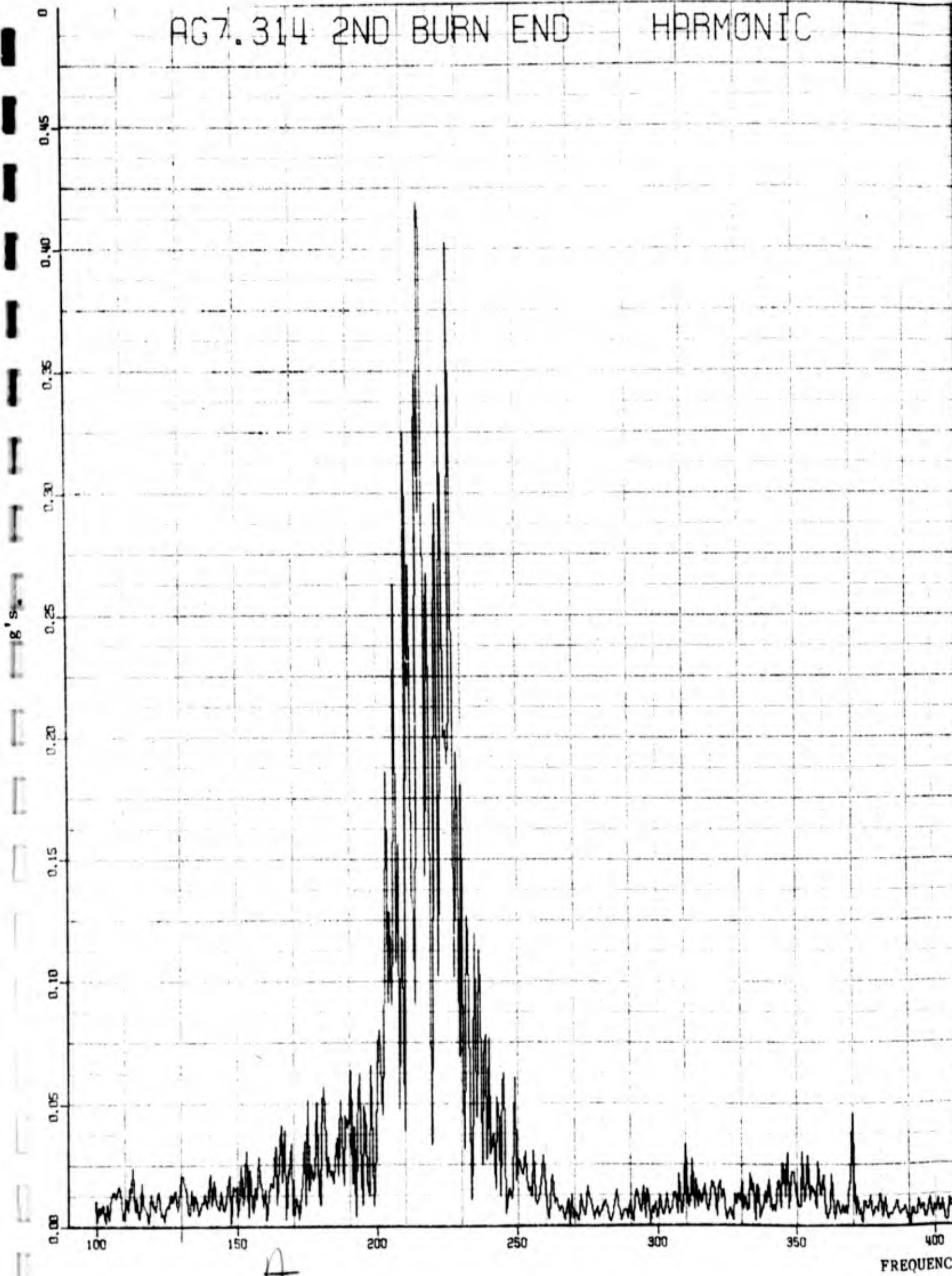
FREQUENCY - Hz

Figure 1-2  
NIR  
light AG 7.316  
Burn - PSD



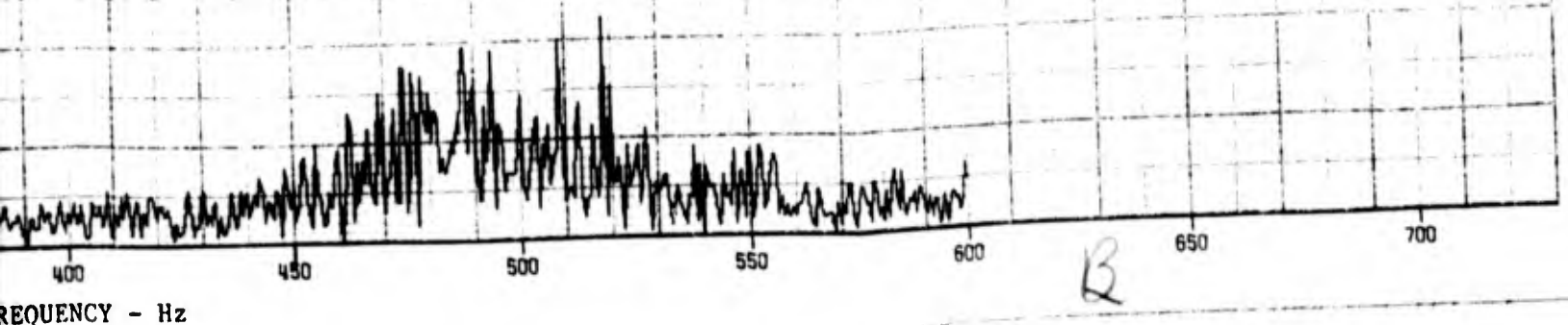
AG7.314 2ND BURN END

HARMONIC



FREQUENCY

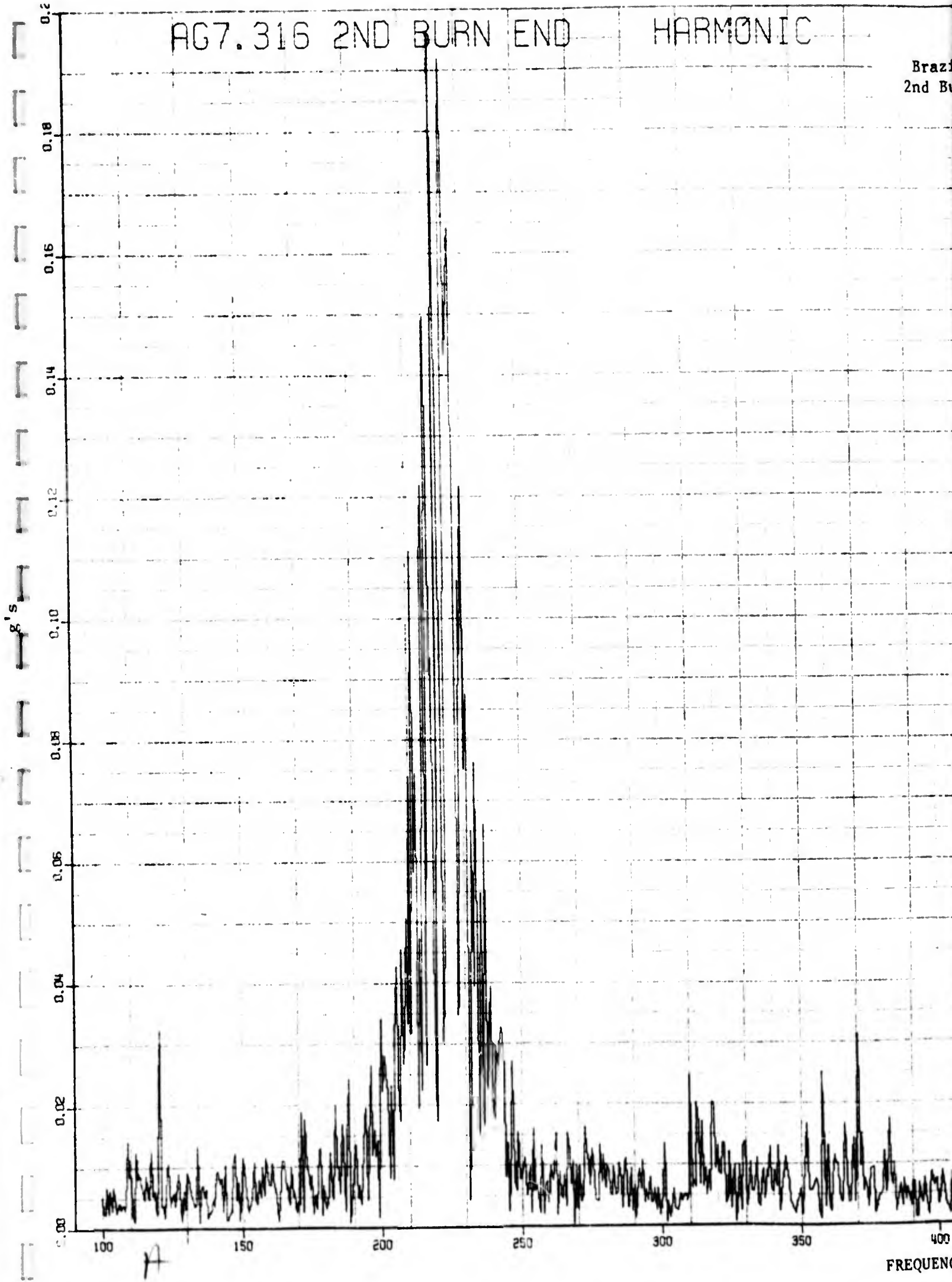
Figure 1-3  
NIRO  
Brazil Flight AG 7.314  
2nd Burn End - Harmonic





AG7.316 2ND BURN END HARMONIC

Braz  
2nd B

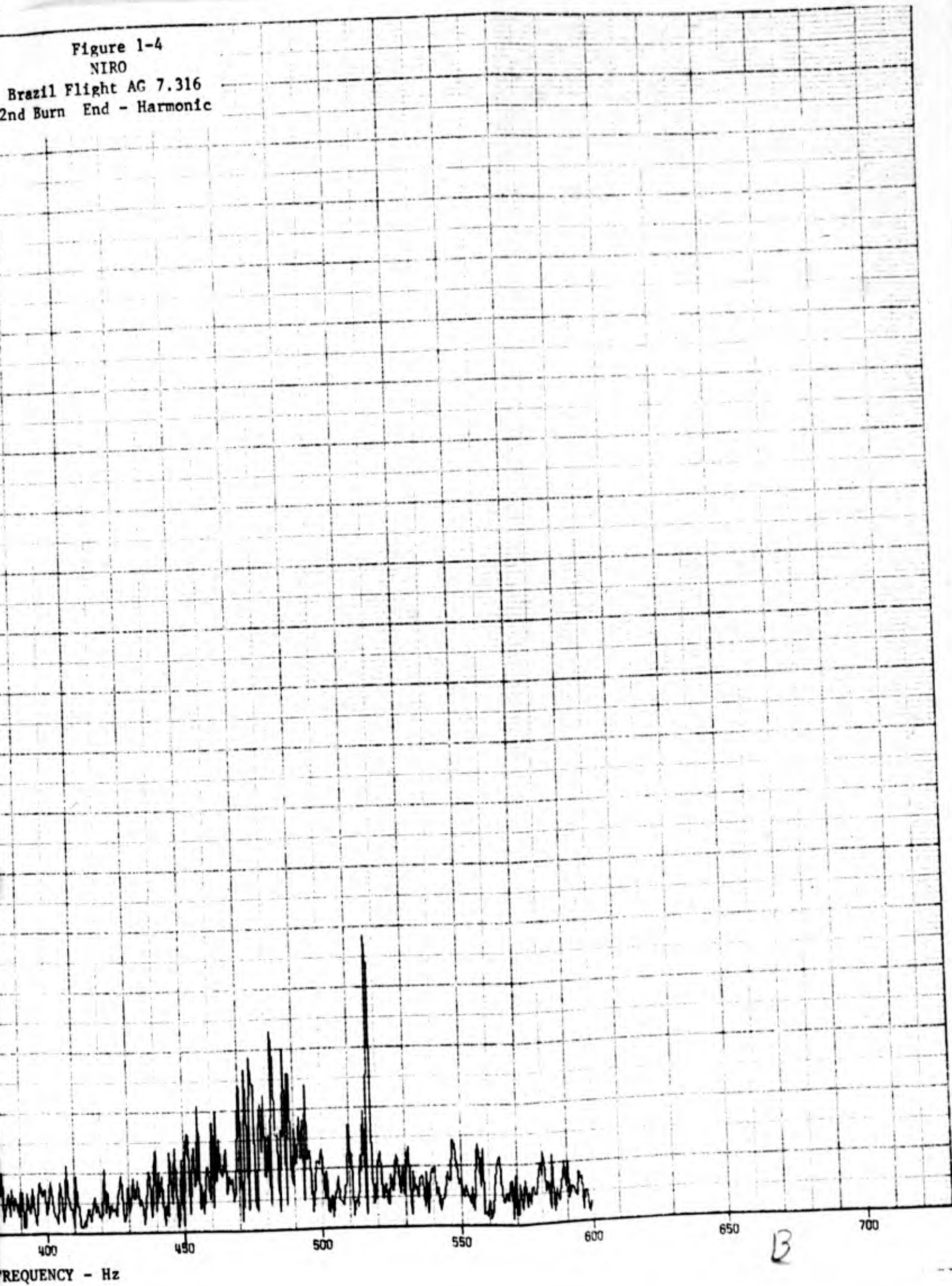


FREQUEN

Figure 1-4

NIRO

Brazil Flight AG 7.316  
2nd Burn End - Harmonic



FREQUENCY - Hz

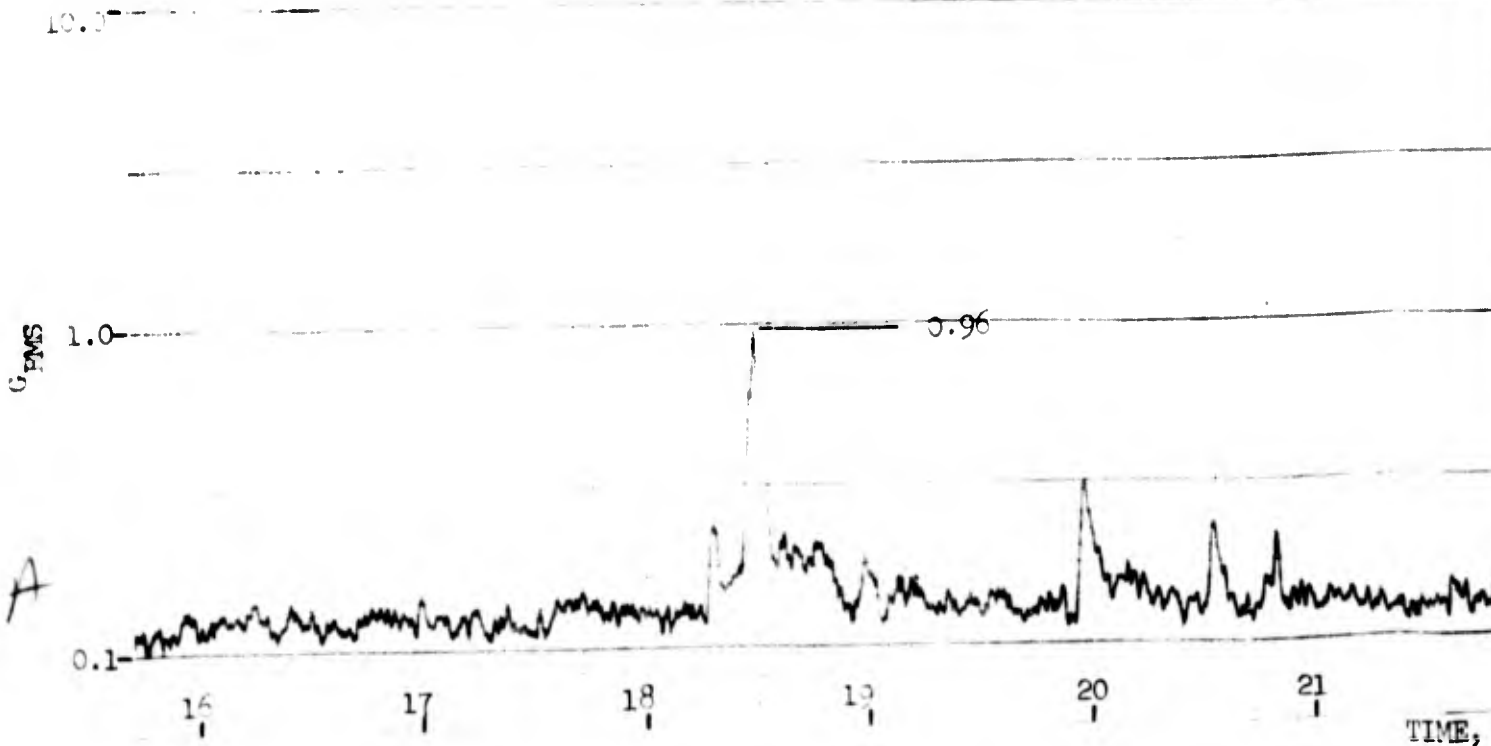
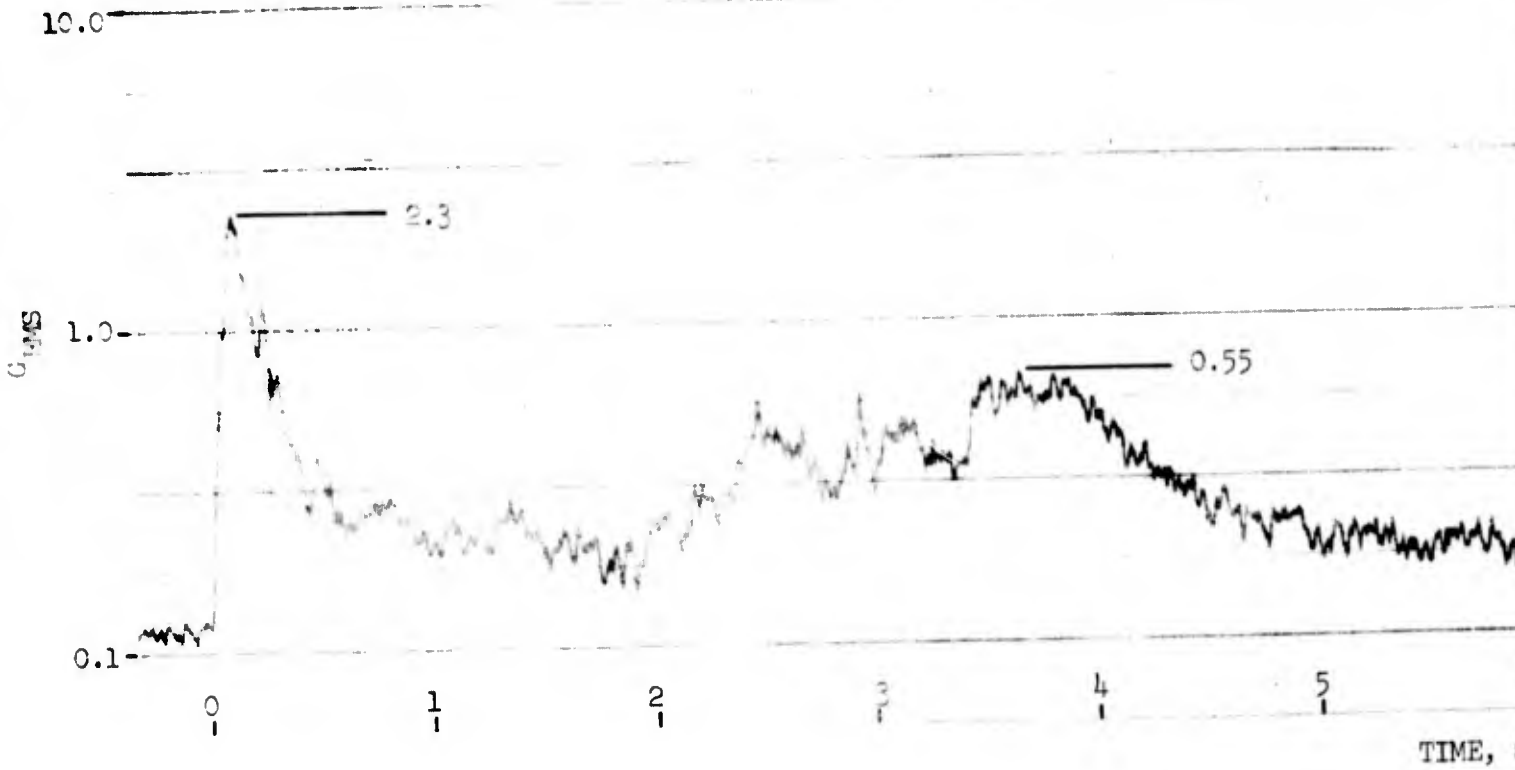
Figure 1-5

NIFO

Brazil Flight AG 7.3

LONGITUDINAL  $G_{RMS}$  vs T

Transducer Located at Payload



A

Figure 1-5  
NIFRO  
Flight AG 7.314  
AL G<sub>RMS</sub> vs TIME  
at Payload Attach Point

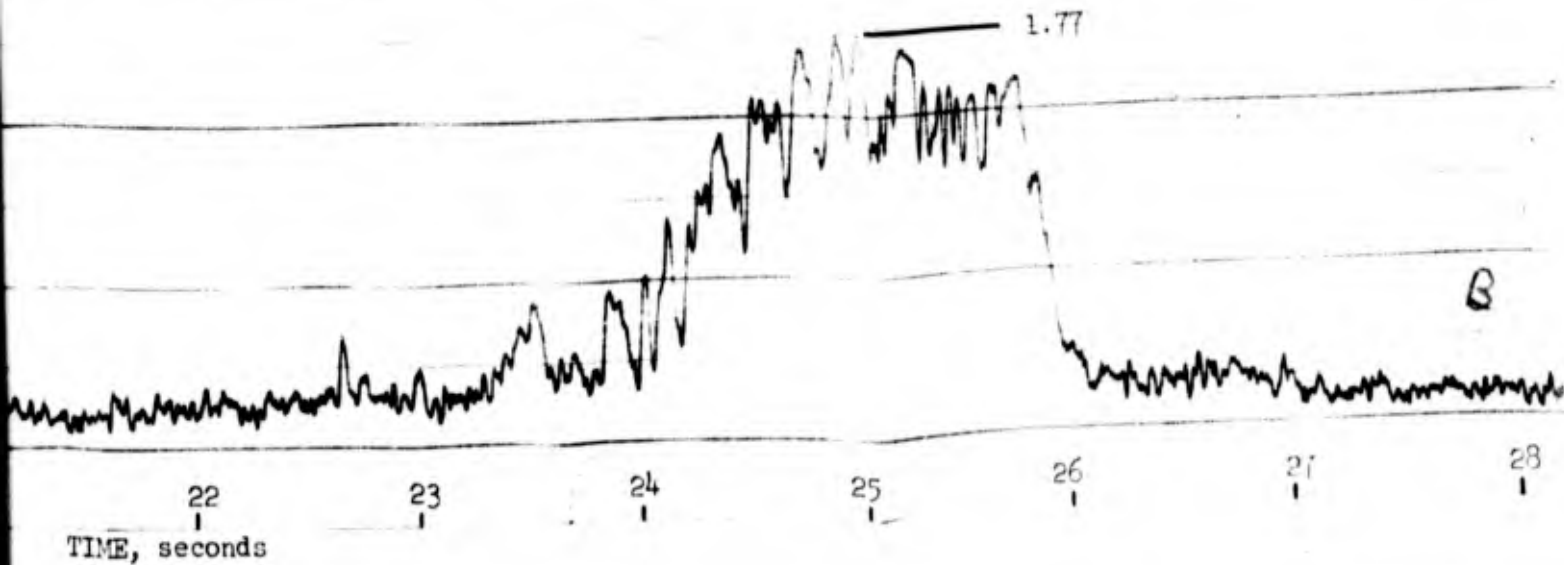
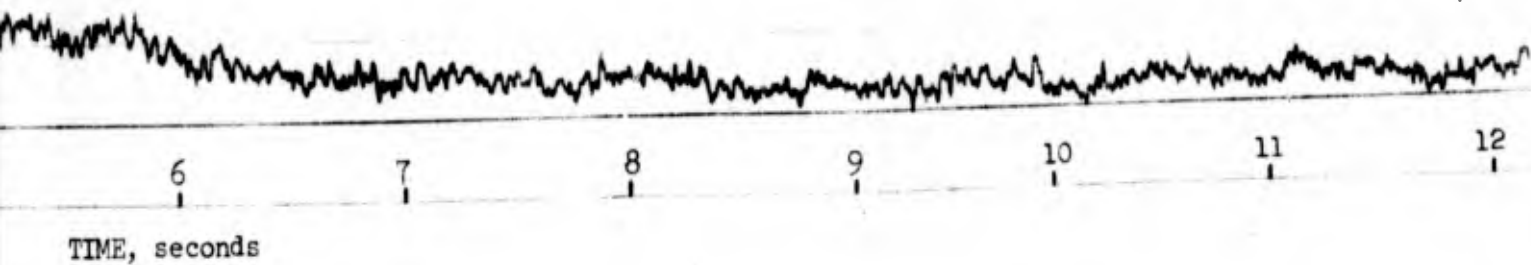




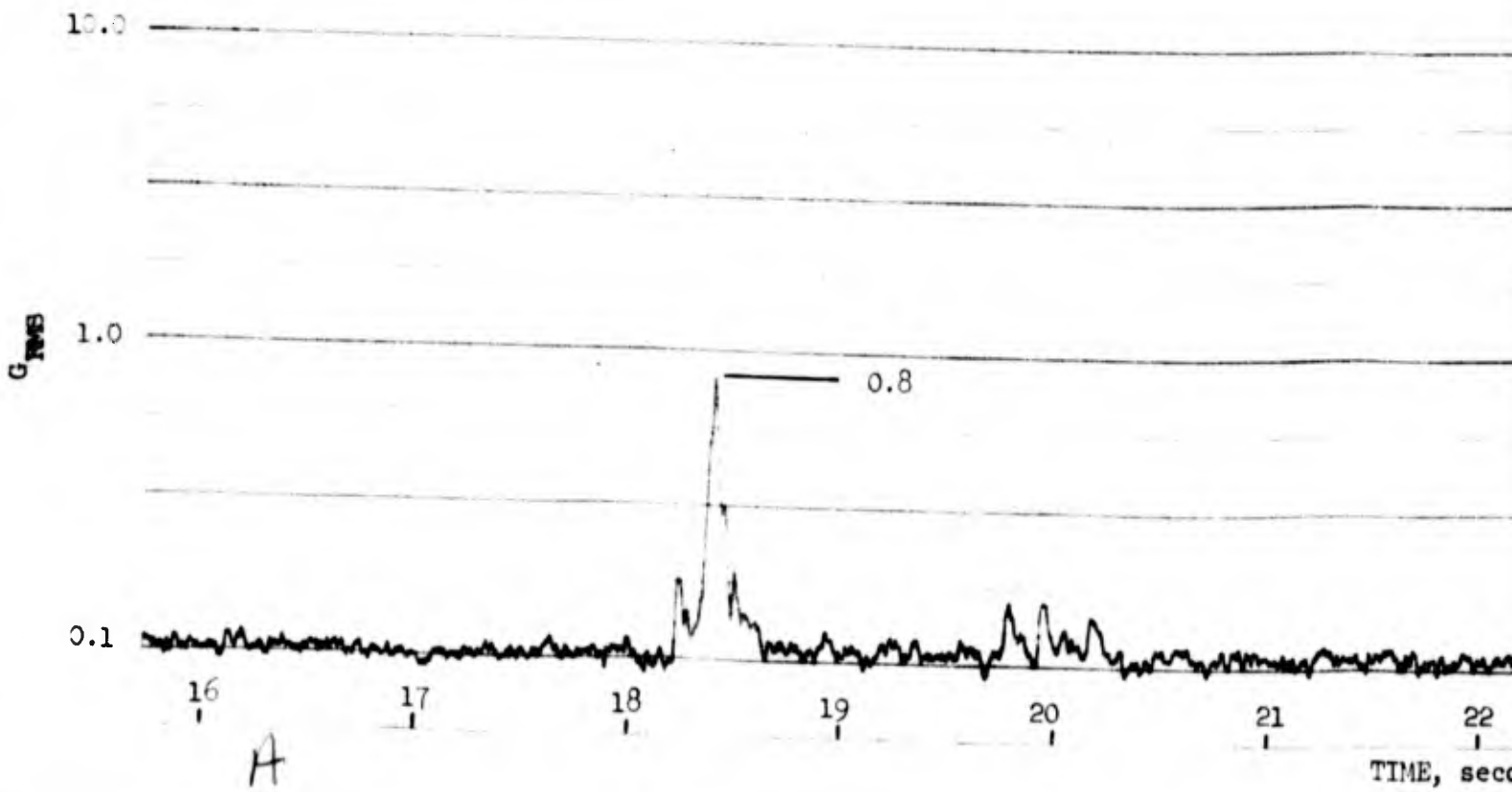
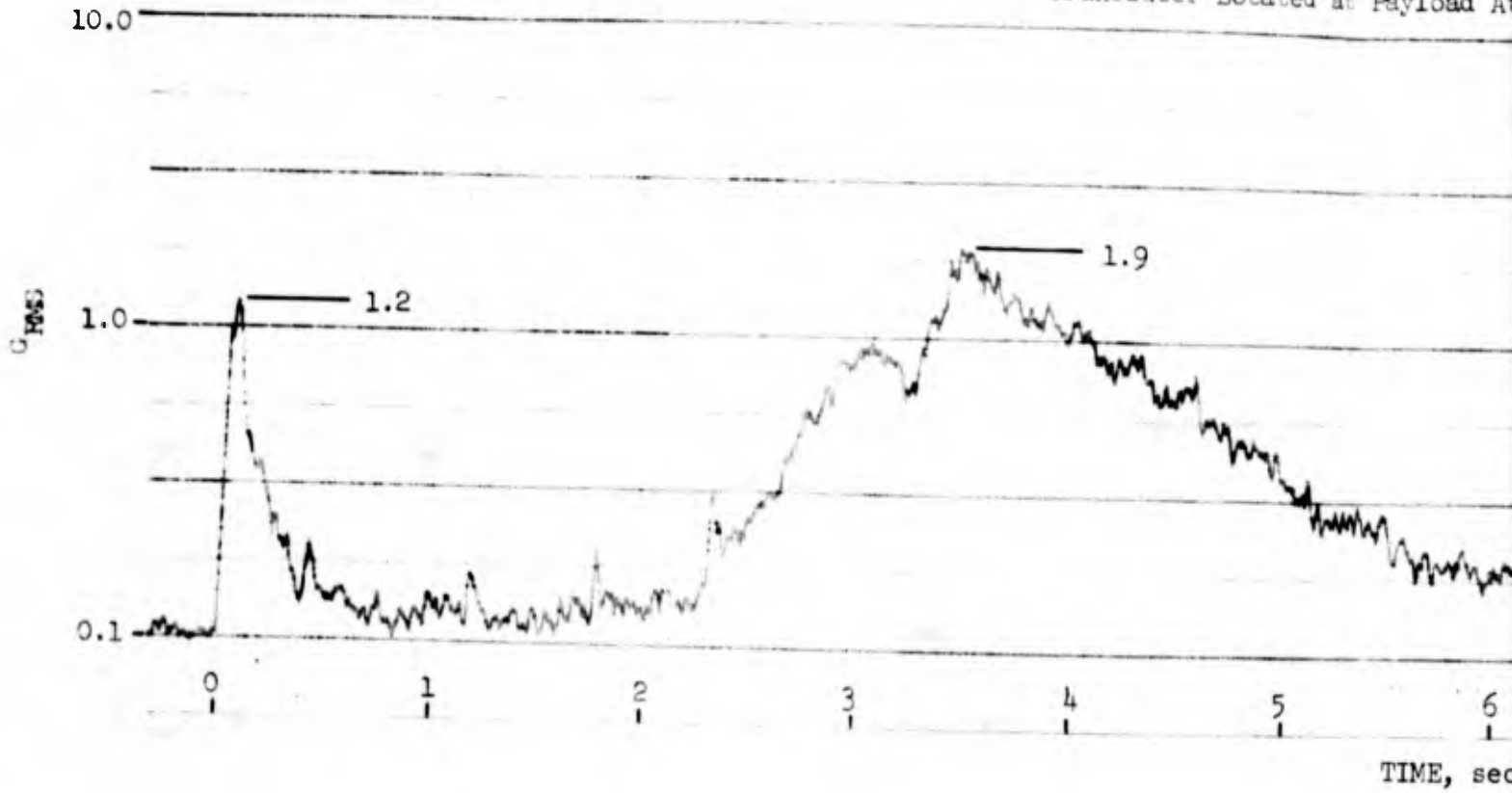
Figure 1-6

NIRO

Brazil Flight AG 7.31

LONGITUDINAL  $G_{RMS}$  vs TIME

Transducer Located at Payload A



A

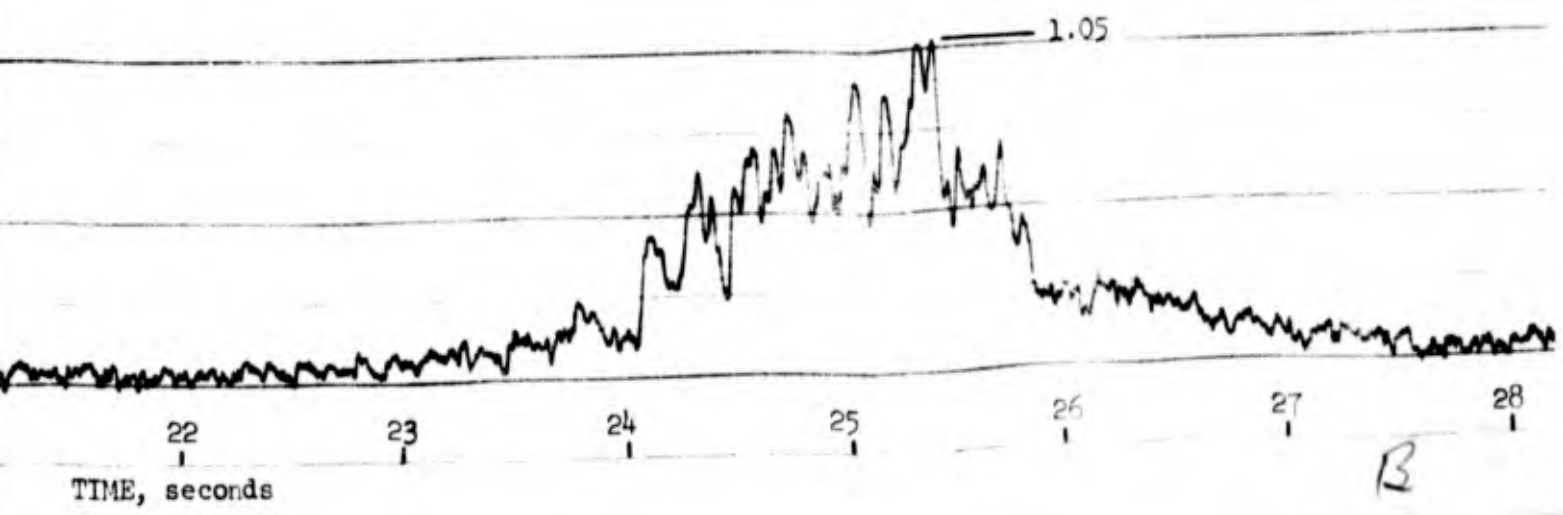
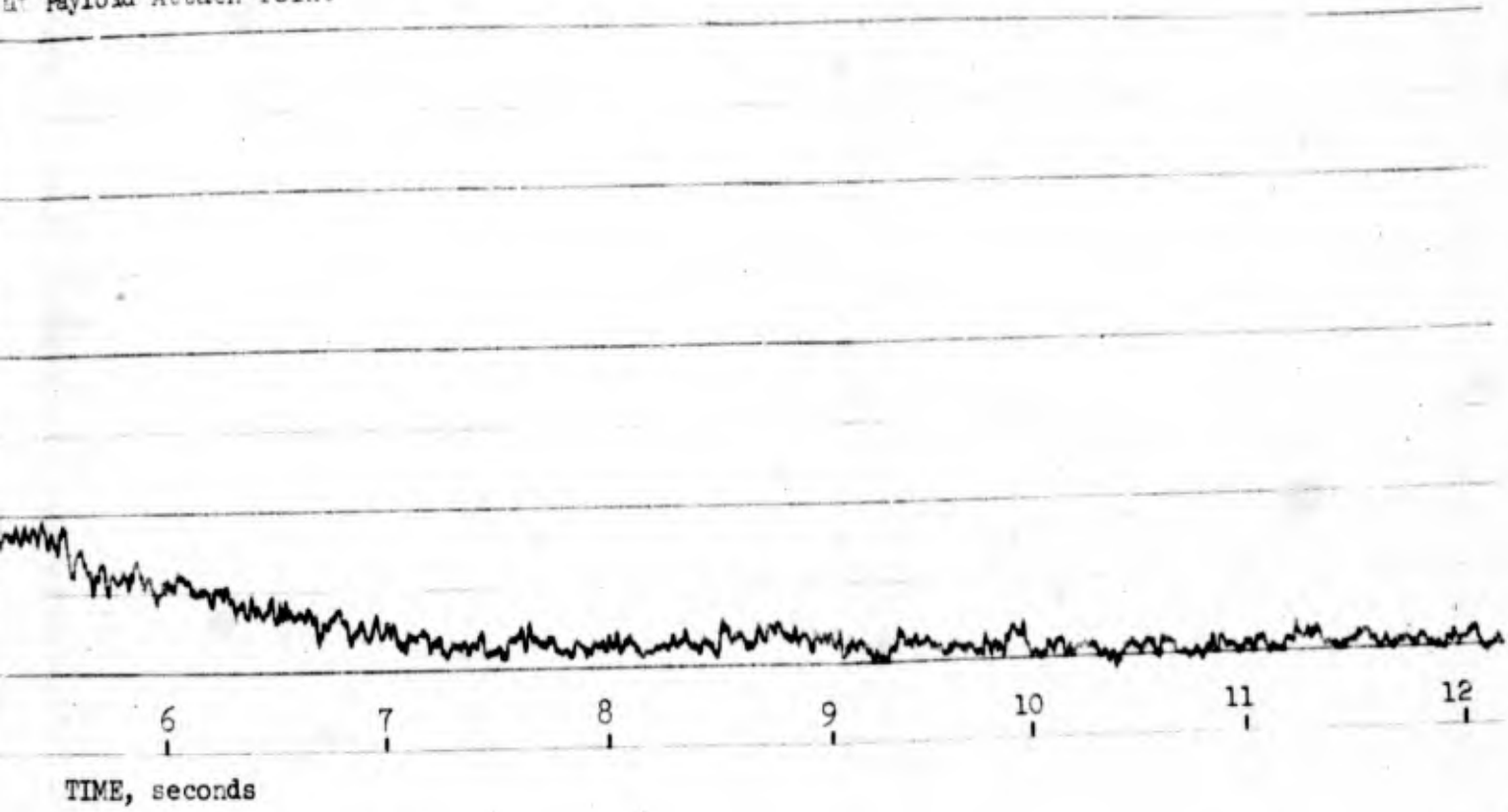
Figure 1-6

NIRO

Flight AG 7.316

L. G. RMS vs TIME

at Payload Attach Point



## Section II

### IROQUOIS JOINT ANALYSIS

#### 2.1 INTRODUCTION

An analysis of the joint between the TE-388, Iroquois, motor assembly in the aft end of the NIRO payload assembly was to be conducted to determine the effect on joint rotation of the following parameters:

- Joint fit tolerances
- Screw preload
- Temperature gradients
- Internal tank pressure
- Flight loads

The analysis was conducted utilizing Aerojet digital computer program No. 0616, for a thin shell (Stress Analysis of Shells). This program determines the radial deflections or rotations at specified increments for each part of the assembly. It allows inputs such as axial and radial loads and bending moments when applied symmetrically to the section. Temperature inputs may vary in both axial and radial directions. The only requirement for all external loads and temperatures is symmetry around the centerline of the section.

The area to be analyzed using the 0616 program is divided into sections called regions. The divisions were determined by changes in geometry, abrupt dimensional change, significant changes in temperature or thickness or application of an external load, such as an applied or radial shear load, bending moment, or axial load. Physical dimensions such as radius or thickness are required input for each region. The modulus of elasticity, Poisson's ratio and thermo coefficient of expansion for each region are also required. The program allows up to 25 regions to be used in each case. The end conditions of the total section must

also be defined. For example, at the end of a cylinder away from all discontinuities one may input a zero bending moment and zero slope or zero shear as defining the required end conditions for the region. The joint between the regions are defined such that one must inform the program which regions are connected to each other. The maximum number of regions which can be joined is three.

The program using all of the above inputs equates the slopes and deflections between the regions and then determines all continuity shears, bending moments throughout each region. Displacements and other parameters are determined by finite difference technique which allows a fine grid to be specified, up to 299 divisions per region, thus the solution has the characteristic of the closed form integral solution while retaining advantages of a finite difference technique.

## 2.2 DISCUSSION

The forward end of the TE-388, Iroquois, motor assembly including a portion of cylindrical case and the head cap was divided into an appropriate number of regions for input into program number 0616. Computations were made using the established vehicle characteristics and various inputs in order to determine the effects on joint rotation of the various parameters. The results of these analyses indicate that the joint rotation effects, due to factors such as internal pressure, caused negligible flange rotation; i. e., less than 0.15 degrees. This unexpected result in the preliminary cases lead to a re-evaluation of the proposed program. A second look at the problem indicated the primary cause of joint rotation must be the body bending moments with the amount of rotation observed associated with the tolerances in the joint itself. This conclusion lead to the questionability of any further attempt to analyze the joint using program 0616.

At this point in time, it was apparent that the joint analysis could not be reoriented and completed within the available contractual time. An adjustment was made in the contract to reduce the scope of effort on this task from that which was originally planned. The contract funding was reduced accordingly. No further work was done on the joint analysis subsequent to this time. The mechanical assumptions, the element data sheets, and the printouts of the computer analysis are contained in Appendix C.

### 2.3 RECOMMENDATIONS

As it has been surmised, the principal magnitude of joint rotation must lie in the effective tolerances associated with the motor head cap-payload joint. It is recommended that the next effort to be performed should involve an oversize layout of the joint to at least a 10 to 1 scale. This layout, which would incorporate the geometric representation of the maximum and minimum tolerances allowable within the joint, would allow a detailed study to be made with more accuracy and much less complication than would be involved in the analytical technique alone. The results of this geometric analysis would then provide direction for further analytical study and/or acceptable tolerance specifications for the motor head cap and the payload attachment. In addition, the effect of screw torque on the tolerance joint should be analyzed. This is not necessarily a straightforward problem and will require some development effort to establish and prove the proper techniques.

## Section III

### NIRO LONGITUDINAL VIBRATION ANALYSIS

#### 3.1 INTRODUCTION

##### 3.1.1 PURPOSE OF THE ANALYSIS

Longitudinal payload vibrations with divergent characteristics were recorded near burnout for NIRO Brazil Flights AG 7.314 and AG 7.316. This report attempts to define the nature and causes of these vibrations by means of a comprehensive structural dynamics analysis. In addition, design data is presented which should allow the payload designer to eliminate or minimize such vibrations for future flights.

##### 3.1.2 BRIEF SUMMARY OF RESULTS

The investigations discussed herein indicate that the adverse vibrations observed were probably due to first mode structural-motor resonance. If so, minimization of these vibrations for future flights can probably best be achieved by frequency separation of the structural and motor first modes. Parametric studies indicate that variation in the payload longeron stiffness is probably the most practical way to achieve this desired frequency separation.

#### 3.2 DISCUSSION

##### 3.2.1 BRAZIL FLIGHTS AG 7.314 AND AG 7.316

###### 3.2.1.1 CONFIGURATION DESCRIPTION

The configurations for NIRO Brazil Flights AG 7.314 and AG 7.316 were nominally identical. Therefore, for purposes of this analysis only one configuration shall be considered. This configuration has the following characteristics:

- Payload Weight = 181 lb
- Payload Diameter = 9.0 inches  
(oversize)
- Payload Length = 115.25 inches

The payload weight includes a payload recovery system between the oversize nose fairing and the sustainer motor. This payload recovery system weighs 35.1 pounds, is 24.6 inches in length and is 7.75 inches in diameter. These recovery system weights and dimensions should be considered as approximate since they were calculated to match overall weights and dimensions.

An inboard profile of the configuration is shown in Figure 3-1. A sketch of the nose fairing structure is presented in Figure 3-2. It should be noted that certain of the dimensions shown on this sketch were scaled from photographs. Most, however, were taken from drawings. Therefore, accuracies of  $\pm 1.0$  inch are probably reasonable in the overall length dimension.

The internal cantilevered payload is comprised of a series of circular shelves upon which are mounted the experimental equipment. These shelves are assembled by means of four full length longerons spaced every 90 degrees around the shelves. These longerons have a rectangular cross section (1.0" x 0.37") and are made of aluminum. The payload assembly is attached to the oversize nose fairing approximately at its midpoint by a series of screws through the skin into one of the equipment shelves. These screws are the only restraint to longitudinal motion. There are guides at each end of the fairing which mate with the longerons. However, these guides restrain only lateral and rotational motions. The weight and CG for this cantilevered assembly is:

Weight = 98.2 lb

CG at Vehicle Station = -61.1

The above figures again should be considered as best estimates. They were obtained from a knowledge of the overall payload weight and CG and an estimate of the nose fairing weight made using the dimensions shown on Figure 3-2.

It should be noted that the midpoint attachment of the payload to the fairing is not the usual method of affixing payloads. Ordinarily the payloads are cantilevered either from their base or are comprised of two separate assemblies, both of which are cantilevered from their bases. The effect of various methods of attachment on structural frequency is discussed later in this report in Section 3.2.2.6.

### 3.2.1.2 LONGITUDINAL VIBRATION DATA NEAR SUSTAINER BURNOUT

#### 3.2.1.2.1 DESCRIPTION

A longitudinal vibration transducer was mounted at the payload rack to skin attach point (midway up the payload) on flights 7.314 and 7.316. Examination of the flight records produced by this instrument indicate a low level, periodic longitudinal vibration commencing several seconds before burnout and continuing to burnout for both flights. The vibration levels for flight 7.314 were more severe than those for flight 7.316. In both cases, the vibration levels tended to increase with time. Also noted in both flights were beats which would indicate the presence of two frequencies of nearly equal value. The vibrations very definitely had single frequency sinusoidal characteristics which would indicate the predominant excitation of one of the structural modes.

The flight records indicate that burnout occurred at 7.75 seconds, rather than at 8 seconds due to temperature conditioning of the motors. The most severe portion of the vibration record commences between 1.6 and 2 seconds prior to burnout and extends to burnout. However, noticeable abnormalities were observed much earlier. Close examination of the records indicate that the vibrations under consideration are probably first evident at about 4.5 seconds. This is most likely the time at which the structural stability margin is crossed. This will be discussed in more detail in the following sections.



### 3.2.1.2.2 $G_{rms}$ VS TIME NEAR SUSTAINER BURNOUT

In order to assess the energy levels of the vibrations under consideration, the flight records were reduced to  $G_{rms}$  time histories. These plots are shown in Figures 3-38 and 3-39. Examination of this data shows a peak value of 1.77 G's at  $t = 25$  seconds for flight 7.314 and a peak value of 1.05 G's at  $t = 25.3$  seconds for flight 7.316. As stated before, this shows that the energy levels for flight 7.314 were higher than those for flight 7.316. Also, it can be seen that the G levels in general tend to increase with time, with some reduction noted just prior to burnout. Although the G levels shown are not necessarily excessive, since no payload failure was noted during these flights, they nonetheless indicate somewhat less than an ideal smooth ride. It is, therefore, one of the goals of this report to provide a means for reducing these levels.

### 3.2.1.2.3 HARMONIC ANALYSIS

As stated previously the vibrations appeared to be primarily sinusoidal in nature with one frequency band predominant. In order to identify the various frequencies present and the distribution of vibrational energy, a harmonic analysis of the data was performed. This analysis was performed by digital means employing Fourier techniques. The results of this analysis are shown in Figures 3-40 and 3-41. The data samples used to perform these analyses were 1.64 seconds in length and were located in the region of maximum vibration levels near sustainer burnout.

The harmonic content of the vibration was determined by the procedure outlined below:

- The vibration data was recovered from the flight-data magnetic tape with standard IRIG FM-FM telemetry discrimination equipment. A 1050 Hz 6th order low pass filter was used to minimize aliasing. The digitizer input to a Varian Data Machines 620i computer was used to digitize a 1.84 second sample of the vibration data at a 5000 sample/second rate. The digitized data was then recorded on a computer magnetic tape.

- The digitized sample was processed with an IBM 360-65 computer to determine the harmonic content. A 1.64 second sample was selected and the static component was removed. The Cooley-Tokey fast Fourier transform was used to determine the magnitudes of sine and cosine components. The absolute magnitude was determined and plotted by creating a special 'plot' magnetic tape which was used to operate a CalComp 565 digital incremental plotter.

An examination of the results shows that, as suspected, most of the energy is concentrated in one frequency band. This is from 210 to 240 cps. Also apparent, especially in the 7.314 results, is the presence of two closely spaced frequencies which would account for the beats which were evident in the records. As will be discussed later, it was found that the first structural frequency and the first motor frequency both are located in this region. At burnout these two frequencies are very nearly equal. This leads one to suspect a resonant condition which would explain the concentration of vibration energy in this frequency band.

The frequency time histories of Figure 3-34 show that the second motor frequency and the second and third structural frequencies are all in the 500 cps region near burnout. An examination of the harmonic analysis shows some concentration of energy in this general frequency region, lending credence to the analytical results. However, the energy levels in this region are very low and do not elicit any concern.

For frequencies between 500 and 1000 cps, the higher frequency resonances predicted by the theory do not have any detectable effect in the data of Figures 3-40 and 3-41.

### 3.2.1.3 CONCLUSIONS FROM THE VIBRATION DATA NEAR SUSTAINER BURNOUT

An examination of the flight vibration data described in Section 3.2.1.2 leads one to several possible conclusions. The first of these is that the observed vibrations are divergent and unstable in nature. This is borne out by the fact that the vibrations are increasing in severity with time and also by the distribution of the energy build up. A stable high amplitude oscillation is characterized

by a rapid build up of energy to a peak with a gradual decrease of energy following the peak. One example of such an oscillation is the case of sounding rocket roll lock-in. Unstable oscillations are characterized by a gradual build up of energy to a high level followed by a more gradual increase of energy which ultimately leads to catastrophe. The vibrational energy build up observed on flights 7.314 and 7.316 appears to be of this latter type. The reason that serious problems did not ensue is the fact the system damping increases with amplitude, thus limiting the vibration amplitudes.

The second conclusion is that the adverse vibrations were possibly due to a resonant condition between the first structural mode and the first motor acoustic mode. The time histories of structural and motor frequencies shown in Figure 3-34 show that these two frequencies converge on each other at burnout. This is further verified by the harmonic analysis which was discussed in Section 3.2.1.2.3. Most of the vibration energy is in the region of the 1st modes and two closely spaced resonances in this region are evident.

It is very important to verify and amplify the foregoing conclusions by means of analysis. Although the vibrations for these particular flights did not prove excessive it is conceivable that some future payload could experience such a condition. Examination of the time histories in Figure 3-34 shows that slight to moderate changes in the vehicle structural natural frequency could possibly put it in an adverse resonant condition with the motor for a much longer time than was experienced by the flights under consideration. It is, therefore, important (as it is done in this report) to define the structural stability limits for various NIRO configurations so that such an adverse condition may be intentionally avoided in the future.

#### 3.2.1.4 ANALYTIC APPROACH

To better understand the vibration characteristics of the configurations under consideration it is required that some knowledge of the structural and motor frequencies and mode shapes be obtained. In order to do this, two tools were employed. The first of these was a large scale digital computer program for finding the eigenvalues and eigenvectors of a large lumped parameter

system. The second was a small program suitable for the Olivetti desk computer. This program employed exact beam theory as applied to a simplified branch beam. The application of these two tools is discussed below:

- a. Lumped Parameter Model - The lumped parameter analysis was chosen as the most accurate method available to define the frequency characteristics of the Flight 7. 314 and 7. 316 configurations. The reasons for this are twofold. The first is the fact that these configurations represent a four branch beam which is shown in Figure 3-10. This is quite simple to represent by a lumped parameter system. Exact solutions for this type of beam, although possible, are somewhat involved. Secondly, the lumped parameter system is considerably more accurate in its representation of mass and stiffness distributions than is an exact theory model. Exact theory models are fairly well limited to readily definable functions (such as uniform, for example) for these distributions. As will be shown later, the distribution of these values is an important consideration. The lumped parameter analysis was used primarily to determine time histories (see Figures 3-33 and 3-34) of the vehicle structural frequencies so that some assessment of the resonances involved could be made. These time histories were used to establish the structural vibrational stability limits of the vehicle. The time histories were determined both with and without an equivalent acoustic branch to represent the elastic behavior of the motor gases. The derivation of this acoustic branch is discussed in Section 3.2.2 and in Appendix A to this report. Due to its simplicity of representation, the lumped parameter model was also used to investigate the effect on vehicle frequency of a variation in the position of the payload attach point. This is discussed in Section 3.2.2.6.
- b. Exact Theory Model - The exact theory model was set up for the Olivetti desk computer so that a large number of parametric variations could easily be studied. The model used assumed uniform mass and stiffness over each of three structural branches. The payload branch was attached at its base. In addition an equivalent acoustic branch was included as was done for the lumped parameter model. This simplified model was far more suitable for a large number of cases than the lumped parameter model due to the set up times involved. The simplified, but exact theory model, was also used to determine the accuracy of results obtained from the lumped parameter analysis. This will be discussed in detail in Section 3.2.2.4. The simplified model was used to study variations in payload weight and stiffness. From this study, consideration

being taken for the accuracies involved, structural stability limits were established in terms of payload (longeron) stiffness and weight. This is discussed in Section 3.2.3.

### 3.2.1.5 RANDOM VIBRATION NEAR BOOSTER BURNOUT

#### 3.2.1.5.1 DESCRIPTION OF THE DATA

The flight vibration records for Brazil flights 7.314 and 7.316 show a noticeable random type vibration occurring near Nike booster burnout and continuing beyond staging. In order to ascertain how much energy was in these vibrations, the flight records were reduced to  $G_{rms}$  time histories. These are shown in Figure 3-38 for Flight 7.314 and Figure 3-39 for Flight 7.316. Examination of the records show that for both flights the energy level was highest just at staging (about 3.35 sec). For Flight 7.314 the maximum level at this time was  $0.8 G_{rms}$  and for Flight 7.316 the level was  $1.9 G_{rms}$ .

It was desired to determine the vibrational energy distribution with frequency for these vibrations in order to see if any significant resonances were present. In order to do this, power spectral density analyses were performed on the data in this region. The method used to perform these analyses is presented in Section 3.2.1.5.2. In all cases the data samples used for the analyses were 1.64 seconds in length. Since the data are non-stationary in character, two samples with slightly different time origins were used for each case. This gives some idea of the variations in results possible with this type of data by using different data samples in the same general region. The cases analyzed were as follows:

| <u>Flight No.</u> | <u>PSD No.</u> | <u>Time Origin<br/>sec</u> | <u>Sample Length<br/>sec</u> |
|-------------------|----------------|----------------------------|------------------------------|
| 7.314             | 1              | 3.28 sec                   | 1.64                         |
| 7.314             | 2              | 3.32 sec                   | 1.64                         |
| 7.316             | 1              | 3.69 sec                   | 1.64                         |
| 7.316             | 2              | 3.81 sec                   | 1.64                         |

Notice that the data for Flight 7.314 commence before staging (3.35 sec) and extend beyond staging. This should be kept in mind when interpreting the results since two separate conditions are present in the data, viz. power-on and power-off. The data for Flight 7.316 are all beyond staging and are therefore of one type, viz. power-off.

The power spectral density diagrams are presented in Figures 3-42 and 3-43 for Flight 7.314 and in Figures 3-44 and 3-45 for Flight 7.316. For both flights and both samples the data appear to be generally "white" in character with no high energy resonances apparent. Sharp spikes are visible in both flights which very likely represent structural resonances, but they do not contain enough energy to be of particular interest.

#### 3.2.1.5.2 METHOD OF ANALYSIS USED TO OBTAIN POWER SPECTRAL DENSITY DATA

The Power Spectral Density (PSD) of the vibration was determined by the procedure outlined below:

- The vibration data were recovered from the flight-data magnetic tape with standard IRIG FM-FM telemetry discrimination equipment. A 1050 Hz 6th order low pass filter was used to minimize aliasing. The digitizer input to a Varian Data Machines 620i computer was used to digitize a 1.84 second sample of the vibration data at a 5000 sample/second rate. The digitized data was then recorded on a computer magnetic tape.
- The digitized sample was processed with an IBM 360-65 computer to produce the PSD. The sample was first filtered with a digital filter that simulates a 2nd order RC filter with a 12 Hz breakpoint frequency. Any residual static component was removed from the data. In some cases a third order least-square polynomial fit was determined, and this polynomial was then removed from the data to eliminate drifts during the sample period. The discrete Fourier transform of a 1.64 second sample of the data was calculated using the Cooley-Tukey fast Fourier transform method. The square of the transform was determined and the components below 10 Hz removed. The auto correlation function was determined by inverse transformation. A Parzen data window was applied to this function to achieve spectral smoothing. A Fourier transform was applied to the result to yield the PSD of the vibration data. The PSD was plotted by creating a special 'plot' magnetic tape which was used to operate a CalComp Model 565 digital incremental plotter.

### 3.2.2 LUMPED PARAMETER ANALYSIS

#### 3.2.2.1 DETERMINATION OF LUMPED MASSES AND STIFFNESSES

##### 3.2.2.1.1 CONFIGURATION

The configuration analyzed is that which is discussed in Section 3.2.1.1. It is representative of NIRO Flights AG 7.314 and AG 7.316. An inboard profile of the vehicle with the Brazil payload attached is shown in Figure 3-1. A sketch of the oversize (9-foot diameter) nose fairing structure is shown in Figure 3-2. Note that the configuration includes a payload recovery system.

##### 3.2.2.1.2 WEIGHT AND STIFFNESS DATA

The payload weight distributions used to obtain the lumped masses are shown in Figure 3-5 for nose fairing and recovery system and in Figure 3-3 for the cantilevered internal payload. These distributions were derived from a knowledge of the overall payload weight and center of gravity and an estimate of the weight and center of gravity of the nose fairing and tip, based on the data shown in Figure 3-2. The data in Figure 3-2 is based on payload drawings and on photographs of the payload. No detailed data regarding the cantilevered payload distribution was available. Therefore the total weight and center of gravity of this segment were matched by means of a trapezoidal distribution. A summary of the weight and CG's calculated for the various payload components is as follows:

| <u>Item</u>                               | <u>Weight<br/>(lb)</u> | <u>Station of CG<br/>(in.)</u> |
|---|------------------------|--------------------------------|
| Split Tipe Nose Cone                      | 9.4                    | -98.0                          |
| Shell Surrounding<br>Cantilevered Payload | 38.3                   | -58.4                          |
| Cantilevered Payload                      | 98.2                   | -61.1                          |
| Payload Recovery System                   | <u>35.1</u>            | <u>-12.3</u>                   |
| Total                                     | 181.0                  | -52.98                         |



The weight distributions of the NIRO motor for various flight times are shown in Figure 3-7. These data were obtained from Reference 3-2. The flight times considered for the analysis were 0, 4, 6, and 8 sec.

The stiffness distribution,  $AE$ , for the nose fairing branch is shown in Figure 3-6. This again was derived from the data in Figure 3-2. The stiffness distribution for the cantilevered internal payload is shown in Figure 3-4. It is based on longeron stiffness only. The stiffness for the motor was considered uniform and is shown in Figure 3-8.

The computer program accepts stiffness in terms of spring constants, rather than  $AE$ 's. These are readily obtainable as follows:

$$k_n = (AE)_n / \Delta l_n$$

where:  $k_n$  = Spring constant for the nth segment

$A$  = Cross section area

$E$  = Young modulus of elasticity

$\Delta l_n$  = Length of Segment under consideration

In the case where a discontinuity in stiffness occurred between two masses, an equivalent spring constant was calculated from the relationship for two springs in series as follows:

$$k_{\text{equivalent}} = \frac{k_1 k_2}{k_2 + k_1}$$

A diagram showing the lumped mass configuration for the Brazil configuration is shown in Figure 3-10. Note that this is a four branch beam. This arises from the fact that the internal payload is cantilevered at approximately its midpoint (also see Figure 3-2).

A summary of the lumped masses and stiffnesses for the Brazil payload is presented in Table 3-1 for the four different flight times under consideration. Note that the cantilevered payload and fairing branches are the same for all times.



### 3.2.2.2 EQUIVALENT ACOUSTIC BRANCH

It was desired to consider the structure and pulsating motor gases as a coupled system rather than as two separate systems. An analysis of this type will show the change in frequency of either system due to the interaction of both of the systems. In order to do this, an equivalent lumped mass and stiffness branch representing the motor gases had to be added to the structural model. This branch could be considered as a sort of pneumatic spring. The motor in this case was considered as a simple organ pipe closed at both ends. The effects of an open nozzle were considered too complex to be considered at this time. The relationships regarding the mass and "stiffness" of the gas are derived in Appendix A of this report. In summary they are as follows:

$$a. \quad \mu_{\text{gas}} = p_o S \gamma / C^2$$

$$b. \quad AE_{\text{gas}} = p_o S \gamma$$

where:

$$\mu_{\text{gas}} = \text{Equivalent mass distribution}$$

$$AE_{\text{gas}} = \text{Equivalent extensional stiffness}$$

$$p_o = \text{Motor chamber pressure}$$

$$S = \text{cross sectional area of the motor port}$$

$$\gamma = \text{Ratio of specific heats}$$

$$C = \text{Speed of sound in the motor gases}$$

The port area,  $S$ , is determined from the following relationship:

$$c. \quad S = \pi \frac{d^2}{4} - \frac{W}{\rho l_G}$$

where:

$d$  = Outside diameter of the propellant grain

$W$  = Propellant weight

$\rho$  = Propellant density

$l_G$  = Propellant grain length

The values used for the calculations were:

$d$  = 7.39 inches

$W$  = Variable with time. Values used were from Reference 3-2.

$\rho$  = .0588 lb/in<sup>3</sup>

$l_G$  = 88.15 in.

The values of chamber pressure versus time which were used for the calculations are shown in Figure 3-9. These data are from Reference 3-3. The value of the ratio of specific heats,  $\gamma$ , which was used was 1.142. The speed of sound used was 3535 ft/sec.

The mass and stiffness distributions for the above are considered to be uniform. The distribution magnitudes, however, vary with time since the port area increases as propellant is consumed. The lumped mass configuration used to represent this acoustic branch is shown in Figure 3-14. The values used for the lumped masses and stiffnesses are presented in Table 3-6 for the various time points under consideration.

In order to evaluate the effects of structural-acoustic coupling on the acoustic branch, the frequency of the acoustic branch as a separate uncoupled system must be known. To do this the acoustic branch was considered as a clamped-clamped uniform beam. The frequency was then obtained from the following relationship (see Reference 3-6) using the equivalent mass and stiffness:

$$\omega_n = n\pi \sqrt{\frac{AE}{\mu l^2}}, \quad n = 1$$

where:

$\omega_n$  = Natural frequency

$l$  = Beam (or motor) length

The fundamental frequency obtained from the above was 241 cps. The same input data were also run on the lumped parameter digital computer program as a separate case. The fundamental frequency obtained in this manner was 239 cps. Therefore, use of the lumped parameter model introduces errors in the acoustic branch on the order of  $\pm 2$  cps.

It was found that the structural and acoustic branches were very lightly coupled. This is discussed in Section 3.2.2.5. The two systems, structural and acoustic, can reasonably be treated as separate systems without introduction of significant errors.

### 3.2.2.3 METHOD OF ANALYSIS

#### 3.2.2.3.1 SOLUTION FOR EIGENVALUES AND EIGENVECTORS

The natural frequencies and modes shapes for the lumped parameter system were found by means of a large scale digital computer program employing the Jacobi Method. This method of analysis is discussed in detail in Reference 3-4. The program used is documented in Reference 3-5. The equations considered in the analysis are as follows:

- a. The equation of motion for an n-lumped mass system is:

$$[M] \{\ddot{Y}\} + [K] \{Y\} = 0 \quad (1)$$

where:  $[M]$  = Diagonal Mass Matrix

$[K]$  = Rectangular symmetric stiffness matrix

$\{Y\}$  = Column deflection matrix

$\{\ddot{Y}\}$  = Column acceleration matrix

- b. Equation (1) may be expressed in the form of a real eigenvalue problem, assuming free sinusoidal vibration at a frequency  $\omega$ , as follows:

$$\omega^2 [M] \{Y\} = [K] \{Y\} \quad (2)$$

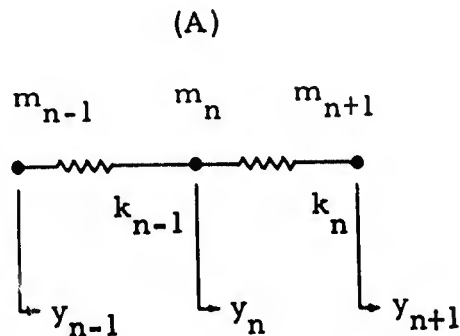
where:  $\ddot{Y} = \omega^2 Y$

Equation (2) is the form which is solved in the computer program. The method programmed determines as many eigenvalues and sets of eigenvectors as there are masses. However, only the first ten will be presented herein. Of these ten, it turns out that only the first three elastic modes are of any real interest. This, of course, is because nearly 100 percent of the vibrational energy noted is in these three modes, with the bulk of the energy residing in the first structural elastic mode.

### 3.2.2.3.2 DEVELOPMENT OF THE STIFFNESS MATRIX

Since all of the structural models analyzed in this report are free ended branch beams, some discussion should be presented on the development of the required stiffness matrices  $[k]$ , and on the representation of the branch points in these stiffness matrices.

Consider the following free-free simple beam with 3 lumped masses and 2 stiffnesses:



The equation of motion for the  $n$ th mass is:

$$m_n \ddot{y}_n - k_{n-1} y_{n-1} + (k_{n-1} + k_n) y_n - k_n y_{n+1} = 0 \quad (3)$$

The above equation applies to all of the masses in the system except those at the free ends and at branch points. The equations at the free ends are:

$$m_{n-1} \ddot{y}_{n-1} + k_{n-1} y_{n-1} - k_{n-1} y_n = 0 \quad (4)$$

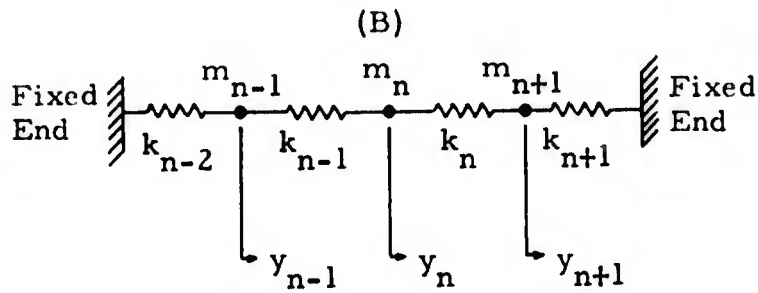
$$m_{n+1} \ddot{y}_{n+1} + k_n y_{n+1} - k_n y_n = 0 \quad (5)$$

The spring forces,  $\{F\}$ , of the foregoing equations in matrix form are:

$$\begin{Bmatrix} F_{n-1} \\ F_n \\ F_{n+1} \end{Bmatrix} = \begin{bmatrix} k_{n-1} & -k_{n-1} & 0 \\ -k_{n-1} & (k_{n-1} + k_n) & -k_n \\ & -k_n & k_n \end{bmatrix} \begin{Bmatrix} y_{n-1} \\ y_n \\ y_{n+1} \end{Bmatrix} \quad (6)$$

Note that the above stiffness matrix is symmetric with a generally diagonalized character.

If the example in (A) were considered as a fixed-fixed beam, as was the case for the acoustic branch alone calculations, the equations would assume the following form:



The equation for the nth mass is the same as before as shown in Equation (3). The equations for the n-1 and n+1 masses become:

$$m_{n-1} \ddot{y}_{n-1} + (k_{n-2} + k_{n-1}) y_{n-1} - k_{n-1} y_n = 0 \quad (7)$$

$$m_{n+1} \ddot{y}_{n+1} + (k_n + k_{n+1}) y_{n+1} - k_n y_n = 0 \quad (8)$$

The stiffness matrix then becomes:

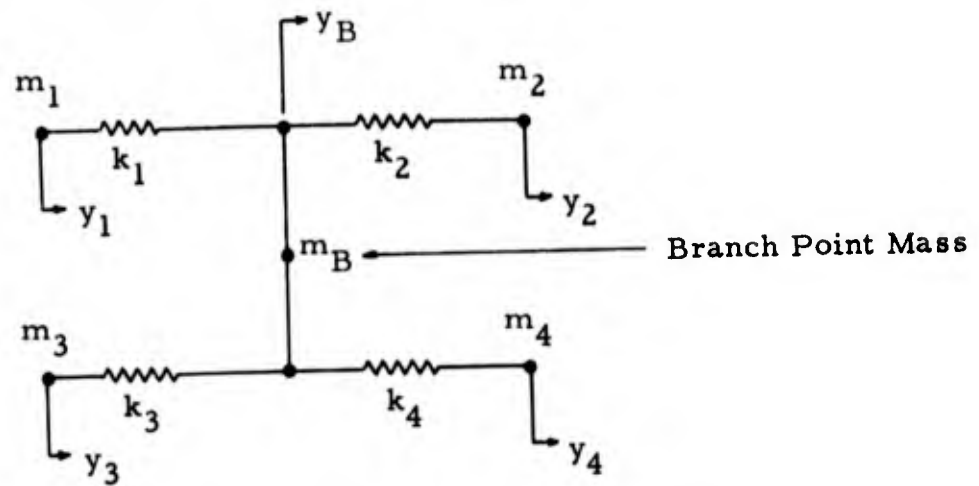
$$\begin{bmatrix} k_{n-2} + k_{n-1} & -k_{n-1} & 0 \\ -k_{n-1} & k_{n-1} + k_n & -k_n \\ 0 & -k_n & k_n + k_{n+1} \end{bmatrix} = [k] \quad (9)$$

Note the similarity of the two matrices in Equations (9) and (6). The end conditions were modified by merely adding in the fixed end stiffnesses to the first and last terms of the free-free matrix.

Finally, consider a free-ended four branch beam similar to the ones analyzed herein, but with fewer masses.



(C)



The equations of motion are written in a manner similar to the previous examples and are as follows:

The equations for the masses at the four free ends are:

$$m_1 \ddot{y}_1 + k_1 y_1 - k_1 y_B = 0 \quad (10)$$

$$m_2 \ddot{y}_2 + k_2 y_2 - k_2 y_B = 0 \quad (11)$$

$$m_3 \ddot{y}_3 + k_3 y_3 - k_3 y_B = 0 \quad (12)$$

$$m_4 \ddot{y}_4 + k_4 y_4 - k_4 y_B = 0 \quad (13)$$

The equation for the branch point mass is:

$$m_B \ddot{y}_B + (k_1 + k_2 + k_3 + k_4) y_B - k_1 y_1 - k_2 y_2 - k_3 y_3 - k_4 y_4 = 0 \quad (14)$$

Writing the spring forces,  $\{F\}$ , of the foregoing equations in matrix form gives:

$$\begin{Bmatrix} F_1 \\ F_2 \\ F_3 \\ F_4 \\ F_B \end{Bmatrix} = \begin{bmatrix} k_1 & 0 & 0 & 0 & -k_1 \\ 0 & k_2 & 0 & 0 & -k_2 \\ 0 & 0 & k_3 & 0 & -k_3 \\ 0 & 0 & 0 & k_4 & -k_4 \\ -k_1 & -k_2 & -k_3 & -k_4 & (k_1+k_2+k_3+k_4) \end{bmatrix} \begin{Bmatrix} y_1 \\ y_2 \\ y_3 \\ y_4 \\ y_B \end{Bmatrix}$$

All of the stiffness matrices used for the lumped parameter analysis were derived in a manner similar to that described in the foregoing discussion. It can be seen that it is quite easy to vary end conditions or branch conditions by simple modifications of the stiffness matrix. For this reason, the lumped parameter method was chosen as the tool for studying the variation of branch point on vehicle frequency. This is discussed in Section 3.2.2.6. For further discussion regarding development of stiffness matrices the reader is referred to material presented in References 3-1 and 3-6.

#### 3.2.2.4 COMPARISON OF THE LUMPED PARAMETER MODEL WITH EXACT THEORY

The structural stability limits of the structure were established (see Section 3.2.3.1.2) using frequency data obtained from the lumped parameter analysis. The lumped parameter model was used for this purpose since it most accurately represented the four branch beam and the mass and stiffness distributions of the actual Brazil flights.

It was desirable, therefore, to establish the accuracies of the results produced by the lumped parameter analysis. To do this, an exact theory model was set up to represent a simplified three branch beam with uniform mass and stiffness distributions. Derivation of this simplified model is presented in Appendix A of this report. The same configuration was then run through both the exact theory analysis and the lumped parameter analysis to obtain frequencies and mode shapes.

The model analyzed in both cases had uniform distributions of mass and stiffness. The payload was considered attached at its base. The mass distribution values used were for  $t = 6.0$  sec of sustainer burn time. The lumped mass configuration used is shown in Figure 3-11. The values of lumped masses and stiffnesses used are shown in Table 3-5.

The frequencies obtained from the two methods are compared in Table 3-9. It can be seen that the fundamental frequencies compare quite favorably. The error is approximately 2 cps. As one would expect the errors increase for the higher modes. In the third structural mode, for example, the error is 15 cps. However, since the first mode is the one of primary concern, the accuracies obtained are quite satisfactory. Therefore, the fundamental frequencies obtained for the actual flight configurations should be accurate within approximately 2 cps.

A comparison of the mode shapes obtained by the two methods is presented in Figures 3-15 through 3-17. Again, the fundamentals agree almost exactly, while the higher modes show some variation.

An acoustic branch, as described in Section 3.2.2.2, was added to both representations. The frequencies obtained by both methods including this acoustic branch are also presented in Table 3-9. Note that the modes which are primarily acoustic in nature are denoted with an asterisk. It can be seen that addition of the acoustic branch produced little or no change in the structural frequencies. The slight difference in acoustic frequencies between the two methods can be primarily attributed to the slightly different lengths used for this branch. In the exact theory model the acoustic branch length was equal to 88.15 inches which is the exact motor length. For the lumped parameter model the length used for the sake of convenience, was 85 inches. Note also that the acoustic frequency of the coupled acoustic-structural system is nearly identical to that obtained for the acoustic branch alone (241 cps, see Section 3.2.2.2). It can be fairly concluded from the foregoing that there is very little coupling between the acoustic and structural branches.

Finally, a comparison was made, again at  $t = 6$  seconds between the simplified uniform distribution model and between a lumped parameter model using exact mass and stiffness distributions and with the payload attached at its base. The comparison here was less favorable. The simplified model frequency was 231 cps while the exact distribution model frequency was 210 cps. Therefore, it would appear that an error of 21 cps can be made by using uniform distributions instead of exact distributions. This error has been considered in the stability margins which are discussed in Section 3.2.3.

### 3.2.2.5 TIME HISTORIES OF FREQUENCIES AND MODE SHAPES

Time histories of the Brazil configuration structural frequencies both with and without an acoustic contribution were calculated by means of the lumped parameter model. As stated previously, this model was used since it most accurately represents the actual Brazil flight configurations. These time histories are presented in Table 3-7 and Figure 3-33 for the structure without acoustics and in Table 3-8 and Figure 3-34 for the structure including acoustics.

The time histories were obtained from lumped parameter models representing the flight times of  $t = 0, 4, 6$  and 8 seconds. The lumped masses and stiffnesses used for the analysis are presented in Table 3-1 for these various flight times.

The natural frequencies produced by the program are printed in descending order. As can be seen in Figure 3-34, several frequencies, both acoustic and structural, are often grouped in a particular bandwidth. For this reason it was difficult to determine whether a particular frequency was primarily structural or primarily acoustic in nature. This assessment had to be made by plotting the mode shapes both with and without the acoustic branch. Typical plots without the acoustic branch are shown in Figures 3-18 through 3-20. Typical plots with the acoustic branch are shown in Figures 3-21 through 3-25. It becomes quite evident which modes are primarily acoustic and which modes are primarily structural from a comparison of these mode shapes. The values shown in Table 3-8 and in Figure 3-34 have been identified by this procedure.

Examination of the data obtained shows that inclusion of an acoustic contribution produces only slight changes in the basic structural frequencies. At  $t = 8$  seconds for example, the fundamental frequency is 3 cps higher for the coupled case than for the uncoupled case. In the higher modes differences of 7 cps may be noted.

The acoustic fundamental frequency shown in Figure 3-34 and Table 3-8 is about 5 cps higher than the acoustic branch alone frequency of 241 cps. As stated previously this difference may be primarily attributed to the slightly shorter than actual (3 inches) motor length which was used.

Figure 3-34 shows that the fundamental structural and motor frequencies converge on each other at burnout and are nearly equal at this time. The second and third structural frequencies and the second acoustic frequency are closely grouped at all times with the third structural and second acoustic frequencies intersecting each other at about 5.5 seconds. The fourth structural and third acoustic frequencies intersect each other near burnout.

From the foregoing it can be seen that many possible structural-acoustic resonances or near resonances exist in the time history. However, one would expect that most of the vibration energy due to these resonances would probably reside primarily in the lower modes. An examination of the harmonic analysis, discussed in Section 3.2.1.2.3, shows that this is indeed true. Most of the energy is in the region of the first structural mode with a much smaller concentration of energy in the region of the second and third structural modes.

A separation of the fundamental motor and structural frequencies would probably be helpful in reducing the amplitude of vibrations noted in this frequency band. As is discussed in Section 3.2.3, it was found that variation in payload longeron stiffness was a convenient way to achieve this frequency separation. The amount of separation required may be established from Figure 3-34 by a knowledge of the time at which the adverse vibrations first became evident. This is discussed in detail in Section 3.2.3.

### 3.2.2.6 VARIATION OF VEHICLE FREQUENCY WITH PAYLOAD ATTACH POINT

Pursuant to the concept of separating the structural and motor frequencies, it was decided to investigate the effect on structural frequency of varying the payload attach point. It was decided to use the lumped parameter model for this purpose due to its ease of representation of the branch points. This is discussed in Section 3.2.2.3.

The model used for this study was the Brazil configuration using exact mass and stiffness distributions. The time point considered was  $t = 6.0$  of sustainer burn time. The frequencies and mode shapes were obtained with the payload attached as follows:

| <u>Attach Point</u>                       | <u>Station of Attachment, in.</u> |
|---|-----------------------------------|
| Base                                      | -26.186                           |
| Midpoint<br>(The Brazil Flights as flown) | -63.75                            |
| Quarter Point                             | -78.25                            |
| Forward End                               | -89.38                            |

The lumped masses and stiffnesses used for this investigation are shown in Table 3-2 for base attachment, in Table 3-1 for midpoint attachment, in Table 3-4 for quarter point attachment, and in Table 3-3 for forward end attachment. The lumped mass configurations used for the foregoing are shown in Figures 3-11, 3-10, 3-12, and 3-13, respectively.

The frequencies obtained from the analysis are presented in Table 3-10. A plot of the fundamental frequency versus payload attach point is shown in Figure 3-32. The mode shapes obtained are presented in Figures 3-26, 3-27 and 3-28 for base attachment, and in Figures 3-29, 3-30, and 3-31 for forward end attachment.

It can be seen that attachment at the midpoint (as was the case for the Brazil flights) produces the highest frequency. This is also the most adverse attach point from the point of view of frequency separation. A decrease of 10 cps is obtained by attaching the payload at its base. By using an unconventional forward attach point the frequency may be reduced by 33 cps.



It can be concluded from this investigation that it is more favorable to attach payloads at their base than at their midpoint. Attachment at the forward end is even more favorable from a frequency point of view. However, such an attachment is not recommended since adverse effects from other aspects might exist due to such an unconventional arrangement. As is pointed out later, it was found that variation in payload longeron stiffness is probably the best way to achieve frequency separation.

### 3.2.3 STRUCTURAL LONGITUDINAL VIBRATION STABILITY LIMITS

#### 3.2.3.1 GENERAL DISCUSSION

Examination of the time histories of Figure 3-34 and the harmonic analysis of Brazil flights shown in Figures 3-40 and 3-41 tends to suggest that an adverse structural-motor fundamental mode resonant condition existed for these flights. These vibrations did not prove excessive, but they did result in somewhat less than an ideal smooth ride. It is conceivable that some future configuration could fall into a more severe resonant condition which could produce payload failure. This is borne out by the time histories of vehicle frequency for various payload weights and stiffnesses which are shown in Figures 3-35 and 3-36. It can be seen that certain of these configurations, using payload stiffnesses similar to the Brazil flights, indeed do fall closer to the motor frequency than did the Brazil flights. For these reasons, it would be desirable to know the structural vibrational stability limits of the various NIRO configurations normally flown. A knowledge of these limits would allow the payload designer to maintain a frequency separation between the motor and structural fundamentals which would preclude any adverse resonant conditions.

Frequency separation can be achieved by variation of the motor frequency and/or the structural frequency. Variation of the motor frequency is difficult and usually impractical since such variations often have adverse effects on desired performance characteristics. This leaves the structure as the frequency variable. Payload weight variation can be used to change the structural frequency. However, payload weight is dictated by mission requirements and restriction of this aspect would severely limit the versatility

of the rocket system. Therefore, variation of the payload stiffness and/or attach point seem to be the most practical ways to vary vehicle frequency. The variations obtained from different attachment configurations are discussed in Section 3.2.2.6. The variations due to payload stiffness are discussed herein. Vibrational stability limits are established in terms of payload weight and payload longeron stiffness.

### 3.2.3.2 ESTABLISHMENT OF THE STABILITY LIMITS

Pursuant to the goal of frequency separation it must be established how much of a separation is required. This may be determined from an examination of the flight records and of the time histories shown in Figure 3-34. The flight records indicate that the neutrally stable vibrations were first evident at about 4.5 seconds into sustainer burn. Burnout occurred at 7.75 seconds. Based on a theoretical burn time of 8.0 seconds, the adverse vibrations could be expected to start at 4.65 seconds. Examination of the time histories at 4.65 seconds indicate a structural-motor frequency separation of about 30 cps. For separations less than 30 cps it is assumed that adverse structural-motor excitation is possible. Therefore, structural stability limits of 240 cps  $\pm$ 30 cps can reasonably be assumed.

The stability limit calculations performed herein are based upon a simplified model using uniform mass and stiffness distributions. In Section 3.2.2.4 it was shown that there was a 20 cps variation in frequency between uniform distribution models and exact distribution models. Therefore, to make the stability limits more realistic an additional  $\pm$ 20 cps should be incorporated. This would result in limits of 290 cps on the high side and 190 cps on the low side. These were the limits which were used for the stability calculations herein.

Once the stability limits have been determined, it remains to determine the payload longeron stiffness which will keep the vehicle frequency time history out of the critical region of 240 cps  $\pm$ 50 cps. This is discussed in Section 3.2.3.5.

### 3.2.3.3 CONFIGURATIONS ANALYZED

The configurations analyzed for the stability analysis are shown in Figure 3-1. A summary of pertinent data is as follows:

| <u>Type</u> | <u>Diameter<br/>in.</u> | <u>Weight<br/>lb</u> | <u>Length<br/>in.</u> |
|-------------|-------------------------|----------------------|-----------------------|
| Standard    | 7.75                    | 140                  | 103.73                |
|             | 7.75                    | 100                  | 79.04                 |
|             | 7.75                    | 40                   | 42.00                 |
| Oversize    | 9.0                     | 180                  | 117.67                |
|             | 9.0                     | 140                  | 94.47                 |
|             | 9.0                     | 100                  | 71.26                 |

The above data were obtained from Reference 3-2. It should be noted that for each payload diameter a constant payload density is assumed. Therefore for each weight a characteristic length is established. These lengths are considered representative of real payloads. For example, the length of the 181 pound Brazil payload was 115.29 inches as compared to 117.67 inches for the 180 pound payload shown in the table.

The calculations did not include a payload recovery system per se. However, since the payload recovery system is included in payload weight and length, configurations employing it should be reasonable well covered by the conditions analyzed.

### 3.2.3.4 METHOD OF ANALYSIS

The frequencies for the stability analysis were obtained from a simplified three branch model employing an exact theoretical solution. The payload was attached at its base and uniform mass and stiffness distributions were assumed over each of the three branches. Since it was found that the acoustic branch had little effect on the structural frequencies it was not included in these calculations. The theoretical relationships for this simplified three branch beam are derived in the Appendix A to this report.

### 3.2.3.5 RESULTS OF THE ANALYSIS

#### 3.2.3.5.1 TIME HISTORIES FOR VARIOUS PAYLOAD WEIGHTS AND STIFFNESSES

In order to gain some understanding as to where various configurations fall with regard to the stability limits, it was decided to obtain fundamental frequency time histories for each of the configurations with four different values of payload stiffness. These stiffnesses were:

$$AE_1 = 5 \times 10^6 \text{ lb}$$

$$AE_2 = 15 \times 10^6 \text{ lb}$$

$$AE_3 = 45 \times 10^6 \text{ lb}$$

$$AE_4 = \infty \text{ (Rigid)}$$

The time histories obtained for the various configurations are shown in Figures 3-35 and 3-36. When examining this data it should be kept in mind that an  $AE = 15 \times 10^6 \text{ lb}$  is representative of the stiffness actually flown on the Brazil flights. It can be seen that several configurations with this stiffness fall closer to the motor frequency than did the Brazil flights. Also a large number of the configurations fall at least partially in the critical region between 190 cps and 290 cps.

#### 3.2.3.5.2 STRUCTURAL VIBRATIONAL STABILITY LIMITS

The structural vibrational stability limits may be defined as the stiffnesses for each payload weight which cause the entire time history to fall either entirely above or entirely below the critical region of 190 cps to 290 cps. Examination of the time histories in Figures 3-35 and 3-36 shows that these limits may be obtained by cross plotting stiffness versus frequency for each of the weights at burnout and at ignition. The stiffnesses obtained in this manner at 290 cps for  $t = 0$  seconds establish the upper limit and the stiffnesses obtained at 190 cps for  $t = 8$  seconds establish the lower limit.

Stiffnesses between these two points represent unstable values while all other stiffnesses outside these limits represent stable values.

It can be seen from the time histories that the upper limit of stability cannot be surpassed for certain of the configurations, even with an infinitely stiff payload. In these cases a limiting weight may be established, beyond which it is not possible to achieve stability by stiffening the payload. This may be determined by plotting weight versus frequency for the infinitely stiff cases. The weight at 290 cps represents this limit. It can also be seen that in all cases stability may always be achieved by reducing the payload stiffness.

The stability limits obtained in the manner described are presented in Figure 3-37 in terms of payload longeron stiffness versus payload weight for 9.0-inch and 7.75-inch diameter payloads. The limiting weight beyond which stability may not be achieved by payload stiffening is 110 pounds for both 9.0-inch and 7.75-inch payloads. This is shown on the figure. It can be seen that for the lighter 7.75-inch payloads that stability may be readily achieved by stiffening the longerons. In the case of the heavier payloads complete assurance of stability may only be accomplished by making the payload less stiff. This has several adverse implications which will be mentioned in Section 3.2.3.5.3.

### 3.2.3.5.3 APPLICATION OF THE RESULTS

Figure 3-37 provides the payload designer with a tool which he may use to minimize adverse longitudinal vibrations for NIRO configurations by means of payload stiffness adjustments. It should be kept in mind, considering all of the assumptions discussed herein, that this tool should be considered as a general guideline rather than an absolute authority.

It is expected, due to any number of considerations, that longeron stiffnesses will often be chosen which fall into the unstable region. When this happens, the time histories of Figures 3-35 and 3-36 may be consulted to provide some indication as to the severity of the stiffness chosen. Also, when using the data in Figure 3-37, it should be remembered that a value of  $AE = 15 \times 10^6$  pound is representative of current values of payload stiffness.

It should be cautioned that reduction in longeron stiffnesses from values currently in use might have several adverse implications. Reduction of longitudinal stiffness, for example, also reduces the bending stiffness, which might lead to handling difficulties. Higher payload deflections in the longitudinal direction due to any disturbance may be expected for the case of reduced longeron stiffness. One such disturbance which could prove troublesome in this regard is the motor start-up transient which could impose a severe shock load on the payload with resulting adverse deflection magnitude.

#### 3.2.3.5.4 ACCURACIES INVOLVED

The accuracies involved in the stability calculations have been mentioned elsewhere in this report in several different sections. For convenience they will be summarized here as follows:

|    | <u>Item</u>   | <u>Accuracy</u> |
|----|---|-----------------|
| a. | Motor fundamental frequency   | <u>+6</u> cps   |
| b. | Structural fundamental frequency                                      | <u>+2</u> cps   |
| c. | Difference between exact and uniform mass and stiffness distributions | <u>+20</u> cps  |

#### 3.3 CONCLUSIONS

The conclusions which may be drawn from the analysis presented herein may summarized as follows:

- a. The adverse longitudinal vibrations noted on NIRO Brazil flights 7.314 and 7.316 were apparently divergent in nature.
- b. Evidence points to the fact that the adverse vibrations of (a) were due to fundamental mode structural-motor resonance.
- c. A reduction of vibration levels in future NIRO flights is possible by using longeron stiffnesses which keep the vehicle structural frequency adequately separated from the motor frequency. Data are presented herein as guidelines for this purpose.
- d. If frequency reduction is required to separate the structural-motor frequencies due caution should be observed with regard to the consequences of such a reduction.



### 3.4 RECOMMENDATIONS

The following recommendations are presented as a result of the information determined from this analysis.

- a. Payload stiffnesses for future NIRO payloads should be determined using the stiffness data presented herein as guidelines.
- b. One or more flights, whose payloads have been designed according to the stiffness guidelines, should be instrumented to verify the results presented herein.
- c. Further analysis should be performed to determine the frequency characteristics of payloads which are divided into two or more separate branches. These types of payloads are generally more typical of actual payloads than the ones analyzed in this report and therefore should be examined.
- d. Further calculations to determine the effect of the open nozzle on the acoustic frequencies should be made.

## REFERENCES

- 3-1 Maun, E. K., Dr.; Arnold, R. P.; "NIRO Vehicle Dynamics Analysis," Space-General Corp., Report No. SGC 497R-3; Jan. 1965.
- 3-2 Taylor, J. P.; Arnold, R. P.; "Aerodynamics and Flight Performance Analysis for the NIRO Sounding Rocket," Space-General Corp., Scientific Report No. 1; March, 1966.
- 3-3 Mallick, J.; "Monthly Report #29 on Contract AF 19(628)-1634 for "Study Means of Minimizing Outgassing from Solid Propellant Rocket Motors," Letter from Thiokol Chemical Corp., Elkton Div. to Mr. C. Hault, AFCRL, Bedford, Mass., November 17, 1964.
- 3-4 "Mathematical Methods for Digital Computer," John Wiley & Sons, New York, 1960.
- 3-5 Kaplan, M. A.; Faulkner, P.H.; "Determination of the Eigenvalues and Eigenvectors of Lumped Parameter System by the Jacobi Method; Structural Dynamics Program D-10," Space-General Corp. Report No. SGC SR-13, 1 November 1962.
- 3-6 Den Hartog, J. P.; "Mechanical Vibrations," McGraw-Hill Book Co., Inc., New York and London, 1947.

Table 3-1

NIRO

Flight 7.314

LUMPED MASSES AND STIFFNESSES  
 Payload Cantilevered at Midpoint as Flown

| Type                          | Designation | Coordinate<br>in. | Weight<br>lb | Stiffness<br>lb/in   |
|-------------------------------|-------------|-------------------|--------------|----------------------|
| FORWARD<br>FAIRING<br>BRANCH  | 1           | -107.395          | 1.613        | $2.118 \times 10^6$  |
|                               | 2           | -98.430           | 2.198        | $7.019 \times 10^6$  |
|                               | 3           | -93.803           | 7.945        | $28.398 \times 10^6$ |
|                               | 4           | -89.683           | 4.384        | $11.118 \times 10^6$ |
|                               | 5           | -84.700           | 2.637        | $6.543 \times 10^6$  |
|                               | 6           | -78.250           | 2.678        | $6.029 \times 10^6$  |
|                               | 7           | -71.250           | 3.090        | $5.553 \times 10^6$  |
| FORWARD<br>INTERNAL<br>BRANCH | 8           | -89.38            | 14.09        | $1.825 \times 10^6$  |
|                               | 9           | -81.27            | 11.91        | $1.973 \times 10^6$  |
|                               | 10          | -73.77            | 11.64        | $2.136 \times 10^6$  |
|                               | 11          | -66.84            | 9.62         | $4.639 \times 10^6$  |
| AFT<br>INTERNAL<br>BRANCH     | 12          | -29.32            | 8.30         | $2.129 \times 10^6$  |
|                               | 13          | -36.27            | 9.99         | $1.971 \times 10^6$  |
|                               | 14          | -43.78            | 10.31        | $1.976 \times 10^6$  |
|                               | 15          | -51.27            | 10.61        | $1.829 \times 10^6$  |
|                               | 16          | -59.36            | 12.67        | $3.450 \times 10^6$  |
| FAIRING AFT<br>BRANCH         | 17          | -63.75            | 3.090        | $5.703 \times 10^6$  |
|                               | 18          | -56.25            | 3.090        | $5.627 \times 10^6$  |
|                               | 19          | -48.75            | 3.090        | $5.627 \times 10^6$  |
|                               | 20          | -41.25            | 3.090        | $6.161 \times 10^6$  |
|                               | 21          | -34.40            | 2.554        | $12.007 \times 10^6$ |
|                               | 22          | -29.786           | 4.380        | $29.175 \times 10^6$ |
|                               | 23          | -26.187           | 3.849        | $7.393 \times 10^6$  |
|                               | 24          | -19.80            | 13.680       | $4.550 \times 10^6$  |
|                               | 25          | -11.25            | 10.680       | $5.187 \times 10^6$  |
|                               | 26          | -3.75             | 10.680       | $6.098 \times 10^6$  |

See Figure 3-10 for Diagram

Table 3-1 - contd.

NIRO

Flight 7.314

LUMPED MASSES AND STIFFNESSES

| Type                                | Designation | Coordinate<br>in. | Weight<br>lb | Stiffness<br>lb/in   |
|-------------------------------------|-------------|-------------------|--------------|----------------------|
| SUSTAINER AFT BRANCH<br>(t = 0 sec) | 27          | 2.96              | 22.89        | $4.845 \times 10^6$  |
|                                     | 28          | 12.00             | 25.2         | $5.006 \times 10^6$  |
|                                     | 29          | 20.75             | 21.68        | $4.735 \times 10^6$  |
|                                     | 30          | 30.00             | 25.5         | $4.380 \times 10^6$  |
|                                     | 31          | 40.00             | 25.5         | $4.380 \times 10^6$  |
|                                     | 32          | 50.00             | 25.5         | $4.380 \times 10^6$  |
|                                     | 33          | 60.00             | 25.5         | $4.380 \times 10^6$  |
|                                     | 34          | 70.00             | 25.5         | $4.867 \times 10^6$  |
|                                     | 35          | 79.00             | 20.4         | $7.169 \times 10^6$  |
|                                     | 36          | 85.11             | 19.90        | $12.550 \times 10^6$ |
|                                     | 37          | 88.60             | 12.90        | $9.419 \times 10^6$  |
|                                     | 38          | 93.25             | 14.63        | $6.738 \times 10^6$  |
| 39                                  | 99.75       | 14.63             | ---          |                      |

Table 3-1 - contd.

NIRO

Flight 7.314

LUMPED MASSES AND STIFFNESSES

| Type                                  | Designation | Coordinate<br>in. | Weight<br>lb | Stiffness<br>lb/in   |
|---------------------------------------|-------------|-------------------|--------------|----------------------|
| SUSTAINER AFT BRANCH<br>(t = 4.0 sec) | 27          | 2.96              | 15.87        | $4.845 \times 10^6$  |
|                                       | 28          | 12.00             | 16.74        | $5.006 \times 10^6$  |
|                                       | 29          | 20.75             | 13.60        | $4.735 \times 10^6$  |
|                                       | 30          | 30.00             | 16.0         | $4.380 \times 10^6$  |
|                                       | 31          | 40.00             | 16.0         | $4.380 \times 10^6$  |
|                                       | 32          | 50.00             | 16.0         | $4.380 \times 10^6$  |
|                                       | 33          | 60.00             | 16.0         | $4.380 \times 10^6$  |
|                                       | 34          | 70.00             | 16.0         | $4.867 \times 10^6$  |
|                                       | 35          | 79.00             | 12.8         | $7.169 \times 10^6$  |
|                                       | 36          | 85.11             | 16.87        | $12.550 \times 10^6$ |
|                                       | 37          | 88.60             | 12.60        | $9.419 \times 10^6$  |
|                                       | 38          | 93.25             | 14.63        | $6.738 \times 10^6$  |
|                                       | 39          | 99.75             | 14.63        | ---                  |

Table 3-1 - contd.

NIRO

Flight 7.314

LUMPED MASSES AND STIFFNESSES

| Type                                     | Designation | Coordinate<br>in. | Weight<br>lb | Stiffness<br>lb/in   |
|--|-------------|-------------------|--------------|----------------------|
| SUSTAINER<br>AFT BRANCH<br>(t = 6.0 sec) | 27          | 2.96              | 11.54        | $4.845 \times 10^6$  |
|  | 28          | 12.00             | 11.52        | $5.006 \times 10^6$  |
|  | 29          | 20.75             | 8.75         | $4.735 \times 10^6$  |
|  | 30          | 30.00             | 10.03        | $4.380 \times 10^6$  |
|  | 31          | 40.00             | 10.03        | $4.380 \times 10^6$  |
|  | 32          | 50.00             | 10.03        | $4.380 \times 10^6$  |
|  | 33          | 60.00             | 10.03        | $4.380 \times 10^6$  |
|  | 34          | 70.00             | 10.03        | $4.867 \times 10^6$  |
|  | 35          | 79.00             | 10.03        | $7.169 \times 10^6$  |
|  | 36          | 85.11             | 18.56        | $12.550 \times 10^6$ |
|  | 37          | 88.60             | 11.45        | $9.419 \times 10^6$  |
|  | 38          | 93.25             | 14.63        | $6.738 \times 10^6$  |
|  | 39          | 99.75             | 14.63        | ---                  |



Table 3-1 - concluded

NIRO

Flight 7.314

LUMPED MASSES AND STIFFNESSES

| Type   | Designation | Coordinate<br>in. | Weight<br>lb        | Stiffness<br>lb/in   |
|--|-------------|-------------------|---------------------|----------------------|
| SUSTAINER AFT BRANCH<br>(t = 8.0 sec, Burnout) | 27          | 2.96              | 7.32                | $4.845 \times 10^6$  |
|  | 28          | 12.00             | 6.48                | $5.006 \times 10^6$  |
|  | 29          | 20.75             | 3.825               | $4.735 \times 10^6$  |
|  | 30          | 30.00             | 4.500               | $4.380 \times 10^6$  |
|  | 31          | 40.00             | 4.500               | $4.380 \times 10^6$  |
|  | 32          | 50.00             | 4.500               | $4.380 \times 10^6$  |
|  | 33          | 60.00             | 4.500               | $4.380 \times 10^6$  |
|  | 34          | 70.00             | 4.500               | $4.867 \times 10^6$  |
|  | 35          | 79.00             | 3.600               | $7.169 \times 10^6$  |
|  | 36          | 85.11             | 11.705              | $12.550 \times 10^6$ |
|  | 37          | 88.60             | 10.875              | $9.419 \times 10^6$  |
| 38   | 93.25       | 14.630            | $6.738 \times 10^6$ |                      |
| 39   | 99.75       | 14.630            | ---                 |                      |

LUMPED MASSES AND STIFFNESSES  
 FLIGHT 7.314 PAYLOAD CANTILEVERED FROM THE BASE

$$t = 6.0 \text{ sec}$$

| Type                       | Designation                                   | Coordinate<br>in. | Weight<br>lb | Stiffness<br>lb/in.  |
|----------------------------|---|-------------------|--------------|----------------------|
| FAIRING BRANCH             | 1   | -107.395          | 1.613        | $2.118 \times 10^6$  |
|                            | 2   | - 98.430          | 2.198        | $7.019 \times 10^6$  |
|                            | 3   | - 93.803          | 7.945        | $28.398 \times 10^6$ |
|                            | 4   | - 89.683          | 4.384        | $11.118 \times 10^6$ |
|                            | 5   | - 84.700          | 2.637        | $6.543 \times 10^6$  |
|                            | 6   | - 78.250          | 2.678        | $6.029 \times 10^6$  |
|                            | 7   | - 71.250          | 3.090        | $5.553 \times 10^6$  |
|                            | 8   | - 63.750          | 3.090        | $5.703 \times 10^6$  |
|                            | 9   | - 56.25           | 3.090        | $5.627 \times 10^6$  |
|                            | 10  | - 48.75           | 3.090        | $5.627 \times 10^6$  |
|                            | 11  | - 41.25           | 3.090        | $6.161 \times 10^6$  |
|                            | 12  | - 34.40           | 2.554        | $12.007 \times 10^6$ |
|                            | 13  | - 29.786          | 4.380        | $29.175 \times 10^6$ |
| INTERNAL<br>PAYLOAD BRANCH | 14  | - 89.38           | 14.09        | $1.825 \times 10^6$  |
|                            | 15  | - 81.27           | 11.91        | $1.973 \times 10^6$  |
|                            | 16  | - 73.77           | 11.64        | $2.136 \times 10^6$  |
|                            | 17  | - 66.84           | 9.62         | $1.980 \times 10^6$  |
|                            | 18  | - 59.36           | 12.67        | $1.829 \times 10^6$  |
|                            | 19  | - 51.27           | 10.61        | $1.976 \times 10^6$  |
|                            | 20  | - 43.78           | 10.31        | $1.971 \times 10^6$  |
|                            | 21  | - 36.27           | 9.99         | $2.129 \times 10^6$  |
|                            | 22  | - 29.32           | 8.30         | $4.72 \times 10^6$   |
|                            | SUSTAINER BRANCH<br>( $t = 6.0 \text{ sec}$ ) | 23                | - 26.187     | 3.849                |
| 24                         |   | - 19.80           | 13.680       | $4.550 \times 10^6$  |
| 25                         |   | - 11.25           | 10.680       | $5.187 \times 10^6$  |
| 26                         |   | - 3.75            | 10.680       | $6.098 \times 10^6$  |
| 27                         |   | 2.96              | 11.54        | $4.845 \times 10^6$  |
| 28                         |   | 12.00             | 11.32        | $5.006 \times 10^6$  |
| 29                         |   | 20.75             | 8.75         | $4.735 \times 10^6$  |
| 30                         |   | 30.00             | 10.03        | $4.380 \times 10^6$  |
| 31                         |   | 40.00             | 10.03        | $4.380 \times 10^6$  |
| 32                         |   | 50.00             | 10.03        | $4.380 \times 10^6$  |
| 33                         |   | 60.00             | 10.03        | $4.380 \times 10^6$  |
| 34                         |   | 70.00             | 10.03        | $4.867 \times 10^6$  |
| 35                         |   | 79.00             | 10.03        | $7.169 \times 10^6$  |
| 36                         |   | 85.11             | 18.96        | $12.550 \times 10^6$ |
| 37                         |   | 88.60             | 11.45        | $9.419 \times 10^6$  |
| 38                         |   | 93.25             | 14.63        | $6.738 \times 10^6$  |
| 39                         |   | 99.75             | 14.63        | -                    |

See Figure 3-11 for Diagram

Table 3-3

NIRO

LUMPED MASSES AND STIFFNESSES

FLIGHT 7.314 PAYLOAD CANTILEVERED FROM NOSE

t = 6.0 sec

| TYPE                       | DESIGNATION | COORDINATE<br>in. | WEIGHT<br>lb | STIFFNESS<br>lb/in   |
|----------------------------|-------------|-------------------|--------------|----------------------|
| FORWARD<br>BRANCH          | 1           | -107.395          | 1.613        | $2.118 \times 10^6$  |
|                            | 2           | - 98.430          | 2.198        | $7.019 \times 10^6$  |
|                            | 3           | - 93.803          | 7.945        | $28.398 \times 10^6$ |
| INTERNAL<br>PAYLOAD BRANCH | 4           | - 29.32           | 8.30         | $2.129 \times 10^6$  |
|                            | 5           | - 36.27           | 9.99         | $1.971 \times 10^6$  |
|                            | 6           | - 43.78           | 10.31        | $1.976 \times 10^6$  |
|                            | 7           | - 51.27           | 10.61        | $1.829 \times 10^6$  |
|                            | 8           | - 59.36           | 12.67        | $1.980 \times 10^6$  |
|                            | 9           | - 66.84           | 9.62         | $2.136 \times 10^6$  |
|                            | 10          | - 73.77           | 11.64        | $1.973 \times 10^6$  |
|                            | 11          | - 81.27           | 11.91        | $1.825 \times 10^6$  |
|                            | 12          | - 89.38           | 14.09        | $50.512 \times 10^6$ |
|                            | AFT BRANCH  | 13                | - 89.683     | 4.384                |
| 14                         |             | - 84.700          | 2.637        | $6.543 \times 10^6$  |
| 15                         |             | - 78.250          | 2.678        | $6.029 \times 10^6$  |
| 16                         |             | - 71.250          | 3.090        | $5.553 \times 10^6$  |
| 17                         |             | - 63.750          | 3.090        | $5.703 \times 10^6$  |
| 18                         |             | - 56.250          | 3.090        | $5.627 \times 10^6$  |
| 19                         |             | - 48.750          | 3.090        | $5.627 \times 10^6$  |
| 20                         |             | - 41.250          | 3.090        | $6.161 \times 10^6$  |
| 21                         |             | - 34.40           | 2.554        | $12.007 \times 10^6$ |
| 22                         |             | - 29.786          | 4.380        | $29.175 \times 10^6$ |
| 23                         |             | - 26.187          | 3.849        | $7.393 \times 10^6$  |
| 24                         |             | - 19.80           | 13.680       | $4.550 \times 10^6$  |
| 25                         |             | - 11.25           | 10.680       | $5.187 \times 10^6$  |
| 26                         |             | - 3.75            | 10.680       | $6.098 \times 10^6$  |
| 27                         |             | 2.96              | 11.54        | $4.845 \times 10^6$  |
| 28                         |             | 12.00             | 11.32        | $5.006 \times 10^6$  |
| 29                         |             | 20.75             | 8.75         | $4.735 \times 10^6$  |
| 30                         |             | 30.00             | 10.03        | $4.380 \times 10^6$  |
| 31                         |             | 40.00             | 10.03        | $4.380 \times 10^6$  |
| 32                         |             | 50.00             | 10.03        | $4.380 \times 10^6$  |
| 33                         |             | 60.00             | 10.03        | $4.380 \times 10^6$  |
| 34                         |             | 70.00             | 10.03        | $4.867 \times 10^6$  |
| 35                         |             | 79.00             | 10.03        | $7.169 \times 10^6$  |
| 36                         |             | 85.11             | 18.96        | $12.550 \times 10^6$ |
| 37                         |             | 88.60             | 11.95        | $9.419 \times 10^6$  |
| 38                         |             | 93.25             | 14.63        | $6.738 \times 10^6$  |
| 39                         |             | 99.75             | 14.63        | ----                 |

See Figure 3-13 for Diagram

Table 3-4

NIRO

## LUMPED MASSES AND STIFFNESSES

Flight 7.314 Payload Cantilevered at Quarter Point

t = 6.0 sec

| Type  | Designation | Coordinate<br>in. | Weight<br>lb | Stiffness<br>lb/in   |
|---|-------------|-------------------|--------------|----------------------|
| FORWARD<br>FAIRING<br>BRANCH                    | 1           | -107.395          | 1.613        | $2.118 \times 10^6$  |
|   | 2           | - 98.430          | 2.198        | $7.019 \times 10^6$  |
|   | 3           | - 93.803          | 7.945        | $28.398 \times 10^6$ |
|   | 4           | - 89.683          | 4.384        | $11.118 \times 10^6$ |
|   | 5           | - 84.700          | 2.637        | $6.543 \times 10^6$  |
| FORWARD<br>INTERNAL<br>BRANCH                   | 6           | - 89.38           | 14.09        | $1.825 \times 10^6$  |
|   | 7           | - 81.27           | 11.91        | $4.900 \times 10^6$  |
| INTERNAL<br>BRANCH                              | 8           | - 29.32           | 8.30         | $2.129 \times 10^6$  |
|   | 9           | - 36.27           | 9.99         | $1.971 \times 10^6$  |
|   | 10          | - 43.78           | 10.31        | $1.976 \times 10^6$  |
|   | 11          | - 51.27           | 10.61        | $1.829 \times 10^6$  |
|   | 12          | - 59.36           | 12.67        | $1.980 \times 10^6$  |
|   | 13          | - 66.84           | 9.62         | $2.136 \times 10^6$  |
|   | 14          | - 73.77           | 11.69        | $3.400 \times 10^6$  |
| AFT FAIRING AND SUSTAINER BRANCH<br>t = 6.0 sec | 15          | - 78.25           | 2.678        | $6.029 \times 10^6$  |
|   | 16          | - 71.25           | 3.050        | $5.553 \times 10^6$  |
|   | 17          | - 63.75           | 3.050        | $5.703 \times 10^6$  |
|   | 18          | - 56.25           | 3.090        | $5.627 \times 10^6$  |
|   | 19          | - 48.75           | 3.090        | $5.627 \times 10^6$  |
|   | 20          | - 41.25           | 3.090        | $6.161 \times 10^6$  |
|   | 21          | - 34.40           | 2.554        | $12.007 \times 10^6$ |
|   | 22          | - 29.786          | 4.380        | $29.179 \times 10^6$ |
|   | 23          | - 26.187          | 3.849        | $7.393 \times 10^6$  |
|   | 24          | - 19.800          | 13.680       | $4.550 \times 10^6$  |
|   | 25          | - 11.25           | 10.680       | $5.187 \times 10^6$  |
|   | 26          | - 3.75            | 10.680       | $6.098 \times 10^6$  |
|   | 27          | 2.96              | 11.540       | $4.845 \times 10^6$  |
|   | 28          | 12.00             | 11.32        | $5.006 \times 10^6$  |
|   | 29          | 20.75             | 8.75         | $4.735 \times 10^6$  |
|   | 30          | 30.00             | 10.03        | $4.380 \times 10^6$  |
|   | 31          | 40.00             | 10.03        | $4.380 \times 10^6$  |
|   | 32          | 50.00             | 10.03        | $4.380 \times 10^6$  |
|   | 33          | 60.00             | 10.03        | $4.380 \times 10^6$  |
|   | 34          | 70.00             | 10.03        | $4.867 \times 10^6$  |
|   | 35          | 79.00             | 10.03        | $7.169 \times 10^6$  |
|   | 36          | 85.11             | 18.96        | $12.550 \times 10^6$ |
|   | 37          | 88.60             | 11.45        | $9.419 \times 10^6$  |
|   | 38          | 93.25             | 14.63        | $6.738 \times 10^6$  |
|   | 39          | 99.75             | 14.63        | ---                  |

See Figure 3-12 for Diagram

Table 3-5

NIRO

LUMPED MASSES AND STIFFNESS  
UNIFORMLY DISTRIBUTED OVER EACH OF THREE BRANCHES

These Values were used to Check Exact Solution  
Payload Cantilevered at Base as in Figure 3-11

$$t = 6.0 \text{ sec}$$

| TYPE                       | DESIGNATION                           | COORDINATE<br>in. | WEIGHT<br>lb | STIFFNESS<br>lb/in   |
|----------------------------|---------------------------------------|-------------------|--------------|----------------------|
| FAIRING BRANCH             | 1                                     | -108.875          | 5.10         | $4.444 \times 10^6$  |
|                            | 2                                     | - 98.75           | 3.00         | $8.182 \times 10^6$  |
|                            | 3                                     | - 93.25           | 1.40         | $12.676 \times 10^6$ |
|                            | 4                                     | - 89.70           | 1.44         | $9.000 \times 10^6$  |
|                            | 5                                     | - 84.70           | 2.56         | $6.977 \times 10^6$  |
|                            | 6                                     | - 78.25           | 2.60         | $6.429 \times 10^6$  |
|                            | 7                                     | - 71.25           | 3.00         | $6.000 \times 10^6$  |
|                            | 8                                     | - 63.25           | 3.00         | $6.000 \times 10^6$  |
|                            | 9                                     | - 56.25           | 3.00         | $6.000 \times 10^6$  |
|                            | 10                                    | - 48.75           | 3.00         | $6.000 \times 10^6$  |
|                            | 11                                    | - 41.25           | 3.00         | $6.569 \times 10^6$  |
|                            | 12                                    | - 34.40           | 2.48         | $9.474 \times 10^6$  |
|                            | 13                                    | - 29.65           | 1.32         | $13.433 \times 10^6$ |
| INTERNAL PAYLOAD<br>BRANCH | 14                                    | - 89.35           | 12.18        | $1.852 \times 10^6$  |
|                            | 15                                    | - 81.25           | 10.50        | $2.000 \times 10^6$  |
|                            | 16                                    | - 73.75           | 10.50        | $2.166 \times 10^6$  |
|                            | 17                                    | - 66.825          | 8.89         | $2.000 \times 10^6$  |
|                            | 18                                    | - 59.325          | 12.11        | $1.858 \times 10^6$  |
|                            | 19                                    | - 51.25           | 10.50        | $2.000 \times 10^6$  |
|                            | 20                                    | - 43.75           | 10.50        | $2.000 \times 10^6$  |
|                            | 21                                    | - 36.25           | 10.50        | $2.158 \times 10^6$  |
|                            | 22                                    | - 29.30           | 9.10         | $5.000 \times 10^6$  |
|                            | SUSTAINER AFT BRANCH<br>(t = 6.0 sec) | 23                | - 26.30      | 1.36                 |
| 24                         |                                       | - 19.80           | 3.84         | $5.263 \times 10^6$  |
| 25                         |                                       | - 11.25           | 3.00         | $6.000 \times 10^6$  |
| 26                         |                                       | - 3.75            | 3.00         | $6.000 \times 10^6$  |
| 27                         |                                       | 3.75              | 10.58        | $5.455 \times 10^6$  |
| 28                         |                                       | 12.00             | 12.69        | $5.143 \times 10^6$  |
| 29                         |                                       | 20.79             | 11.99        | $4.865 \times 10^6$  |
| 30                         |                                       | 30.00             | 14.10        | $4.500 \times 10^6$  |
| 31                         |                                       | 40.00             | 14.10        | $4.500 \times 10^6$  |
| 32                         |                                       | 50.00             | 14.10        | $4.500 \times 10^6$  |
| 33                         |                                       | 60.00             | 14.10        | $4.500 \times 10^6$  |
| 34                         |                                       | 70.00             | 14.10        | $5.000 \times 10^6$  |
| 35                         |                                       | 79.00             | 11.28        | $7.500 \times 10^6$  |
| 36                         |                                       | 85.00             | 5.64         | $12.857 \times 10^6$ |
| 37                         |                                       | 88.50             | 4.23         | $9.474 \times 10^6$  |
| 38                         |                                       | 93.25             | 9.17         | $6.923 \times 10^6$  |
| 39                         |                                       | 99.75             | 9.17         | ---                  |

Table 3-6  
 NIRO  
 LUMPED MASSES AND STIFFNESSES  
 ACOUSTIC BRANCH OF SUSTAINER

| Type                           | Designation | Coordinate<br>in. | Weight<br>lb | Stiffness<br>lb/in |
|--------------------------------|-------------|-------------------|--------------|--------------------|
| ACOUSTIC BRANCH<br>t = 0 sec   | 39          | -                 | -            | 1930               |
|                                | 40          | 5                 | .0083        | 386                |
|                                | 41          | 15                | .0083        | 386                |
|                                | 42          | 25                | .0083        | 386                |
|                                | 43          | 35                | .0083        | 386                |
|                                | 44          | 45                | .0083        | 386                |
|                                | 45          | 55                | .0083        | 386                |
|                                | 46          | 65                | .0083        | 386                |
|                                | 47          | 75                | .0083        | 424                |
|                                | 48          | 84.075            | .00675       | 850                |
| ACOUSTIC BRANCH<br>t = 4.0 sec | 39          | -                 | -            | 8280               |
|                                | 40          | 5                 | .0357        | 1655               |
|                                | 41          | 15                | .0357        | 1655               |
|                                | 42          | 25                | .0357        | 1655               |
|                                | 43          | 35                | .0357        | 1655               |
|                                | 44          | 45                | .0357        | 1655               |
|                                | 45          | 55                | .0357        | 1655               |
|                                | 46          | 65                | .0357        | 1655               |
|                                | 47          | 75                | .0357        | 1825               |
|                                | 48          | 84.075            | .0291        | 3650               |
| ACOUSTIC BRANCH<br>t = 6.0 sec | 39          | -                 | -            | 13600              |
|                                | 40          | 5                 | .0585        | 2720               |
|                                | 41          | 15                | .0585        | 2720               |
|                                | 42          | 25                | .0585        | 2720               |
|                                | 43          | 35                | .0585        | 2720               |
|                                | 44          | 45                | .0585        | 2720               |
|                                | 45          | 55                | .0585        | 2720               |
|                                | 46          | 65                | .0585        | 2720               |
|                                | 47          | 75                | .0585        | 2997               |
|                                | 48          | 84.075            | .04767       | 6000               |
| ACOUSTIC BRANCH<br>t = 8.0 sec | 39          | -                 | -            | 18650              |
|                                | 40          | 5                 | .0800        | 3730               |
|                                | 41          | 15                | .0800        | 3730               |
|                                | 42          | 25                | .0800        | 3730               |
|                                | 43          | 35                | .0800        | 3730               |
|                                | 44          | 45                | .0800        | 3730               |
|                                | 45          | 55                | .0800        | 3730               |
|                                | 46          | 65                | .0800        | 3730               |
|                                | 47          | 75                | .0800        | 4110               |
|                                | 48          | 84.075            | .0653        | 8230               |

Note: See Figure 3-14 for Diagram



Table 3-7

NIRO

BRAZIL FLIGHT 7.314

LONGITUDINAL MODAL NATURAL FREQUENCIES

Payload Weight = 181 lb

No Acoustics Included

Payload Attached at Midpoint as Flown

| Mode Number | MODAL NATURAL FREQUENCIES, cps |           |           |                        |
|-------------|--------------------------------|-----------|-----------|------------------------|
|             | t = 0 sec<br>(Ignition)        | t = 4 sec | t = 6 sec | t = 8 sec<br>(Burnout) |
| 1           | 199                            | 212       | 220       | 242                    |
| 2           | 403                            | 440       | 453       | 457                    |
| 3           | 462                            | 467       | 482       | 516                    |
| 4           | 646                            | 674       | 687       | 720                    |
| 5           | 730                            | 807       | 883       | 1060                   |
| 6           | 972                            | 1085      | 1130      | 1155                   |
| 7           | 1135                           | 1165      | 1260      | 1345                   |
| 8           | 1240                           | 1342      | 1345      | 1523                   |
| 9           | 1345                           | 1435      | 1600      | 1730                   |
| 10          | 1500                           | 1690      | 1720      | 1943                   |



Table 3-8

NIRO

Brazil Flight 7.314

LONGITUDINAL MODAL NATURAL FREQUENCIES

Payload Weight = 181 lb

Payload Attached at Midpoint as Flown

Acoustic Contribution Included

| Mode Number | MODAL NATURAL FREQUENCIES, cps |           |           |           |
|-------------|--------------------------------|-----------|-----------|-----------|
|             | t = 0 sec                      | t = 4 sec | t = 6 sec | t = 8 sec |
| 1           | 199                            | 211       | 220       | 239       |
| 2           | 246                            | 246       | 247       | 250       |
| 3           | 403                            | 440       | 453       | 457       |
| 4           | 462                            | 466       | 489       | 521       |
| 5           | 484                            | 484       | 479       | 483       |
| 6           | 646                            | 671       | 689       | 711       |
| 7           | 706                            | 705       | 706       | 707       |
| 8           | 739                            | 806       | 885       | 1058      |
| 9           | 907                            | 906       | 907       | 908       |
| 10          | 973                            | 1092      | 1122      | 1148      |
| 11          | 1080                           | 1078      | 1080      | 1081      |

Table 3-9

NIRO

COMPARISON OF EXACT THEORY AND LUMPED PARAMETER RESULTS  
WITH AND WITHOUT ACOUSTICS

Uniform Mass and Stiffness Distributions  
Payload Attached at Base

$t = 6.0$  sec

| Mode Number | LONGITUDINAL FREQUENCY, cps |                |                  |                |
|-------------|-----------------------------|----------------|------------------|----------------|
|             | EXACT THEORY                |                | LUMPED PARAMETER |                |
|             | No Acoustics                | With Acoustics | No Acoustics     | With Acoustics |
| 1           | 231                         | 230.4          | 229              | 228            |
| 2*          | -                           | 241.5          | -                | 247            |
| 3           | 379                         | 378.0          | 392              | 392            |
| 4*          | -                           | 481.8          | -                | 484            |
| 5           | 620                         | 619.2          | 635              | 635            |
| 6           | 700                         | 699.96         | 690              | 689            |
| 7*          | -                           | 722.73         | -                | 706            |

\* Denotes a mode which is primarily acoustic in nature.

Note: The Acoustic Branch for the Exact Theory Model was 88" in length and equal to the exact motor length. The Acoustic Branch for the Lumped Parameter Model was only 85" in length. This would account for the slightly higher acoustic frequencies obtained from the Lumped Parameter Model.

Table 3-10

LONGITUDINAL FREQUENCIES FOR VARIOUS PAYLOAD ATTACH POINTS

Flight 7.314 Payload = 181 lb

t = 6.0 sec

No Acoustics Included

| Mode Number | FREQUENCY, cps |          |               |         |
|-------------|----------------|----------|---------------|---------|
|             | Base           | Midpoint | Quarter Point | Forward |
| 1           | 210            | 220      | 204           | 187     |
| 2           | 338            | 453      | 388           | 362     |
| 3           | 574            | 482      | 526           | 529     |
| 4           | 664            | 687      | 853           | 789     |
| 5           | 890            | 883      | 905           | 890     |
| 6           | 1099           | 1130     | 1108          | 1199    |
| 7           | 1270           | 1260     | 1241          | 1268    |
| 8           | 1504           | 1345     | 1461          | 1564    |
| 9           | 1598           | 1600     | 1579          | 1641    |
| 10          | 1842           | 1720     | 1794          | 1823    |

Base @ Station - 26.187

Midpoint @ Station - 63.75

Quarter Point @ Station - 78.25

Forward @ Station - 89.38

PAYLOAD CONFIGURATIONS USED FOR PARAMETRIC STUDIES

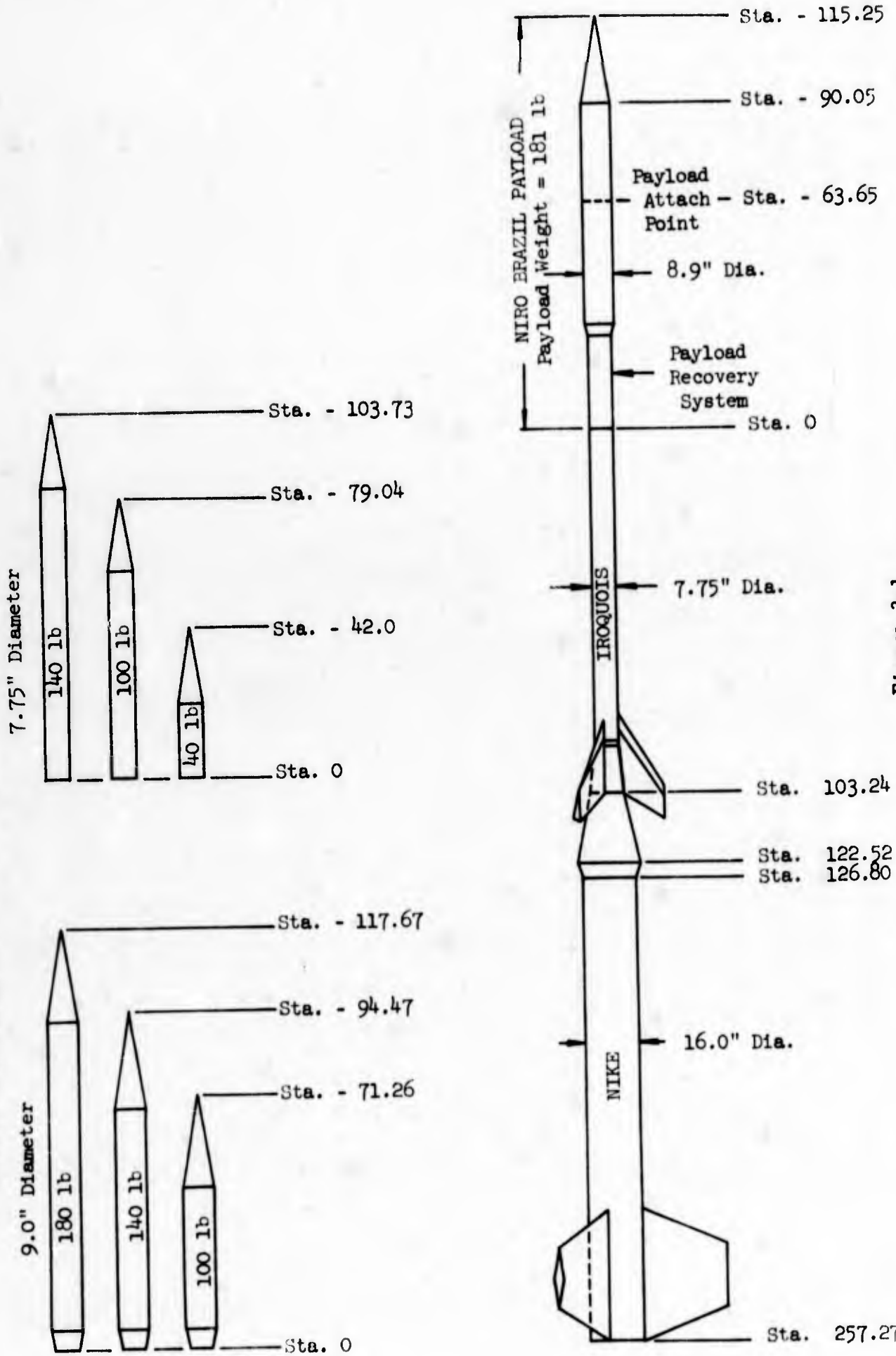
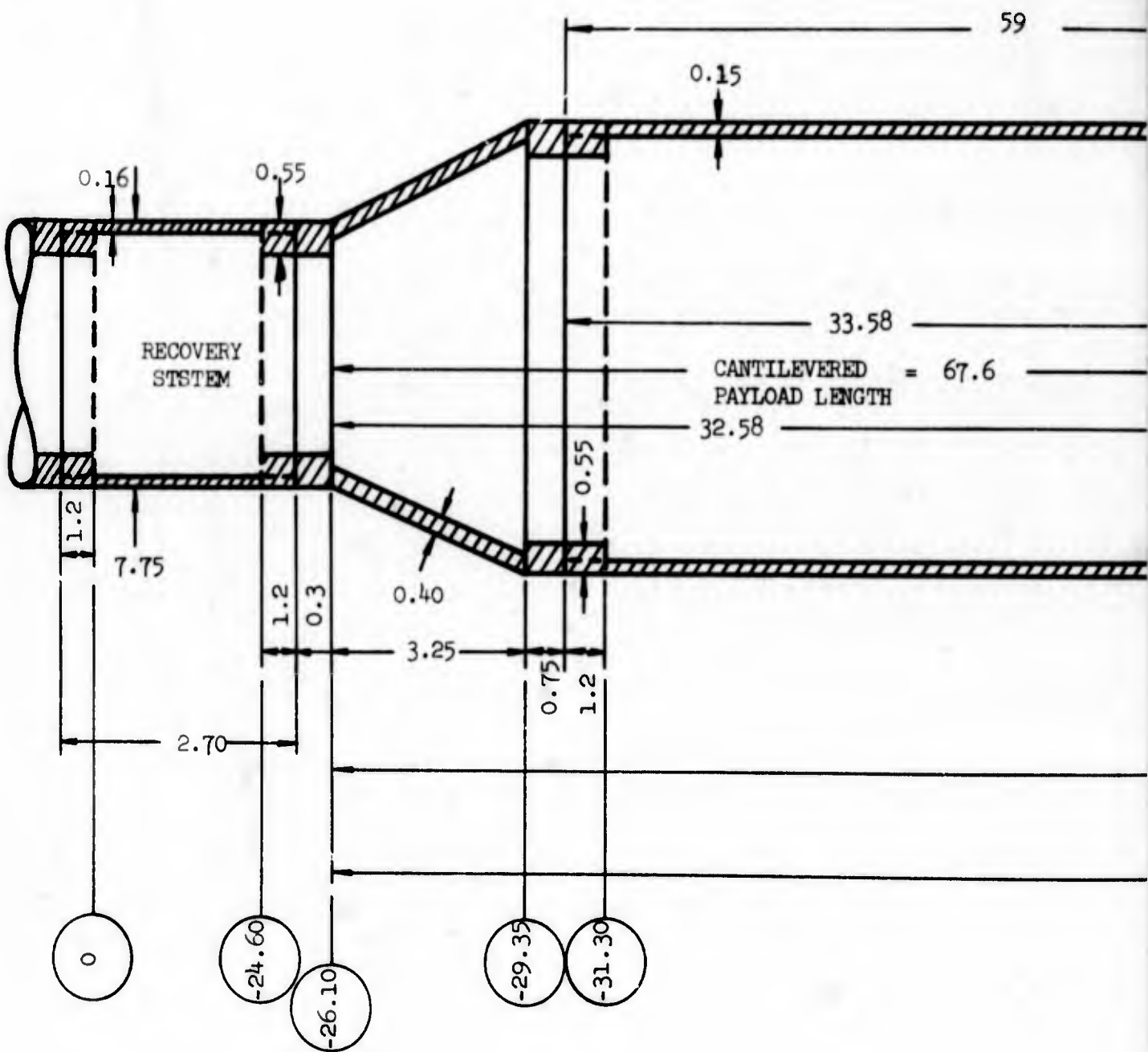
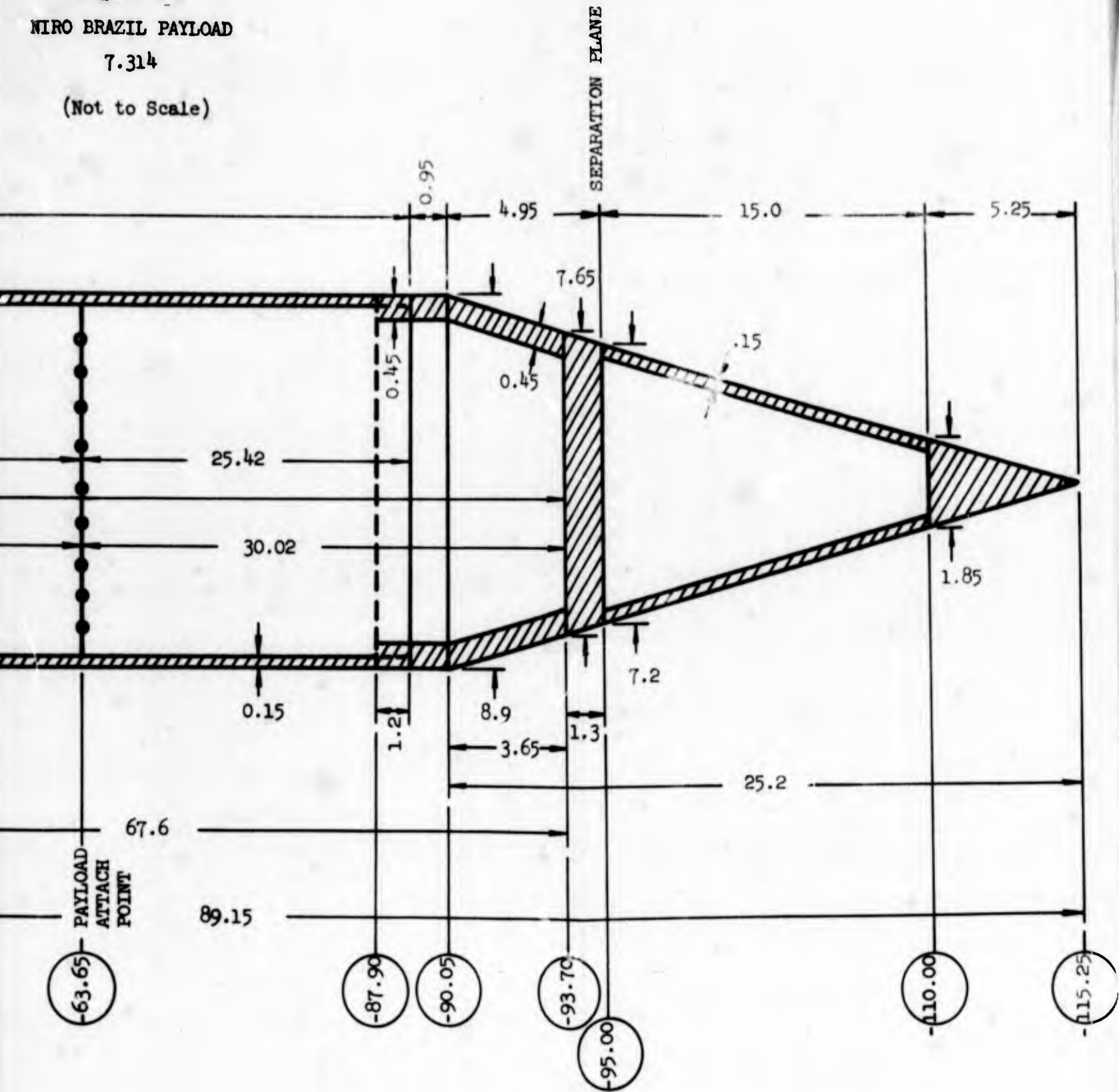


Figure 3-1  
NIRO CONFIGURATION



#

Figure 3-2  
 NIRO BRAZIL PAYLOAD  
 7.314  
 (Not to Scale)



Material: 6061-T6 Aluminum  
 $E_{Avg} = 10.0 \times 10^6 \text{ lb/in}^2$   
 $\rho = 0.098 \text{ lb/in}^3$

All dimensions shown are in inches

Figure 3-3

MIRO

PAYLOAD WEIGHT DISTRIBUTION

Brazil Flight Number 7.314

Cantilevered Payload Only

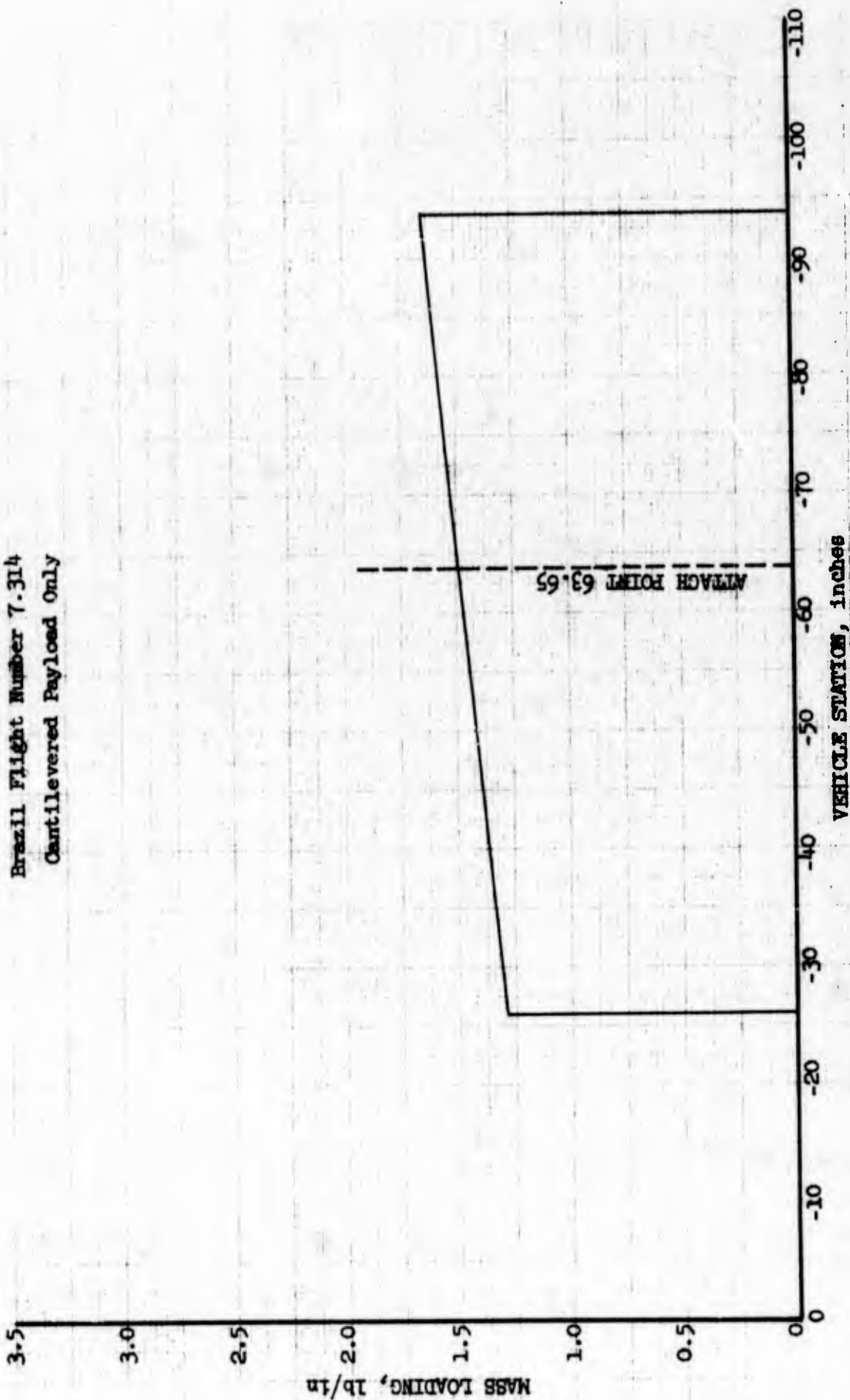




Figure 3-4

HIND

PAYLOAD EXTENSIONAL STIFFNESS (AE)

Cantilevered Payload Only

Brazil Flight Number 7.314

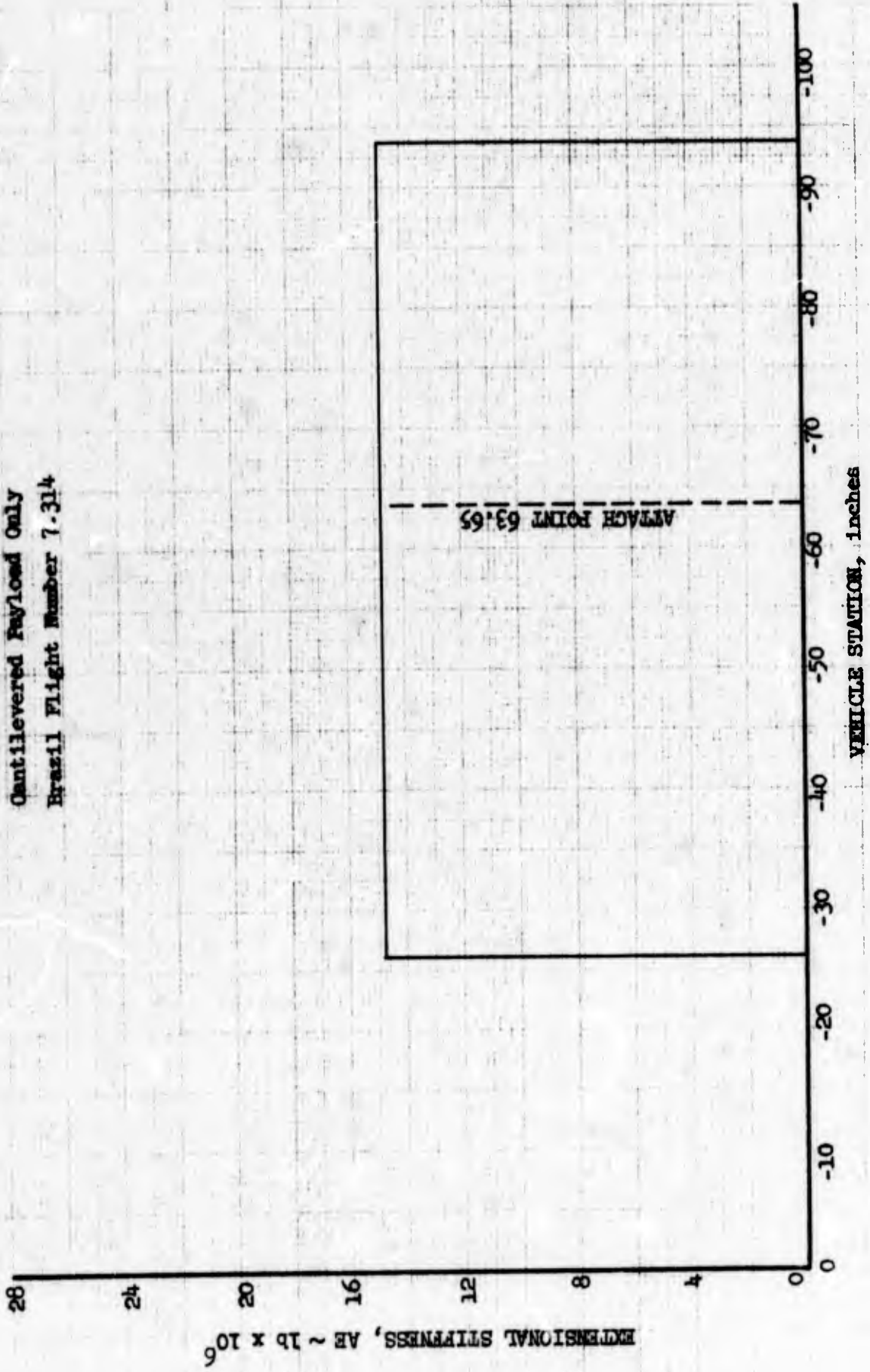


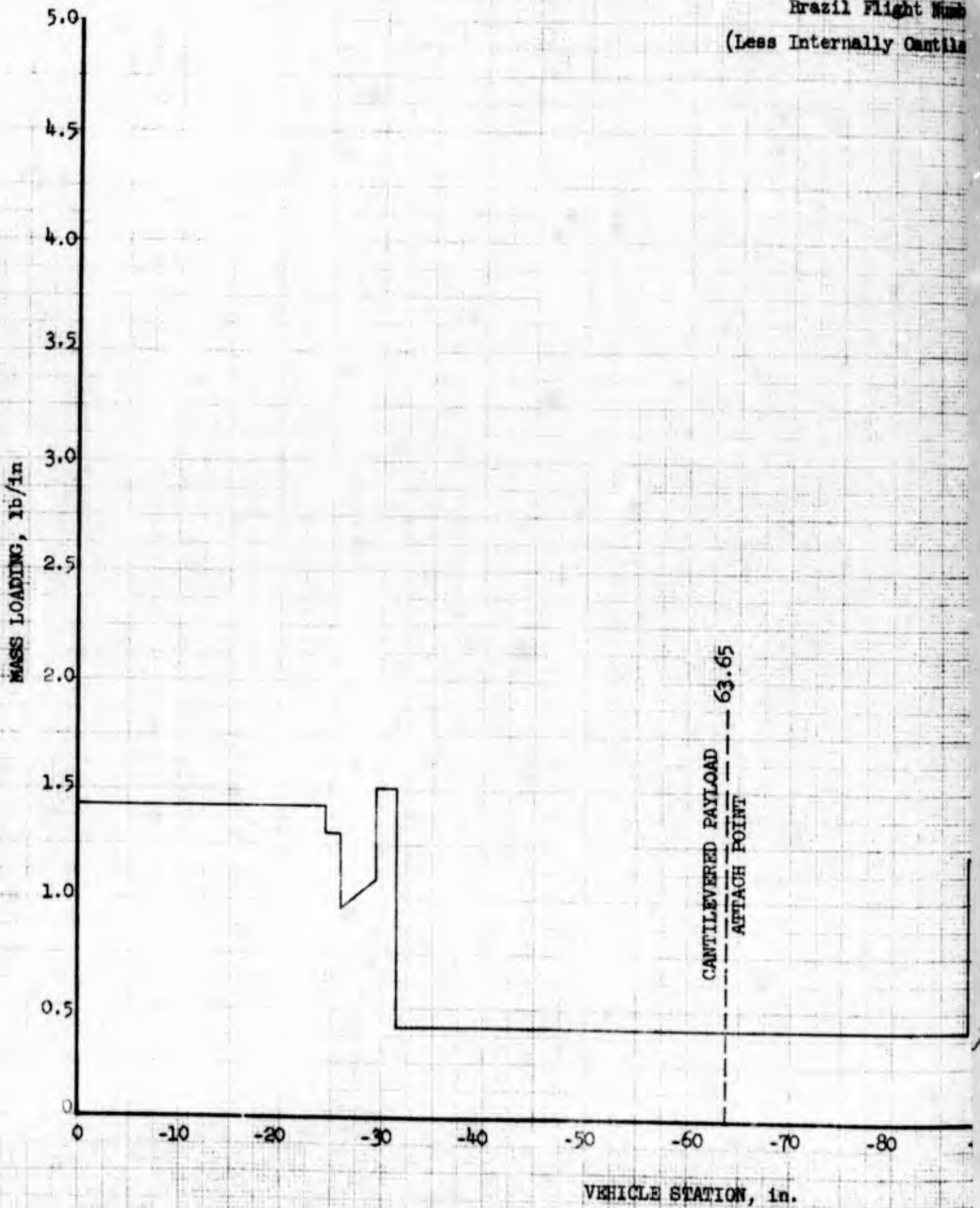
Figure 3-3

WERO

PAYLOAD WEIGHT DATA

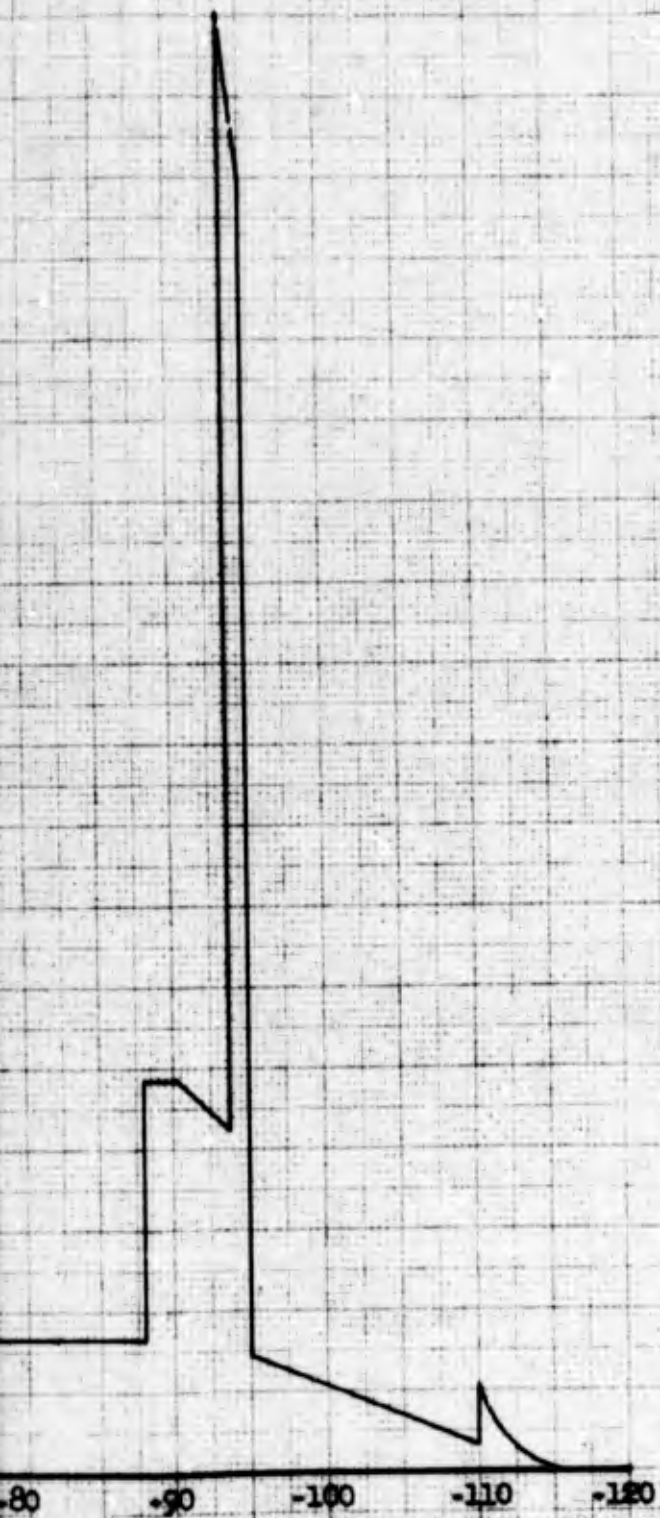
Brazil Flight Wagon

(Less Internally Cantilevered)



A

Figure 3-5  
WIND  
WIND DISTRIBUTION  
Light Number 7.314  
(Cantilevered Payload)



B

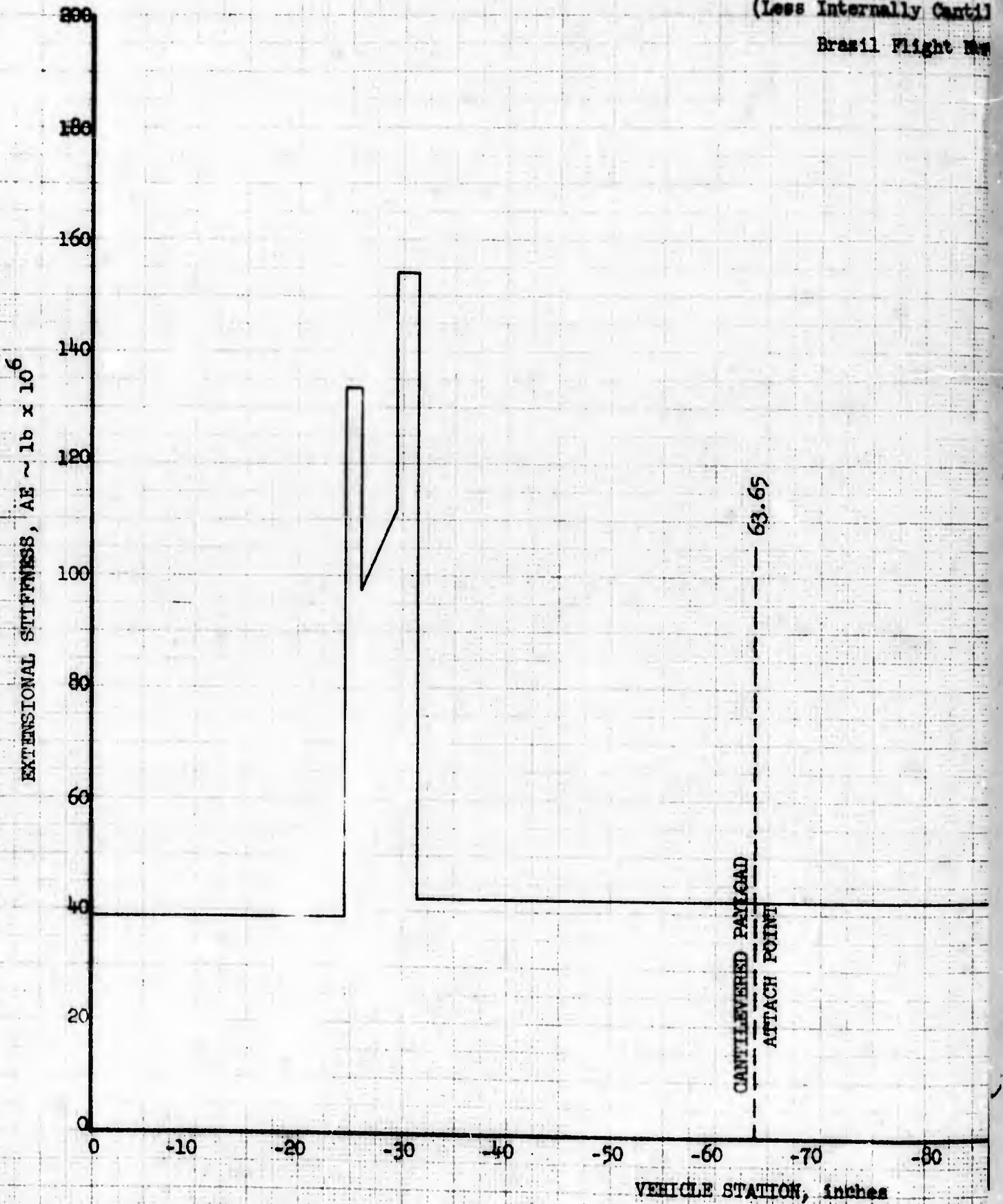
Figure 3-

MIRCO

PAYLOAD EXTENSIONAL STIFFNESS

(Less Internally Cantilevered Payload)

Brasil Flight Data



A



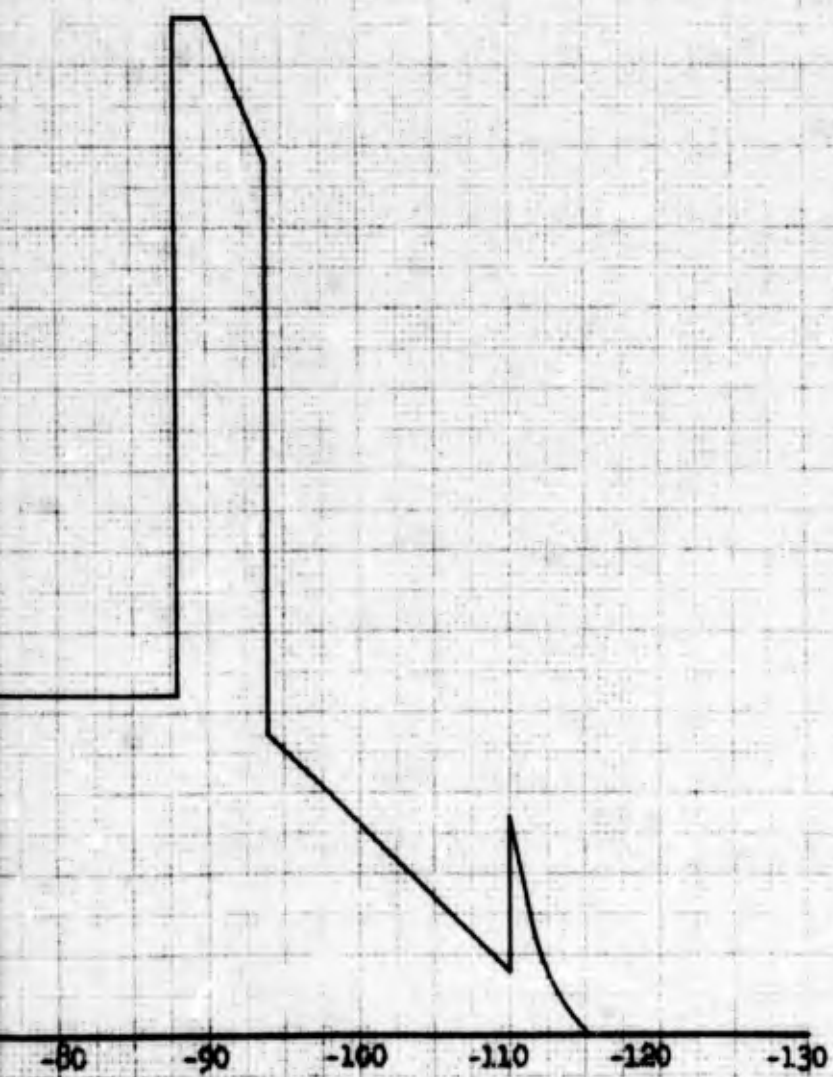
Figure 3-6

MIRQ

RESIGNAL STIFFNESS (AE)

ly Cantilevered Payload)

Flight Number 7.314



B

Figure 3-7

NIRO

SUSTAINER MASS DISTRIBUTION

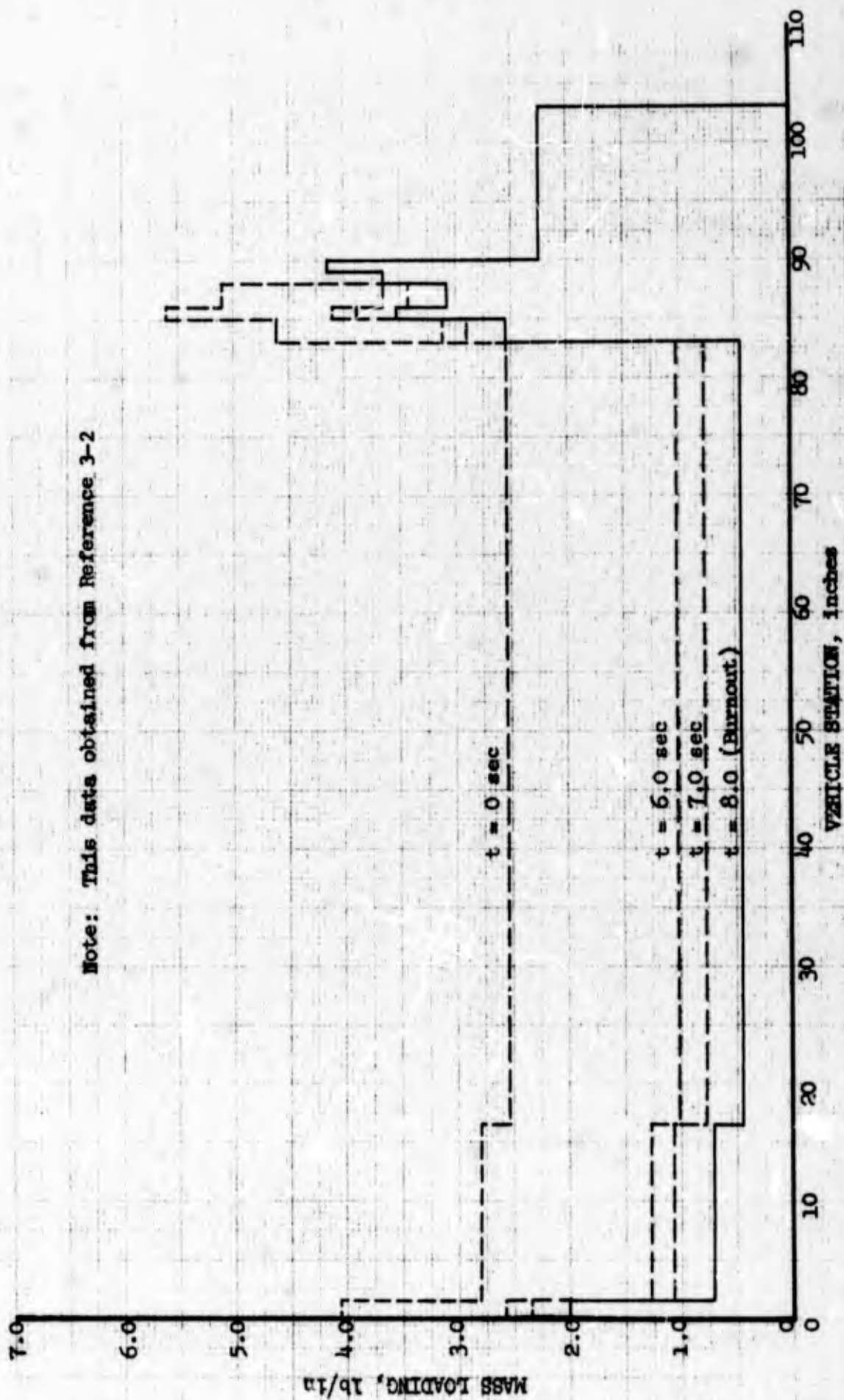


Figure 3-8

MEMO

SUSPENSION EXTENSIONAL STIFFNESS (AE)

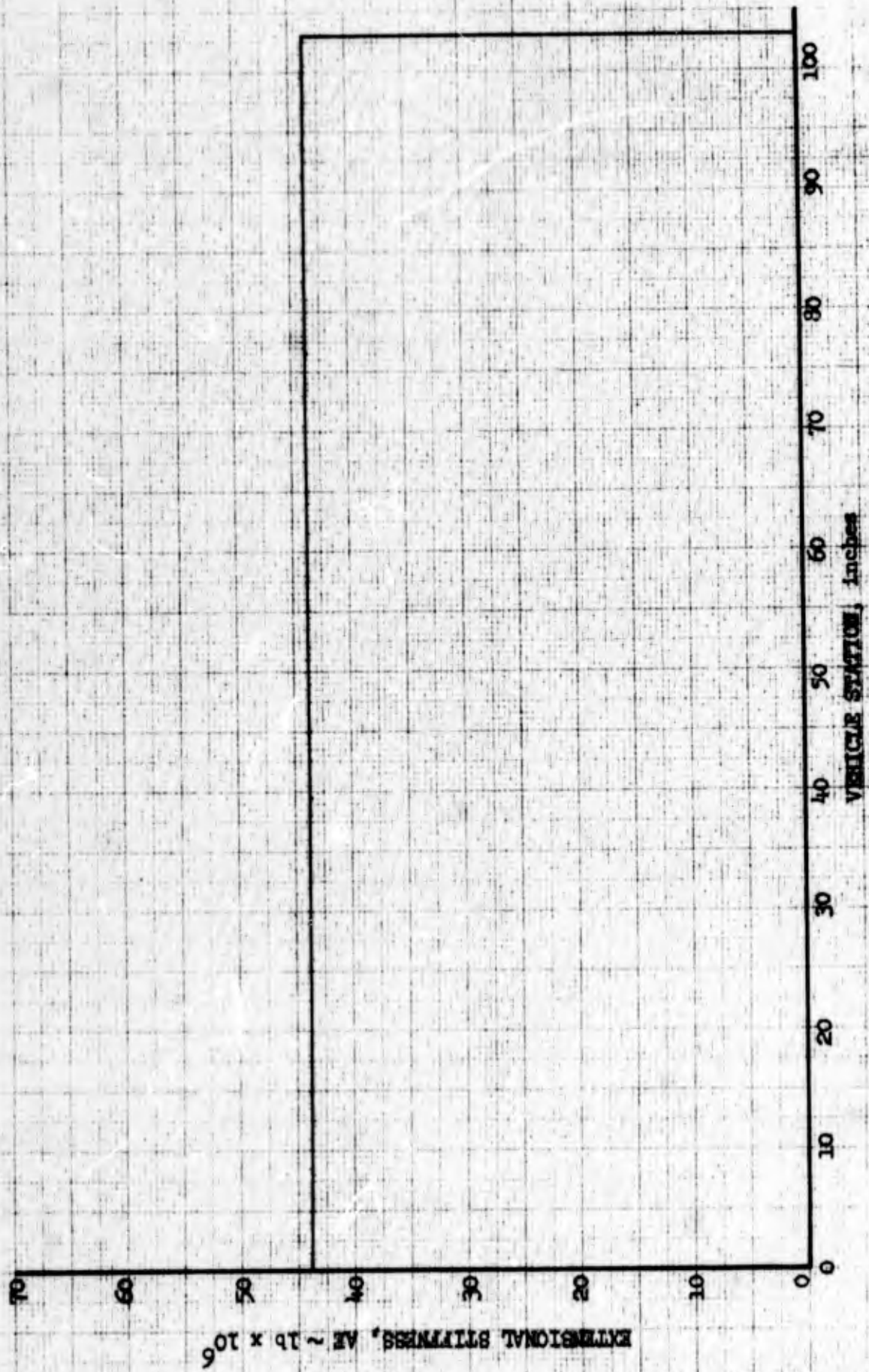




Figure 3-9

HEBO

SUSTAINER CHAMBER PRESSURE VS TIME

Note: This data obtained from Reference 3-3



gd. 11/2/61

Figure 3-10

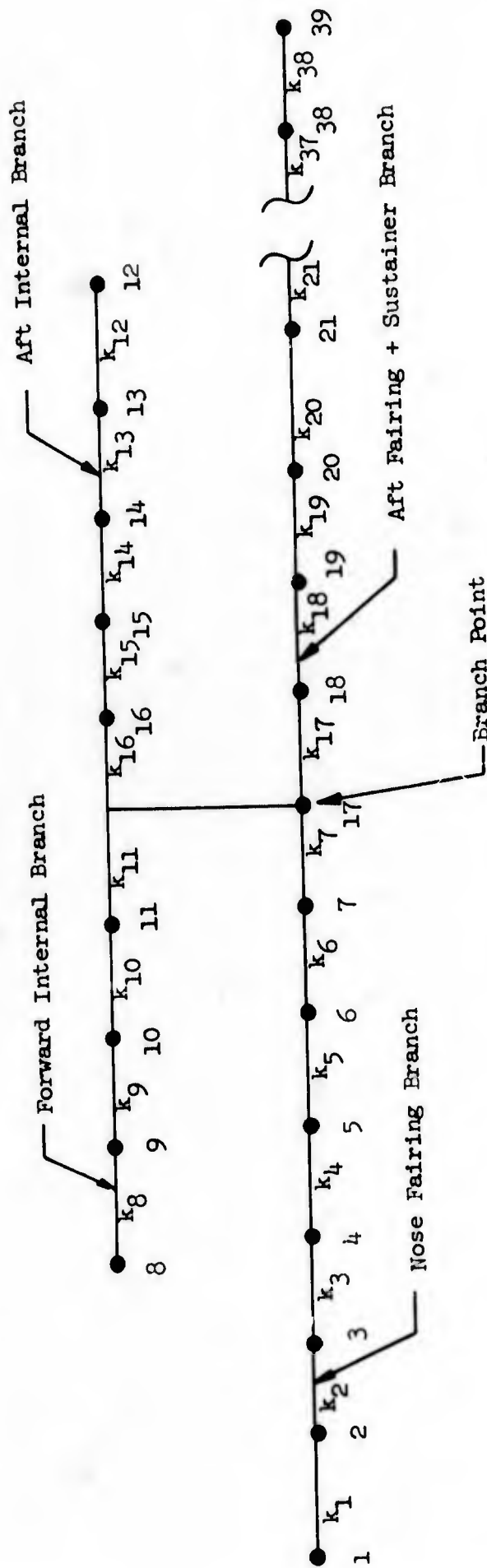
NIRO

LUMPED MASS AND STIFFNESS REPRESENTATION:

BRAZIL FLIGHT 7.314

PAYLOAD BRANCHED AT MIDPOINT (As Actually Flown)

(Not to Scale)

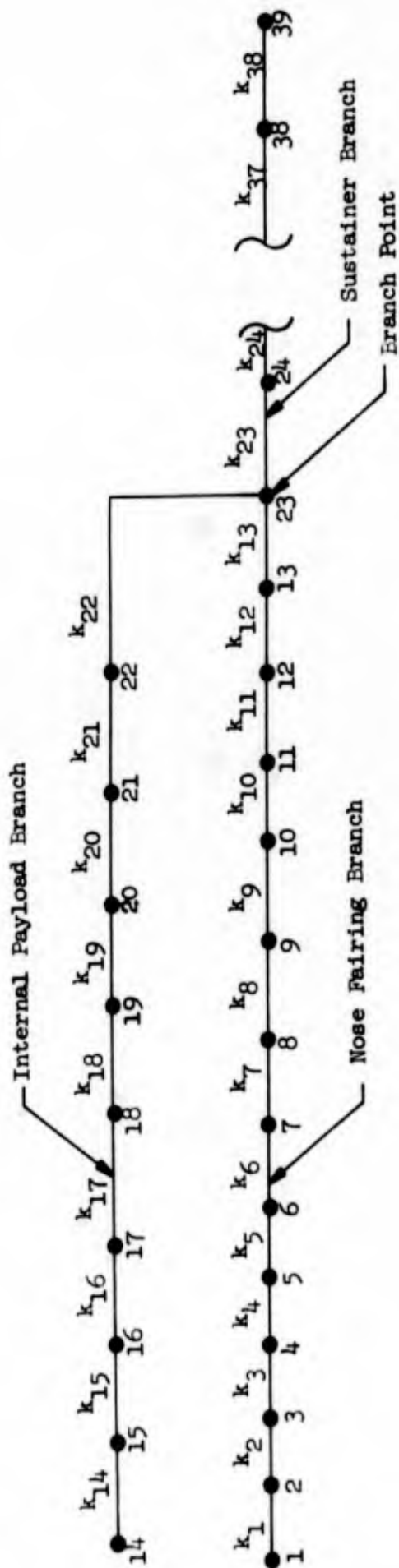


Note: See Table 3-1 for Coordinates

Figure 3-11

NIRO

LUMPED MASS AND STIFFNESS REPRESENTATION  
PAYLOAD BRANCHED AT BASE  
(Not to Scale)

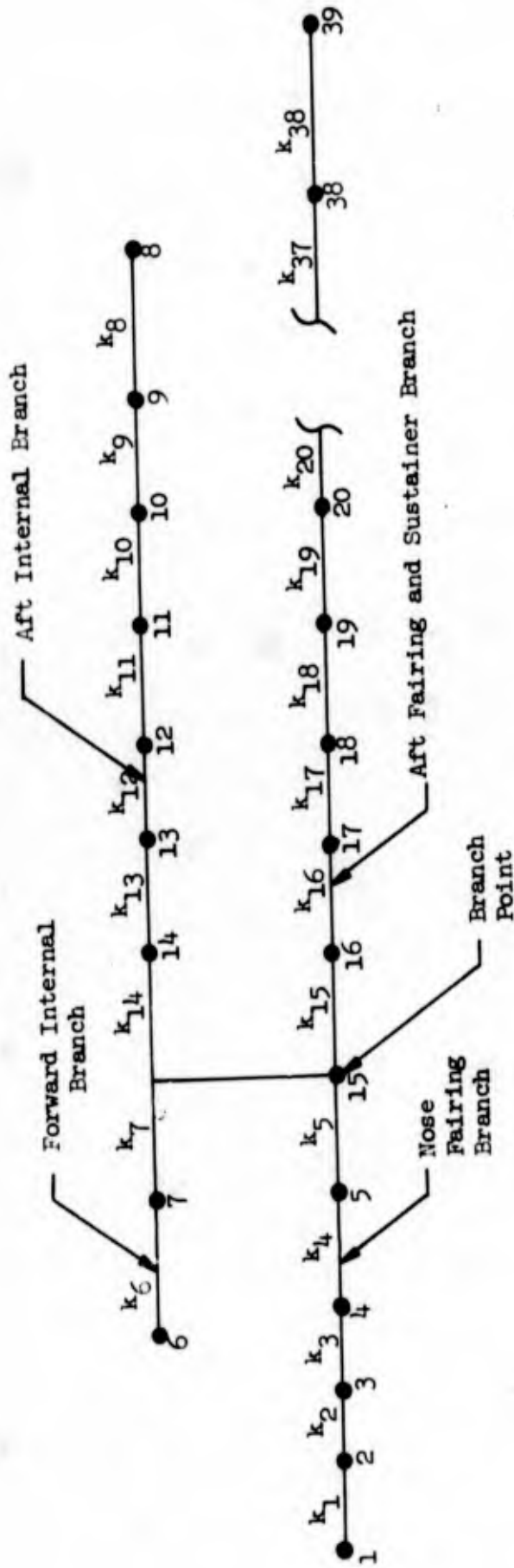


Note: See Table 3-2 for Coordinates

Figure 3-12

NIRO

LUMPED MASS AND STIFFNESS REPRESENTATION  
PAYLOAD BRANCHED AT QUARTER POINT  
(Not to Scale)



Note: See Table 3-4 for Coordinates

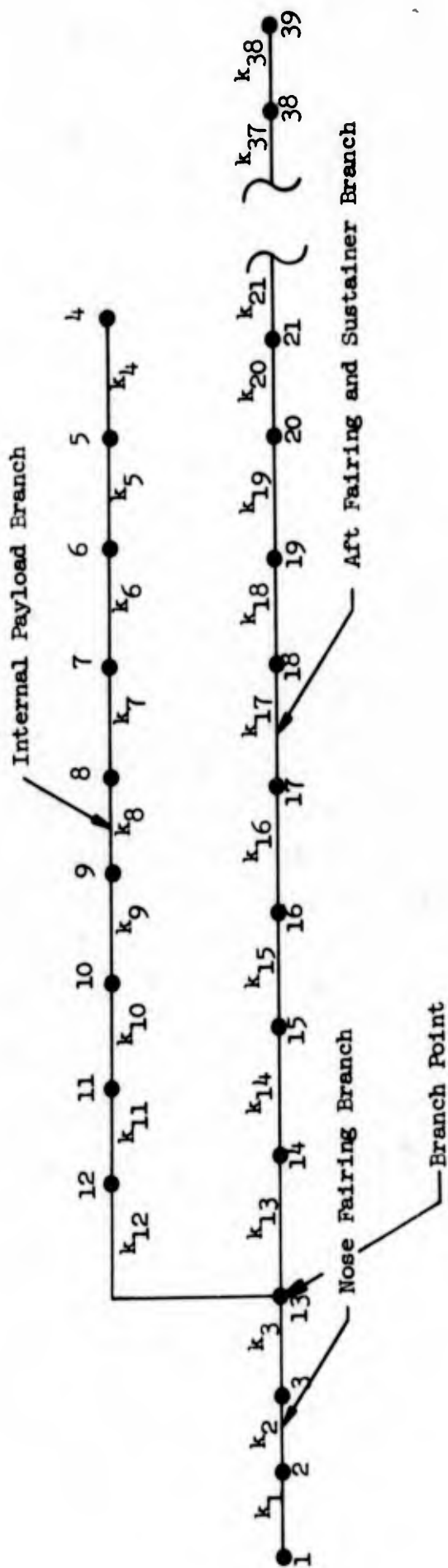
Figure 3-13

NIRO

LUMPED MASS AND STIFFNESS REPRESENTATION

PAYLOAD BRANCHED AT FRONT

(Not to Scale)



Note: See Table 3-3 for Coordinates

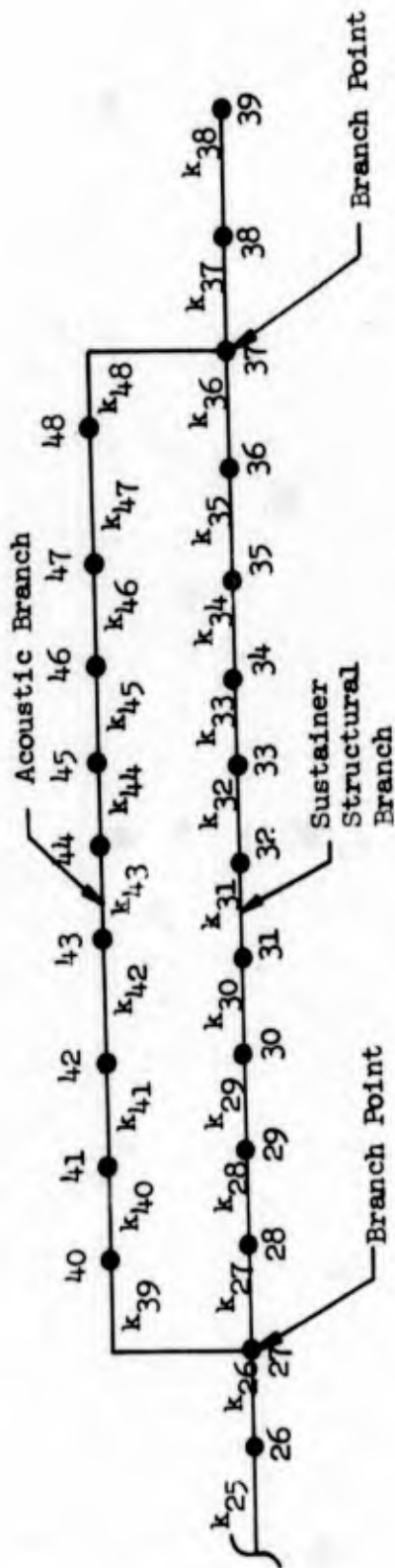
Figure 3-14

NIRO

LUMPED MASS AND STIFFNESS REPRESENTATION

ACOUSTIC BRANCH OF SUSTAINER

(Not to Scale)



Note: See Table 3-6 for Coordinates



Figure 3-15

W190

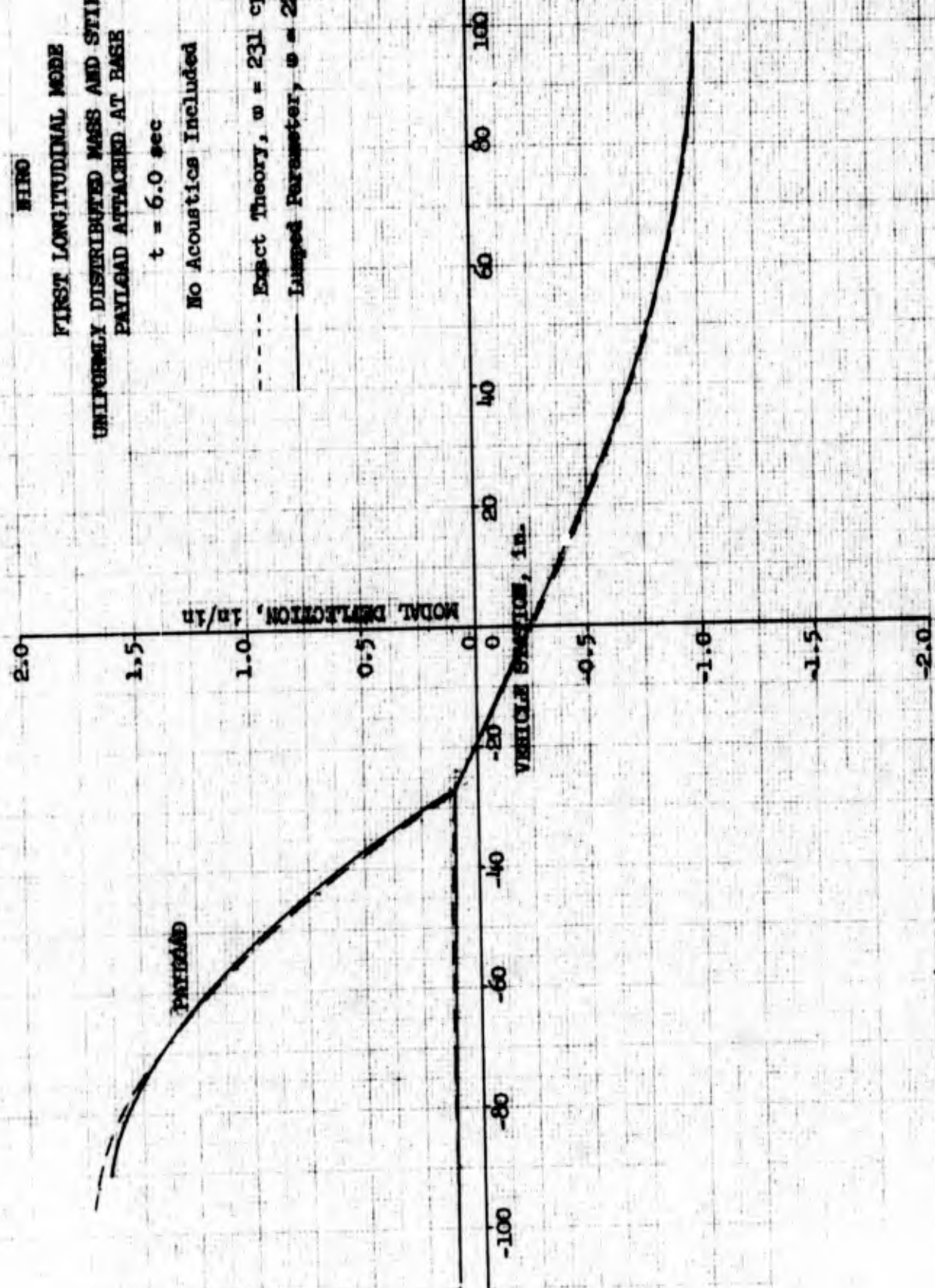
FIRST LONGITUDINAL MODE  
UNIFORMLY DISTRIBUTED MASS AND STIFFNESS  
PAVLOAD ATTACHED AT BASE

$t = 6.0 \text{ sec}$

No Acoustics Included

--- Exact Theory,  $\omega = 231 \text{ cps}$

— Lumped Parameter,  $\omega = 229 \text{ cps}$



*g. Miller*



Figure 3-16

MIRO

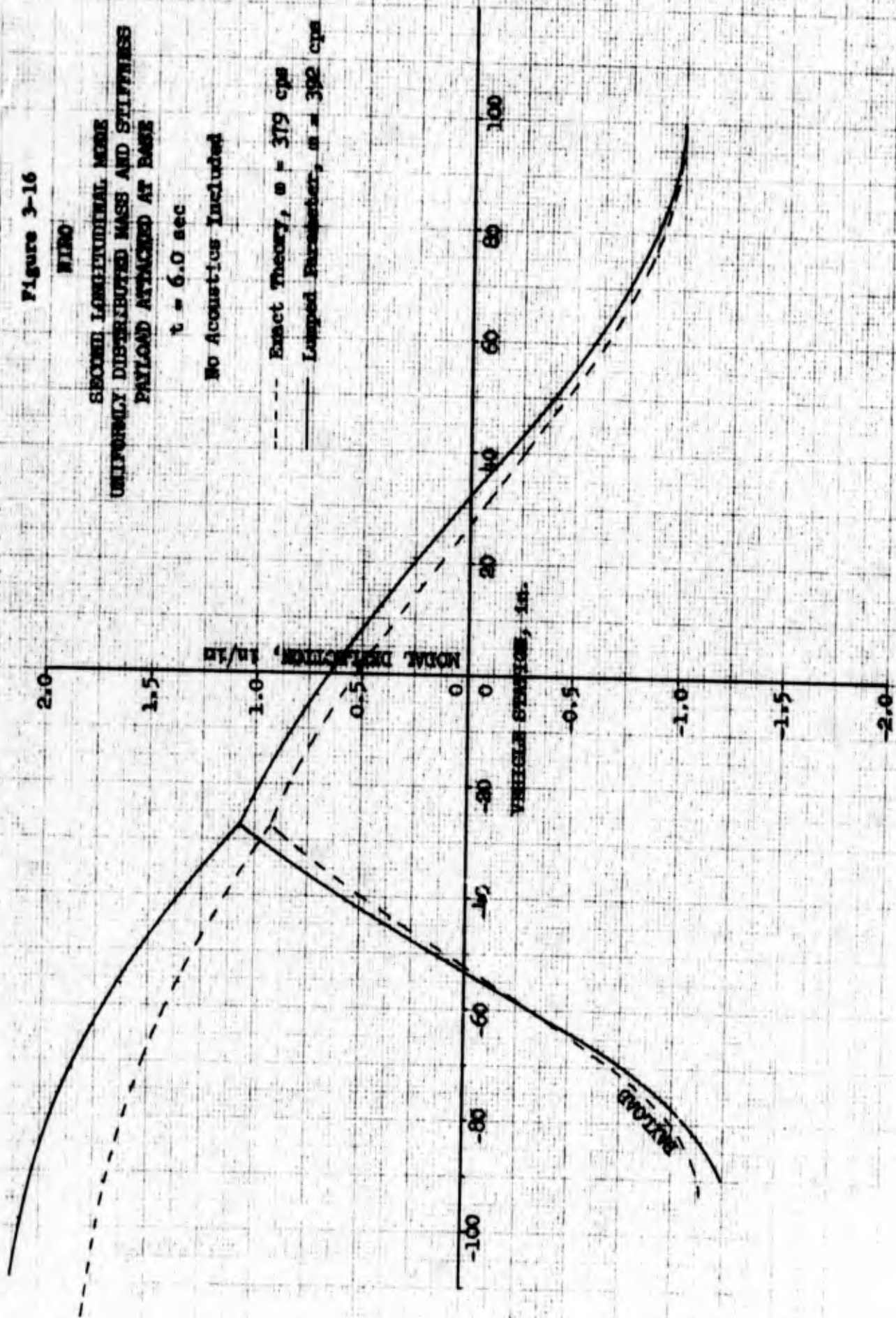
SECOND LONGITUDINAL MODE  
UNIFORMLY DISTRIBUTED MASS AND STIFFNESS  
PAYLOAD ATTACHED AT BASE

$t = 6.0$  sec

No Acoustics Included

--- Exact Theory,  $\omega = 379$  cps

— Lumped Parameter,  $\omega = 392$  cps



A. H. H.

Figure 3-17

MIRO

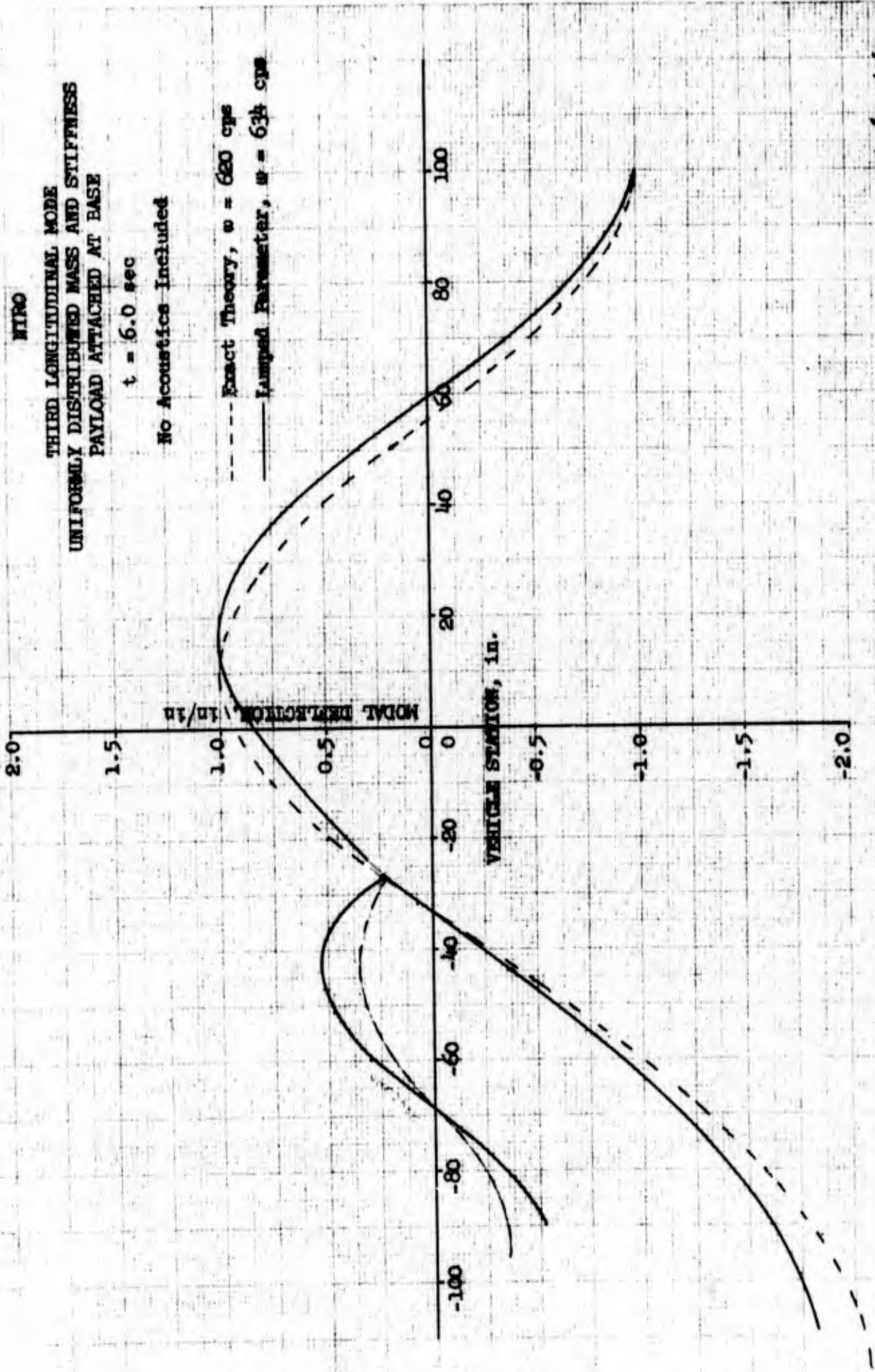
THIRD LONGITUDINAL MODE  
UNIFORMLY DISTRIBUTED MASS AND STIFFNESS  
PAYLOAD ATTACHED AT BASE

$t = 6.0 \text{ sec}$

No Acoustics Included

--- Exact Theory,  $\omega = 620 \text{ cps}$

— Lumped Parameter,  $\omega = 634 \text{ cps}$



*pl. slides*

Figure 3-18

NIRG

FIRST LONGITUDINAL MODE

Bresil Flight 7.314 Payload

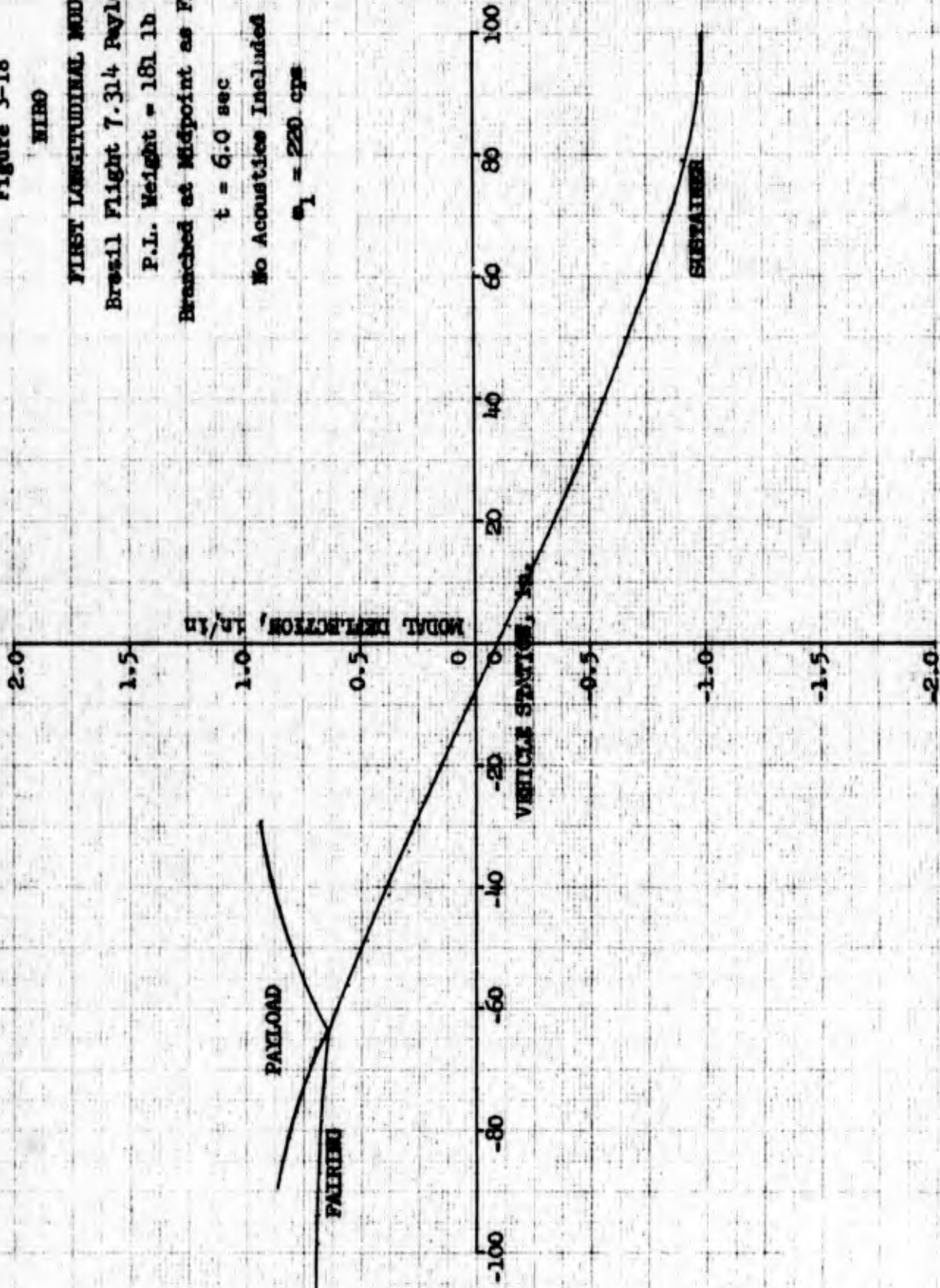
P.L. Weight = 181 lb

Branched at Midpoint as Flown

$t = 6.0$  sec

No Acoustics Included

$\omega_1 = 220$  cps



gpk 8/12/68



Figure 3-19

**MIRO**

**SECOND LONGITUDINAL MODE**

Brazil Flight 7.314 Payload

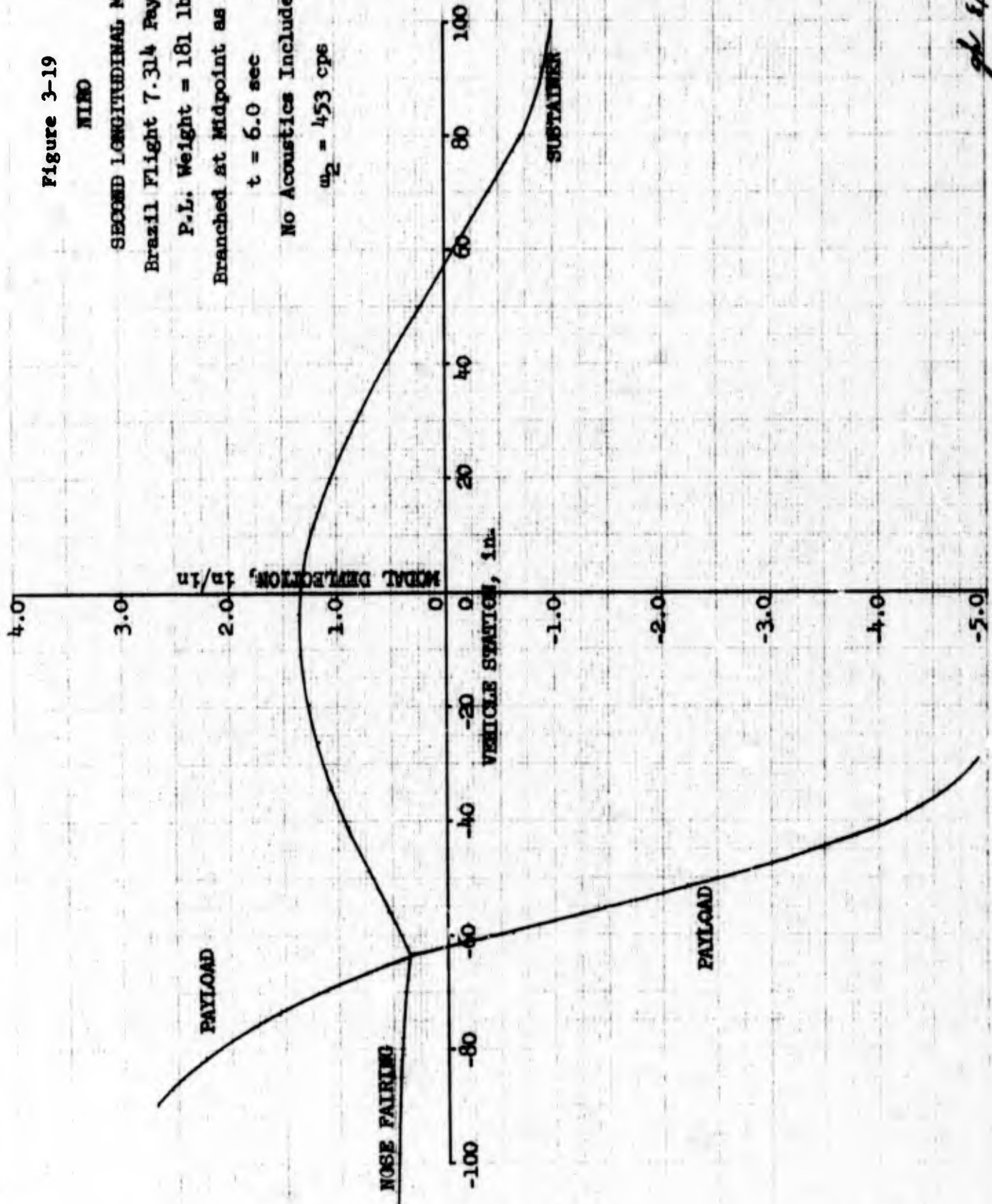
P.L. Weight = 181 lb

Branched at Midpoint as Flown

$t = 6.0$  sec

No Acoustics Included

$\omega_2 = 453$  cps



*gh 8/13/68*

Figure 3-20

MILMO

THIRD LONGITUDINAL MODE

Brazil Flight 7.314 Payload

P.L. Weight = 181 lb

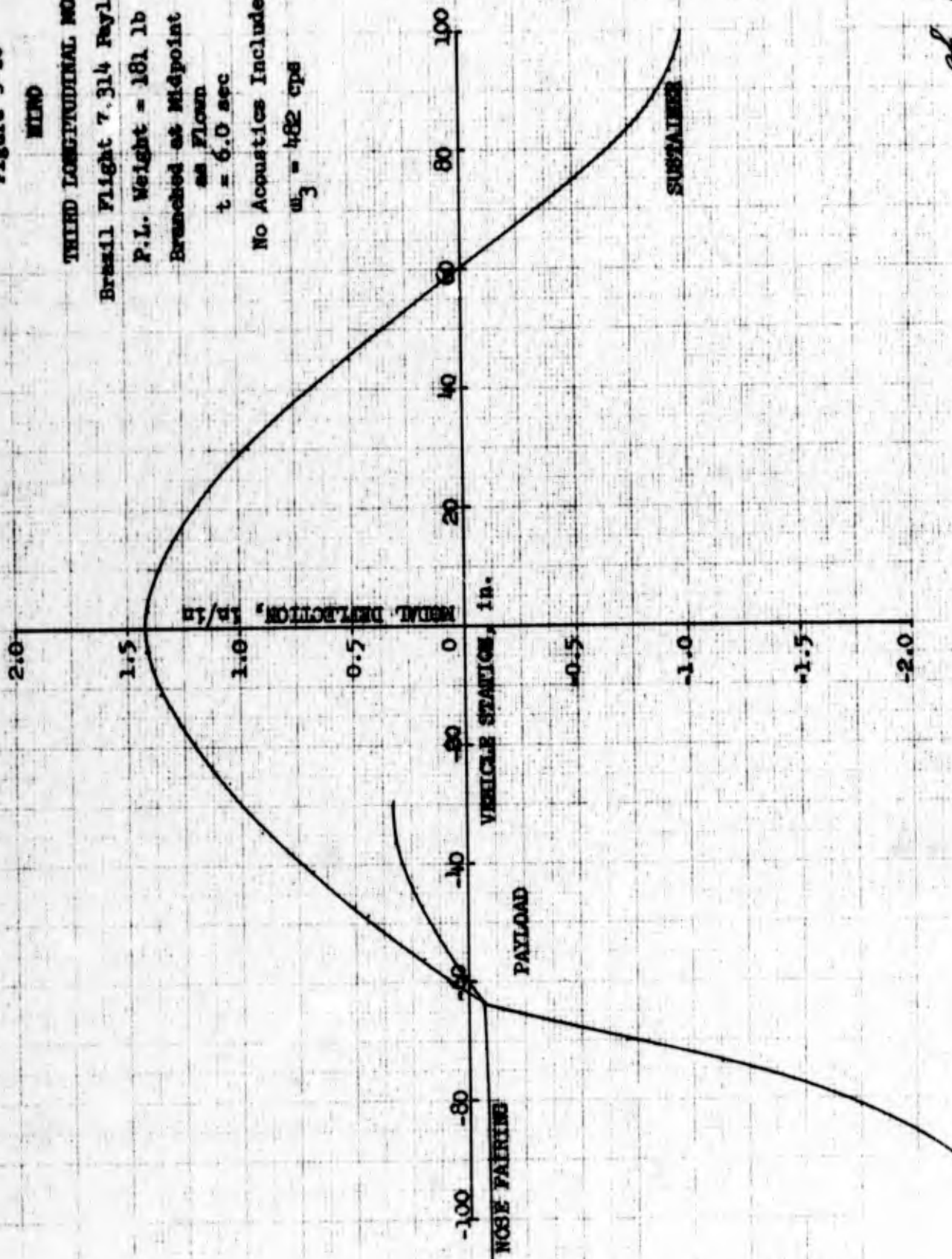
Branched at Midpoint

as Flown

t = 6.0 sec

No Acoustics Included

$\omega_3 = 482$  cps



gpl 8/12/68

Figure 3-21

MIRO

FIRST LONGITUDINAL MODE

Brazil Flight 7.314

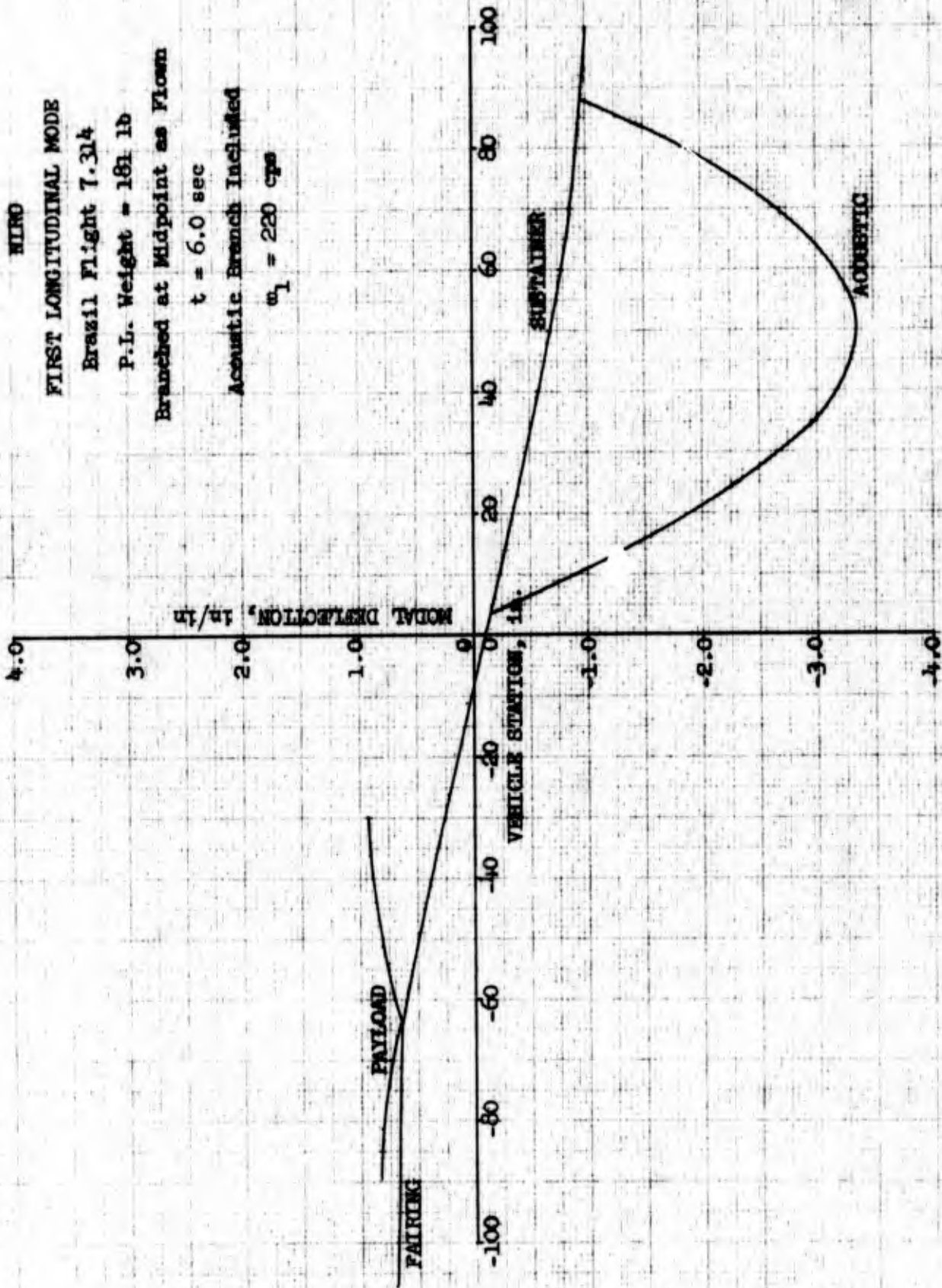
P.L. Weight = 181 lb

Branched at Midpoint as Flown

$t = 6.0$  sec

Acoustic Branch Included

$\omega_1 = 220$  cps



gh. states

Figure 3-22

WIND

SECOND LONGITUDINAL MODE

Brazil Flight 7.314

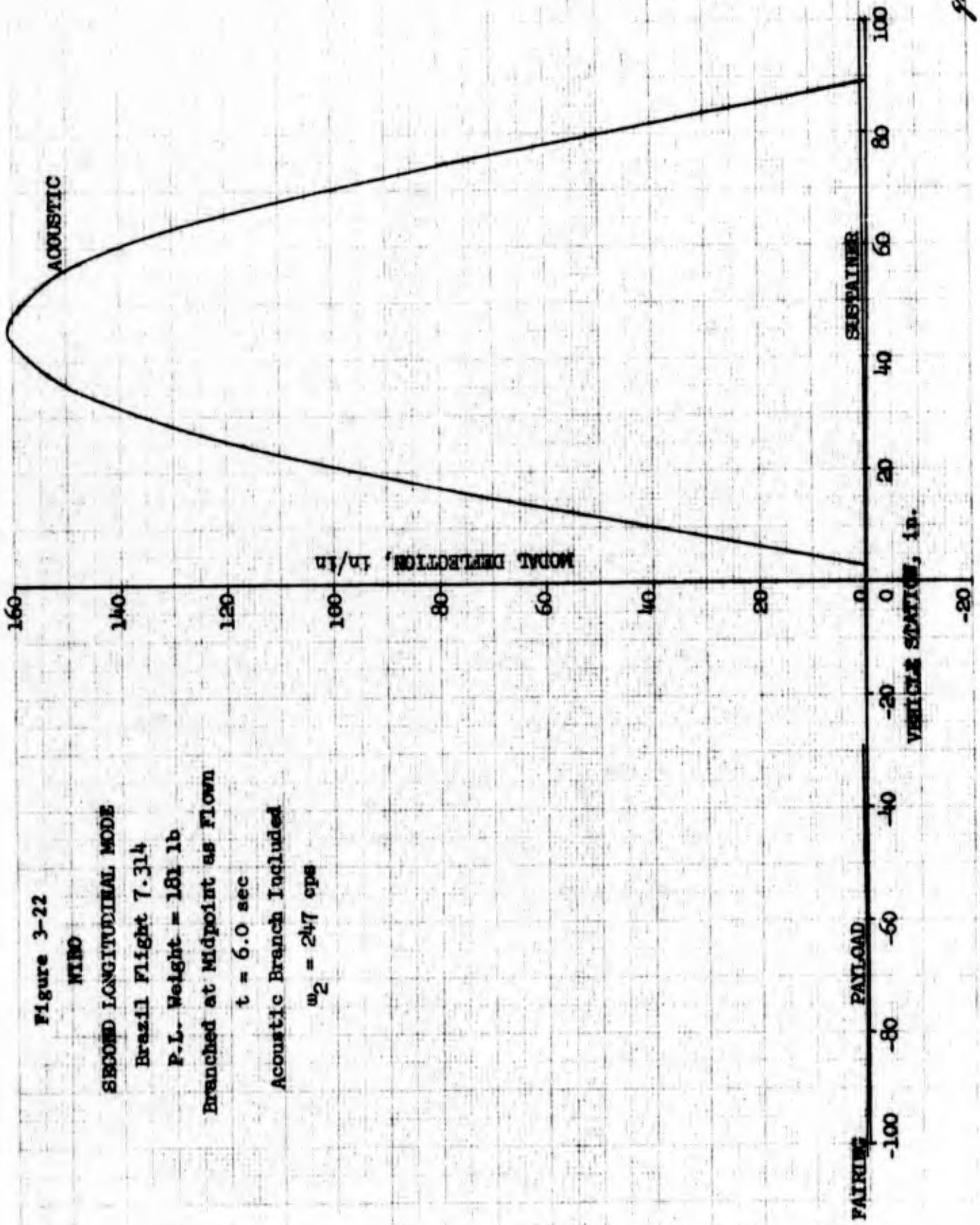
P.L. Weight = 181 lb

Branched at Midpoint as Flown

$t = 6.0$  sec

Acoustic Branch Included

$\omega_2 = 247$  cps



gt 8/19/68



Figure 3-23

MIRO

THIRD LONGITUDINAL MODE

Brazil Flight 7-314

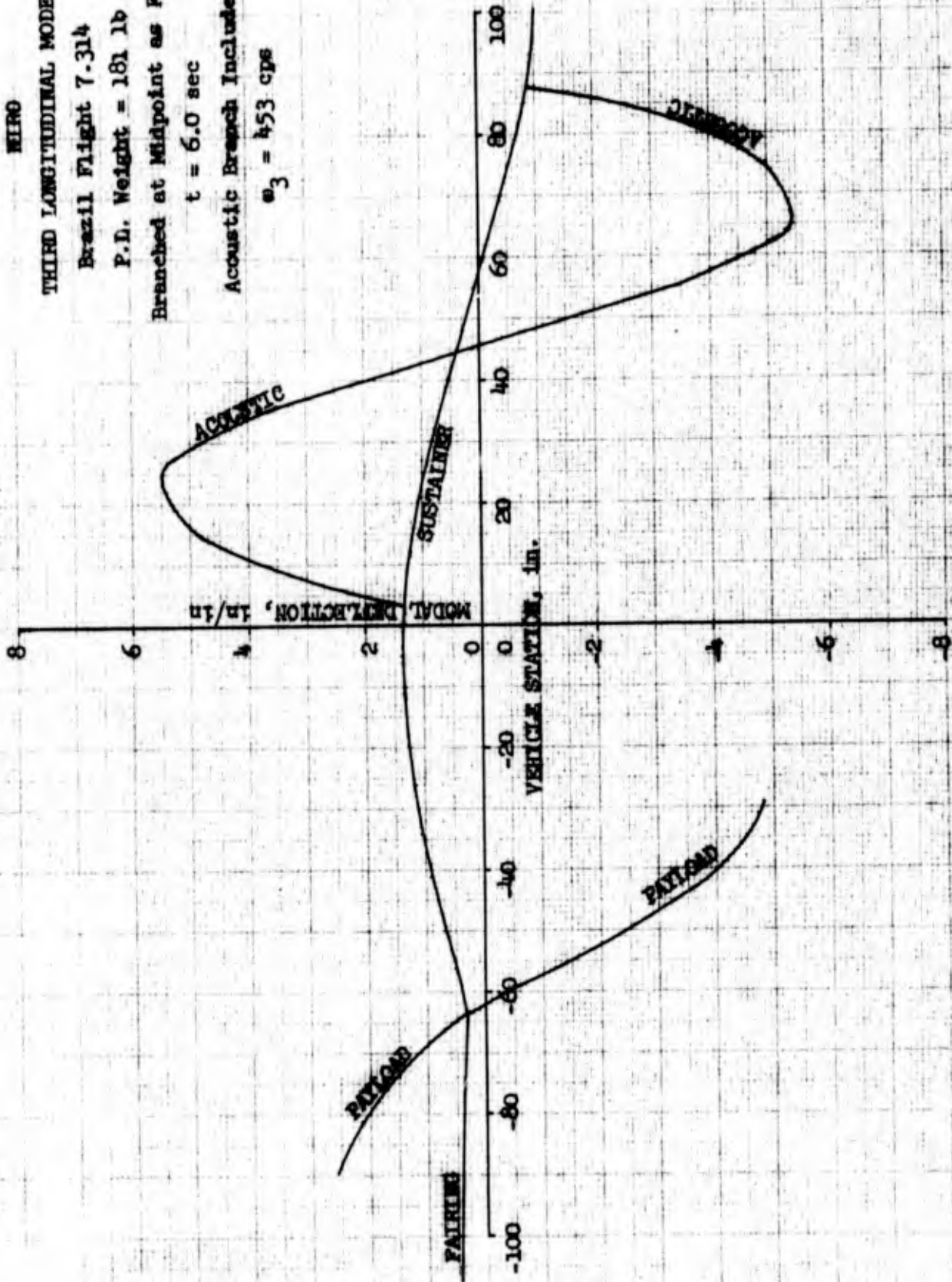
P.L. Weight = 181 lb

Branched at Midpoint as Flown

$t = 6.0$  sec

Acoustic Branch Included

$\omega_3 = 453$  cps



pk slaked

Figure 3-24

WIND

FOURTH LONGITUDINAL MODE

Brazil Flight 7.314

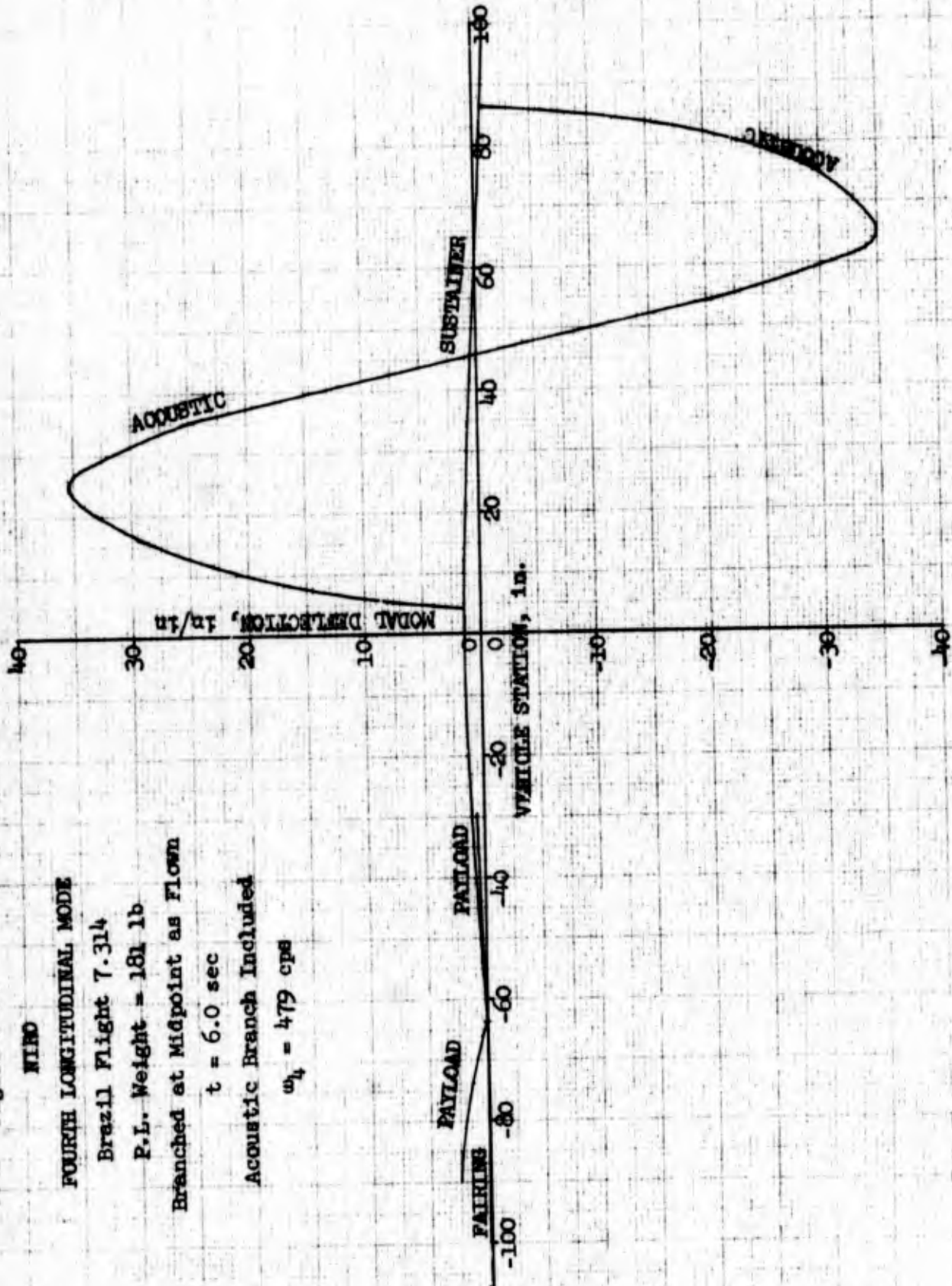
P.L. Weight = 181 lb

Branched at Midpoint as Flown

$t = 6.0$  sec

Acoustic Branch Included

$\omega_4 = 479$  cps



gd 8/19/68

Figure 3-25

NIRO

FIFTH LONGITUDINAL MODE

Brazil Flight 7.314

P.L. Weight = 181 lb

Branched at Midpoint as Flown

$t = 6.0$  sec

Acoustic Branch Included

$\omega_5 = 489$  cps

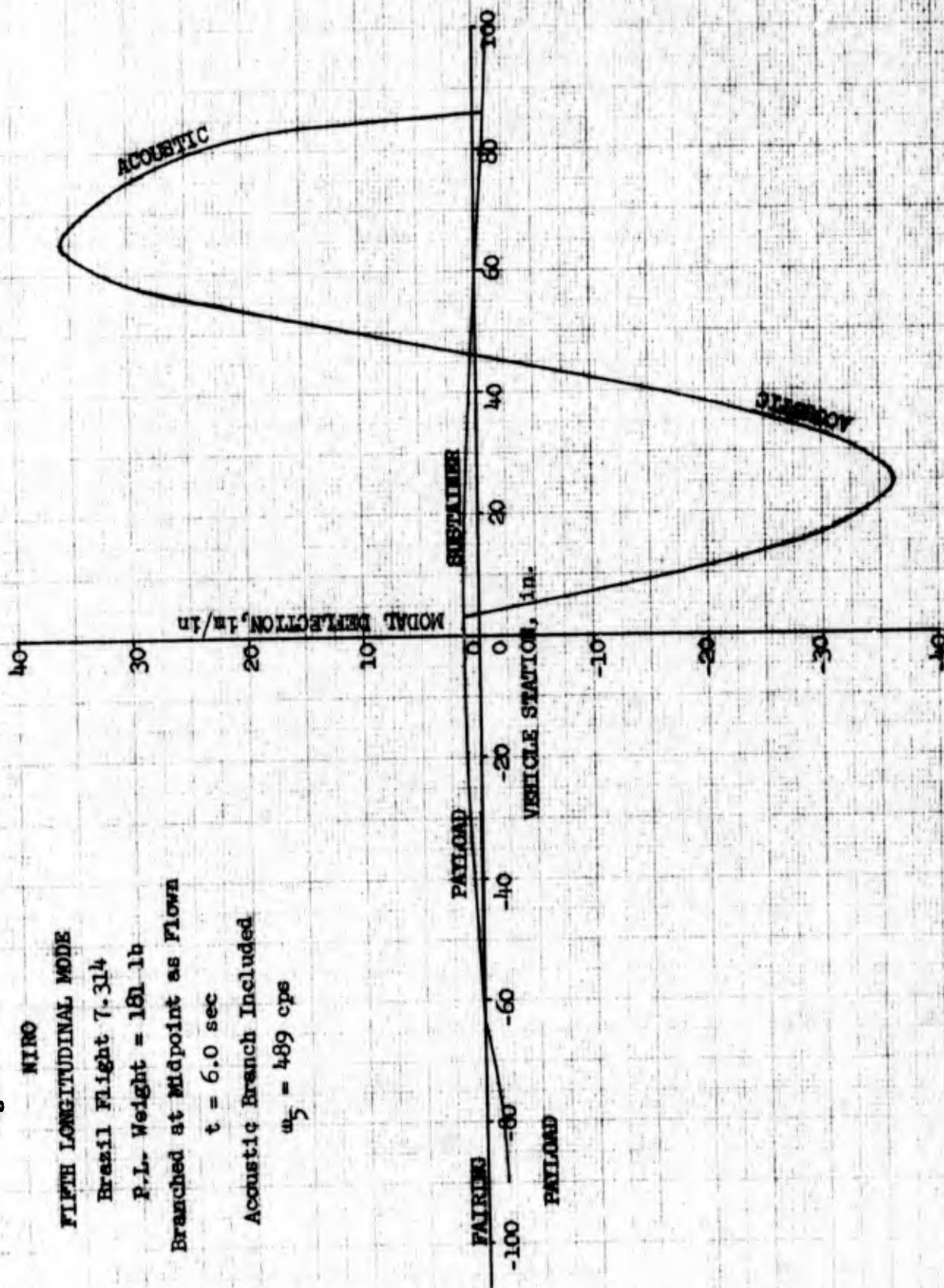




Figure 3-26

MIRO

FIRST LONGITUDINAL MODE

Flight 7.314 Rayloed

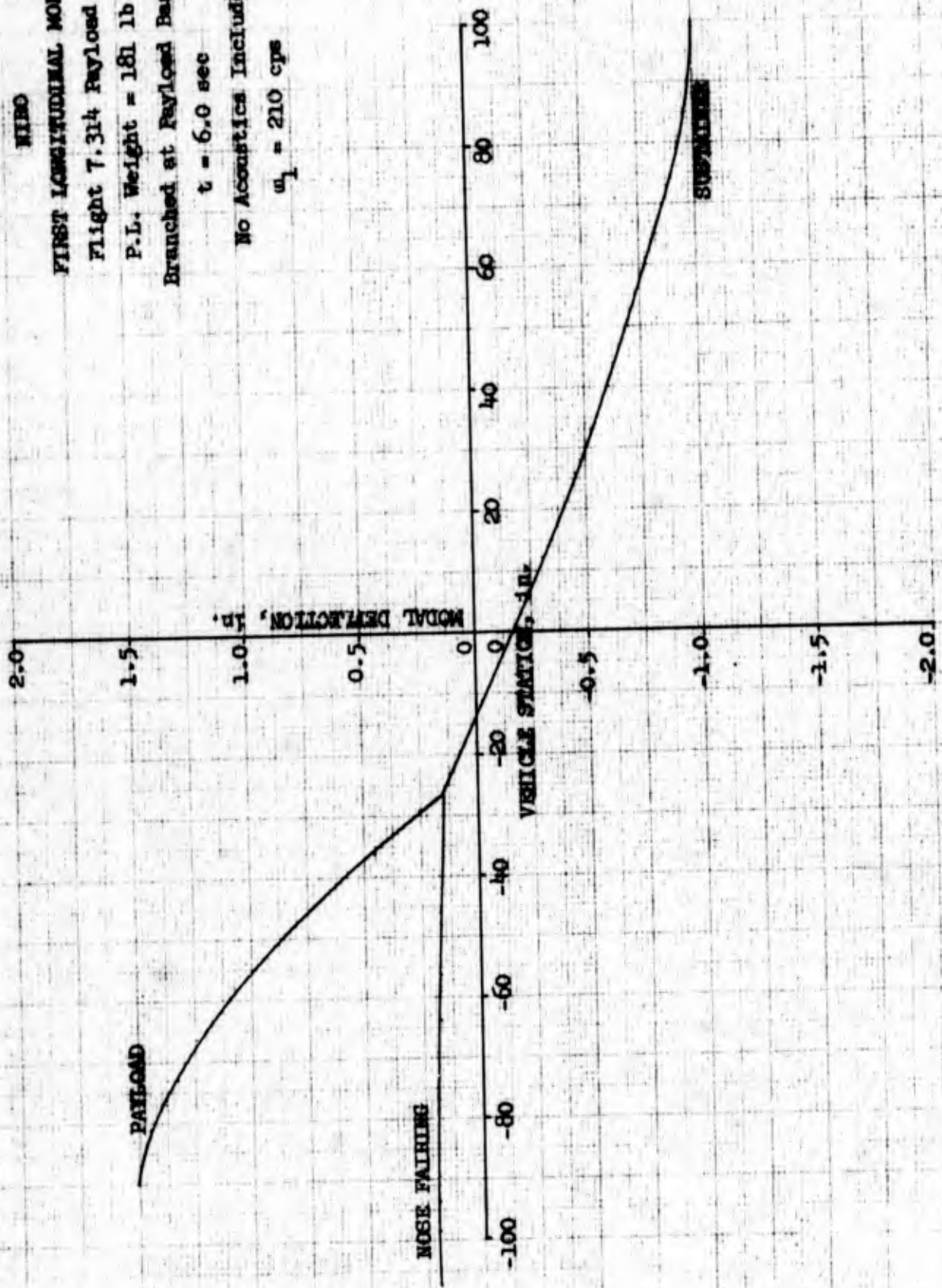
P.L. Weight = 181 lb

Branched at Rayloed Base

$t = 6.0$  sec

No Acoustics Included

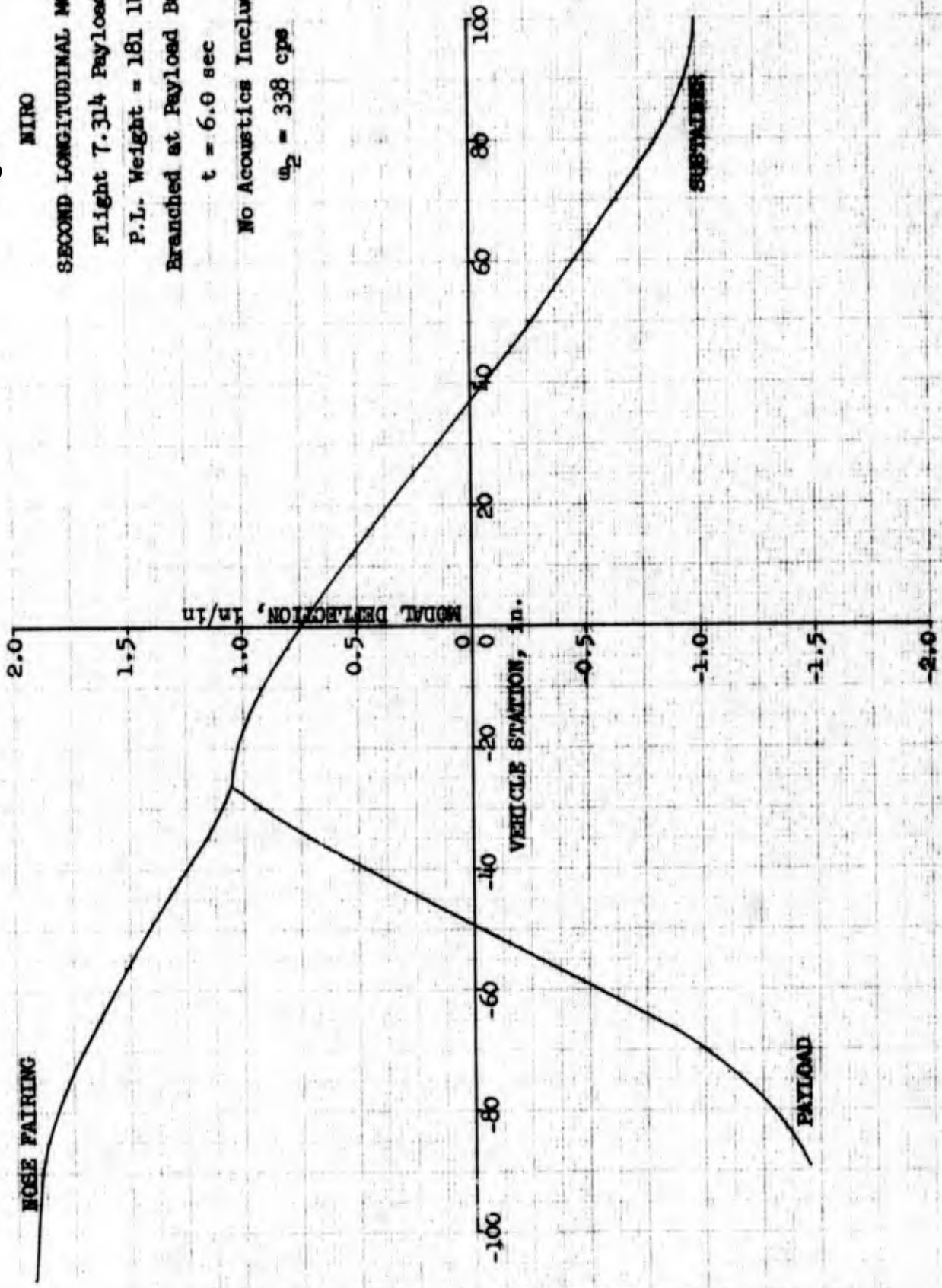
$\omega_1 = 210$  cps



gk 1/1/68

Figure 3-27

**MIRO**  
**SECOND LONGITUDINAL MODE**  
**Flight 7-314 Payload**  
**P.L. Weight = 181 lb**  
**Branched at Payload Base**  
**t = 6.0 sec**  
**No Acoustics Included**  
 **$\omega_2 = 338$  cps**



*ph r/m/66*

Figure 3-28

W190

THIRD LONGITUDINAL MODE

Flight 7.314 Payload

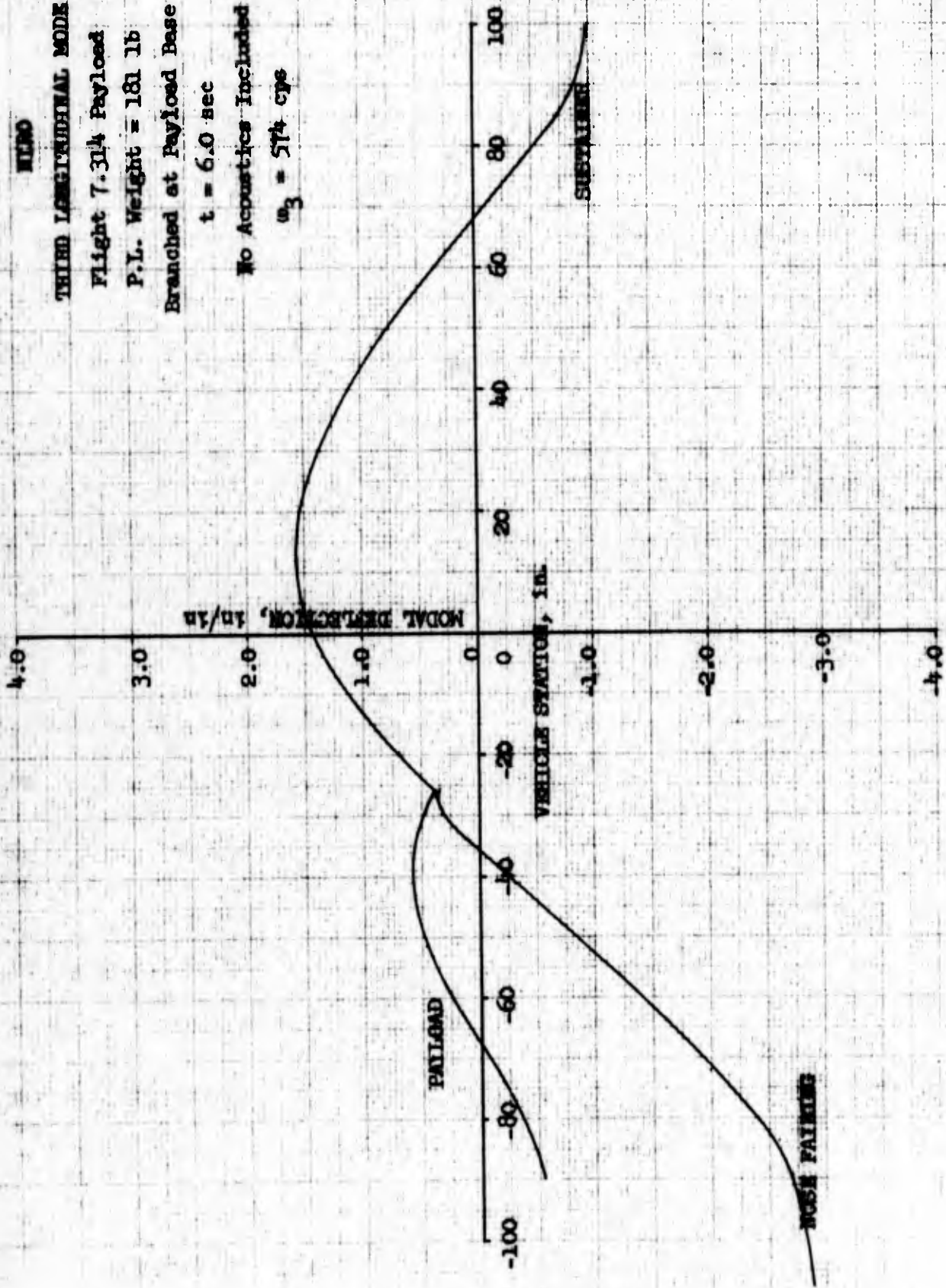
P.L. Weight = 181 lb

Branched at Payload Base

$t = 6.0$  sec

No Acoustics Included

$\omega_3 = 574$  cps



pk slides

Figure 3-29

WING

FIRST LONGITUDINAL MODE

Flight 7.314 Payload

Payload Wt. = 181 lb

Branched at Forward End of Payload

$t = 6.0$  sec

No Acoustics Included

$\omega_1 = 187$  cps

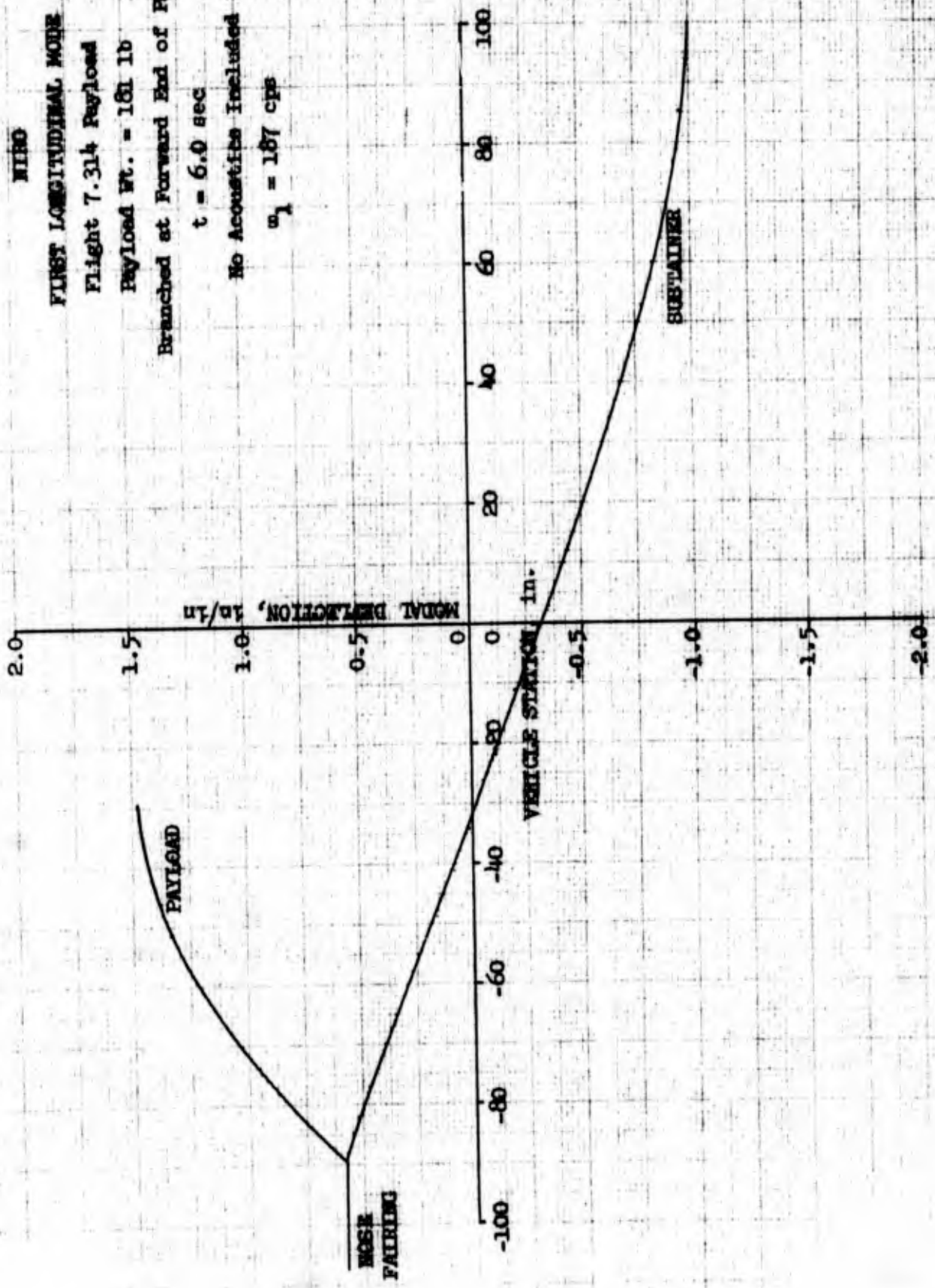




Figure 3-30

IIRO

SECOND LONGITUDINAL MODE

Flight 7.314 Payload

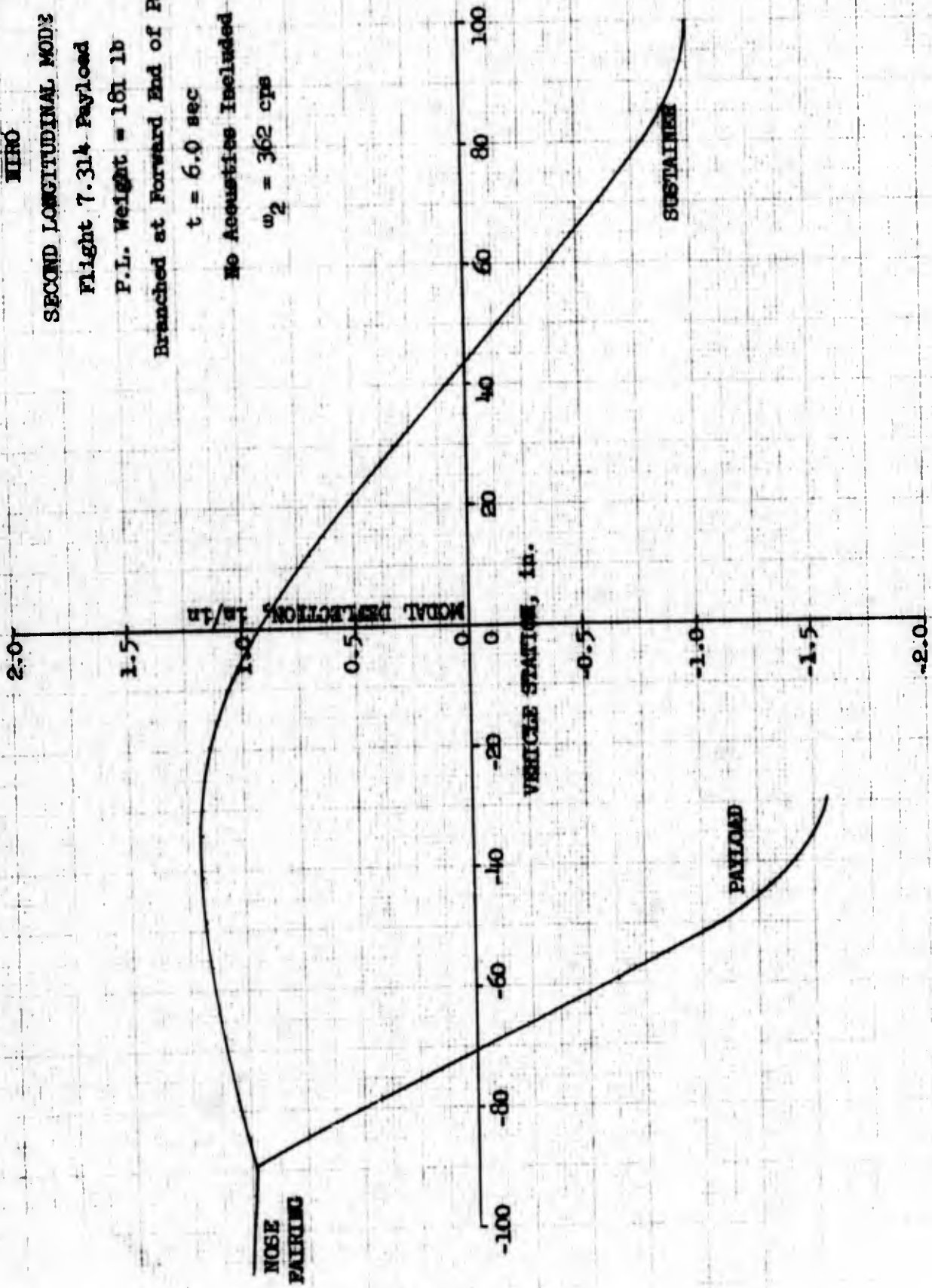
P.L. Weight = 161 lb

Branched at Forward End of Payload

$t = 6.0$  sec

No Acoustics Included

$\omega_2 = 362$  cps



gp 8/13/68

Figure 3-31

THIRD LANGUINAL MODE  
NIBO

Flight 7-314 Payload

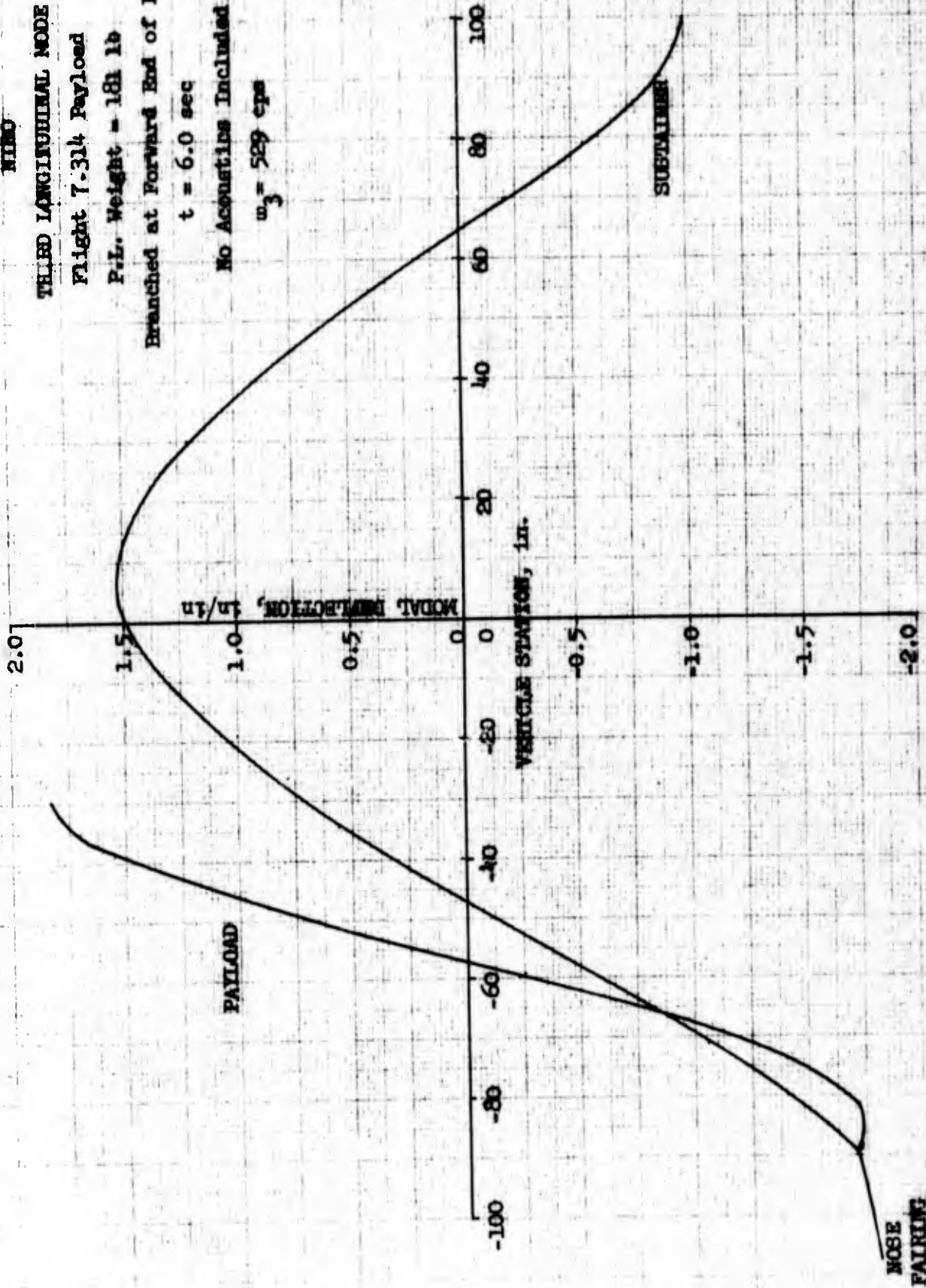
P.L. Weight = 181 lb

Branched at Forward End of Payload

$t = 6.0$  sec

No Acoustics Included

$\omega_3 = 529$  cps



*Handwritten signature*

Figure 3-32

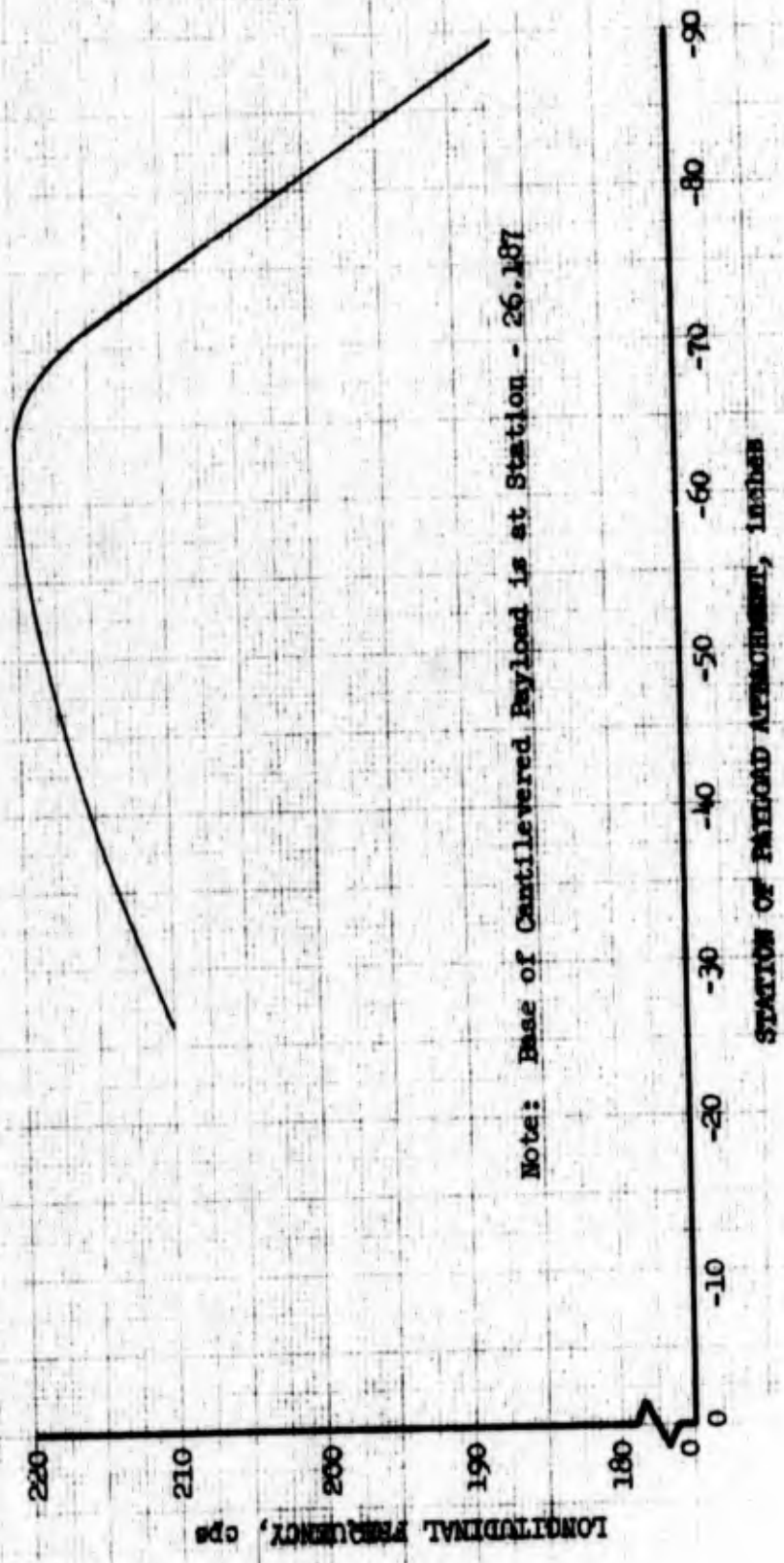
MINI

VARIATION OF LONGITUDINAL FIRST MODE NATURAL FREQUENCY WITH PAYLOAD ATTACH POINT

P.L. Weight = 181 lb

P.L. Length = 115.25

Configuration Includes a Payload Recovery System



Note: Base of Cantilevered Payload is at Station - 26.187

Figure 3-33

MIRO

LONGITUDINAL MODAL FREQUENCIES VS TIME

Brazil Flight 7,314 Payload

P.L. Weight = 161 lb

Payload Attached at Midpoint as Flown

No Acoustics Included

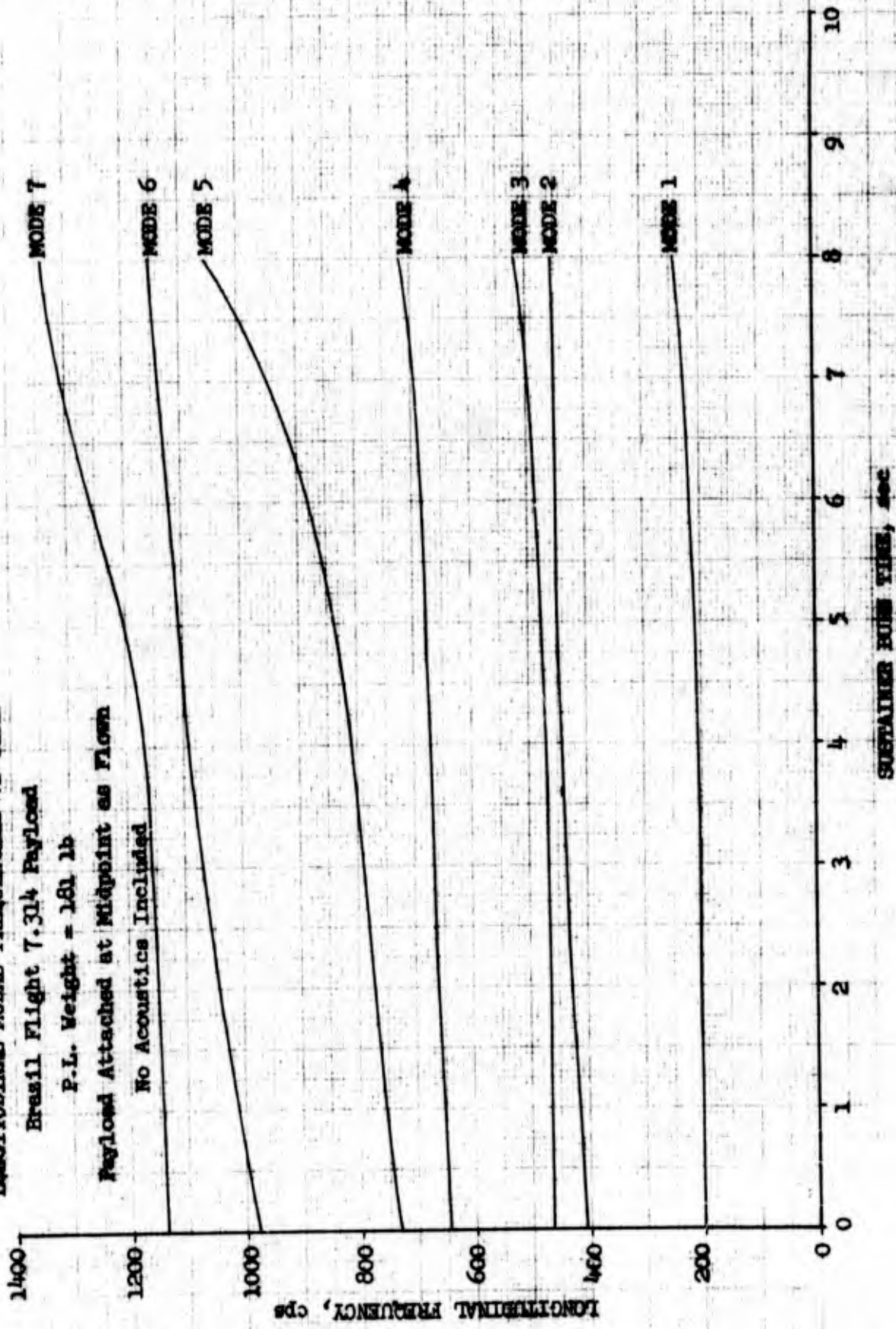




Figure 3-34

SHIP

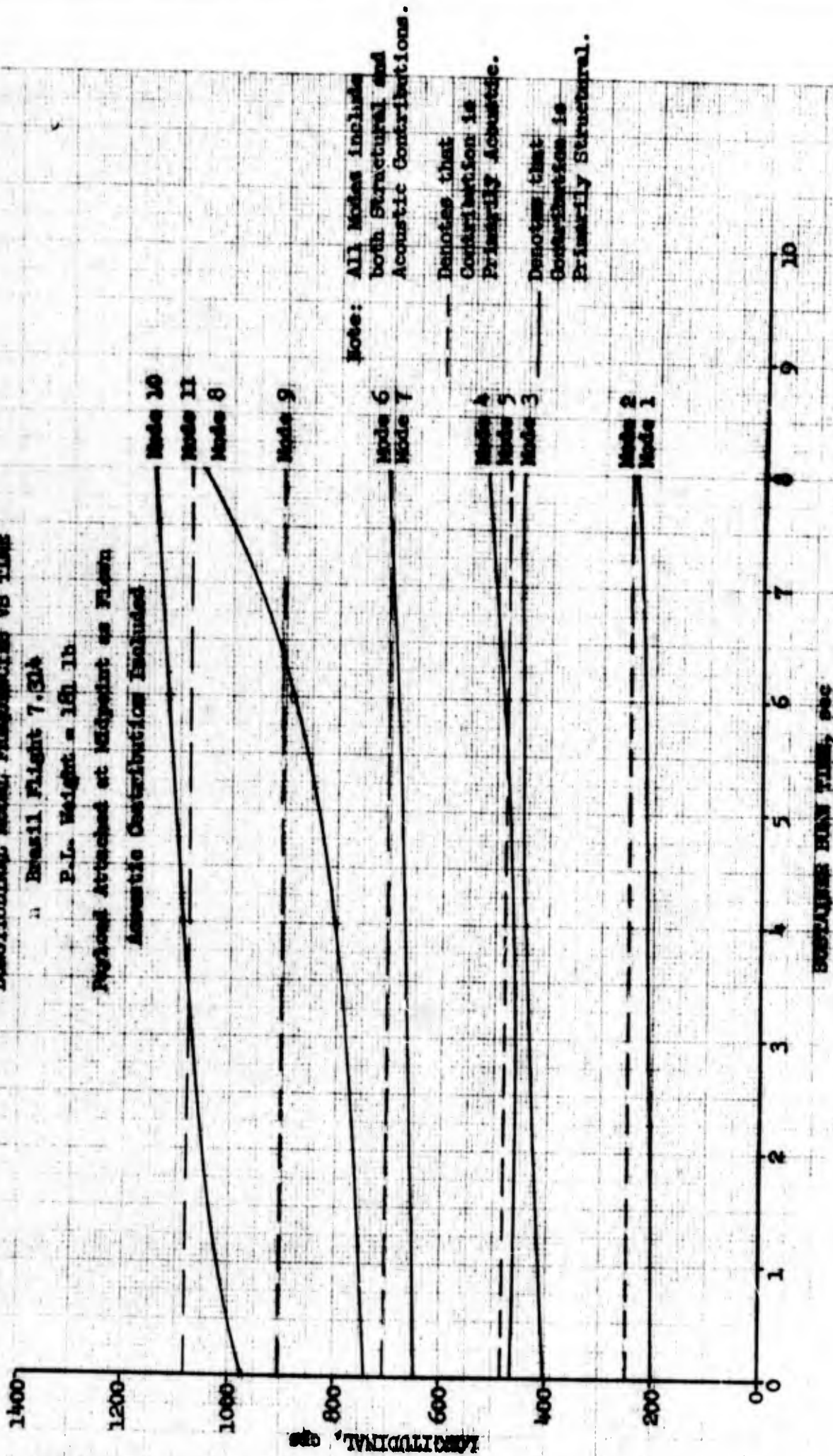
LONGITUDINAL MODES, FREQUENCIES VS TIME

" Basil Flight 7.504

P.L. Weight = 181 lb

Reform Attached at Midpoint as Flown

Acoustic Contribution Included



Note: All Modes include both Structural and Acoustic Contributions.

--- Denotes that Contribution is Primarily Acoustic.

— Denotes that Contribution is Primarily Structural.

Figure 3-35

NIRO

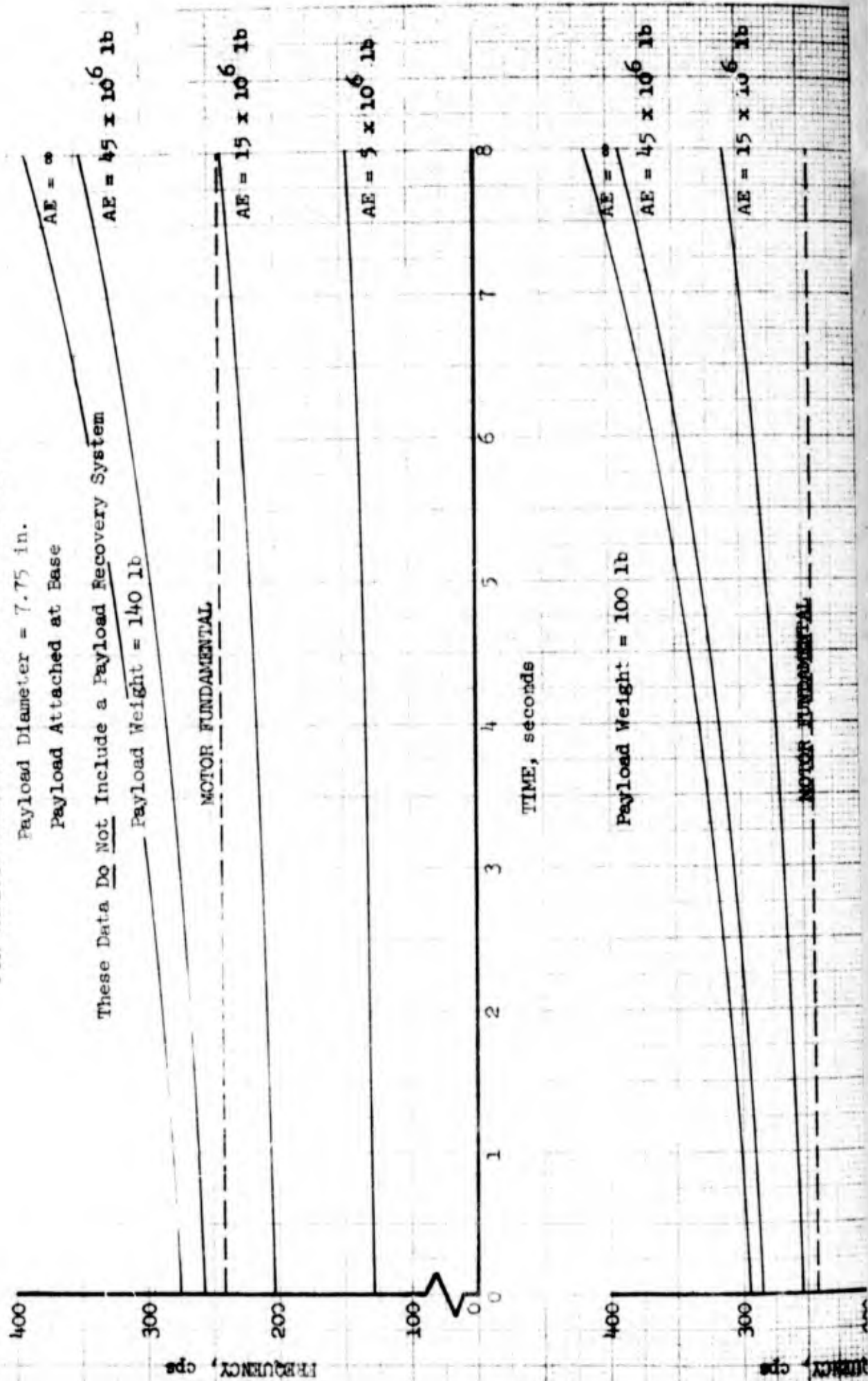
FIRST LONGITUDINAL STRUCTURAL FREQUENCY VS TIME  
FOR VARIOUS PAYLOAD LONGERON STIFFNESSES (AE)

Payload Diameter = 7.75 in.

Payload Attached at Base

These Data Do Not Include a Payload Recovery System

Payload Weight = 140 lb



A

MOTOR FUNDAMENTAL

$$AE = 5 \times 10^6 \text{ lb}$$

TIME, seconds

Payload Weight = 40 lb

$$AE = \infty$$

$$AE = 45 \times 10^6 \text{ lb}$$

$$AE = 15 \times 10^6 \text{ lb}$$

$$AE = 5 \times 10^6 \text{ lb}$$

MOTOR FUNDAMENTAL

Note: 1) All values shown were obtained by means of a simplified model assuming uniform mass and stiffness distributions.  
2) The payload configurations analyzed are shown in Figure

TIME, seconds

B



Figure 3-36

NIRO

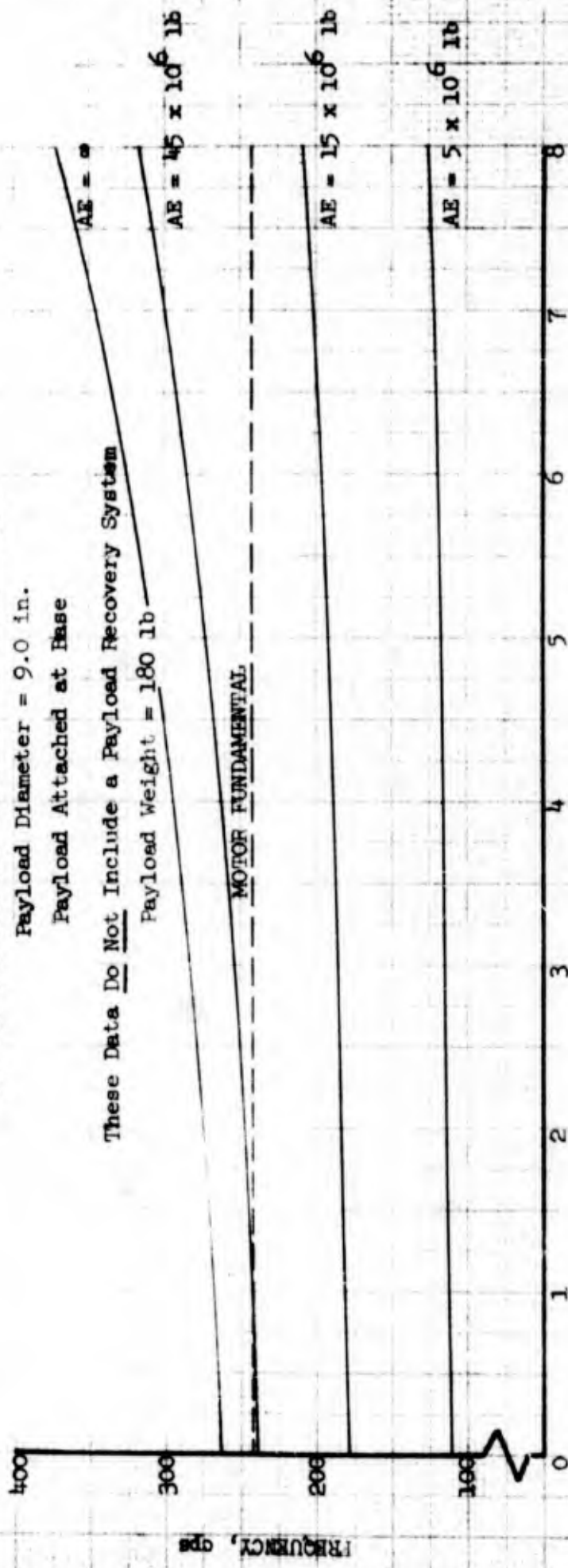
FIRST LONGITUDINAL STRUCTURAL FREQUENCY VS TIME  
FOR VARIOUS PAYLOAD LONGERON STIFFNESSES (AE)

Payload Diameter = 9.0 in.

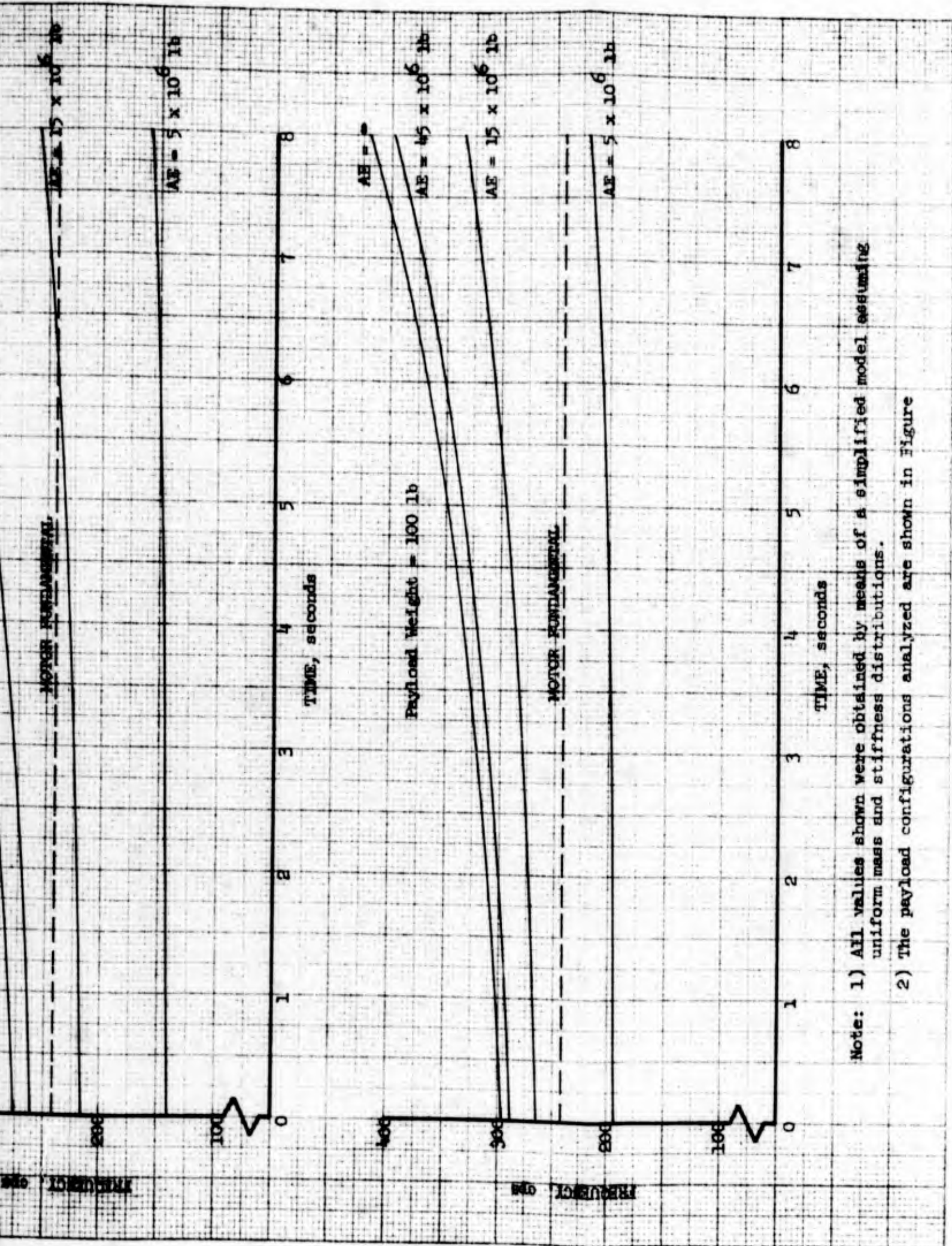
Payload Attached at Base

These Data Do Not Include a Payload Recovery System

Payload Weight = 180 lb



T



Note: 1) All values shown were obtained by means of a simplified model assuming uniform mass and stiffness distributions.  
 2) The payload configurations analyzed are shown in Figure

B



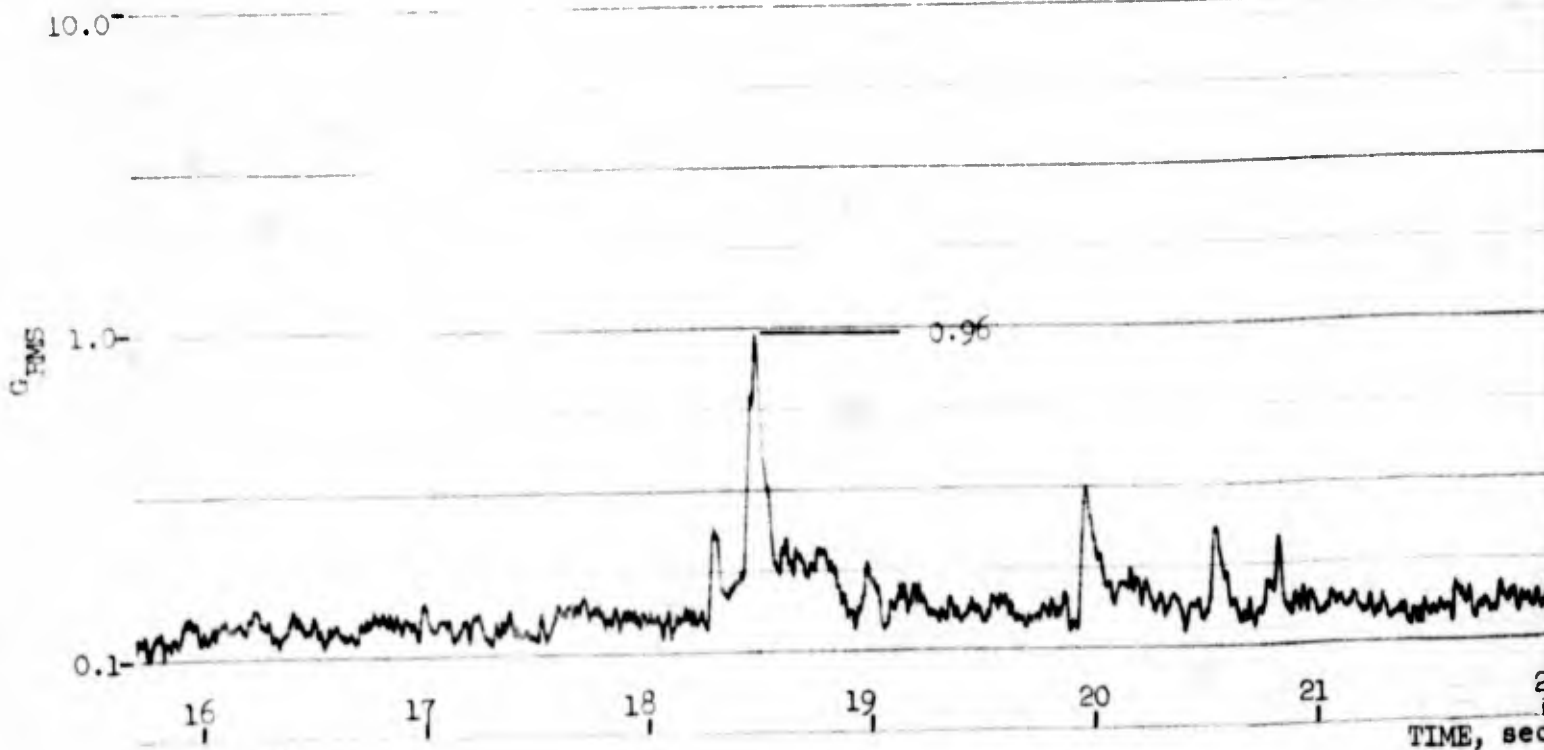
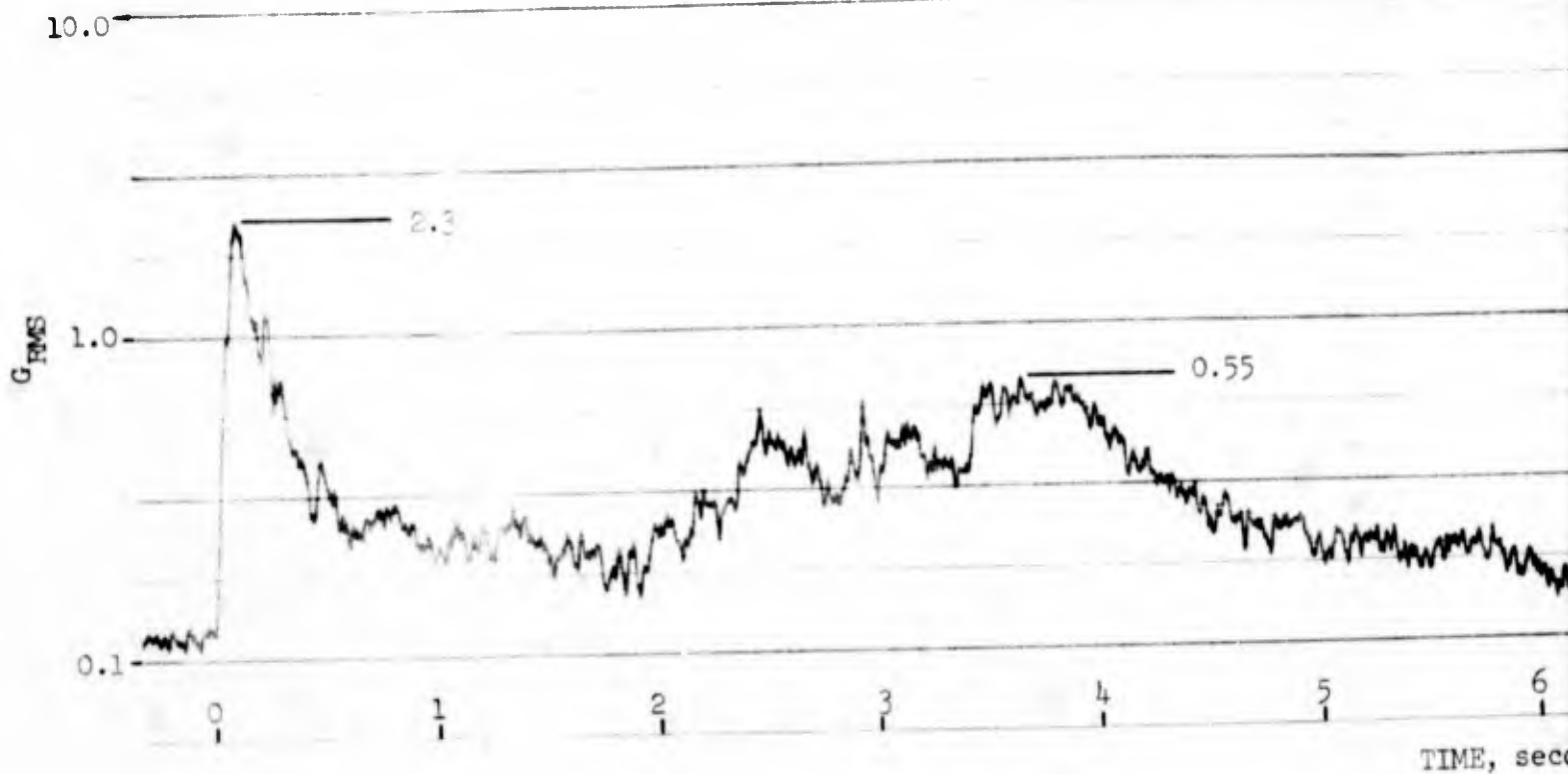
Figure 3-38

NIRO

Brazil Flight AG 7.314

LONGITUDINAL  $G_{RMS}$  vs TIME

Transducer Located at Payload Att.

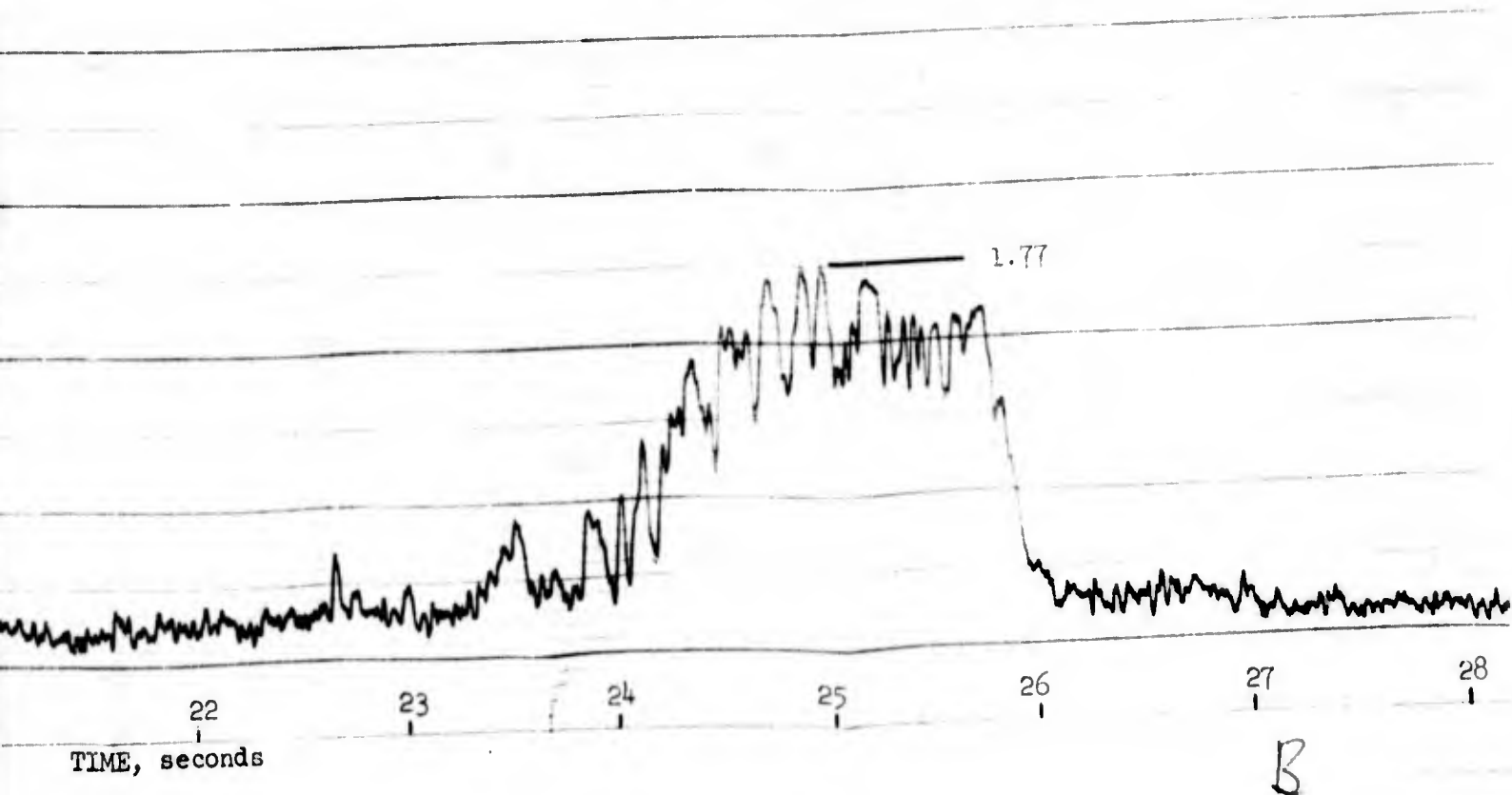
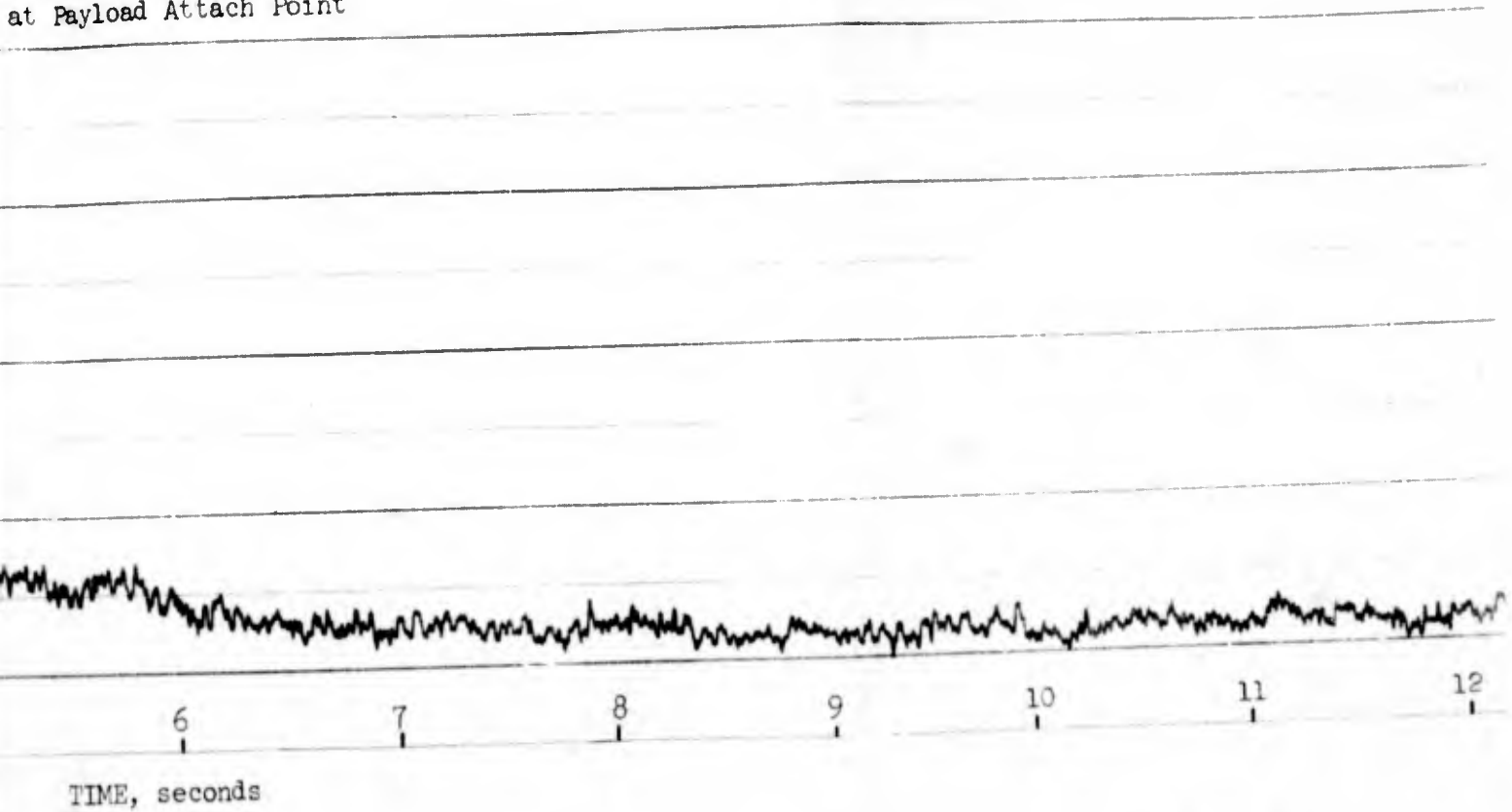


A



Figure 3-38

NIRO  
Flight AG 7.314  
ALG RMS vs TIME  
at Payload Attach Point



B

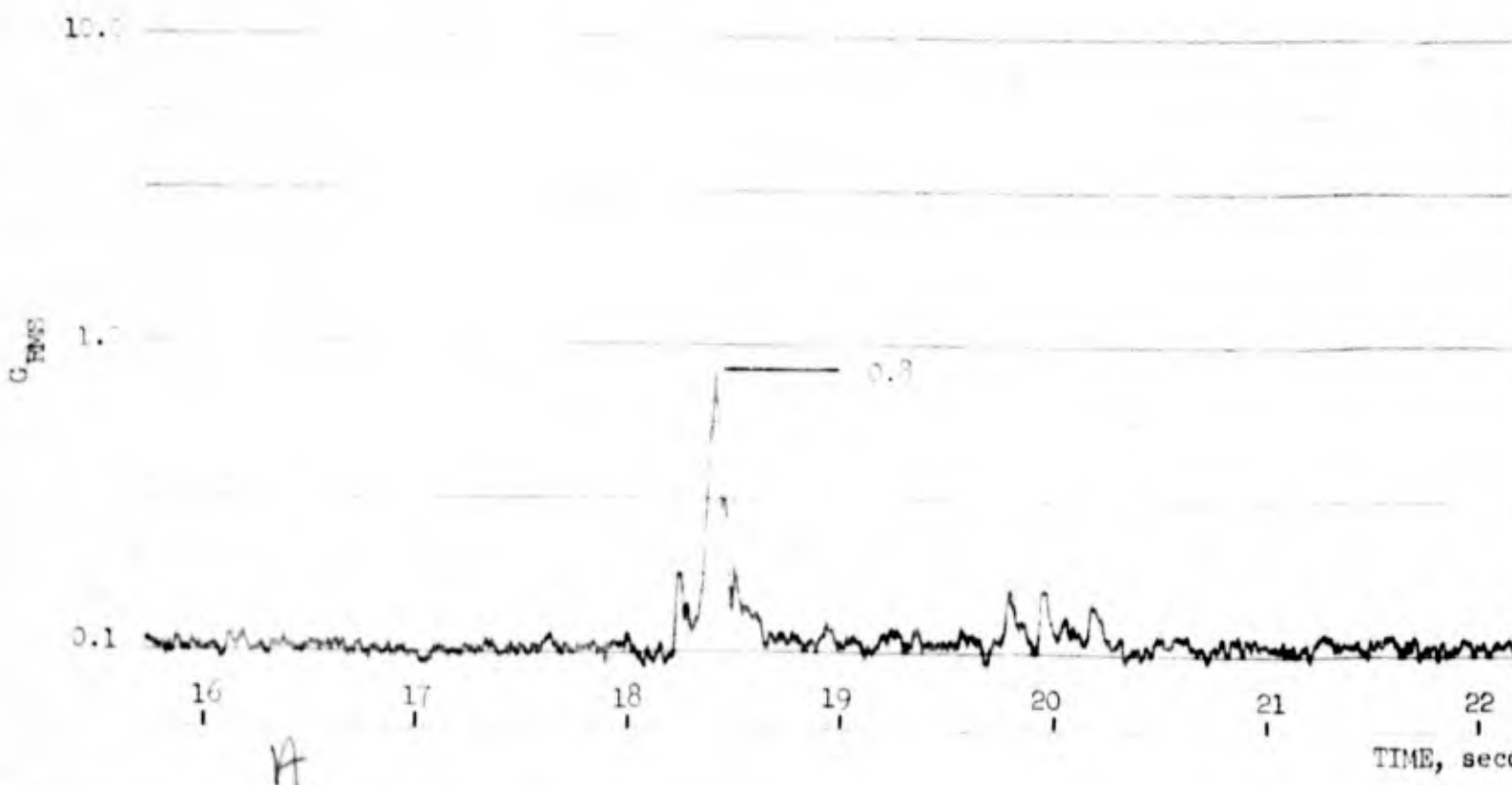
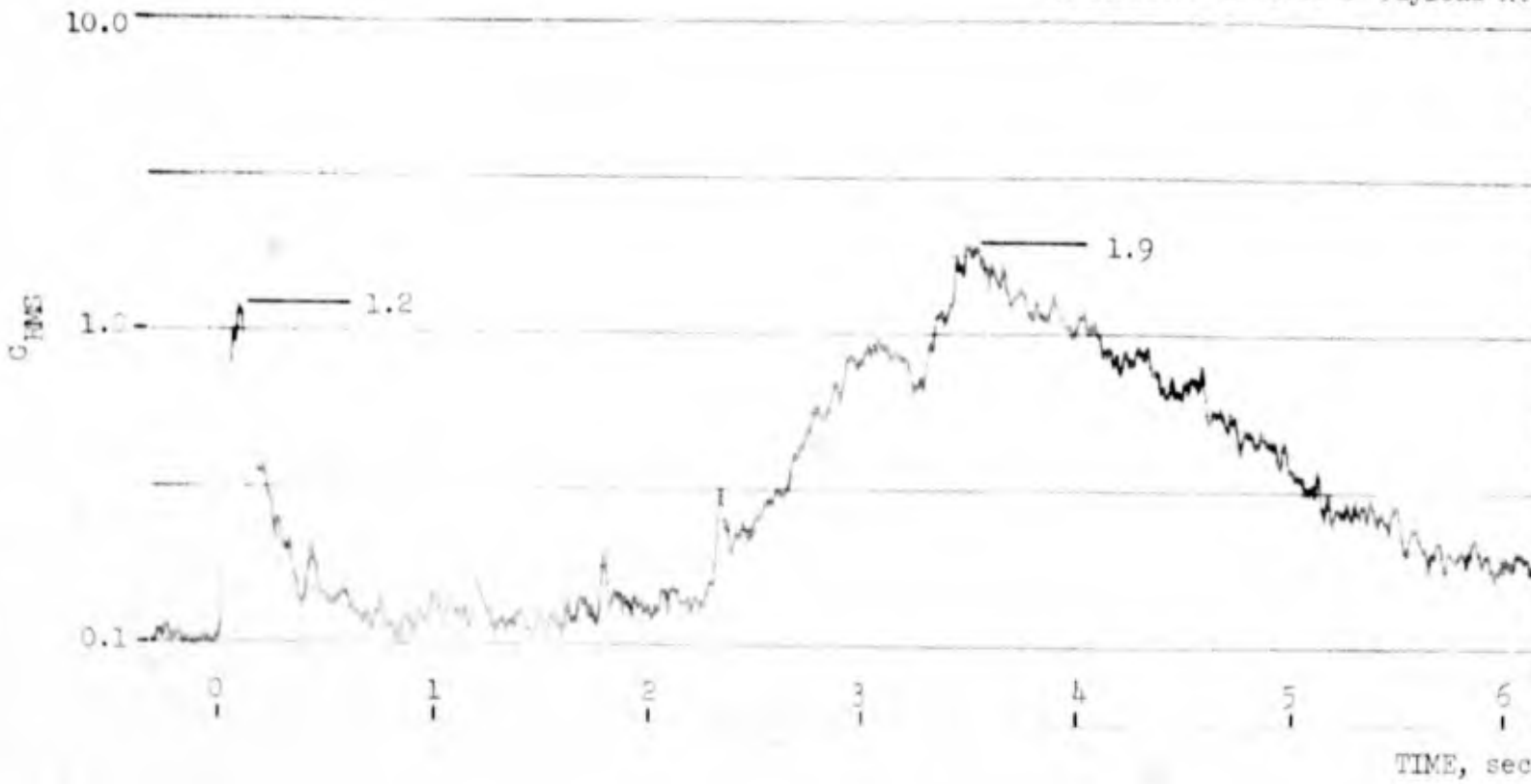
Figure 3-39

NIRO

Brazil Flight AG 7.316

LONGITUDINAL  $G_{RMS}$  vs TIME

Transducer Located at Payload Att



A

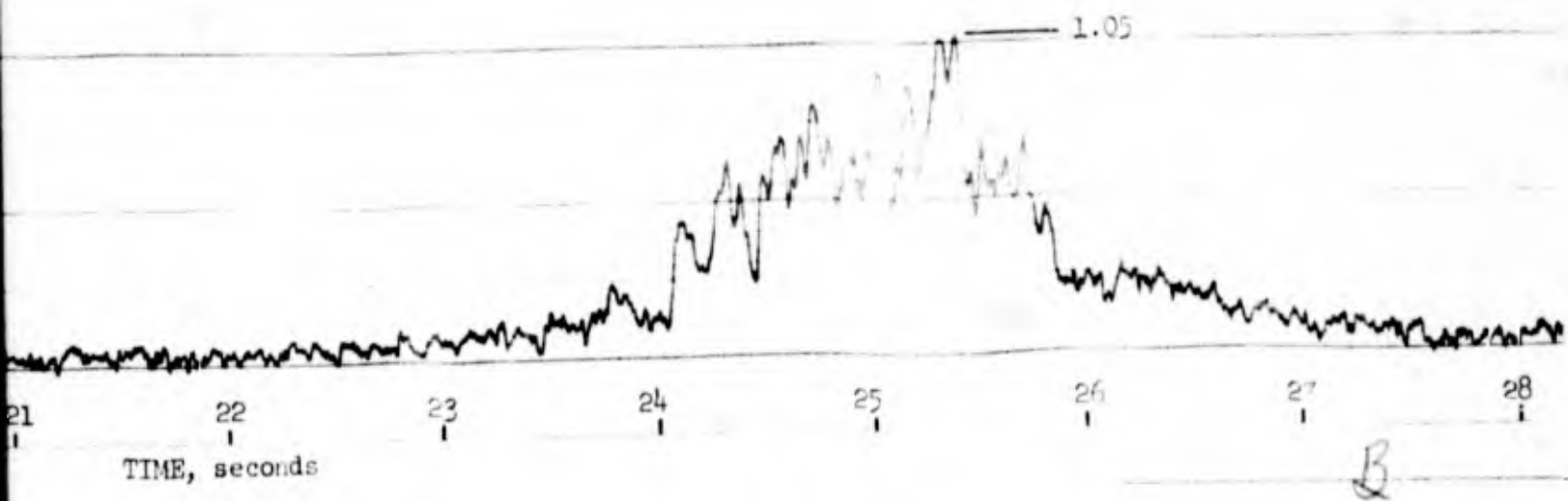
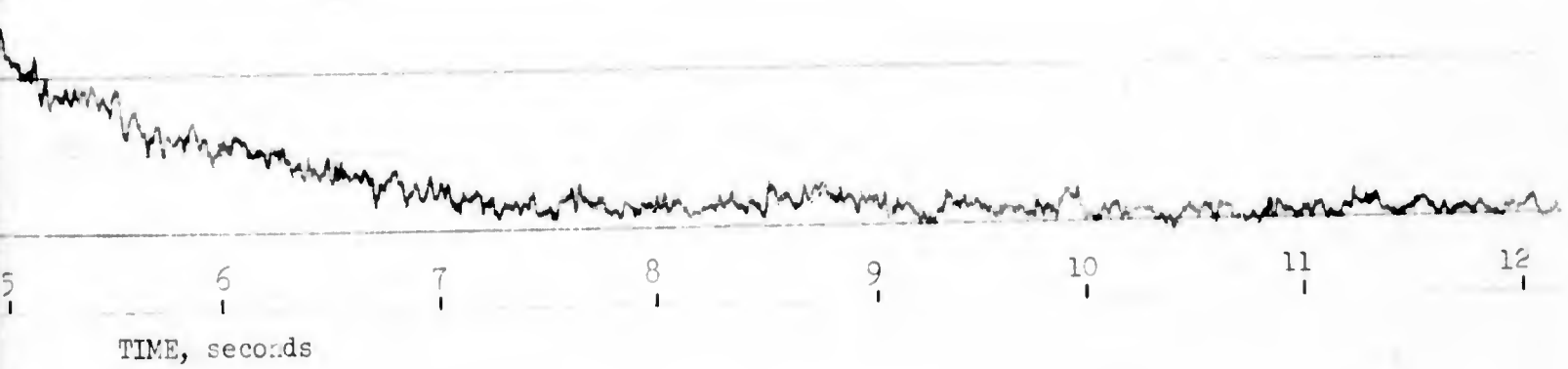
Figure 3-39

NIRO

Flight AG 7.316

ORIGINAL G<sub>RMS</sub> vs TIME

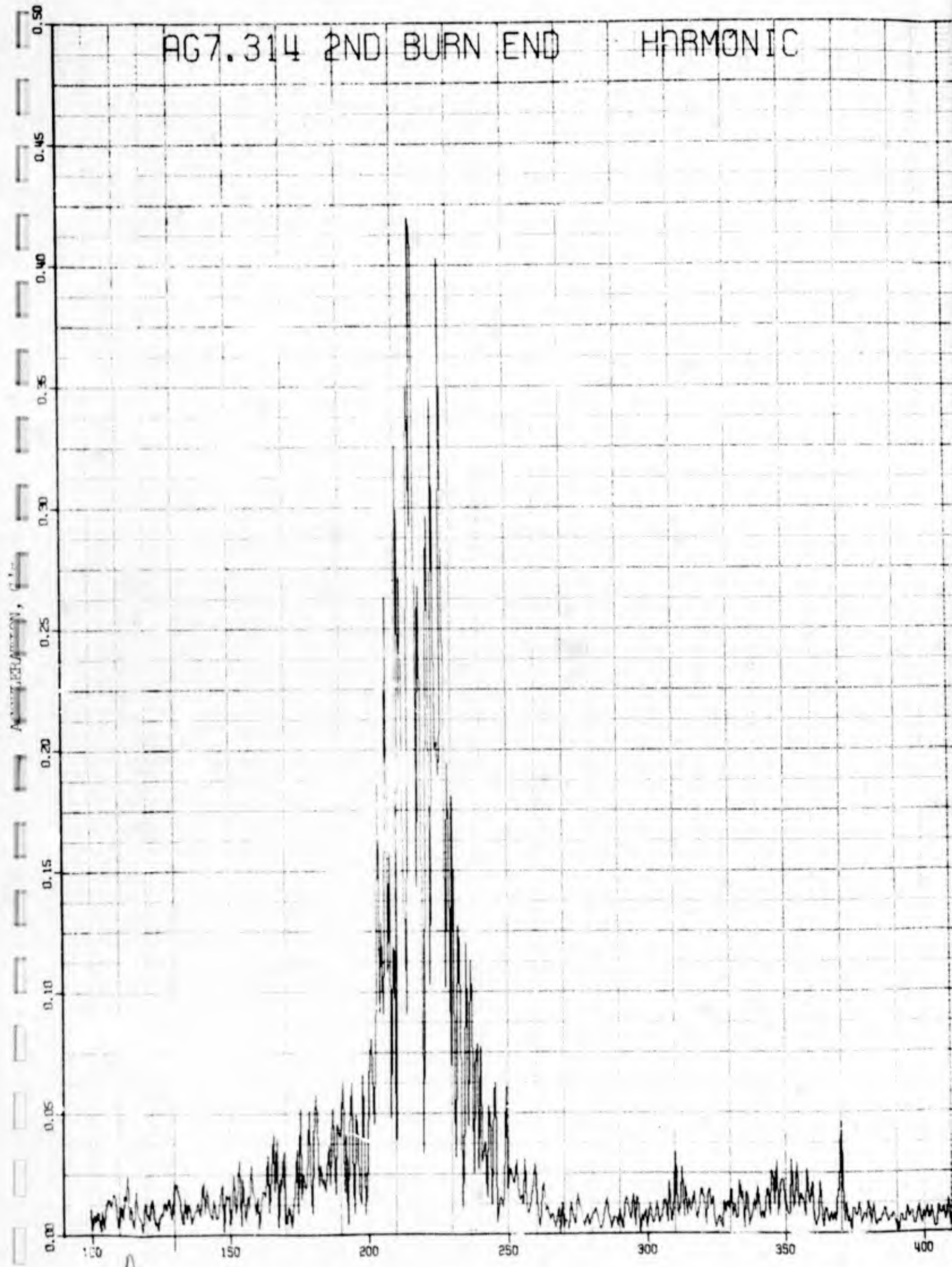
Recorded at Payload Attach Point



B



AG7.314 2ND BURN END HARMONIC



A

Figure 3-40

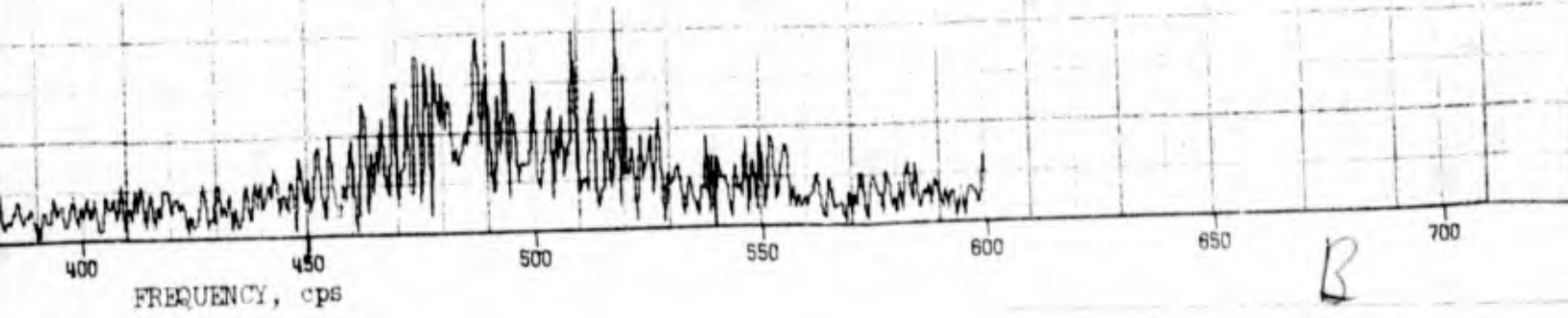
NIFO

Brazil Flight AG 7.314

HARMONIC ANALYSIS OF LONGITUDINAL VIBRATION  
DATA JUST PRIOR TO SUSTAINER BURSTOUT

Transducer Located at Payload Attach Point

Data Sample is 1.6 sec in Length



B

AG7.316 2ND BURN END HARMONIC

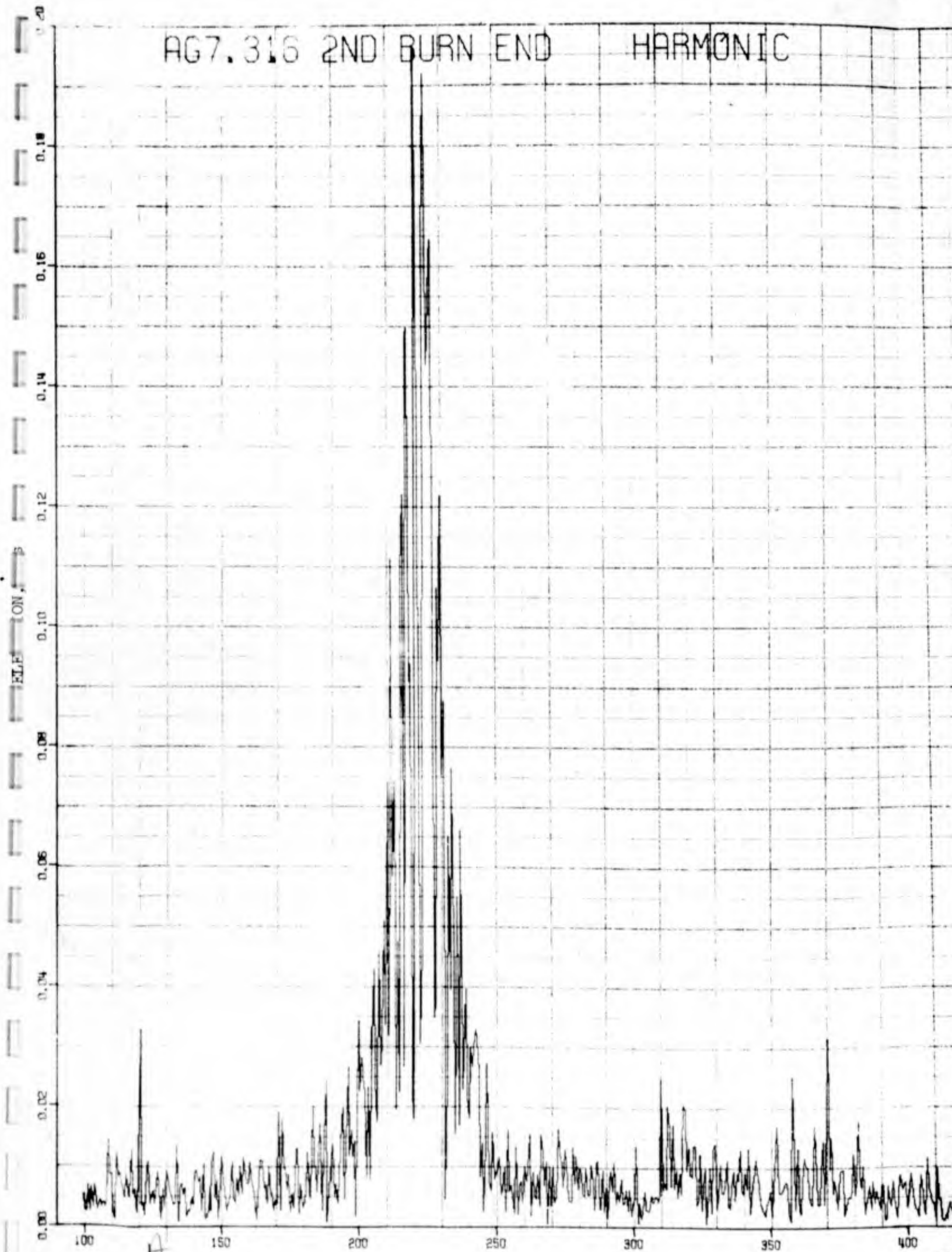


Figure 3-41

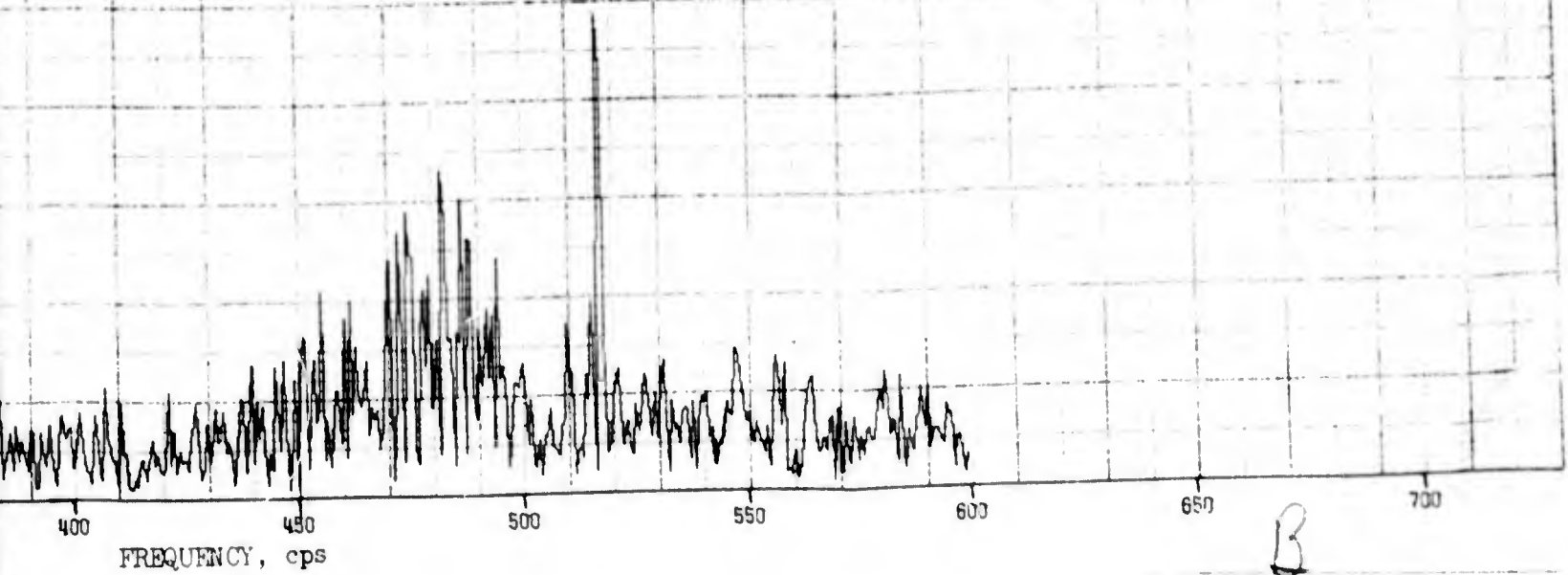
NIRO

Brazil Flight AG 7.316

HARMONIC ANALYSIS OF LONGITUDINAL VIBRATION  
DATA JUST PRIOR TO SUSTAINER BURNOUT

Transducer Located at Payload Attach Point

Data Sample is 1.64 sec in Length

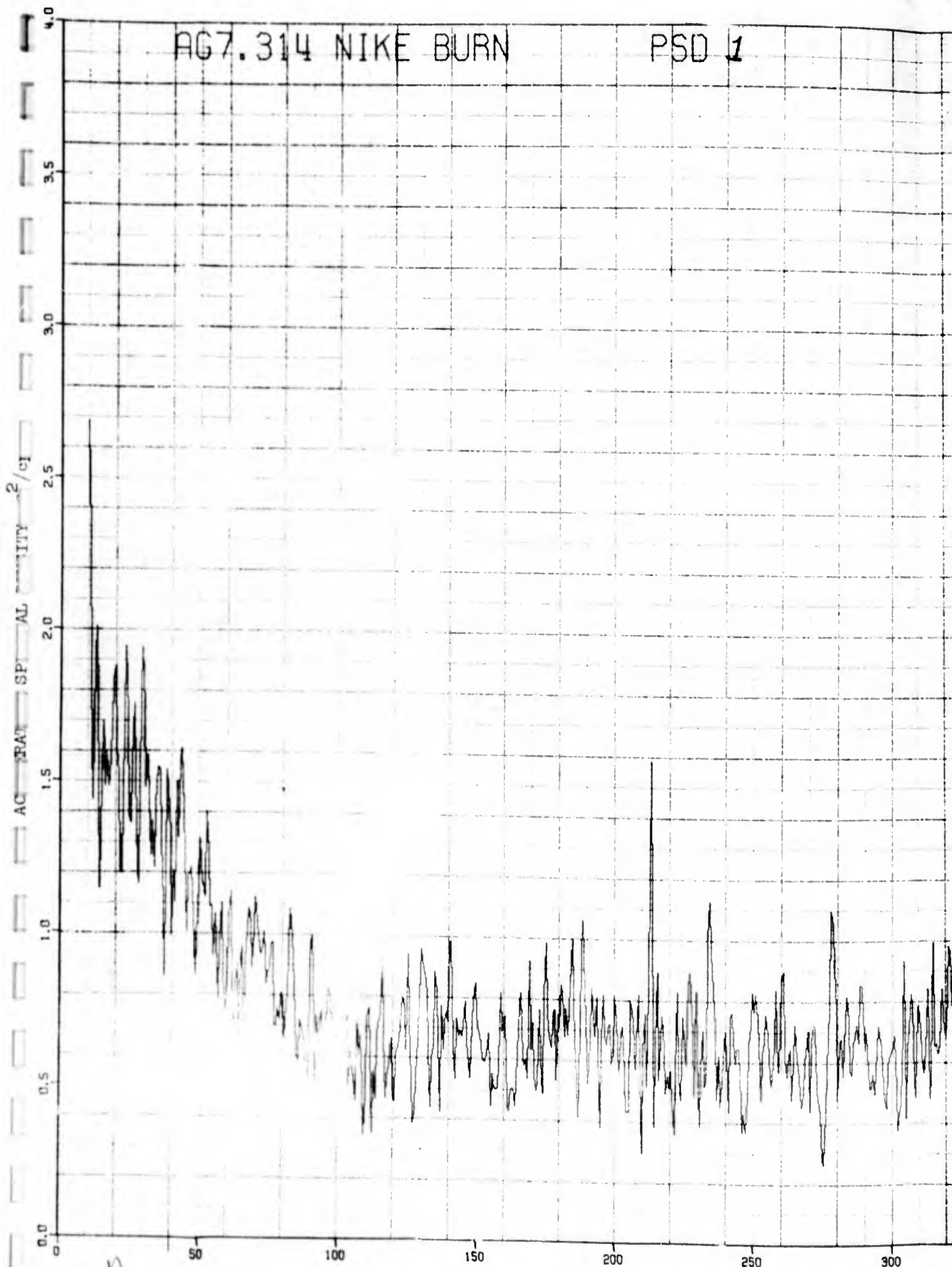


B



AG7.314 NIKE BURN

PSD 1



A

FREQU

Figure 3-42

NIRO

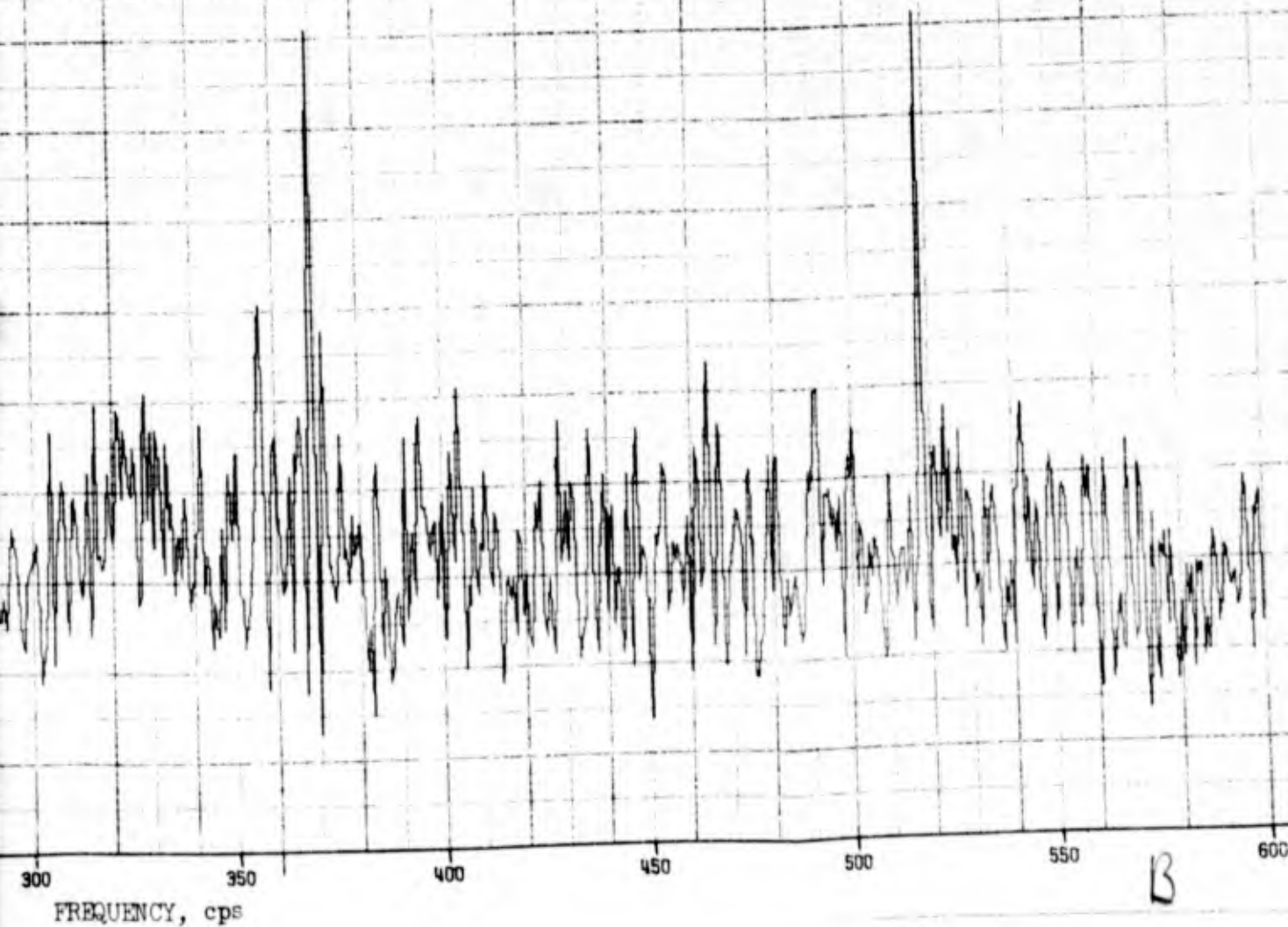
Brazil flight AG 7.314

POWER SPECTRAL DENSITY OF LONGITUDINAL  
VIBRATIONS AT STAGING

Transducer Located at Payload Attach Point

Data Sample is 1.64 sec in Length

Time Origin = 3.28 seconds



B



AG7.314 NIKE BURN

PSD 2

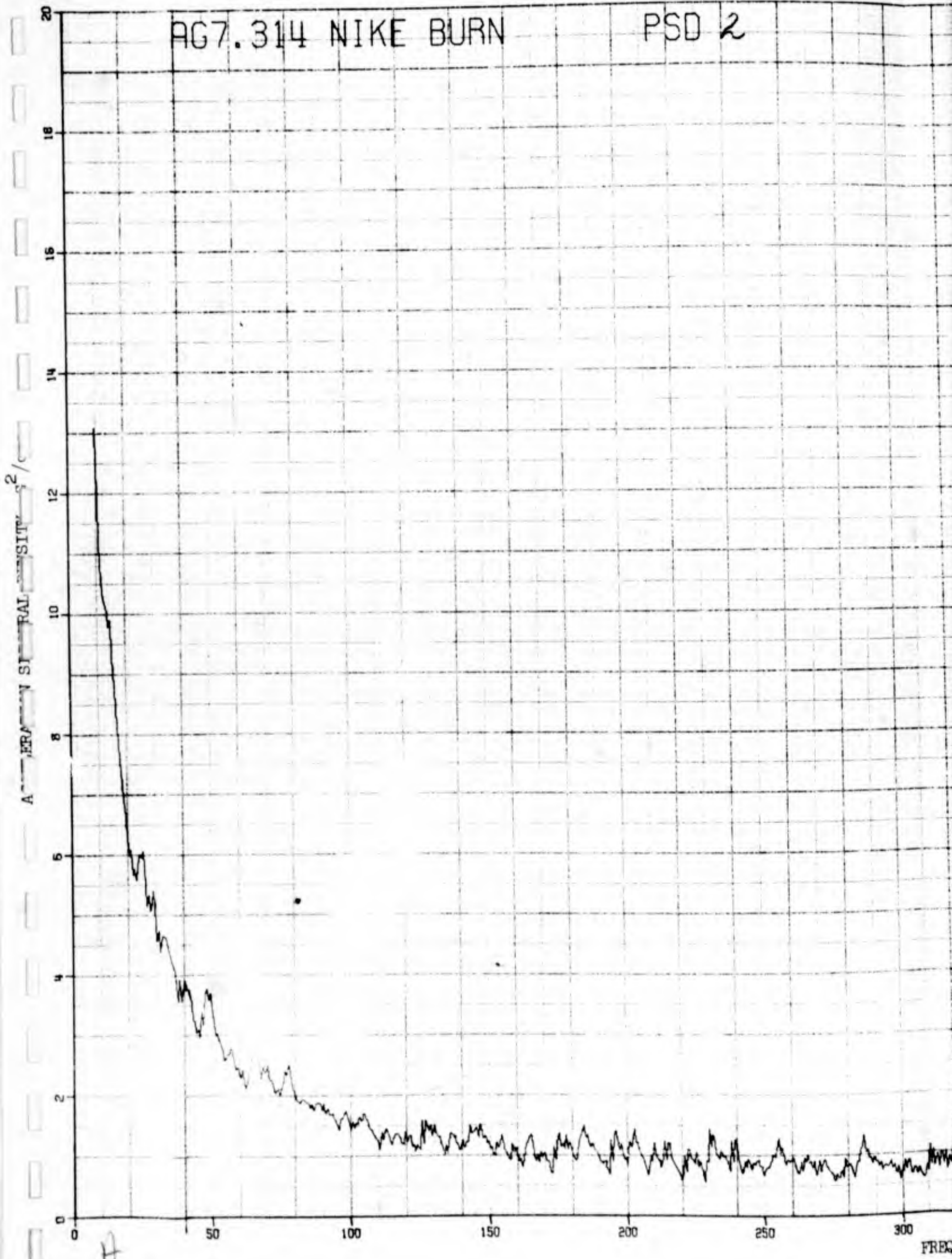


Figure 3-43

NIRO

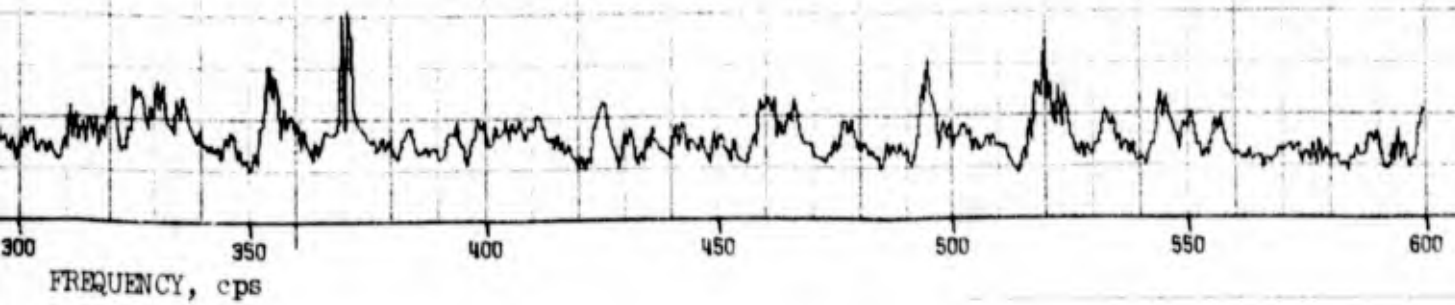
Brazil Flight AG 7.314

POWER SPECTRAL DENSITY OF LONGITUDINAL  
VIBRATIONS AT STAGING

Transducer Located at Payload Attach Point

Data Sample is 1.64 sec in Length

Time Origin = 3.32 seconds



AG7.316-NIKE BURN

PSD 1

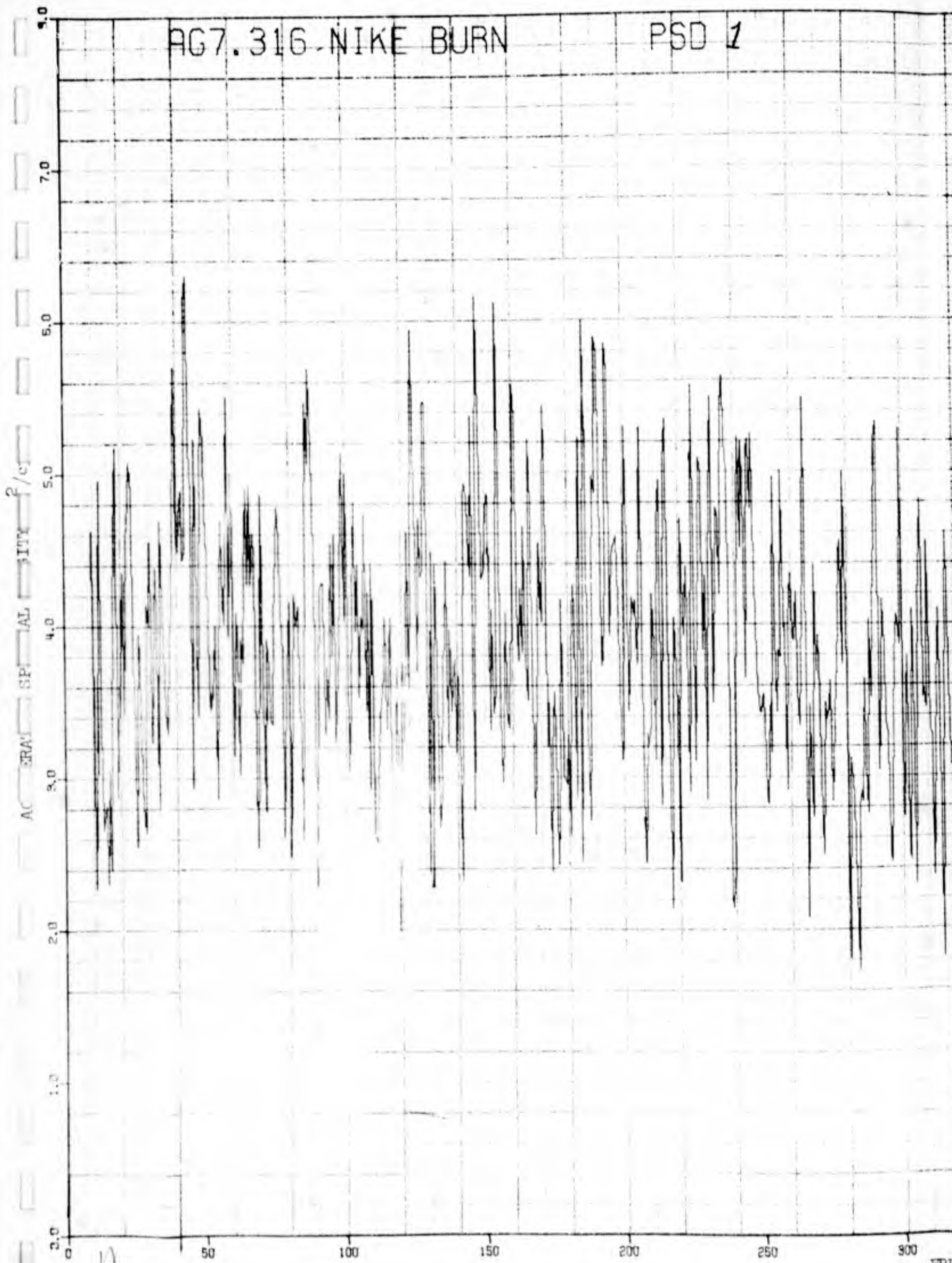


Figure 3-44

NIRO

Brazil Flight AG 7.316

POWER SPECTRAL DENSITY OF LONGITUDINAL  
VIBRATIONS JUST AFTER STAGING

Transducer Located at Payload Attach Point

Data Sample is 1.64 sec in Length

Time Origin = 3.69 seconds





AG7.316 NIKE BURN

PSD 2

ACCELERATION SPECTRAL DENSITY,  $\text{g}^2/\text{cps}^2$

20  
18  
16  
14  
12  
10  
8  
6  
4  
2  
0

A

50 100 150 200 250 300

FREQU

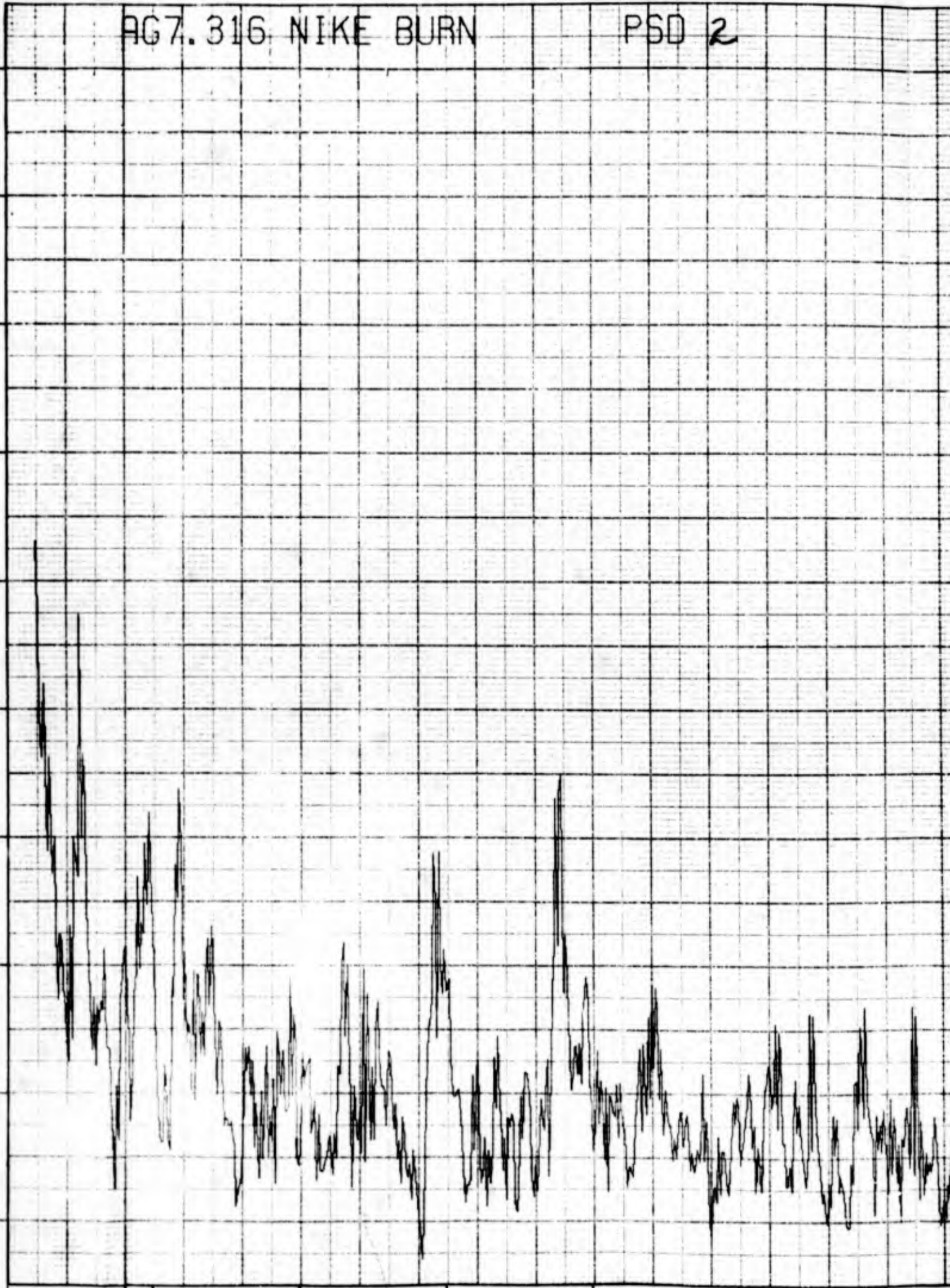


Figure 3-45

NIRO

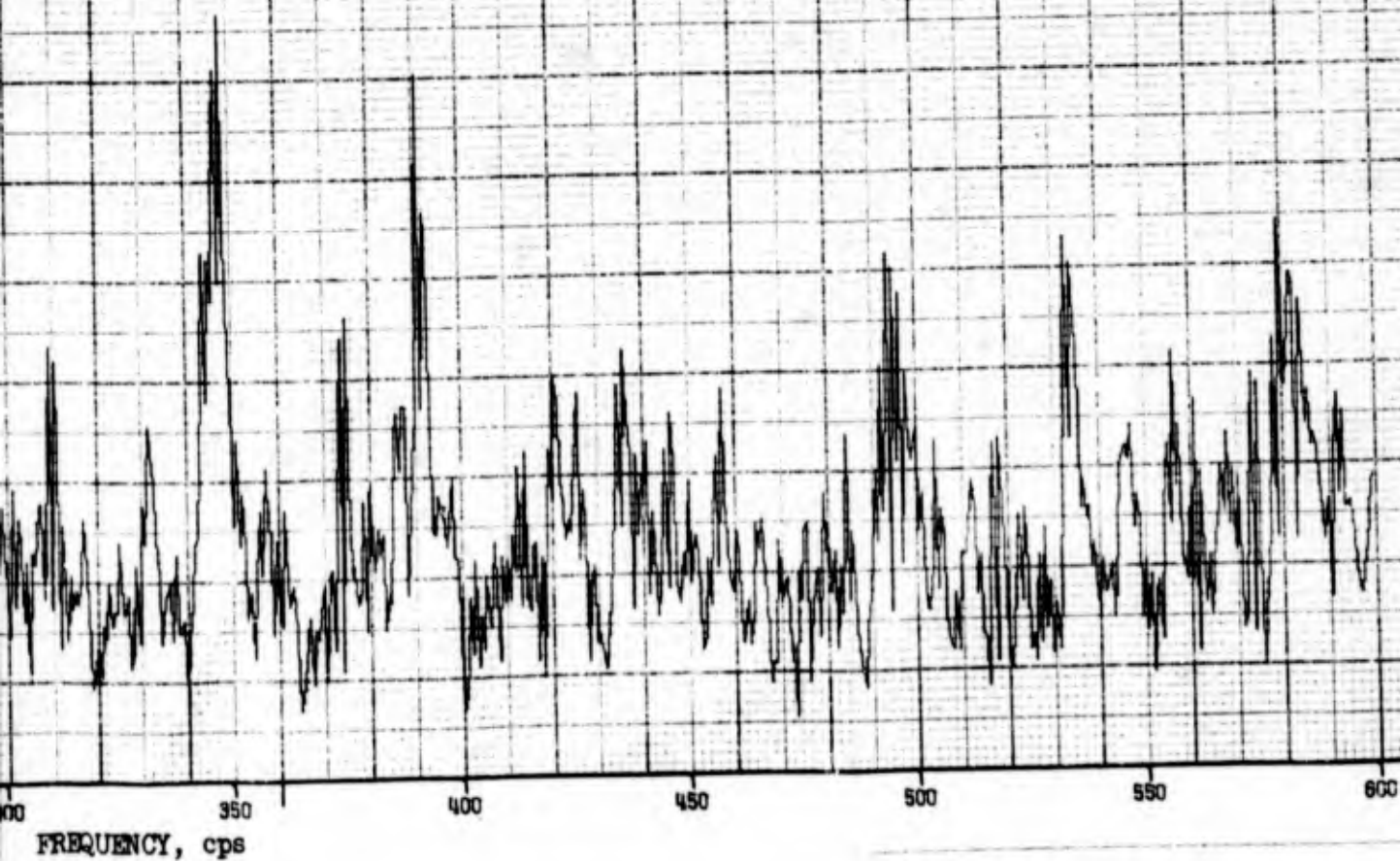
Brazil Flight AG 7 316

POWER SPECTRAL DENSITY OF LONGITUDINAL  
VIBRATIONS JUST AFTER STAGING

Transducer Located at Payload Attach Point

Data Sample is 1.64 sec in Length

Time Origin = 3.81 seconds





## Section IV

### NIRO MARS PLATFORM ANALYSIS

#### 4.1 INTRODUCTION

The MARS roll stabilized platform, built by Whittaker Corporation, is frequently used in sounding rockets to monitor the attitude histories of these vehicles. The output of this platform is a set of three angles which define vehicle orientation relative to the orientation at uncage. These angles, unfortunately, are not in a coordinate system such as to be immediately of great general interest and use. Therefore, work was initiated to develop a computer program which would manipulate the MARS data to provide time histories of a number of parameters of interest to the flight dynamicist. MARS data for NIRO Flight AF7-387 were available on magnetic tape and these data were selected for a test case for the computer program.

#### 4.2 RESULTS AND RECOMMENDATIONS

A computer program has been written in Fortran IV, for use on an IBM 360 Digital Computer, for the purpose of manipulating the output of a MARS roll stabilized platform and presenting this output in terms of variables which are of interest to the flight dynamicist. However, problems have been encountered in using the NIRO Flight AF7-387 MARS data tape which have precluded checkout and demonstration of the program.

The tape was prepared by Whittaker Corporation from the telemetered MARS output. This tape presents only five data points per second and has a number of errors which represent either errors in assigning a quadrant to a measured angle, or in the commutator segment assumed in decommutating the data. Thus, the errors are multiples of either  $90^{\circ}$  or  $20^{\circ}$ . The present program was written to attempt to resolve these errors automatically before proceeding with the balance of the data manipulation. It was decided to perform

this function by making a least-square fit to a number of preceding points and predicting the next data point. In the event of a large difference between the predicted value and the value on the tape, the value on the tape was to be incremented or decremented by  $10^0$  until the closest possible agreement was found. Due to the low data rate, as compared to the expected vehicle frequencies, a second order least squares fit to only five data points was selected for this error correcting routine. It was found that this extrapolation was unstable, and could not be used for its intended purpose. It appears necessary to either start the analysis from the telemetered data, which has a much higher data rate, or to develop a more sophisticated technique for testing the low data rate tape for errors. It is recommended that additional work be performed along one or the other of these lines and the program be brought to operational status, since it is apparent that much useful data are contained in the MARS records; albeit in a very inconvenient form.

#### 4.3 DISCUSSION

The work performed for this study may be divided into several steps, the first being the development of the equations defining the operations to be performed by the computer program, the second the programming itself, and the third the "debugging" of the program. Since the debugging could not be completed, there is no output from the program to report, and the program listing included in this volume as Appendix B is not operational.

##### 4.3.1 THE DEFINING EQUATIONS

Reference 4-1 defines several axis systems used to define the orientation of the vehicle. These are: the MARS coordinate system ( $x_m, y_m, z_m$ ), the uncage coordinate system ( $x_u, y_u, z_u$ ) and the launch site coordinate system ( $x_l, y_l, z_l$ ). All three are orthogonal, right-handed systems. The MARS coordinate system is fixed in the vehicle (body axis), with  $x_m$  forward. At launch, the uncage coordinate system is coincident with the MARS coordinate system. The uncage system is fixed relative to the launcher orientation at the time of launch. The orientation of the uncage system relative to the launch site coordinate system is given by three angles:  $\beta$ ,  $\gamma$ , and  $\Omega$ .

The launch site coordinate system is oriented so that  $x_l$  is north,  $y_l$  is east and  $z_l$  is down. To get from the launch site orientation to the uncage orientation, three successive rotations are made. The first is an azimuth rotation,  $\gamma$ , about  $z_l$  to the launcher azimuth. The second rotation is about the rotated  $y_l$  axis through the launcher elevation angle,  $\beta$ . After these rotations, the rotated  $x_l$  axis is coincident with the  $x_u$  axis, the rotated  $y_l$  axis is horizontal, and the rotated  $z_l$  axis is in a vertical plane, with a downward component for elevations ( $\beta$ ) less than  $90^\circ$ . Reference 4-1 gives the third axis rotation as  $\Omega - 90^\circ$  about the  $x_u$  axis.  $\Omega$  is denoted as the notch roll angle, referring to the platform mounting ring notch which is used as a roll reference. This notch is located along the  $-z_u$  axis. For a notch roll angle of  $90^\circ$  (equivalent to the vehicle being mounted on the depressed launcher so that the platform mounting ring notch is up), the third rotation (through  $\Omega - 90^\circ$ ) vanishes.

Three Euler rotations must be made to go from the uncage axis system to the MARS axis system. Using the notation of Reference 4-1, these are: first a rotation of  $\theta$  (denoted pitch in the reference) about the  $y_u$  axis; next a rotation of  $\psi$  (denoted yaw in the reference) about the rotated  $z_u$  axis; and finally a rotation of  $\phi$  (denoted roll in the reference) about the rotated  $x_u$  axis. It may be observed that the pitch and yaw designations have the generally accepted meanings only for a  $90^\circ$  notch roll angle ( $\Omega$ ). The "pitch" output of the MARS platform, denoted  $P_m$ , is not a true pitch angle, and must be modified, as shown in Reference 4-1.

$$\theta = -\tan^{-1} (\cos \psi \tan P_m) \quad (1)$$

Two transformation matrices define the rotations from the body (MARS) axes to the launch site axes:

$$A = \begin{bmatrix} \cos \gamma \cos \beta & -\cos \gamma \sin \beta \cos \Omega & \cos \gamma \sin \beta \sin \Omega \\ \sin \gamma \cos \beta & -\sin \gamma \sin \beta \cos \Omega & \sin \gamma \sin \beta \sin \Omega \\ -\sin \beta & -\cos \beta \cos \Omega & \cos \beta \sin \Omega \end{bmatrix} \quad (2)$$

to go from the uncage axes to the launch site axes, and,

$$B = \begin{bmatrix} \cos \theta \cos \psi & -\cos \theta \sin \psi \cos \phi & \cos \theta \sin \psi \sin \phi \\ \sin \psi & \cos \psi \cos \phi & -\cos \psi \sin \phi \\ -\sin \theta \cos \psi & +\cos \theta \sin \phi & +\cos \theta \cos \phi \end{bmatrix} \quad (3)$$

to go from the body (MARS) axes to the uncage axes. Defining:

$$C = AB, \quad (4)$$

then

$$\{\xi_l\} = C \{\xi_m\} \quad (5)$$

where  $\{\xi_l\}$  is a vector resolved in the launch site axis system and  $\{\xi_m\}$  is the same vector in the body axes. From Reference 4-2,

$$\dot{\xi} = \left( \frac{-d}{dt} [C]^{-1} \right) [C] \quad (6)$$

where

$$\dot{\xi} = \begin{bmatrix} 0 & -r & q \\ r & 0 & -p \\ -q & p & 0 \end{bmatrix} \quad (7)$$

and p, q, and r are the body axis components of the vehicles angular rates, along  $x_m$ ,  $y_m$ , and  $z_m$ , respectively. Since A is time invariant,

$$\frac{d}{dt} [C]^{-1} = \left( \frac{d}{dt} [B]^{-1} \right) [A]^{-1} \quad (8)$$

and,

$$\tilde{\omega} = \left( \frac{d}{dt} [B]^{-1} \right) [B] \quad (9)$$

performing the operations denoted by Equation (9) yields:

$$p = \dot{\phi} + \dot{\theta} \sin \psi \quad (10)$$

$$q = \dot{\theta} \cos \psi \cos \phi + \dot{\psi} \sin \phi \quad (11)$$

$$r = \dot{\psi} \cos \phi - \dot{\theta} \cos \psi \sin \phi \quad (12)$$

It is important to note from Equation (10) that the spin rate, p, is not equivalent to the time rate of change of the roll angle ( $\dot{\phi}$ ). This makes assessment of the spin rate from a casual inspection of the roll history inaccurate and misleading, except when the angle  $\psi$  is nearly zero, or  $\dot{\theta}$  is nearly zero.

The angular accelerations of the vehicle are given by differentiation of Equation (10) through (12):

$$\dot{p} = \ddot{\phi} + \ddot{\theta} \sin \psi + \dot{\theta} \dot{\psi} \cos \psi \quad (13)$$

$$\dot{q} = \ddot{\theta} \cos \psi \cos \phi - \dot{\theta} \dot{\psi} \sin \psi \cos \phi - \dot{\theta} \dot{\phi} \cos \psi \sin \phi + \ddot{\psi} \sin \phi + \dot{\psi} \dot{\phi} \cos \phi \quad (14)$$

$$\dot{r} = \ddot{\psi} \cos \phi - \dot{\psi} \dot{\phi} \sin \phi - \ddot{\theta} \cos \psi \sin \phi + \dot{\theta} \dot{\psi} \sin \psi \sin \phi - \dot{\theta} \dot{\phi} \cos \psi \cos \phi \quad (15)$$

The first and second derivations of  $\psi$ ,  $\phi$ , and  $\theta$  needed in Equation (10) through (15) are approximated by fitting three successive values of each of the variables to a quadratic in time and differentiating this quadratic as necessary. The evaluation is always done at the interior point of the fitted set.



The angular momentum components, in body axes, are evaluated as,

$$H_x = p I_x \quad (16)$$

$$H_y = q I \quad (17)$$

$$H_z = r I \quad (18)$$

where  $I_x$  is the roll moment of inertia and  $I$  is the transverse moment of inertia. The coning angle is evaluated as

$$\phi_c = \tan^{-1} \left[ (H_y^2 + H_z^2)^{1/2} / H_x \right] \quad (19)$$

The net moments acting on the vehicle, i. e., those which cause changes in trim, are given by:

$$L = I_x \dot{p} \quad (20)$$

$$M = I \dot{q} + (I_x - I) p r \quad (21)$$

$$N = I \dot{r} + (I - I_x) p q \quad (22)$$

Since the  $\dot{p}$  and  $\dot{r}$  terms do not appear on the right side of the equations, the moment components  $L$ ,  $M$ , and  $N$  (along the  $x_m$ ,  $y_m$ ,  $z_m$  axes, respectively) contain the complete terms usually denoted as jet damping.

Equation (5) is used to define the orientation, relative to the launch site axes, of the angular momentum vector and of the vehicle's spin axis. The angular momentum components, in launch site axes, are given by:

$$\begin{Bmatrix} H_{x_l} \\ H_{y_l} \\ H_{z_l} \end{Bmatrix} = C \begin{Bmatrix} H_x \\ H_y \\ H_z \end{Bmatrix} \quad (23)$$

The azimuth of the angular momentum vector is given by

$$\psi_H = \tan^{-1} \left( H_{y_l} / H_{x_l} \right)$$

and the elevation of this vector by:

$$\theta_H = \tan^{-1} \left[ -H_{z_l} / \left( H_{y_l}^2 + H_{x_l}^2 \right)^{1/2} \right] \quad (24)$$

The directional cosines of the spin axis ( $x_m$ ) in the launch site system are:

$$\begin{Bmatrix} a_{x_l} \\ a_{y_l} \\ a_{z_l} \end{Bmatrix} = C \begin{Bmatrix} 1 \\ 0 \\ 0 \end{Bmatrix} \quad (25)$$

The azimuth of the spin axis is given by

$$\psi_x = \tan^{-1} \left( a_{y_l} / a_{x_l} \right) \quad (26)$$

and the elevation by

$$\theta_x = \tan^{-1} \left[ -a_{z_l} / \left( a_{x_l}^2 + a_{y_l}^2 \right)^{1/2} \right] \quad (27)$$

The roll orientation of the transverse rate is measured counterclockwise (looking in the  $+x_m$  direction) from the  $z_m$  axis, and is given by:

$$\phi_Q = \tan^{-1} (q/r) \quad (28)$$

The roll orientation of the net transverse moment (using the same convention as  $\phi_Q$ ) is given by:

$$\phi_M = \tan^{-1} (M/N) \quad (29)$$

It is apparent that if a velocity vector history were available, a great many more parameters of interest to flight dynamicists would be derivable if this velocity data were used in combination with the MARS data.

#### 4.4 COMPUTER PROGRAM

The computer program which was written to interpret the MARS platform output data is written in Fortran IV and is compatible with an IBM 360 digital computer. The subroutines which produce automatic plots are facility dependent, and those in the program are compatible with the Calcomp Automatic Plotter at the Aerojet-General Space Division Facility. However, little change should be necessary to adapt the program to other plotters.

Appendix B gives a listing of the program as it is presently constituted. It must be emphasized that this program is not yet operational. The program is organized in conventional form, having a main program and a number of subroutines. To perform various phases of the job, the main program calls four subroutines, once each. The first call from the main program is to the subroutine  $\text{OUTFIT}$ , and this call results in the printing of headings for a listing of the results of the subroutine  $\text{FIXTPE}$ , which smooths and decommutates the input data. The second call from the main program is to  $\text{FIXTPE}$ .  $\text{FIXTPE}$  reads a tape which has a number of binary records of the form (time,  $\phi$ ,  $\theta$ ,  $\psi$ ) or (time,  $\phi$ ,  $P_m$ ,  $\psi$ ). The number of records to be read is denoted by an input variable  $\text{NP}\text{OINT}$ . A flag  $\text{IF}\text{OORTH}$  denotes whether  $\theta$  or  $P_m$  is being read. If  $\text{IF}\text{OORTH}$  is equal to zero,  $\theta$  is determined from  $P_m$  using Equation (1). If  $\text{IF}\text{OORTH}$  is non-zero, the program assumes that  $\theta$  has been read. As the input tape is read, corrections to particular items on the tape may be made by input cards which identify the record in which the change is to be made ( $\text{NPT}$ ), which words in the record are to be changed (by flags  $\text{K}(1)$  through  $\text{K}(4)$ , which are set to a non-zero value when a word is to be changed) and the value to be inserted ( $\text{Y}(1)$  through  $\text{Y}(4)$ ).  $\text{FIXTPE}$  produces a new data set which varies from the original input tape in that the changes input by cards are included, and the angles (which are initially read in degrees) are converted to radian measure. The next function of  $\text{FIXTPE}$  is to complete the decommutation of the data, and optionally to remove errors produced in the earlier decommutation. The tape which has been input to this program should be considered only partially decommutated since the MARS platform output which has a  $20^\circ$  bandwidth has been converted to a  $360^\circ$  bandwidth. Since the data are to be differentiated, it is necessary that the angle

representations be continuous (i. e., that  $0^\circ$  and  $360^\circ$  are not equivalent). Therefore, FIXTPE appropriately increments or decrements the angle data prepared in the first pass by  $2\pi$  until the data are continuous. If a non-zero value of the flag IFFIX is input, this subroutine also removes errors in the initial decommutation. This is done by making a running second order least squares fit to five consecutive values of each of the three Euler angles and comparing a predicted next value of each angle with the next value found on the data set being processed. When the disagreement exceeds  $5^\circ$ , the value read is incremented or decremented by  $10^\circ$  until the value agrees with the predicted value within  $5^\circ$ . The second order least squares fit is performed by the subroutine FIT2ND, which uses the method of determinants, and for this purpose employs the function subroutine DETMNT. Since 5 points are required for the least squares fit, the first 5 points on the input data set are not smoothed, nor are the first five points of each stage. In order to identify staging points, the number of staging points is input as the variable NSTGE (which may be as great as 5) and the staging times are input in the array TSTGE. In order for the program to be able to correlate the staging times with the data on the input tape, the appropriate time data points should be overwritten (during the first pass in FIXTPE) with the exact values entered in TSTGE. After FIXTPE has prepared a smooth decommutated data set defining the Euler angles, control is returned to the main program.

The main program next calls FIRST which, using the final data set created by FIXTPE, performs the operations defined by Equation (2) through (29) to produce the desired output variables. When FIRST is initially entered, it clears the data storage areas and then calls INPUT, which handles the inputting of time dependent tables of the roll and transverse moments of inertia, the time scale of the curves to be plotted (TPERIN, in seconds/inch) the angles  $\beta$ ,  $\gamma$ , and  $\Omega$ , and the flight time to which data are to be processed. Subroutine INPUT is a generalized input routine, to allow for the inputting of additional data in the event of program growth. After control of the program is returned to FIRST, this subroutine computes the variables to be output, for

each record on the data set prepared by FIXTPE, until the upper time limit (TEND) is reached. At the end of the computations of each time point, FIRST calls IPRINT to create a printed output report, and ITAPE to prepare a data set containing the calculated parameters. When TEND is reached, the time in the last record transmitted to ITAPE is made negative to act as an end of file flag for the routine using the data set prepared by ITAPE. Control is then returned to the main program.

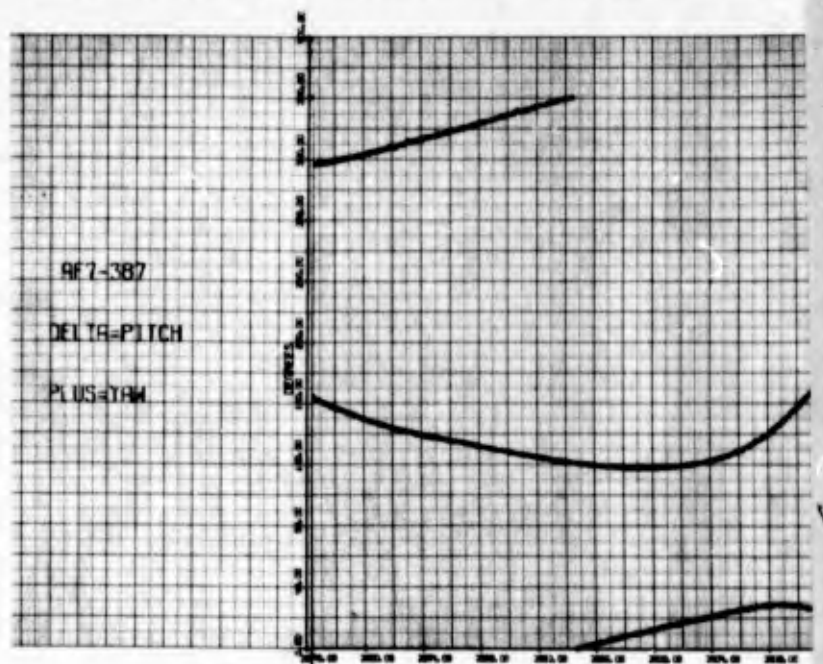
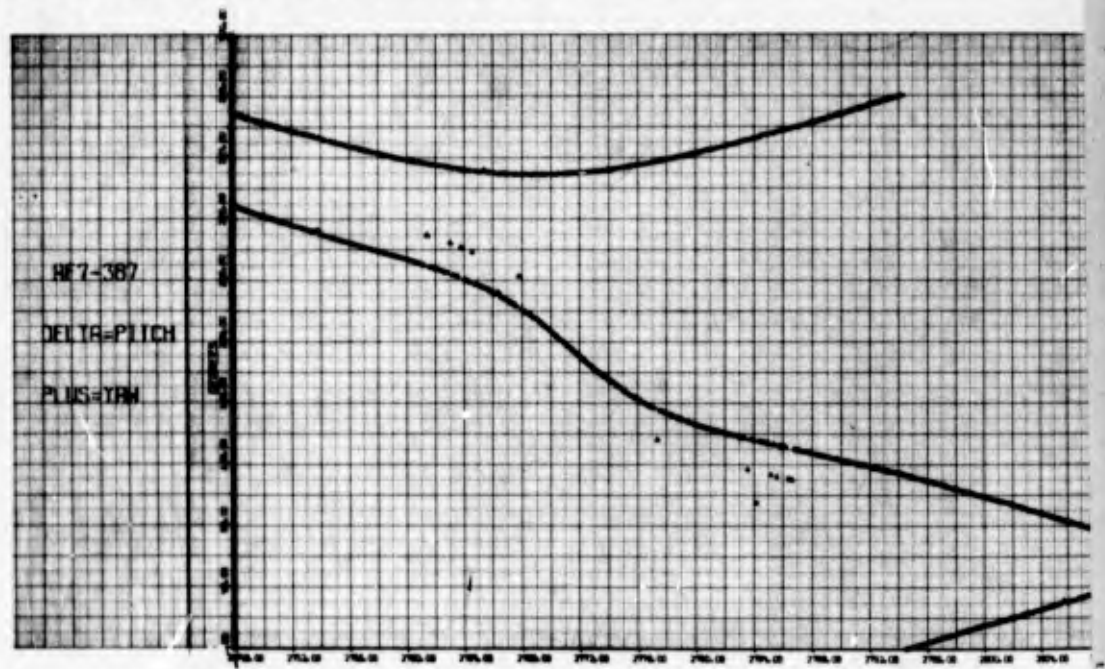
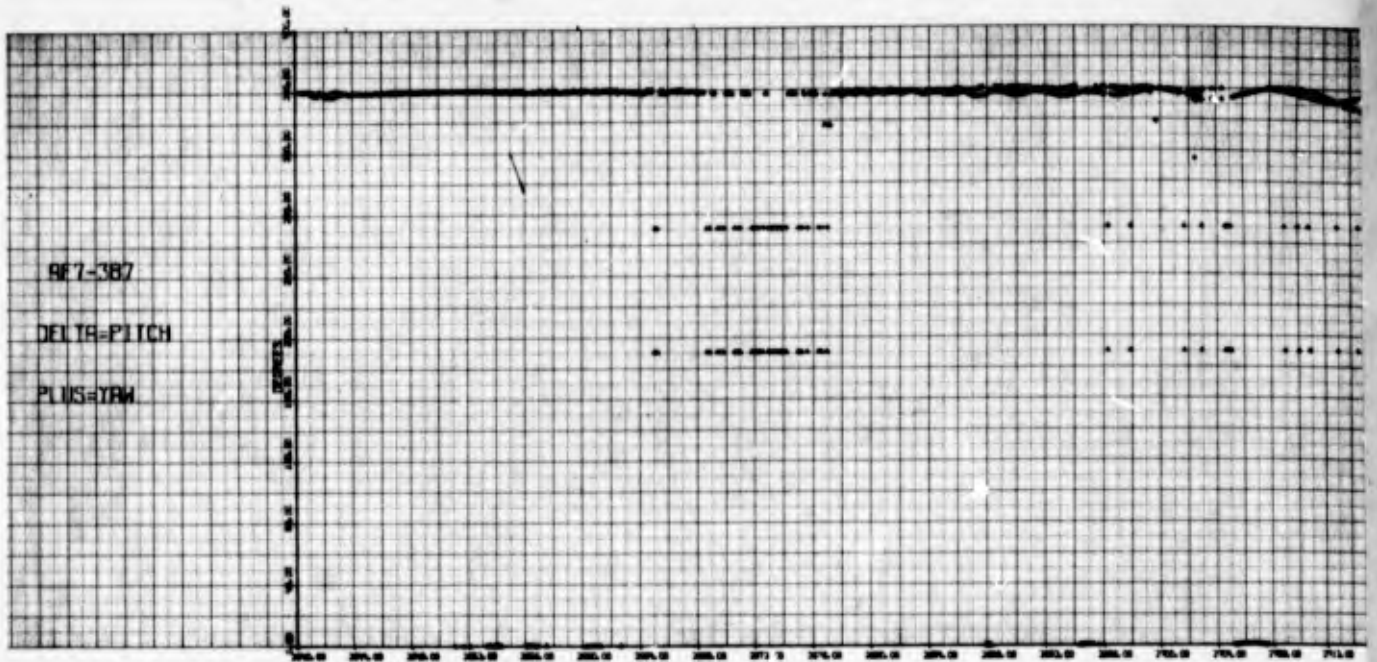
The main program next calls the subroutine SECØND. SECØND sets up the dependent variable scaling factors for the curves to be plotted. Then, for each parameter to be plotted, SECØND calls subroutine DØAXIS, which puts a message on an output tape which will cause the plotter to draw and label the axes, and then calls SYMBOL repeatedly until all the desired data points (i. e., until a negative time is encountered) have been read off the data set prepared by ITAPE. The subroutine SYMBOL puts records on the output tape which will cause the automatic plotter to plot each data point with a symbol. The subroutine SYMBOL, as well as the subroutine PLOTS, PLOT, and SCALE called by SECØND, and the subroutine AXIS called by DØAXIS are in the Systems Library of the IBM 360/65 at Aerojet-General Von Karman Center. These are substantially identical to subroutines distributed by the manufacturer of the CalComp Plotter. When the plotter tape has been prepared, SECØND returns control to the main program, and the job ends, except for plotting the tape which has been generated.

The printed output and the plots present time histories of the same parameters. These are: the coning angle ( $\phi_c$ ), angular momentum vector azimuth ( $\psi_M$ ) and elevation ( $\theta_M$ ), the vehicle azimuth ( $\psi_x$ ) and elevation ( $\theta_x$ ), the transverse rate orientation ( $\phi_Q$ ), the transverse moment orientation ( $\phi_M$ ), the phase angle  $\phi_M - \phi_Q$ , the body axis angular rates (p, q, and r), the body axis angular accelerations ( $\dot{p}$ ,  $\dot{q}$ , and  $\dot{r}$ ), and the body axis net moments (L, M, and N).



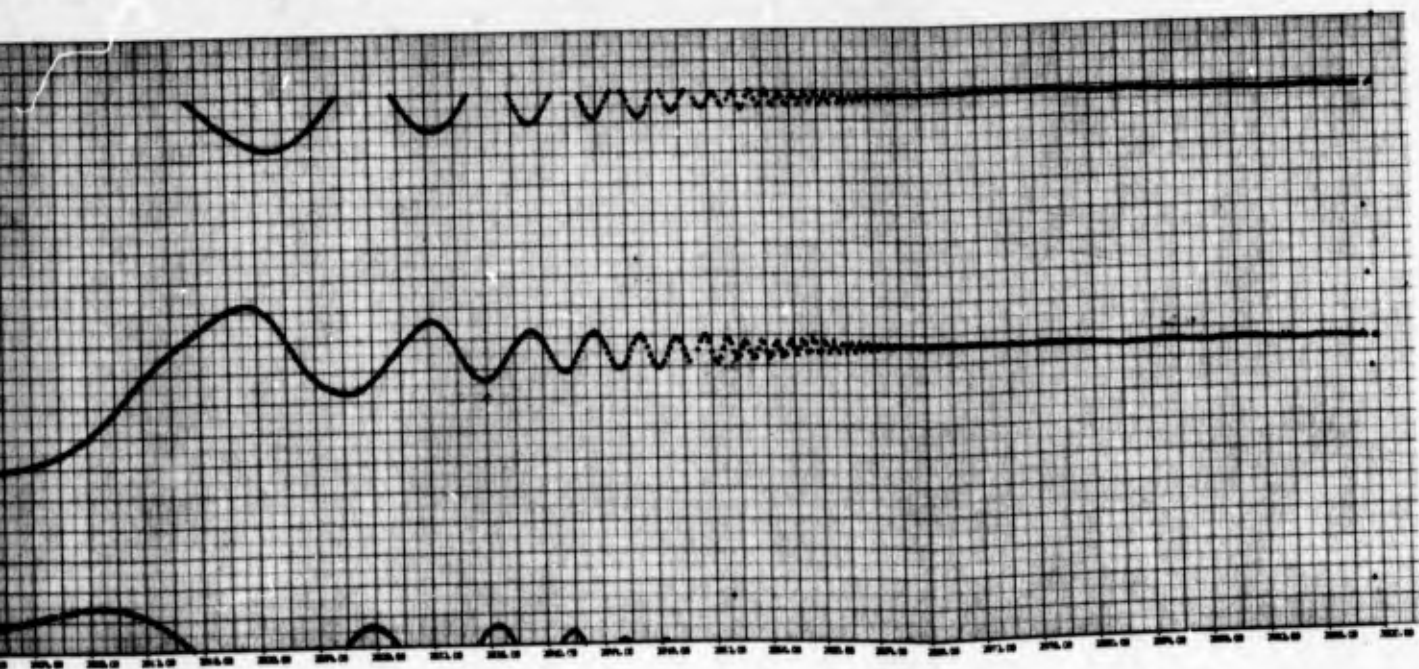
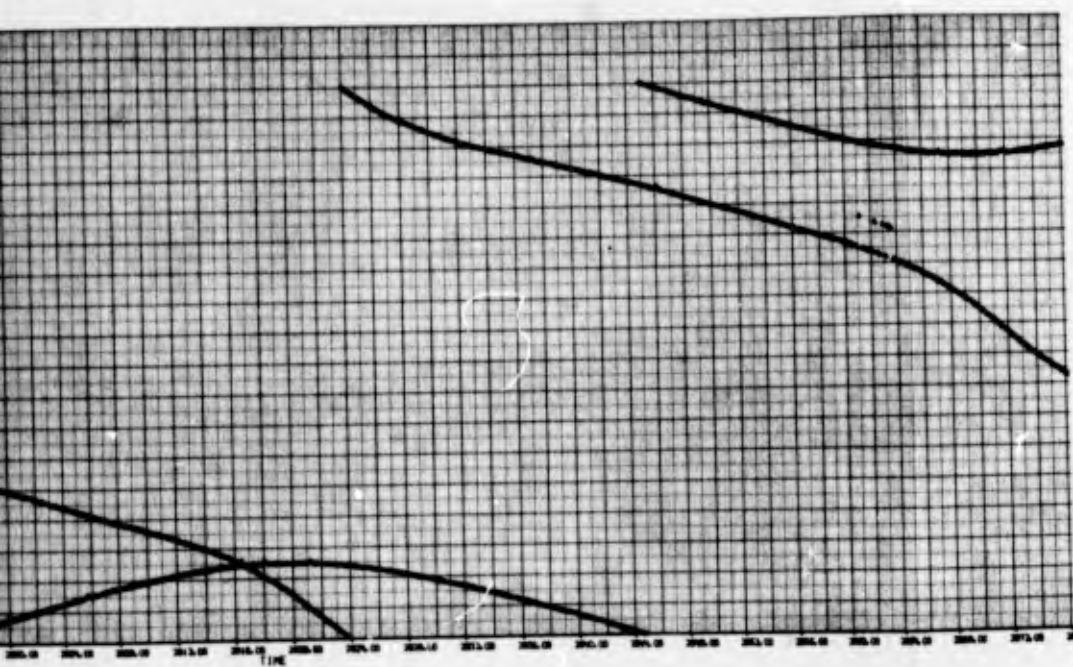
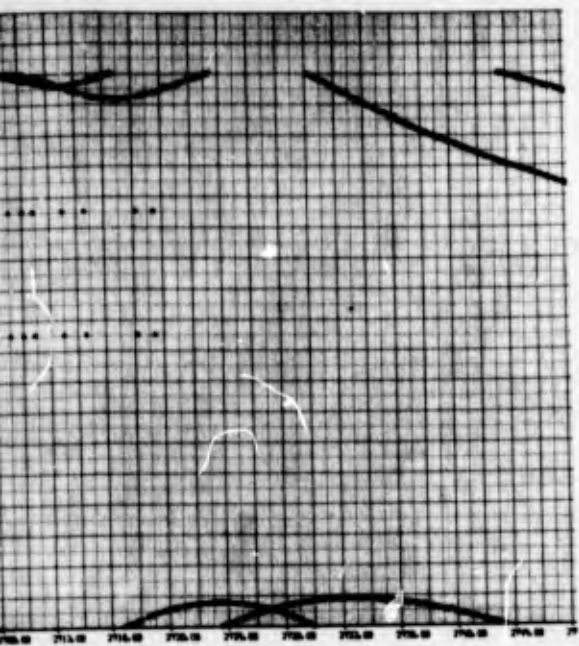
4.5 REFERENCES

- 4-1 MARS Data Reduction; Memorandum prepared by Whittaker Corporation.
- 4-2 Elementary Matrices; R. A. Frazer, W. J. Duncan, A. R. Collar;  
Cambridge Press, 1963.

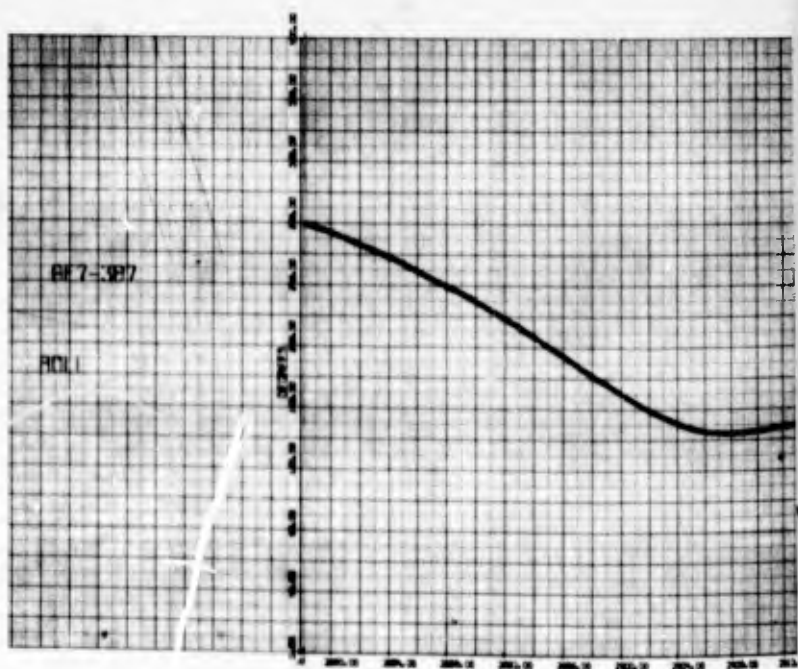
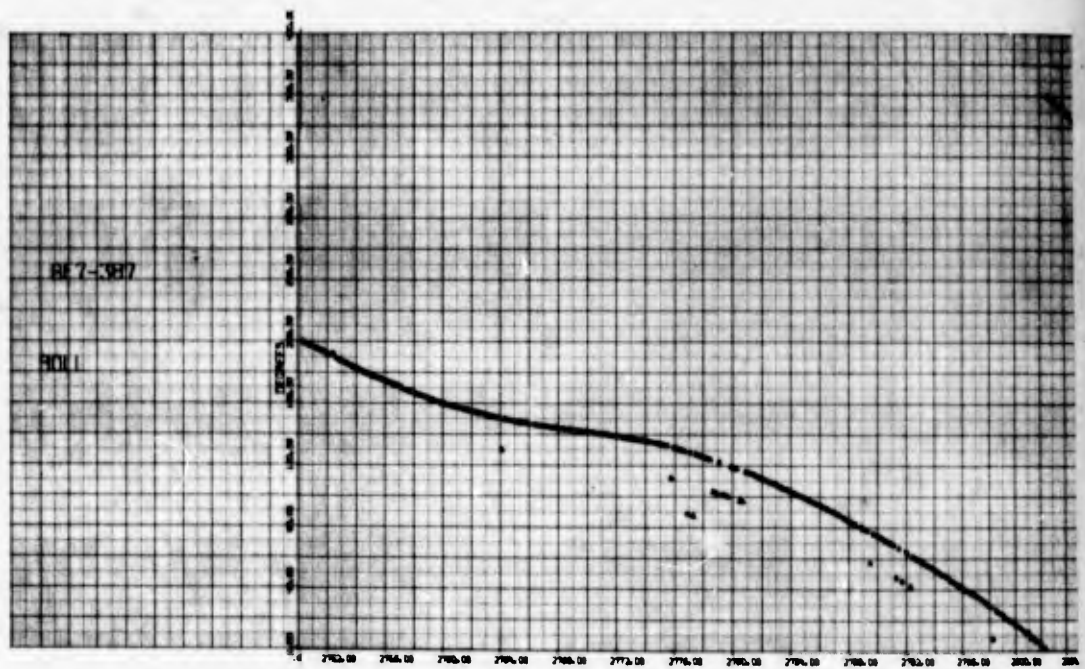
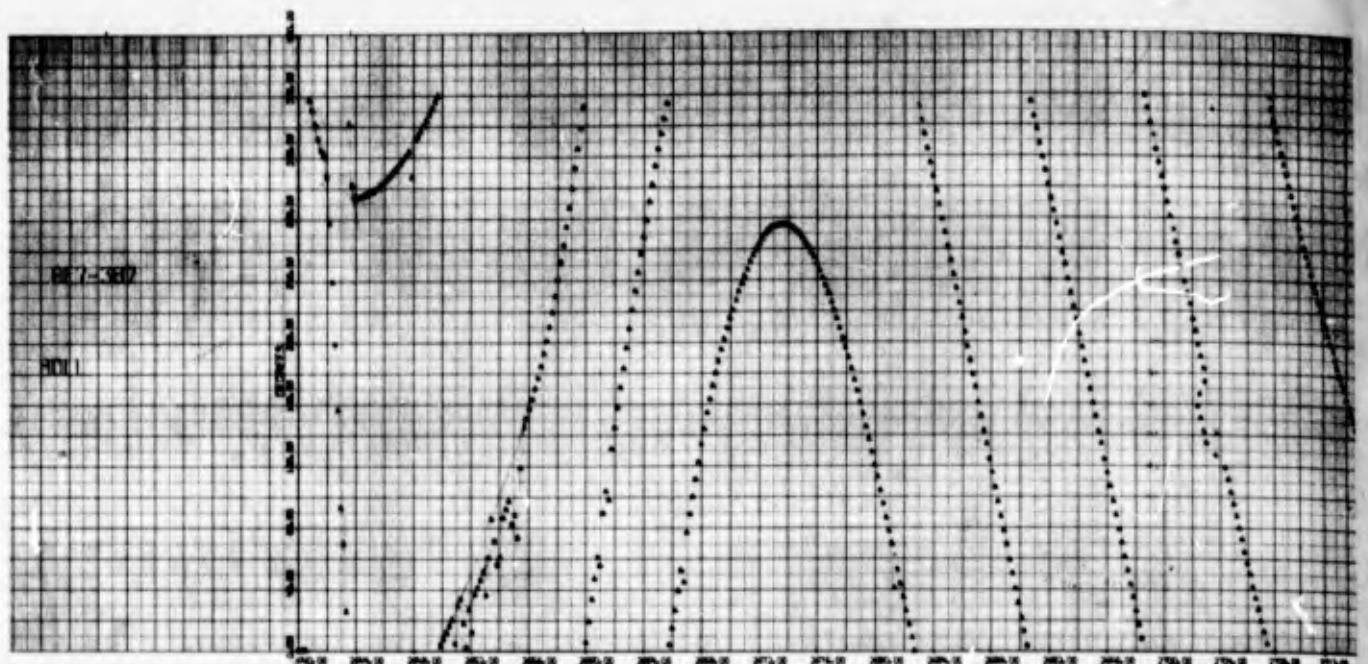


A

Figure 4-1. AF 7-387 Pitch and

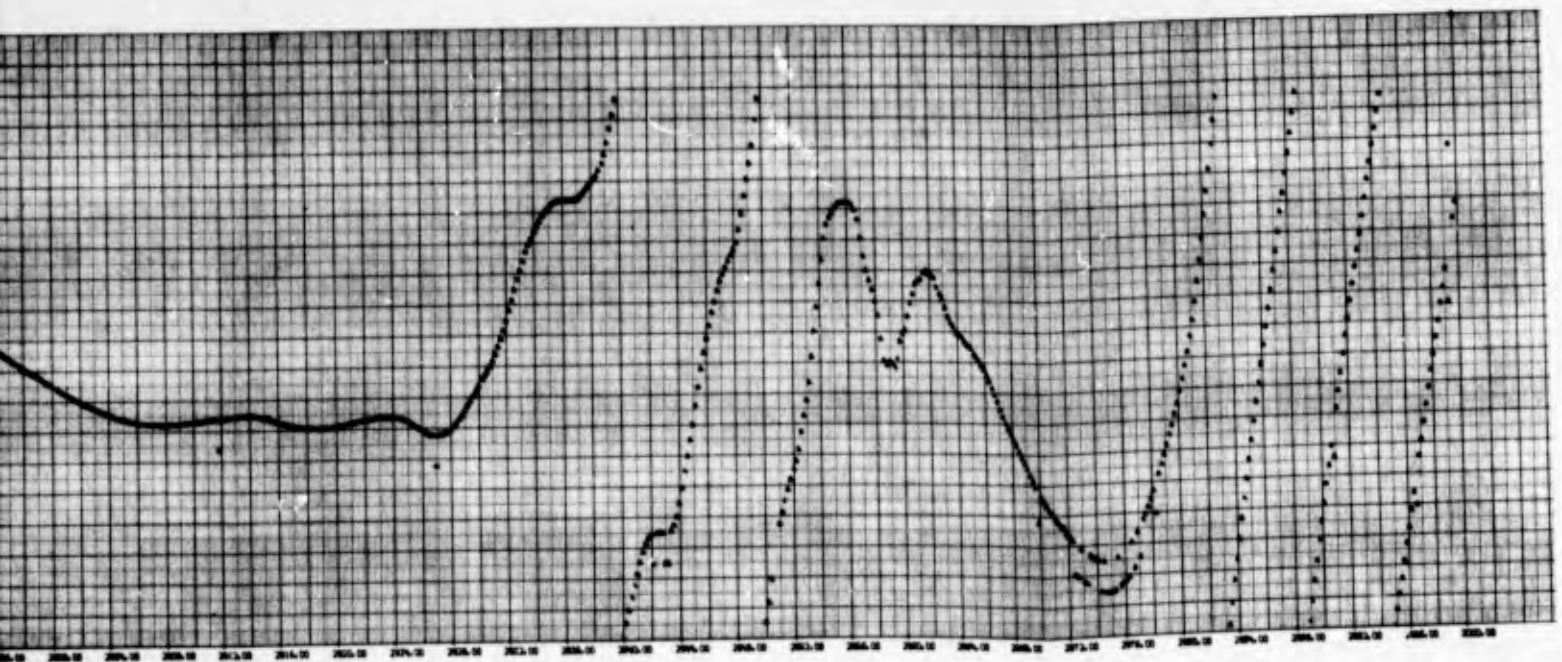
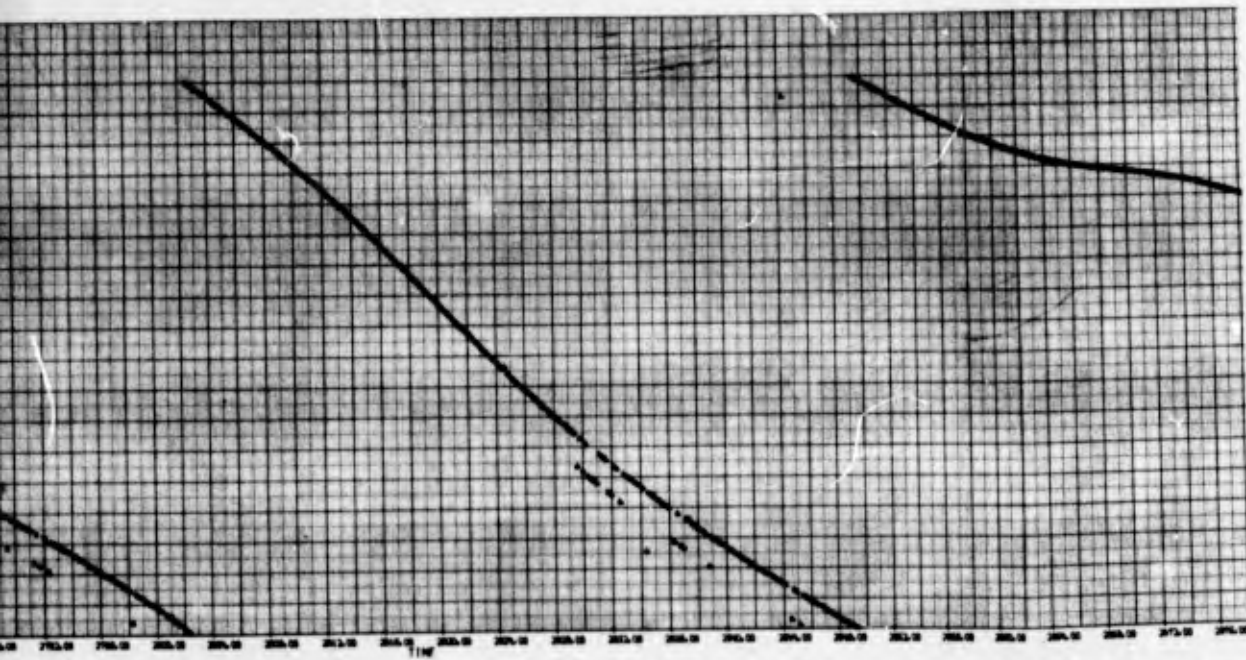
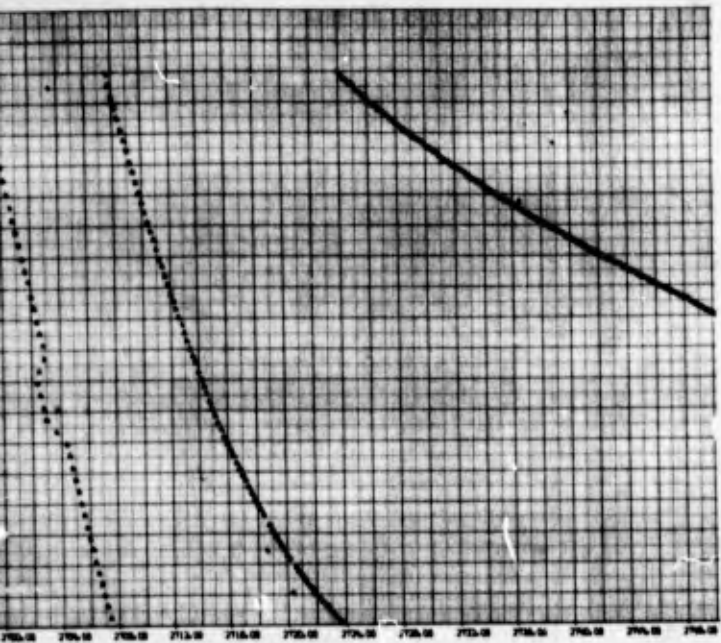






A

Figure 4-2. AF 7-387





**Appendix A**

**SIMPLIFIED VIBRATION ANALYSIS METHODS**

## Appendix A

### SIMPLIFIED VIBRATION ANALYSIS METHODS

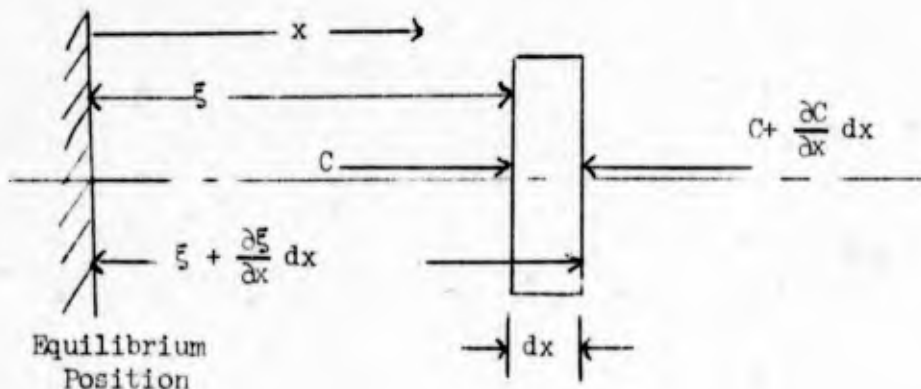
The purpose of this appendix is to document the derivations for some of the formulae used in this report. For the most part, these calculations are not terribly fancy, but may be regarded as forming the theoretical backbone of the kind of vibration analysis which seems to be important in sounding rocket work.

#### A.1 ANALYSIS OF AN ELASTIC COLUMN

First let

- $\mu$  = mass per unit length,
- $\xi(x,t)$  = displacement from equilibrium,
- $C(x,t)$  = compressive force,
- $\epsilon$  = strain,
- $A$  = column cross-section area,
- $E$  = Young's modulus for the column material, and
- $x,t$  = spatial and temporal coordinates.

Now consider an element of column of length  $dx$  as shown in the sketch below:



Applying Newton's law to this element of mass gives

$$C - \left( C + \frac{\partial C}{\partial x} dx \right) = (\mu dx) \frac{\partial^2 \xi}{\partial t^2}, \text{ or} \quad (1.1)$$

$$\frac{\partial C}{\partial x} + \mu \frac{\partial^2 \xi}{\partial t^2} = 0.$$

Now, using Hooke's law we can write

$$C = AE\epsilon = AE \frac{\xi - \left( \xi + \frac{\partial \xi}{\partial x} dx \right)}{dx} = -AE \frac{\partial \xi}{\partial x}. \quad (1.2)$$

Substituting (1.2) into (1.1) yields the wave equation for longitudinal vibrations:

$$\frac{\partial}{\partial x} \left( -AE \frac{\partial \xi}{\partial x} \right) + \mu \frac{\partial^2 \xi}{\partial t^2} = 0. \quad (1.3)$$

As an example, let us analyze the free-free vibrations of a uniform beam of length  $L$ . That is, we must solve

$$\frac{AE}{\mu} \frac{\partial^2 \xi}{\partial x^2} - \frac{\partial^2 \xi}{\partial t^2} = 0$$

subject to

$$\xi(0,t) = \xi(L,t) = 0, \text{ or}$$

$$\frac{\partial \xi}{\partial x}(0,t) = \frac{\partial \xi}{\partial x}(L,t) = 0. \quad (1.4)$$

Letting

$$a^2 = \frac{AE}{\mu}, \quad (1.5)$$

a separated solution is

$$\xi = \left[ C_1 \sin \frac{\Omega}{a} x + C_2 \cos \frac{\Omega}{a} x \right] \left[ \sin \Omega t + C_3 \cos \Omega t \right] \quad (1.6)$$

Applying the boundary conditions leads to

$$\begin{aligned} C_1 &= 0, \text{ and} \\ C_2 \frac{\Omega}{a} \sin \frac{\Omega L}{a} &= 0. \end{aligned} \tag{1.7}$$

This implies that  $C_2$  is arbitrary, and that the frequency  $\Omega$  must take on one of the values

$$\begin{aligned} \frac{\Omega}{a} &= K\pi, \quad K = 0, 1, 2, \dots, \text{ or} \\ \Omega_K &= \frac{K\pi a}{L} = \frac{K\pi}{L} \sqrt{\frac{AE}{\mu}}. \end{aligned} \tag{1.8}$$

The mode shapes are

$$\xi_K = C_K \cos K\pi \frac{x}{L}, \tag{1.9}$$

where  $C_K$  is an arbitrary constant.

## A.2 ACOUSTIC ANALYSIS OF A GAS COLUMN

Now let

- $\rho$  = mass density of the gas,
- $u$  = gas velocity,
- $\gamma$  = ratio of specific heats,
- $c$  = sound speed,
- $p$  = pressure,
- $s$  = entropy,
- $S$  = port area,
- $R$  = gas constant,
- $T$  = temperature,
- $F$  = end closure perturbation force,

$\phi$  = velocity potential, and  
 $x, t$  = spatial and temporal coordinates.

The gas motion is assumed to be one dimensional, isentropic, and perfect. Under these conditions conservation, of mass, momentum and entropy require that

$$\frac{\partial \rho}{\partial t} + u \frac{\partial \rho}{\partial x} + \rho \frac{\partial u}{\partial x} = 0,$$

$$\frac{\partial u}{\partial t} + u \frac{\partial u}{\partial x} + \frac{1}{\rho} \frac{\partial p}{\partial x} = 0, \text{ and} \tag{2.1}$$

$$\frac{p}{p_0} = \left( \frac{\rho}{\rho_0} \right)^\gamma.$$

The equation of state required is

$$p = \rho R T. \tag{2.2}$$

It is convenient to introduce the speed of sound:

$$c^2 = \left( \frac{\partial p}{\partial \rho} \right)_s = \gamma \frac{p}{\rho}. \tag{2.3}$$

Then since

$$\frac{1}{\rho} \frac{\partial p}{\partial x} = \frac{1}{\rho} \frac{\partial p}{\partial \rho} \frac{\partial \rho}{\partial x} = \frac{c^2}{\rho} \frac{\partial \rho}{\partial x},$$

the momentum eqn. may be written as

$$\frac{\partial u}{\partial t} + u \frac{\partial u}{\partial x} + \frac{c^2}{\rho} \frac{\partial \rho}{\partial x} = 0. \tag{2.4}$$

Now introduce the velocity potential, and the subscript notation for differentiation.

$$u = \phi_x. \tag{2.5}$$



With this, eqn. (2.4) becomes

$$\phi_{xt} + \phi_x \phi_{xx} + \frac{c^2}{\rho} \frac{\partial \rho}{\partial x} = 0.$$

Integrating this at constant time gives

$$\phi_t + \frac{1}{2} \phi_x^2 + \int_{\rho_0}^{\rho} \frac{c^2}{\rho} \frac{\partial \rho}{\partial x} dx = f(t) \quad (2.6)$$

From Eqn. (2.3) it is found that

$$\frac{dc}{c} = \frac{(\gamma-1)}{2} \frac{d\rho}{\rho}. \quad (2.7)$$

It follows that

$$\int_{\rho_0}^{\rho} \frac{c^2 d\rho}{\rho} = \frac{c^2 - c_0^2}{\gamma-1}.$$

Then

$$\phi_t + \frac{1}{2} \phi_x^2 + \frac{c^2 - c_0^2}{\gamma-1} = f(t), \quad (2.8)$$

where  $f(t)$  is a function of integration. Differentiating eqn. (2.8) with respect to time, and also with respect to  $x$ , and substituting from eqn. (2.7) lets us solve for  $\frac{\partial \rho}{\partial t}$  and  $\frac{\partial \rho}{\partial x}$ . These may be substituted into the first of Eqn's (2.1) to give

$$(c^2 - \phi_x^2) \phi_{xx} - 2 \phi_x \phi_{xt} - \phi_{tt} = -\dot{f}(t) \quad (2.9)$$

Now let

$$\tilde{\phi} = \phi - \int f(t) dt. \quad (2.10)$$

Substituting this into eqns. (2.8) and (2.9) gives

$$\tilde{\phi}_t + \frac{1}{2} \tilde{\phi}_x^2 + \frac{c^2 - c_0^2}{\gamma - 1} = 0, \text{ and} \quad (2.11)$$

$$(c^2 - \tilde{\phi}_x^2) \tilde{\phi}_{xx} - 2\tilde{\phi}_x \tilde{\phi}_{xt} - \tilde{\phi}_{tt} = 0$$

Since all physical quantities associated with  $\tilde{\phi}$  are the same as for  $\phi$ , we can set  $r(t) = 0$  without loss of generality. Finally, eliminating  $c^2$  between eqns. (2.11) gives

$$\left[ c_0^2 - \frac{\gamma+1}{2} \phi_x^2 - (\gamma-1) \phi_t \right] \phi_{xx} - 2\phi_x \phi_{xt} - \phi_{tt} = 0. \quad (2.12)$$

We assume that there is no mean flow inside the motor. If all disturbances are infinitesimal, then to first order,

$$c_0^2 \phi_{xx} - \phi_{tt} = 0. \quad (2.13)$$

We readily find separated solutions to Eqn. (2.13) in the form

$$\phi = e^{i\omega t} \left[ c_1 \sin \frac{\omega}{c_0} x + c_2 \cos \frac{\omega}{c_0} x \right]. \quad (2.14)$$

Let the displacements of the end closures at  $x = 0$  and  $x = L$  be given by  $\xi(0)e^{i\omega t}$  and  $\xi(L)e^{i\omega t}$ . Then appropriate boundary conditions are

$$\phi_x(0, t) = i\omega \xi(0)e^{i\omega t}, \text{ and} \quad (2.15)$$

$$\phi_x(L, t) = i\omega \xi(L)e^{i\omega t}.$$

It is readily found that

$$c_1 = i c_0 \xi(0), \text{ and} \quad (2.16)$$

$$c_2 = i c_0 \left[ \xi(0) \cot \frac{\omega L}{c_0} - \xi(L) \csc \frac{\omega L}{c_0} \right]$$

For a rigid motor case,  $\xi(0) = \xi(L) = 0$ , and the only way for  $c_2$  to be finite is if

$$\sin \frac{\omega L}{c_0} = 0, \text{ or}$$

$$\omega = \frac{c_0 K \pi}{L}, K = 0, 1, 2, \dots \quad (2.17)$$

In spite of its apparent simplicity, eqn. (2.17) usually yields answers to within one or two percent when applied to the large fineness ratio motors employed in sounding rocket work.

It is now necessary to calculate the forces acting on the end closures. From the first of Eqns. (2.11) we find that

$$c^2 - c_0^2 = \gamma R(T - T_0) = -\frac{\gamma - 1}{2} \phi_x^2 - (\gamma - 1) \phi_t,$$

or, to first order,

$$\gamma R \Delta T = -(\gamma - 1) \phi_t. \quad (2.18)$$

Substituting eqns. (2.14) and (2.16) into (2.18) gives

$$\frac{\gamma R \Delta T}{c_0 \omega (\gamma - 1)} = e^{i\omega t} \left[ \xi(0) \sin \frac{\omega x}{c_0} + \left( \xi(0) \cot \frac{\omega L}{c_0} - \xi(L) \csc \frac{\omega L}{c_0} \right) \cos \frac{\omega x}{c_0} \right] \quad (2.19)$$

Now, from the third of Eqns. (2.1) and from Eqn. (2.2), it is found that

$$\frac{p}{p_0} = \left( \frac{T}{T_0} \right)^{\frac{\gamma}{\gamma - 1}},$$

or, again to first order,

$$p - p_0 = \Delta p = \frac{\gamma}{\gamma - 1} p_0 \frac{\Delta T}{T_0} \quad (2.20)$$

The end closure forces are  $\Delta p S$ , or when Eqns. (2.19) and (2.20) are used,

$$\begin{aligned}
 F(0,t) &= \Delta p(0,t)S = \frac{\gamma \omega S p_0}{c_0} \left[ \xi(0) \cot \frac{\omega L}{c_0} - \xi(L) \csc \frac{\omega L}{c_0} \right] e^{i\omega t}, \text{ and} \\
 F(L,t) &= \Delta p(L,t)S = \frac{\gamma \omega S p_0}{c_0} \left[ \xi(0) \csc \frac{\omega L}{c_0} - \xi(L) \cot \frac{\omega L}{c_0} \right].
 \end{aligned}
 \tag{2.21}$$

Note that it assumes that positive forces are outward, i.e.,  $F(0,t)$  and  $F(L,t)$  are in opposite directions.

### A.3 ELASTIC-ACOUSTIC ANALOGY

It is observed from the foregoing that both the elastic column and the closed organ pipe show certain similarities in behavior. First, both systems are described by differential equations (Eqns. (1.3) and (2.13)) which are structurally similar. This equation is known as the wave equation. Since Space Division possessed a working computer program which solved Eqn. (1.3) when this work was started, it was felt that it should be possible to simulate an acoustic branch by inserting a suitable elastic branch in the program.

A comparison of Eqns. (1.3) and (2.13) reveals that the first requirement for similarity is that

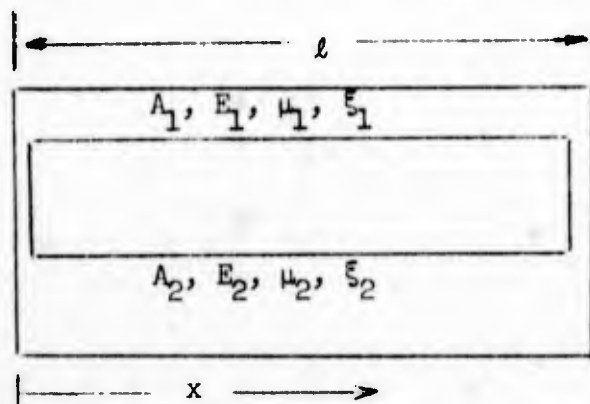
$$\frac{A_g E_g}{\mu_g} = c_0^2,
 \tag{3.1}$$

where the subscript "g" refers to the elastic analog to the real acoustic branch. If Eqn. (3.1) is satisfied the elastic branch will behave between end points just like an organ pipe.

The end points are a little tricky, for this involves matching end forces. Inspection of Eqns. (1.2) and (2.18) and (2.20) indicates apparent difficulties.

The tactic followed here is to compute the natural frequencies of two beams in parallel, and then the natural frequencies of a gas column in parallel with a beam. If the natural frequencies of the two are the same, and if Eqn. (3.1) is satisfied, then end condition similarity is established, and therefore the desired analogy is also established.

Now consider two uniform beams in parallel:



Each beam element must satisfy the wave Eqn., Eqn. (1.3). Then the spatial part of the deformation of each element is in the form

$$\xi_i = c_{1_i} \sin \frac{\Omega}{a_i} x + c_{2_i} \cos \frac{\Omega}{a_i} x, \text{ and} \quad (3.2)$$

$$a_i = \sqrt{\frac{A_i E_i}{\mu_i}},$$

where the subscript "i" refers to the  $i^{\text{th}}$  element, and  $\Omega$  is the oscillation frequency. The compressive load is

$$c_i = \Omega \sqrt{A_i E_i \mu_i} \left[ -c_{1_i} \sin \frac{\Omega}{a_i} x + c_{2_i} \cos \frac{\Omega}{a_i} x \right]. \quad (3.3)$$

It is required that there be no external end force on the ensemble, and that the deformations of the elements match at the ends. These boundary conditions are:



$$\begin{aligned}
\xi_1(0,t) &= \xi_2(0,t), \\
\xi_1(l,t) &= \xi_2(l,t), \\
c_1(0,t) &= c_2(0,t) = 0, \text{ and} \\
c_2(l,t) &= c_2(l,t) = 0
\end{aligned}
\tag{3.4}$$

Substitution of Eqns. (3.2) and (3.3) into Eqn. (3.4), followed by some algebra permits us to eliminate three of the four constants of integration. The fourth, as is the case in all free vibration problems, is indeterminate. The condition that the fourth constant be different from zero is the characteristic equation. For this problem, the characteristic equation is

$$2 \left( 1 - \cos \frac{\Omega l}{a_1} \cos \frac{\Omega l}{a_2} \right) + \frac{A_2 E_2 \mu_2 + A_1 E_1 \mu_1}{\sqrt{A_2 E_2 \mu_2} \sqrt{A_1 E_1 \mu_1}} \sin \frac{\Omega l}{a_1} \sin \frac{\Omega l}{a_2} = 0. \tag{3.5}$$

The roots of Eqn. (3.5) are the natural frequencies of the system.

In the next section of this appendix it is shown that the characteristic equation for a closed organ pipe in parallel with an elastic column is

$$2 \left( 1 - \cos \frac{\Omega l}{c_o} \cos \frac{\Omega l}{a} \right) + \frac{\left( \frac{p_o S \gamma}{c_o} \right)^2 + A E \mu}{\frac{p_o S \gamma}{c_o} \sqrt{A E \mu}} \sin \frac{\Omega l}{c_o} \sin \frac{\Omega l}{a} = 0. \tag{3.6}$$

When Eqns. (3.5) and (3.6) are compared, we see that if the gas-filled tube is replaced with an elastic bar whose properties are

$$\begin{aligned}
\mu_g &= \frac{p_o S \gamma}{c_o}, \text{ and} \\
A_g E_g &= p_o S \gamma,
\end{aligned}
\tag{3.7}$$

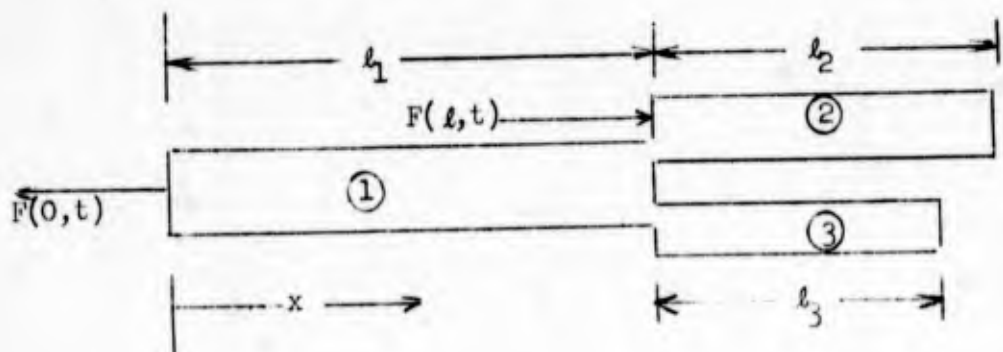
then the natural frequencies of the system are unchanged. Furthermore, since Eqns. (3.7) contain Eqn. (3.1), we are assured that the mode shapes are also unchanged.

The analogy, Eqn. (3.7), has been incorporated into Space Division's computer program to find the longitudinal natural frequencies and mode shapes of rockets.

#### A.4 ACOUSTIC-ELASTIC MODEL OF A SOUNDING ROCKET

In order to get some idea of what is occurring in flight, an approximate analysis of a typical rocket configuration is carried out. The present problem formulation is sufficiently complex as to yield interesting, simplified results.

The model selected has three elastic branches representing the payload nose shell, the payload rack and the motor tube. A closed organ pipe propulsion model is used with the nominal motor length equal to the elastic motor tube length. Correction to the actual acoustic length is accomplished by reducing the sound speed slightly.



For each of the three beam elements, we can write a separated solution of the form

$$\xi_i = \left[ c_{1_i} \sin \frac{\Omega}{a_i} x + c_{2_i} \cos \frac{\Omega}{a_i} x \right] e^{i\Omega t}, \text{ where} \quad (4.1)$$

$$a_i = \sqrt{\frac{A_i E_i}{\mu_i}}.$$

The compressive load is

$$c_i = -\Omega \sqrt{A_i E_i \mu_i} \left[ c_{1_i} \cos \frac{\Omega}{a_i} x - c_{2_i} \sin \frac{\Omega}{a_i} x \right] e^{i\Omega t}. \quad (4.2)$$

The boundary conditions are

$$\begin{aligned} c_1(0, t) &= -F(0, t), \\ c_2(l_1 + l_2, t) &= 0, \\ c_3(l_1 + l_3, t) &= 0, \\ c_1(l_1, t) + F(l_1, t) &= c_2(l_1, t) + c_3(l_1, t), \text{ and} \\ \xi_1(l_1, t) &= \xi_2(l_1, t) = \xi_3(l_1, t). \end{aligned} \quad (4.3)$$

The forces due to the gas pressure in the organ pipe are found from Eqn. (2.21) to be

$$\begin{aligned} F(0, t) &= \frac{p_0 S \gamma \Omega}{c_0} \left[ \xi_1(0, t) \cot \frac{\Omega l_1}{c_0} - \xi_1(l_1, t) \csc \frac{\Omega l_1}{c_0} \right], \text{ and} \\ F(l_1, t) &= \frac{p_0 S \gamma \Omega}{c_0} \left[ \xi_1(l_1, t) \cot \frac{\Omega l_1}{c_0} - \xi_1(0, t) \csc \frac{\Omega l_1}{c_0} \right]. \end{aligned} \quad (4.4)$$

As before, Eqns. (4.1), (4.2), and (4.4) may be substituted into Eqn. 4.3. Eliminating all the constants save one, which must remain finite, implies the characteristic equation:

$$\begin{aligned} & \left( \frac{p_o S \gamma}{c_o} \right)^2 - \frac{2p_o S \gamma}{c_o} \sqrt{A_1 E_1 \mu_1} \left[ \cot \frac{\Omega l_1}{c_o} \cot \frac{\Omega l_1}{a_1} - \csc \frac{\Omega l_1}{c_o} \csc \frac{\Omega l_1}{a_1} \right] \\ & + A_1 E_1 \mu_1 + \left[ \frac{p_o S \gamma}{c_o} \cot \frac{\Omega l_1}{c_o} + \sqrt{A_1 E_1 \mu_1} \cot \frac{\Omega l_1}{a_1} \right] \left[ \sqrt{A_2 E_2 \mu_2} \tan \frac{\Omega l_2}{a_2} + \sqrt{A_3 E_3 \mu_3} \tan \frac{\Omega l_3}{a_3} \right] \\ & = 0. \end{aligned} \tag{4.5}$$

We note that in the terms involving propulsion the ratio  $(l_1/c_o)$  occurs. The appropriate length, L, for the organ pipe is from the forward closure to the initial sonic region of the throat. It has been found that the desired accuracy is obtained if  $l_1/c_o$  is replaced by  $L/c_o$  in Eqn. (4.5). We finally have that

$$\begin{aligned} & \left( \frac{p_o S \gamma}{c_o} \right)^2 - \frac{2p_o S \gamma}{c_o} \sqrt{A_1 E_1 \mu_1} \left[ \cot \frac{\Omega L}{c_o} \cot \frac{\Omega l_1}{a_1} - \csc \frac{\Omega L}{c_o} \csc \frac{\Omega l_1}{a_1} \right] + A_1 E_1 \mu_1 \\ & + \left[ \frac{p_o S \gamma}{c_o} \cot \frac{\Omega L}{c_o} + \sqrt{A_1 E_1 \mu_1} \cot \frac{\Omega l_1}{a_1} \right] \left[ \sqrt{A_2 E_2 \mu_2} \tan \frac{\Omega l_2}{a_2} + \sqrt{A_3 E_3 \mu_3} \tan \frac{\Omega l_3}{a_3} \right] = 0. \end{aligned} \tag{4.6}$$

This change is equivalent to reducing the speed of sound in the original analysis in order to compensate for the fact that the length is incorrect.

Two interesting results may be obtained by specializing Eqn. (4.5). If we first let  $l_2$  and  $l_3$  go to zero, we readily recover Eqn. (3.6).

Second, it has been found in the numerical examples studied that the acoustic branch does not greatly affect the elastic frequencies, and vice versa.

This suggests that we calculate the acoustic frequencies from Eqn. (2.17), and let the mean pressure go to zero in Eqn. (4.7). The results:

$$\sqrt{A_1 E_1 \mu_1} \tan \frac{\Omega l_1}{a_1} + \sqrt{A_2 E_2 \mu_2} \tan \frac{\Omega l_2}{a_2} + \sqrt{A_3 E_3 \mu_3} \tan \frac{\Omega l_3}{a_3} = 0. \quad (4.7)$$

As a representation of reality, this short-cut approach is scarcely inferior to the complete analysis as in Eqn. (4.6). The errors resulting from the uniform beam approximation are usually larger than the errors resulting from neglecting coupling between elastic and acoustic branches.

It remains to calculate the mode shapes associated with the various natural frequencies. Neglecting the acoustic branch, and supposing that  $c_{21}$  is arbitrary, the mode shapes are given by

$$\begin{aligned} \xi_1 &= c_{21} \cos \frac{\Omega x}{a_1}, \\ \xi_2 &= c_{21} \frac{\cos \frac{\Omega l_1}{a_1} \cos \frac{\Omega}{a_2} (l_1 + l_2)}{\cos \frac{\Omega l_2}{a_2}} \left[ \tan \frac{\Omega}{a_2} (l_1 + l_2) \sin \frac{\Omega x}{a_2} + \cos \frac{\Omega x}{a_2} \right], \text{ and} \\ \xi_3 &= c_{21} \frac{\cos \frac{\Omega l_1}{a_1} \cos \frac{\Omega}{a_3} (l_1 + l_3)}{\cos \frac{\Omega l_3}{a_3}} \left[ \tan \frac{\Omega}{a_3} (l_1 + l_3) \sin \frac{\Omega x}{a_3} + \cos \frac{\Omega x}{a_3} \right] \end{aligned} \quad (4.8)$$

The acoustic branch may be readily found to have a sinusoidal mode shape.



Appendix B

LISTING OF MARS PLATFORM PROGRAM

APPENDIX B

THIS LISTING IS OF THE PROGRAM AS PRESENTLY CONSTITUTED  
 THE PROGRAM HAS NOT AS YET BEEN CHECKED OUT

```

C MAIN PROGRAM
COMMON IDATA(100), DATA(1000)
CALL OUTFIT(1,0.0,0.0,0.0,0.0)
CALL FIXTPE(IDIED)
IF(IDIED.EQ.0)GO TO 1
WRITE(6,2)
2 FORMAT(1H1////21H I BLEW THE CURVE FIT)
1 CALL FIRST
CALL SECOND
RETURN
END
SUBROUTINE FIRST
COMMON
DIMENSION
1 TIME(4),
2 PHI(4),
3 CMAT(3,3),
4 DIRCOS(3),
EQUIVALENCE
1(TWOPI,DATA(2)),
2(PI,DATA(105)),
3(SINPI,DATA(108)),
4(COSGAM,DATA(111)),
5(AMAT(1,1),DATA(45)),
6(THETA(1),DATA(37)),
7(KOUNTS,IDATA(1)),
8(DENUM,DATA(104)),
9(K,DATA(83)),
A(THATT,VBLUCK(1,2)),
B(D1THET,VBLUCK(2,2)),
C(D2THET,VBLUCK(3,2)),
D(SINTHT,VBLUCK(4,2)),
E(COSTHT,VBLUCK(5,2)),
F(QDOT,DATA(85)),
EQUIVALENCE
1(HZ,H(3)),
2(HZDOT,DATA(89)),
IDATA(100),
XAXIS(3),
PSI(4),
H(3),
VBLUCK(5,3),
HDUT(3)
(INTIMEI, IDATA(2)),
(XAXIS(1),DATA(11)),
(GAMMA,DATA(106)),
(COSBET,DATA(109)),
(SINOMG,DATA(112)),
(TIME(1),DATA(29)),
(PHI(1),DATA(41)),
(DT1,DATA(102)),
(P,DATA(81)),
(VBLUCK(1,1),DATA(14)),
(PHIATT,VBLUCK(1,3)),
(D1PHI,VBLUCK(2,3)),
(D2PHI,VBLUCK(3,3)),
(SINPHI,VBLUCK(4,3)),
(COSPHI,VBLUCK(5,3)),
(RDOT,DATA(86)),
(HX,H(1)),
(HXDOT,DATA(87)),
(ROLLI,DATA(116)),
DATA(1000),
AMAT(3,3),
THETA(4),
HMAT(3,3),
HCOMP(3),
(PI,DATA(1)),
(RAD,DATA(5)),
(OMEGA,DATA(107)),
(SINGAM,DATA(110)),
(COSOMG,DATA(113)),
(PSI(1),DATA(33)),
(TEND,DATA(114)),
(DT2,DATA(103)),
(IQ,DATA(82)),
(PSIATT,VBLUCK(1,1)),
(DIPSI,VBLUCK(2,1)),
(D2PSI,VBLUCK(3,1)),
(SINPSI,VBLUCK(4,1)),
(CUSPSI,VBLUCK(5,1)),
(PDOT,DATA(84)),
(H(1),DATA(72)),
(HY,H(2)),
(HYDOT,DATA(88)),
(PITCHI,DATA(117)),

```

```

3 (COSM, DATA(115)), (PMAT(1,1), DATA(957)), (CMT(1,1), DATA(6377))
4 (HCOMP(1), DATA(75)), (URCOS(1), DATA(78)), (MAZI, DATA(90)),
5 (MELI, DATA(91)), (XAZI, DATA(92)), (XELI, DATA(93)),
6 (PHIRTE, DATA(119)), (PHIMG, DATA(120)), (DELPHI, DATA(121)),
7 (TIME, DATA(30)), (HDUT(1), DATA(87))

DO 4 I=1,100
4 1 DATA(I)=0
DO 5 I=1,1000
5 DATA(I)=0.0
N TIME I=1
CALL INPUT
PI=3.141593
TWOP=6.283185
XAXIS(1)=1.0
RAD=57.29578
BETA=BETA/RAD
GAMMA=GAMMA/RAD
OMEGA=OMEGA/RAD
SINBET=SIN(BETA)
COSBET=COS(BETA)
SINGAM=SIN(GAMMA)
COSGAM=COS(GAMMA)
SINOMG=SIN(OMEGA)
COSOMG=COS(OMEGA)
AMAT(1,1)=COSGAM*COSBET
AMAT(1,2)=-SINBET*COSOMG+COSGAM-SINGAM*SINOMG
AMAT(1,3)=SINBET*SINOMG+COSGAM-CUSOMG*SINGAM
AMAT(2,1)=SINGAM*COSBET
AMAT(2,2)=-SINBET*CUSOMG+SINGAM+SINOMG*COSGAM
AMAT(2,3)=SINBET*SINOMG+SINGAM+CUSOMG*COSGAM
AMAT(3,1)=-SINBET
AMAT(3,2)=-COSBET*COSOMG
AMAT(3,3)=COSBET*SINOMG
1 READ(1) TIME(4), PHI(4), THETA(4), PSI(4)
IF (TIME(4).GE.TEND) GO TO 100
KOUNTS=KOUNTS+1
DO 2 I=1,3
TIME(I)=TIME(I+1)
PSI(I)=PSI(I+1)
THETA(I)=THETA(I+1)
PHI(I)=PHI(I+1)
IF (KOUNTS.LT.3) GO TO 1
DT1=TIME(2)-TIME(1)
DT2=TIME(3)-TIME(1)
DENOM=DT2*DT1*(DT2-DT1)

```

```

CALL SETUP(1,PSI)
CALL SETUP(2,THETA)
CALL SETUP(3,PHI)
P=D1PHI+D1THET#SINPSI
W=D1THET#COSPSI#COSPHI+D1PSI#SINPHI
R=D1PSI#COSPHI-D1THET#SINPSI+D1THET#D1PSI#COSPSI
PDUOT=D2PHI+D2THET#SINPSI#COSPHI-D1THET#D1PSI#SINPSI#COSPHI
RDUOT=D2THET#COSPSI#SINPHI+D1PSI#D1PHI#COSPHI
ICUSPSI#SINPHI+D2PSI#SINPHI-D1PSI#D1PHI#SINPHI-D2THET#COSPSI#SINPHI+D1THET#
ICUSPSI#SINPHI-D2THET#D1PHI#COSPSI#COSPHI
CALL ITHET
HX=RULLI#P
HY=PITCHI#Q
HZ=PITCHI#R
HXDUOT=RULLI#PDUOT
HYDUOT=PITCHI#QDUOT+(ROLLI-PITCHI)#P#K
HZDUOT=PITCHI#RDUOT+(PITCHI-RULLI)#P#C
CONE=ATAN2(SQRT(HY##2+HZ##2),HX)
RMAT(1,1)=COSTHT#COSPSI
RMAT(1,2)=SINTHT#SINPHI-COSTHT#SINPSI#COSPHI
RMAT(1,3)=COSTHT#SINPSI#SINPHI+SINTHT#COSPHI
RMAT(2,1)=SINPSI
RMAT(2,2)=COSPSI#COSPHI
RMAT(2,3)=-COSPSI#SINPHI
RMAT(3,1)=-SINTHT#COSPSI
RMAT(3,2)=SINTHT#SINPSI#COSPHI+COSTHT#SINPHI
RMAT(3,3)=-SINTHT#SINPSI#SINPHI+COSTHT#COSPHI
DO 3 I=1,3
DO 3 J=1,3
CMAT(I,J)=0.0
DO 3 K=1,3
CMAT(I,J)=CMAT(I,J)+AMAT(I,K)#RMAT(K,J)
CALL CULMPY(H,HCOMP,CMAT)
CALL CULMPY(XAXIS,DIRCOS,CMAT)
HAZI=ATAN2(HCOMP(2),HCOMP(1))
HELI=ATAN2(-HCOMP(3),SORT(HCOMP(1)##2+HCOMP(2)##2))
XAZI=ATAN2(DIRCOS(2),DIRCOS(1))
XELI=ATAN2(-DIRCOS(3),SORT(DIRCOS(1)##2+DIRCOS(2)##2))
IF(HAZI.GT.PI)HAZI=HAZI-TWOPI
IF(HELI.GT.PI)HELI=HELI-TWOPI
IF(XAZI.GT.PI)XAZI=XAZI-TWOPI
IF(XELI.GT.PI)XELI=XELI-TWOPI
PHIRTE=ATAN2(Q,K)
PHIRUM=ATAN2(HDUOT(2),HDUOT(3))

```

```
DELPHI=PHI*1000-PI*1E  
IF(DELPHI.GT.PI)DELPHI=DELPHI-PI
```

```
CALL IPKINT  
CALL ITAPE
```

```
GO TO 1
```

```
100 TIME=-1.0
```

```
CALL ITAPE
```

```
RETURN
```

```
END
```

```
SUBROUTINE SECOND
```

```
COMMON
```

```
  DIMENSION
```

```
  ITITLE(18)
```

```
  DIMENSION
```

```
  EQUIVALENCE
```

```
  1(JVAR, IDATA(5)),
```

```
  2(WDONE, IDATA(6)),
```

```
  3(TPERIN, DATA(4)).
```

```
  CALL PLOTS(BUFF,3000)
```

```
  DO 101 I=1,9
```

```
    SIZIT(1)=AREA(I+27)
```

```
    SIZIT(2)=AREA(I+45)
```

```
    CALL SCALE(SIZIT,10.0,2,1,10.0)
```

```
    AREA(I+9)=SIZIT(3)
```

```
101 AREA(I+27)=SIZIT(4)
```

```
    AREA(2)=0.0
```

```
    AREA(3)=-200.0
```

```
    AREA(4)=-100.0
```

```
    AREA(5)=-200.0
```

```
    AREA(6)=-100.0
```

```
    AREA(7)=-200.0
```

```
    AREA(8)=-200.0
```

```
    AREA(9)=-200.0
```

```
    AREA(20)=20.0
```

```
    AREA(21)=40.0
```

```
    AREA(22)=20.0
```

```
    AREA(23)=40.0
```

```
    AREA(24)=20.0
```

```
    AREA(25)=40.0
```

```
    AREA(26)=40.0
```

```
    AREA(27)=40.0
```

```
  JVAR=1
```

```
102 TEND=0.0
```

```
  JVAR=JVAR+1
```

```
  TIME=TIME
```

```
  IDATA(100),  
  SIZIT(4),  
  DATA(1000)  
  AREA(54),
```

```
  BUFF(3000)  
  (SIZIT(1),DATA(5)),  
  (TEND,DATA(114)),  
  (X,DATA(9)),  
  (TTITLE(1),DATA(182))  
  (AREA(1),DATA(128)),  
  (TSTART,DATA(127)),  
  (Y,DATA(10)),
```



```

REWIND 2
103 TSTART=IEND
    CALL DGAXIS
104 READ(2)(TITLE(I), I=1,14)
105 NDOONE=NDOONE+1
106 X=(TITLE(1)-I*START)/I*PERIN
    Y=(TITLE(JVAR)-A*EA(JVAR))/A*EA(JVAR-14)
    IF(X.LE.TEND)CALL SYMBOL(X,Y,0.04,3,0.0,-1)
    IF(NDOONE.EQ.NPOINT)GO TO 107
    IF(X.LT.TEND)GO TO 104
    CALL PLOT(17.25,0.0,-3)
TSTART=IEND
CALL DGAXIS
GO TO 106

107 CALL PLOT(17.25,0.0,-3)
    IF(JVAR.LT.18)GO TO 102
    CALL PLOT(X,Y,399)
    RETURN
END
SUBROUTINE INPUT
COMMON
3 READ(5,1000)I,J,K
  IF(I.LE.0)RETURN
  K=J+K-1
  GO TO (1,2),I
1 READ(5,1000)(IDATA(M),M=J,K)
  GO TO 3
2 READ(5,2000)(DATA(M),M=J,K)
  GO TO 3
1000 FORMAT(6I12)
2000 FORMAT(6E12.8)
END
SUBROUTINE ITAPE
COMMON
DIMENSION
1 HDUT(3),
  EQUIVLFMCF
1 DIRATE(1),DATA(84),
2 (HAZI,DATA(90)),
3 (XELI,DATA(93)),
4 (DELPHI,DATA(121)),
5 (TWOPI,DATA(2)),
  AREA(1)=TYME
  AREA(2)=CONE*RAD
  AREA(3)=HAZI*RAD
  IDATA(100),
  RATE(3),
  AREA(54)
  (TYME,DATA(30)),
  (HDUT(1),DATA(87)),
  (HELI,DATA(91)),
  (PHIRIE,DATA(119)),
  (AREA(1),DATA(128)),
  (NPOINT, IDATA(4))
  DATA(1000)
  DIRATE(3),
  (RATE(1),DATA(81)),
  (CONE,DATA(115)),
  (XAZI,DATA(92)),
  (PHIMCM,DATA(120)),
  (RAD,DATA(3)),
  DATA(1000)

```

```

AREA(4)=HELI#RAD
AREA(5)=XAZI#RAD
AREA(6)=XELI#RAD
AREA(7)=PHIRTE#RAD
AREA(8)=PHIMOM#RAD
AREA(9)=DELPHI#RAD
DO 1 I=1,3
AREA(I+9)=RATE(I)/TWOPI
AREA(I+12)=HOUT(I)
1 AREA(I+15)=DIRATE(I)/TWOPI
WRITE(2)(AREA(I),I=1,18)
IF(TYME.LT.0.0)RETURN
DO 2 I=1,18
IF(AREA(I).LT.AREA(I+18))AREA(I+18)=AREA(I)
IF(AREA(I).GT.AREA(I+36))AREA(I+36)=AREA(I)
2 CONTINUE
NPOINT=NPOINT+1
RETURN
END
SUBROUTINE DOAXIS
COMMON
DIMENSION
EQUIVALENCE
1(TPERIN,DATA(4)),
CALL AXIS(0.0,0.0,14,HTIME (SECONDS),-14,16.0,0.0,TEND,TPERIN,10.0)
TEND=TEND+16.0#1PERIN
GO TO (2,2,3,4,5,6,7,8,9,10,11,12,13,14,15,16,17,18),JVAK
2 CALL AXIS(0.0,0.0,22,HCUNING ANGLE (DEGREES),22,9.0,90.0,0.0,20.0,1
10.0)
GO TO 100
3 CALL AXIS(0.0,1.0,41,HANGULAR MOMENTUM VECTOR AZIMUTH (DEGREES),41,
18.0,90.0,-160.0,40.0,10.0)
GO TO 100
4 CALL AXIS(0.0,1.0,43,HANGULAR MOMENTUM VECTOR ELEVATION (DEGREES),4
13.8,0,90.0,-80.0,20.0,10.0)
GO TO 100
5 CALL AXIS(0.0,1.0,25,HVEHICLE AZIMUTH (DEGREES),25,8.0,90.0,-160.0,
140.0,10.0)
GO TO 100
6 CALL AXIS(0.0,1.0,27,HVEHICLE ELEVATION (DEGREES),27,8.0,90.0,-80.0
1,20.0,10.0)
GO TO 100
7 CALL AXIS(0.0,1.0,37,TRANSVERSE RATE ORIENTATION (DEGREES),37,8.0,
190.0,-160.0,40.0,10.0)
GO TO 100

```



```

8 CALL AXIS(0.0,1.0,39HTRANSVERSE MOMENT ORIENTATION (DEGREES),39.0,
10,90.0,-160.0,40.0,10.0)
GO TO 100
9 CALL AXIS(0.0,1.0,32HMOMENT-RATE PHASE LEAD (DEGREES),32.8.0,90.0,
1-160.0,40.0,10.0)
GO TO 100
10 CALL AXIS(0.0,0.0,29HSPIN RATE (CYCLES PER SECOND),29,10.0,90.0,AK
1EA(10),AREA(28),10.0)
GO TO 100
11 CALL AXIS(0.0,0.0,37HRATE ABOUT Y-AXIS (CYCLES PER SECOND),37,10.0
1,90.0,AREA(11),AREA(29),10.0)
GO TO 100
12 CALL AXIS(0.0,0.0,37HRATE ABOUT Z-AXIS (CYCLES PER SECOND),37,10.0
1,90.0,AREA(12),AREA(30),10.0)
GO TO 100
13 CALL AXIS(0.0,0.0,28HROLLING MOMENT (FOOT-POUNDS),28,10.0,90.0,ARE
1A(13),AREA(31),10.0)
GO TO 100
14 CALL AXIS(0.0,0.0,33HMOMENT ABOUT Y-AXIS (FOOT-POUNDS),33,10.0,90.
10,AREA(14),AREA(32),10.0)
GO TO 100
15 CALL AXIS(0.0,0.0,33HMOMENT ABOUT Z-AXIS (FOOT-POUNDS),33,10.0,90.
10,AREA(15),AREA(33),10.0)
GO TO 100
16 CALL AXIS(0.0,0.0,48HSPIN ACCELERATION (CYCLES PER SECOND PER SECO
1ND),48,10.0,90.0,AREA(16),AREA(34),10.0)
GO TO 100
17 CALL AXIS(0.0,0.0,58HY-AXIS ANGULAR ACCELERATION (CYCLES PER SECON
1D PER SECOND),58,10.0,90.0,AREA(17),AREA(35),10.0)
GO TO 100
18 CALL AXIS(0.0,0.0,58HZ-AXIS ANGULAR ACCELERATION (CYCLES PER SECON
1D PER SECOND),58,10.0,90.0,AREA(18),AREA(36),10.0)
100 RETURN
END
SUBROUTINE COLMPY(COLIN,COLOUT,SQUARE)
DIMENSION
1 SQUARE(3,3)
DO 1 I=1,3
COLOUT(I)=0.0
DO 1 J=1,3
1 COLOUT(I)=COLOUT(I)+SQUARE(I,J)*COLIN(J)
RETURN
END
SUBROUTINE SETUP(N,VALUE)
DIMENSION
1 DATA(100),
DATA(1000)

```

```

WRITE(6,2006)
2006 FORMAT(104H
      1OUNDS)
      (CYCLES PER SECOND)
      (CYCLES PER SECOND PER SECOND) )
      (FOOT-P
WRITE(6,2007)
2007 FORMAT(104H
      1XIS Z-AXIS
      X-AXIS Y-AXIS Z-AXIS X-AXIS Y-A
      X-AXIS Y-AXIS Z-AXIS )
4 WRITE(6,1000)
ISKIP=0
1 ISKIP=ISKIP+1
IF(ISKIP.GT.11)GO TO 4
TITILE(1)=TYME
TITILE(2)=CONE#RAD
TITILE(3)=HAZI#RAD
TITILE(4)=HELI#RAD
TITILE(5)=XAZI#RAD
TITILE(6)=XELI#RAD
TITILE(7)=PHIRTE#RAD
TITILE(8)=PHIMOM#RAD
TITILE(9)=DELPHI#RAD
DO 3 I=1,3
TITILE(I+9)=RATE(I)/TWOPI
TITILE(I+12)=HDUT(I)
3 TITILE(I+15)=DIRATE(I)/TWOPI
WRITE(6,2008)(TITILE(J),J=1,18)
2008 FORMAT(5X,9F11.3/5X,9F11.3/)
RETURN
END
SUBROUTINE INERT
COMMON
DIMENSION
1APTCHI(50)
EQUIVALENCE
1(NTIMEI,IDATA(2)),
2(AROLLI(1),DATA(250)),(APTCHI(1),DATA(300)),(RATIO,DATA(122))
1 IF(TYME-T(NTIMEI))4,3,2
2 NTIMEI=NTIMEI+1
GO TO 1
3 RATIO=0.0
GO TO 5
4 RATIO=(T(NTIMEI)-TYME)/(T(NTIMEI)-T(NTIMEI-1))
5 ROLLI=AROLLI(NTIMEI)-(AROLLI(NTIMEI)-AROLLI(NTIMEI-1))*RATIO
PITCHI=APTCHI(NTIMEI)-(APTCHI(NTIMEI)-APTCHI(NTIMEI-1))*RATIO
RETURN
END
SUBROUTINE FIT2ND(N,VARIND,VARDEP,A0,A1,A2,IDIED)

```

```

DIMENSION
1 COEFFO(3),
2 SUM(8),
3 VARIND(N),
4 COEFF1(3),
5 RIGHT(3),
6 VARDEP(N),
7 COEFF2(3),
8
9 THIS PROGRAM PERFORMS A LEAST SQUARES FIT OF A QUADRATIC TO N
10 PAIRS OF DATA POINTS. THE ARRAY VARIND CONTAINS VALUES OF THE
11 INDEPENDENT VARIABLE (X) AND VARDEP CONTAINS THE COINCIDENT
12 VALUES OF THE DEPENDENT VARIABLE (Y). THE PROGRAM RETURNS THE
13 COEFFICIENTS OF  $Y=A_0+A_1X+A_2X^2$ . IDIED IS RETURNED AS 0 IF THE
14 EVALUATION IS SUCCESSFUL AND 1 IF THE DETERMINANT IS ZERO.
15 N MUST BE SPECIFIED IN THE CALL TO THIS PROGRAM AND THE ARKAYS
16 CALLING VARIND AND VARDEP MUST BE DIMENSIONED N IN THE CALLING
17 PROGRAM.
18 IDIED=0
19 SUM(1)=N
20 DO 1 I=2,8
21 SUM(I)=0.0
22 DO 2 J=1,N
23 SUM(2)=SUM(2)+VARIND(J)
24 POWER2=VARIND(J)*VARIND(J)
25 SUM(3)=SUM(3)+POWER2
26 POWER3=POWER2*VARIND(J)
27 SUM(4)=SUM(4)+POWER3
28 SUM(5)=SUM(5)+POWER3*VARIND(J)
29 SUM(6)=SUM(6)+VARDEP(J)
30 SUM(7)=SUM(7)+VARDEP(J)*VARIND(J)
31 SUM(8)=SUM(8)+VARDEP(J)*POWER2
32 DO 3 I=1,3
33 COEFFO(I)=SUM(I)
34 COEFF1(I)=SUM(I+1)
35 COEFF2(I)=SUM(I+2)
36 RIGHT(I)=SUM(I+5)
37 DENOM=DETMINT(COEFFO,COEFF1,COEFF2)
38 IF(DENOM.NE.0.0)GO TO 4
39 IDIED=1
40 RETURN
41
42 A0=DETMINT(RIGHT,COEFF1,COEFF2)/DENOM
43 A1=DETMINT(COEFFO,RIGHT,COEFF2)/DENOM
44 A2=DETMINT(COEFFO,COEFF1,RIGHT)/DENOM
45 RETURN
46
47 END
48 FUNCTION DETMINT(CUL1,CUL2,CUL3)
49 DIMENSION
50 COL3(3)
51 DETMINT=COL1(1)*(COL2(2)*COL3(3)-COL2(3)*COL1(2))+COL1(2)*(COL3(2)*
52 COL1(3)-COL3(3)*COL1(2))+COL1(3)*(COL2(1)*COL3(2)-
53 COL2(2)*COL1(3)+COL2(3)*COL1(2)-COL2(1)*COL3(2)+
54 COL2(2)*COL1(3)-COL2(3)*COL1(2))
55
56
57
58
59
60
61
62
63
64
65
66
67
68
69
70
71
72
73
74
75
76
77
78
79
80
81
82
83
84
85
86
87
88
89
90
91
92
93
94
95
96
97
98
99

```



```

RETURN
END
SUBROUTINE FIXTPE(IDIED)
COMMON
DIMENSION
1RTABLE(6),
2DELREF(3),
3X(4),
4VARDEP(5),
5C2(3)
EQUIVALENCE
1(RTABLE(1),DATA(13)),
2(TWOPI,DATA(31)),
3(NPOINT,DATA(2)),
4(Y(1),DATA(35)),
5(TSTGE(1),DATA(43))
6(VARDEP(1),DATA(53)),
7(C1(1),DATA(61)),
8(FIVDEG,DATA(69)),
DO 25 I=1,100
IDATA(I)=0
25 DATA(I)=0.0
TWOPI=6.283185
FIVDEG=0.0872665
TENDEG=0.1745329
KAD=57.29578
NFIRST=0
READ(5,1000)NPOINT,IFFIX,IFORTH
1000 FORMAT(3I12)
IF(IFFIX.EQ.0)FIVDEG=999999.
4 READ(5,1001)NPT,K(1),Y(1),K(2),Y(2),K(3),Y(3),K(4),Y(4)
1001 FORMAT(I12,4(I2,F10.3))
5 READ(9)(X(N),N=1,4)
NFIRST=NFIRST+1
IF(NFIRST.LT.NPT)GO TO 1
DO 2 I=1,4
IF(K(I).NE.0)X(I)=Y(I)
2 CONTINUE
1 DO 26 L=2,4
26 X(L)=X(L)/RAD
WRITE(2)(X(I),I=1,4)
IF(NFIRST.EQ.NPOINT)GO TO 3
IF(NFIRST.EQ.NPT)GO TO 4
GO TO 5
3 REWIND 2
DATA(1000)
TABLE(6),
YTABLE(6),
Y(4),
VARIND(5),
C1(3),
(TTABLE(1),DATA(7)),
(YTABLE(1),DATA(25)),
(NFIRST,DATA(1)),
(K(1),DATA(4)),
(JSTGE,DATA(8)),
(VARIND(1),DATA(48)),
(CO(1),DATA(58)),
(PRED,DATA(67)),
(TRY(1),DATA(1)),
(PTABLE(1),DATA(19)),
(DELREF(1),DATA(32)),
(NPT,DATA(3)),
(X(1),DATA(39)),
(NSTGE,DATA(9)),
(NEXTGO,DATA(10)),
(C2(1),DATA(64)),
(TENDEG,DATA(70))

```

```

JSTGE=1
DO 9 I=1,3
9 DELREF(I)=0.0
NFIRST=1
READ(5,1002)NSTGE,(TSTGE(I),I=1,NSTGE)
1002 FORMAT(112,5E12.8)
READ(2)TTABLE(1),RTABLE(1),PTABLE(1),YTABLE(1)
CALL OUTFIT(2,TTABLE(1),RTABLE(1),PTABLE(1),YTABLE(1))
IF(IFORTH.EQ.0)PTABLE(1)=-ATAN2((SIN(PTABLE(1))*COS(YTABLE(1))),
1COS(PTABLE(1)))
WRITE(1)TTABLE(1),RTABLE(1),PTABLE(1),YTABLE(1)
CALL OUTFIT(3,TTABLE(1),RTABLE(1),PTABLE(1),YTABLE(1))
24 CONTINUE
DO 6 I=2,5
READ(2)TTABLE(1),RTABLE(1),PTABLE(1),YTABLE(1)
CALL OUTFIT(2,TTABLE(1),RTABLE(1),PTABLE(1),YTABLE(1))
IF(IFORTH.EQ.0)PTABLE(1)=-ATAN2((SIN(PTABLE(1))*COS(YTABLE(1))),
1COS(PTABLE(1)))
RTABLE(1)=RTABLE(1)+DELREF(1)
PTABLE(1)=PTABLE(1)+DELREF(2)
YTABLE(1)=YTABLE(1)+DELREF(3)
NFIRST=NFIRST+1
TRY(1)=RTABLE(1)
TRY(2)=PTABLE(1)
TRY(3)=YTABLE(1)
TRY(4)=RTABLE(I-1)
TRY(5)=PTABLE(I-1)
TRY(6)=YTABLE(I-1)
DO 7 N=1,3
IF(ABS(TRY(N)-TRY(N+2)).LT.ABS(TRY(N)+TWOPI-TRY(N+3)))GO TO 8
TRY(N)=TRY(N)+TWOPI
DELREF(N)=DELREF(N)+TWOPI
GO TO 7
8 IF(ABS(TRY(N)-TRY(N+3)).LT.ABS(TRY(N)-TWOPI-TRY(N+3)))GO TO 7
TRY(N)=TRY(N)-TWOPI
DELREF(N)=DELREF(N)-TWOPI
7 CONTINUE
RTABLE(1)=TRY(1)
PTABLE(1)=TRY(2)
YTABLE(1)=TRY(3)
WRITE(1)TTABLE(1),RTABLE(1),PTABLE(1),YTABLE(1)
CALL OUTFIT(3,TTABLE(1),RTABLE(1),PTABLE(1),YTABLE(1))
IF(NFIRST.EQ.NPOINT)GO TO 22
IF(TTABLE(1).LT.TSTGE(JSTGE).OR.JSTGE.GT.NSTGE)GO TO 6
TTABLE(1)=TTABLE(1)

```

\*\*\*

\*\*\*

\*\*\*

\*\*\*

```

RTABLE(1)=RTABLE(I)
PTABLE(1)=PTABLE(I)
YTABLE(1)=YTABLE(I)
JSTGE=JSTGE+1
GO TO 24

6 CONTINUE
23 READ(2)TTABLE(6),RTABLE(6),PTABLE(6),YTABLE(6)
CALL OUTFIT(2,TTABLE(6),RTABLE(6),PTABLE(6),YTABLE(6))
IF(IFORTH.EQ.0)PTABLE(6)=-ATAN2((SIN(PTABLE(6))#COS(YTABLE(6))),
1COS(PTABLE(6)))
RTABLE(6)=RTABLE(6)+DELREF(1)
PTABLE(6)=PTABLE(6)+DELREF(2)
YTABLE(6)=YTABLE(6)+DELREF(3)
NFIRST=NFIRST+1
NEXTGO=1
DO 10 I=1,5
VARIND(I)=TTABLE(I)
10 VARDEP(I)=RTABLE(I)
GO TO 11
12 NEXTGO=2
DO 13 I=1,5
13 VARDEP(I)=PTABLE(I)
GO TO 11
14 NEXTGO=3
DO 15 I=1,5
15 VARDEP(I)=YTABLE(I)
11 CALL FIT2ND(5,VARIND,VARDEP,CO(NEXTGU),C1(NEXTGU),C2(NEXTGU),IDIED
1)
IF(IDIED.GT.0)RETURN
GO TO(12,14,16),NEXTGO
16 TRY(1)=RTABLE(6)
TRY(2)=PTABLE(6)
TRY(3)=YTABLE(6)
DO 17 I=1,3
PREDCO(I)+C1(I)#TTABLE(6)+C2(I)#TTABLE(6)##2
IF(ABS(TRY(I)-PRED).LT.ABS(TRY(I)+TWOPI-PRED))GO TO 18
TRY(I)=TRY(I)+TWOPI
DELREF(I)=DELREF(I)+TWOPI
GO TO 19
18 IF(ABS(TRY(I)-PRED).LT.ABS(TRY(I)-TWOPI-PRED))GO TO 19
TRY(I)=TRY(I)-TWOPI
DELREF(I)=DELREF(I)-TWOPI
19 IF(ABS(TRY(I)-PRED).LE.FIVDEG)GO TO 17
IF(TRY(I).GT.PRED)GO TO 20
TRY(I)=TRY(I)+TENDEG

```

\*\*\*

```

IF(TTABLE(6).EQ.TSTGE(JSTGE))DELREF(I)=DELREF(I)+TENDEG
GO TO 19
20 TRY(I)=TRY(I)-TENDEG
IF(TTABLE(6).EQ.TSTGE(JSTGE))DELREF(I)=DELREF(I)-TENDEG
GO TO 19
17 CONTINUE
RTABLE(6)=TRY(1)
PTABLE(6)=TRY(2)
YTABLE(6)=TRY(3)
DO 21 I=1,5
TTABLE(I)=TTABLE(I+1)
RTABLE(I)=RTABLE(I+1)
PTABLE(I)=PTABLE(I+1)
YTABLE(I)=YTABLE(I+1)
21 WRITE(1)TTABLE(5),RTABLE(5),PTABLE(5),YTABLE(5)
CALL OUTFIT(3,TTABLE(5),RTABLE(5),PTABLE(5),YTABLE(5))
IF(NFIRST.EQ.NPOINT)GO TO 22
IF(TTABLE(5).LT.TSTGE(JSTGE).OR.JSTGE.GT.NSTGE)GO TO 23
TTABLE(1)=TTABLE(5)
RTABLE(1)=RTABLE(5)
PTABLE(1)=PTABLE(5)
YTABLE(1)=YTABLE(5)
JSTGE=JSTGE+1
GO TO 24
22 REWIND 2
REWIND 1
RETURN
END
SUBROUTINE OUTFIT(ISEND,A,B,C,D)
GO TO (1,2,3),ISEND
1 RAD=57.29578
WRITE(6,1001)
1001 FORMAT(1H1//////35H THIS IS THE WAY WE SMOOTH THE DATA//30X,4HTIME)
1,18X,4HROLL,17X,5HPITCH,19X,3HYAW/)
JPAGE=6
RETURN
2 ROUT=B#RAD
COUT=C#RAD
DOUT=D#RAD
WRITE(6,1002)A,B,OUT,C,OUT,DOUT
1002 FORMAT(6X,6HBEFORE,4F22.3)
RETURN
3 ROUT=B#RAD
COUT=C#RAD
DOUT=D#RAD

```

\*\*\*

OUTFIT01  
OUTFIT02  
OUTFIT03  
OUTFIT04  
OUTFIT05  
OUTFIT06  
OUTFIT07  
OUTFIT08  
OUTFIT09  
OUTFIT10  
OUTFIT11  
OUTFIT12  
OUTFIT13  
OUTFIT14  
OUTFIT15  
OUTFIT16  
OUTFIT17

OUTFIT18  
OUTFIT19  
OUTFIT20  
OUTFIT21  
OUTFIT22  
OUTFIT23  
OUTFIT24  
OUTFIT25  
OUTFIT26

WRITE(6,1003)A,ROUT,COUT,DOUT  
1003 FORMAT(7X,5HAFTEK,4F22.3/)  
JPAGE=JPAGE+3  
IF(JPAGE.LT.45)RETURN  
WRITE(6,1004)  
1004 FORMAT(1H1///)  
JPAGE=0  
RETURN  
END

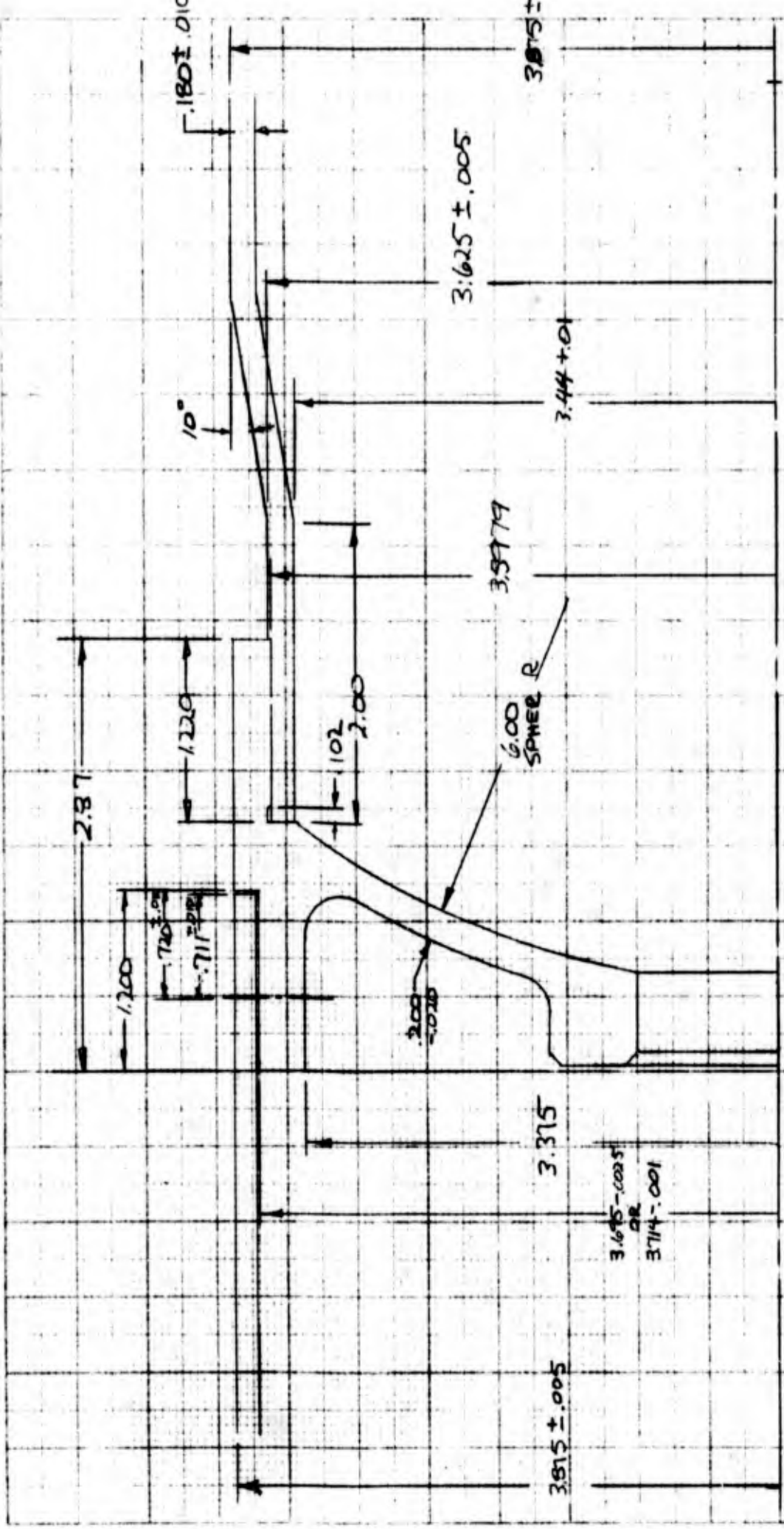
Appendix C

NIRO JOINT STUDY DATA SHEETS AND PRINTOUT

The following data sheets present the assumed geometry and mechanics of the NIRO payload-motor joint used in the computer simulation of the joint rotation. Work sheets for each of the assumed elements are included.

The input and computed output printouts for the NIRO joint analysis as run on Program 0616 are also included.



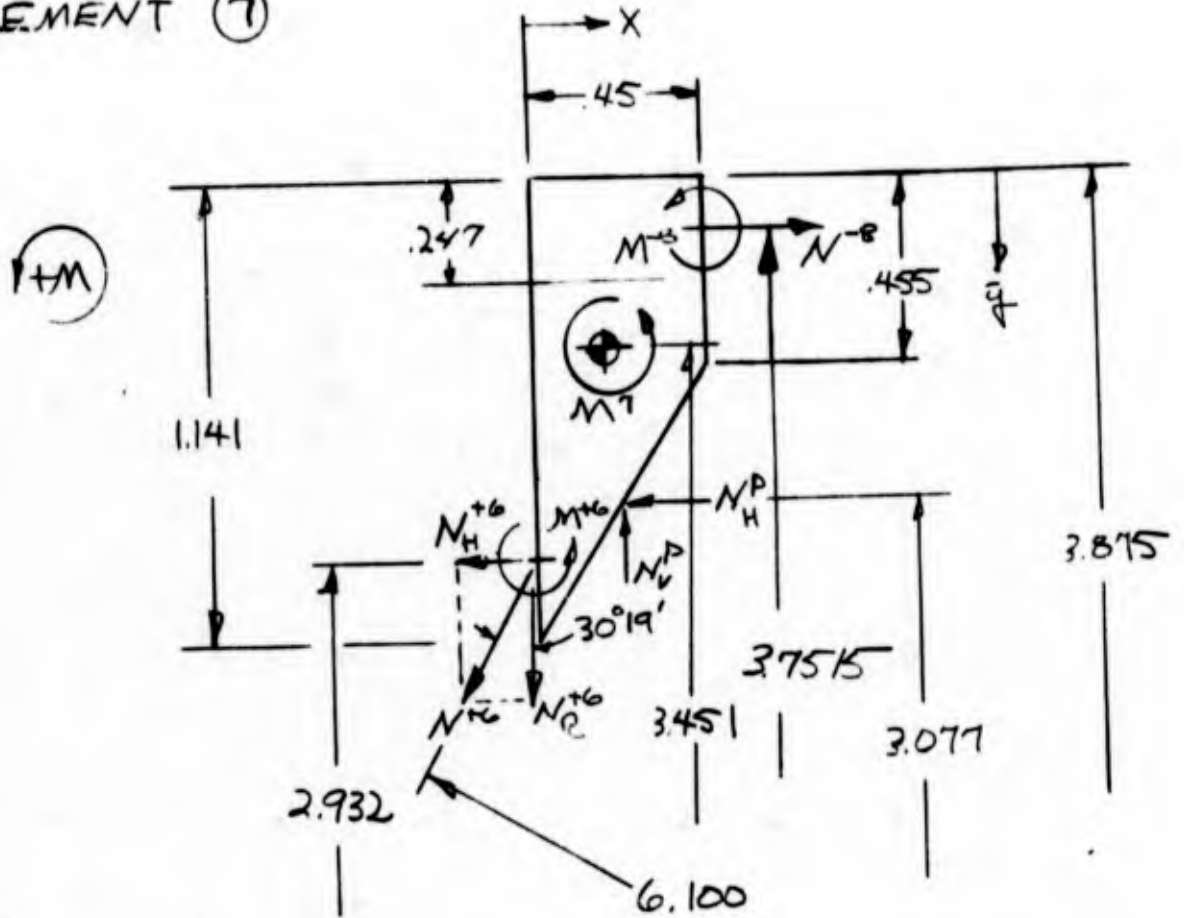


NIRO PAYLOAD-MOTOL JOINT

By CLH  
 Checked \_\_\_\_\_  
 Subject NIRO

Page \_\_\_\_\_ of \_\_\_\_\_  
 Date \_\_\_\_\_  
 Work Order 901320-2010

HEAD CAP  
 ELEMENT ⑦



ELEMENT C.G.

$$\bar{y} = \frac{\sum Ay}{\sum A}$$

$$= \frac{.45(.455)^2(\frac{1}{2}) + (1.141 - .455)(\frac{.45}{2})(.455 + \frac{1.141 - .455}{3})}{.45(.455) + (1.141 - .455)(\frac{.45}{2})}$$

$$= \frac{.04658 + .10552}{.20475 + .15435} = \frac{.15210}{.35910} = .424 \text{ IN.}$$

$$\bar{x} = \frac{\sum Ax}{\sum A} = \frac{.20475(.45)^2(\frac{1}{2}) + .15435(.45)(\frac{1}{3})}{.20475 + .15435}$$

$$= \frac{.06922}{.35910} = .193$$

|         |      |
|---------|------|
| By      | CLH  |
| Checked |      |
| Subject | NIRO |

|            |             |
|------------|-------------|
| Page       | of          |
| Date       |             |
| Work Order | 901320-2010 |

HEAD CAP (CONTD)

ELEMENT ⑦ (CONTD)

MEMBRANE LOADS

$$N^{tg} = \frac{PR}{2} = \frac{1440(6.100)}{2}$$

$$= 4392 \text{ LB./IN.}$$

$$N_H^{tg} = N^{tg} \sin 30^\circ 19' = 4392(.50478)$$

$$= 2217 \text{ LB./IN.}$$

$$N_R^{tg} = N^{tg} \cos 30^\circ 19'$$

$$= 3791 \text{ LB./IN.}$$

$$N^{-B} = \frac{PR}{2} = \frac{1440(3.51895)}{2} \left( \frac{3.51895}{3.7515} \right)$$

$$= 2377 \text{ LB./IN.}$$

$$N_H^D = P^H A^H = 1440 (\sin 56^\circ 44') (1.141-.495)$$

$$= 826 \text{ LB./IN.}$$

$$N_V^D = P^V A^V = 1440 (\cos 53^\circ 44') (.45)$$

$$= 355 \text{ LB./IN.}$$

KICK MOMENT

$$M^T = \left[ 2217(3.451-2.932) + 3791(.193) \right] \left( \frac{2.932}{3.451} \right)$$

$$- 2377(3.7515-3.451) \left( \frac{3.7515}{3.451} \right)$$

$$+ \left[ -826(3.451-3.077) + 355(.225-.193) \right] \left( \frac{3.077}{3.451} \right)$$

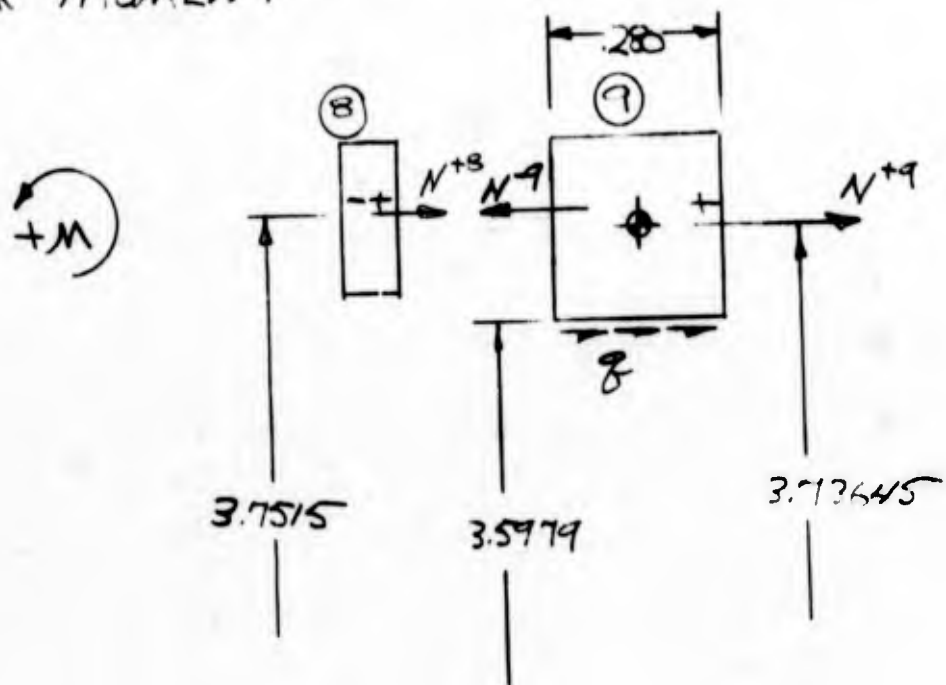
$$= -355.95 - 776.49 - 265.32$$

$$= -1398 \text{ IN. LB./IN.}$$

By CLH  
 Checked \_\_\_\_\_  
 Subject NIRO

Page \_\_\_\_\_ of \_\_\_\_\_  
 Date \_\_\_\_\_  
 Work Order 701320-2010

HEAD CAP (CONT'D)  
 ELEMENTS (8), (9)  
 KICK MOMENT



$$N^{+8} = N^{-8} = 2377 \text{ LB/IN}$$

$$N^{-9} = N^{+8} = 2377 \text{ LB/IN}$$

$$\delta = \frac{PR}{2L} = \frac{1440(3.51895)}{2(1.22-1.02)} \left( \frac{3.51895}{3.5979} \right)$$

$$= 2216.5 \text{ LB/IN/IN}$$

LOAD IN THREAD

$$N^{+9} = N^{-9} - .280 \delta = 2377 - .280(2216.5) \frac{3.5979}{3.73645}$$

$$= 1798.4 \text{ LB/IN}$$

$$M_y = 2377(3.7515 - 3.73645) \frac{3.7515}{3.73645}$$

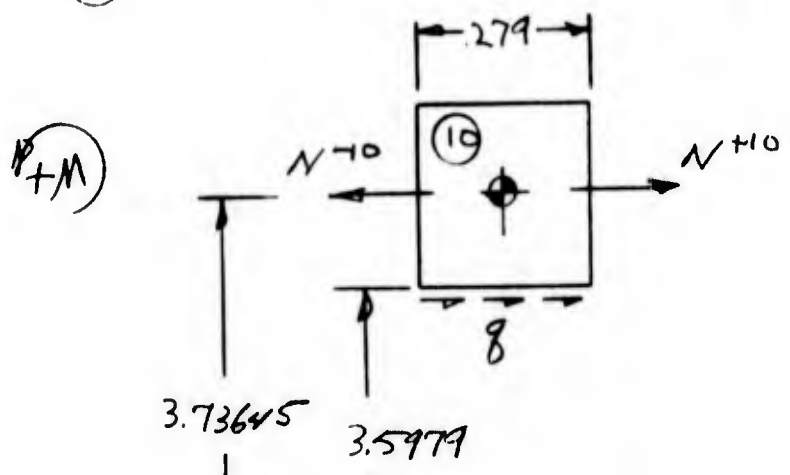
$$+ 2216.5(.280)(3.73645 - 3.5979) \left( \frac{3.5979}{3.73645} \right)$$

$$= 35.9 + 82.8 = 118.7 \text{ IN.LB./IN. Page C-5}$$

By CLH  
 Checked \_\_\_\_\_  
 Subject VIRO

Page \_\_\_\_\_ of \_\_\_\_\_  
 Date \_\_\_\_\_  
 Work Order 901320-2010

HEAD CAP (CONT'D)  
 ELEMENT ⑩



$$g = 2216.5 \text{ LB/IN/IN}$$

$$N^{-10} = N^{+9} = 1788.4 \text{ LB/IN.}$$

$$N^{+10} = N^{-10} - .279 g = 1788.4 - .279(2216.5) \frac{3.5979}{3.73645}$$

$$= 1192.9 \text{ LB/IN}$$

$$M_{10} = 2216.5 (.279)(3.73645 - 3.5979) \frac{3.5979}{3.73645}$$

$$= 82.5 \text{ IN-LB./IN}$$

ELEMENT ⑪

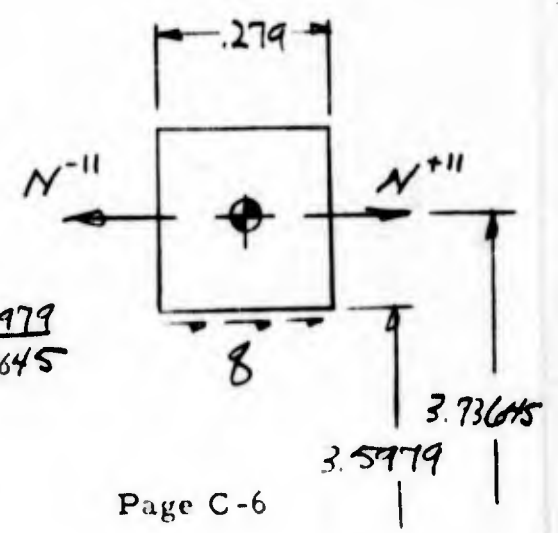
$$N^{-11} = N^{+10} = 1192.9 \text{ LB/IN}$$

$$N^{+11} = N^{-11} - .279 g$$

$$= 1192.9 - .279(2216.5) \frac{3.5979}{3.73645}$$

$$= 597.4 \text{ LB/IN.}$$

$$M_{11} = M_{10} = 82.5 \text{ IN-LB./IN}$$

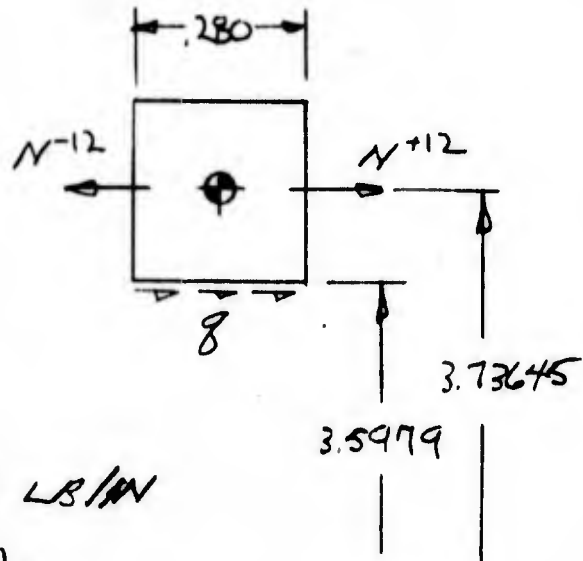


By CLH  
 Checked \_\_\_\_\_  
 Subject NIRO

Page \_\_\_\_\_ of \_\_\_\_\_  
 Date \_\_\_\_\_  
 Work Order 901320-2010

HEAD CAP (CONT'D)

ELEMENT ⑫



$$N^{-12} = N^{+11} = 597.4 \text{ LB/IN}$$

$$\begin{aligned} N^{+12} &= N^{-12} - (.280)g \\ &= 597.4 - (.280)(2216.5) \frac{3.5979}{3.73645} \\ &= 0 \end{aligned}$$

$$\begin{aligned} M_{12} &= 2216.5(.280)(3.73645 - 3.5979) \frac{3.5979}{3.73645} \\ &= 82.8 \text{ IN-LB./IN.} \end{aligned}$$

ELEMENT ⑬

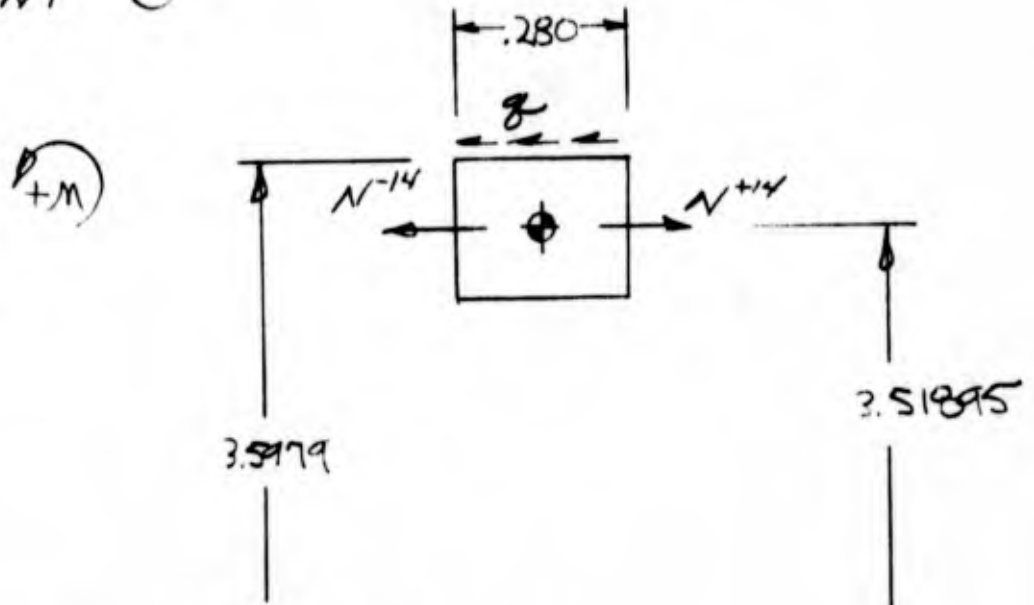
$$N^{-13} = N^{+13} = M_{13} = 0$$



By CLH  
 Checked \_\_\_\_\_  
 Subject NIRO

Page \_\_\_\_\_ of \_\_\_\_\_  
 Date \_\_\_\_\_  
 Work Order 901320-2010

HEAD CAP (CONT'D)  
 ELEMENT ⑭



$$q = 2216.5 \text{ LB/IN/IN}$$

$$N^{-14} = 0$$

$$N^{+14} = N^{-14} + q(.280) = 2216.5(.280) \frac{3.5979}{3.51895}$$

$$= 634.5 \text{ LB/IN.}$$

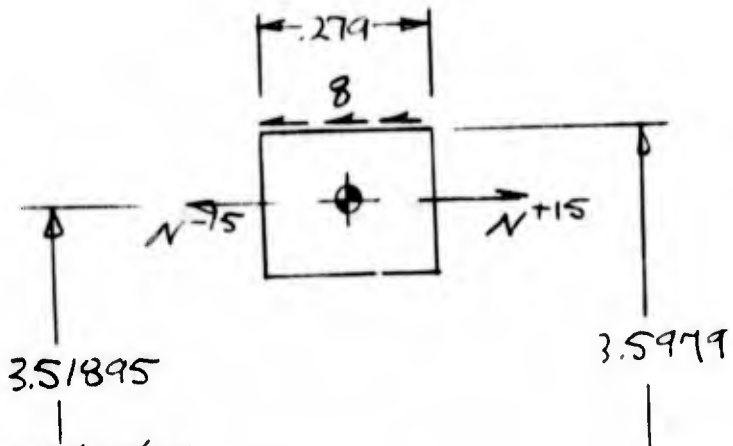
$$M_{14} = 2216.5(.280)(3.5979 - 3.51895) \frac{3.5979}{3.51895}$$

$$= 50.1 \text{ IN-LB/IN}$$

By CLH  
 Checked \_\_\_\_\_  
 Subject NIRO

Page \_\_\_\_\_ of \_\_\_\_\_  
 Date \_\_\_\_\_  
 Work Order 901320-2010

HEAD CAP (CONT'D)  
 ELEMENT (5)



$$g = 2216.5 \text{ LB/IN/IN}$$

$$N^{-15} = N^{+14} = 634.5 \text{ LB/IN}$$

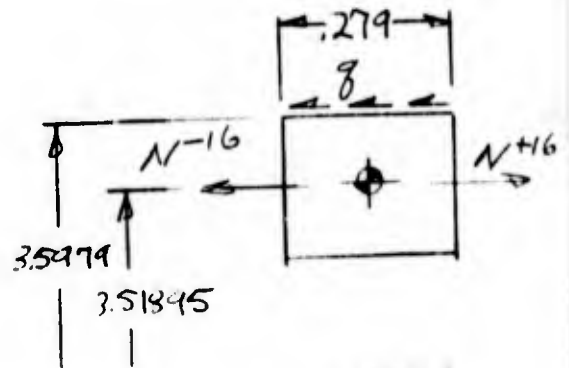
$$N^{+15} = N^{-15} + .279g = 634.5 + .279(2216.5) \frac{3.5979}{3.51895}$$

$$= 1266.8 \text{ LB/IN.}$$

$$M_{15} = 2216.5 (.279) (3.5979 - 3.51895) \frac{3.5979}{3.51895}$$

$$= 49.9 \text{ IN-LB/IN}$$

ELEMENT (16)



$$g = 2216.5$$

$$N^{-16} = N^{+15} = 1266.8 \text{ LB/IN}$$

$$N^{+16} = N^{-16} + .279g = 1266.8 + .279(2216.5) \frac{3.5979}{3.51895}$$

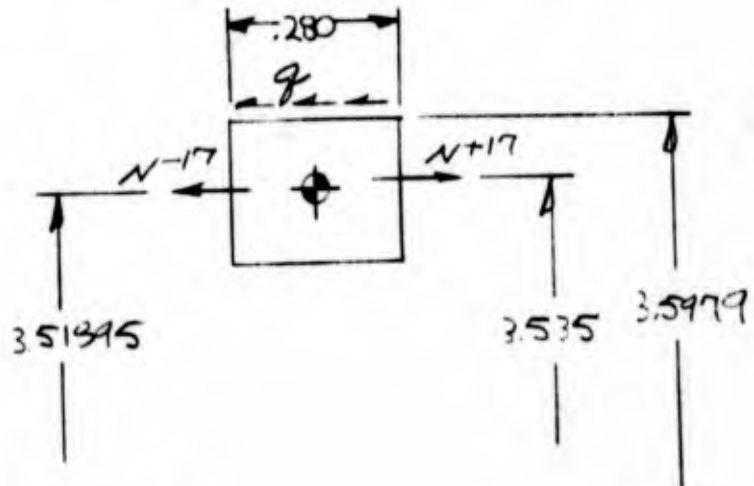
$$= 1899.1 \text{ LB/IN}$$

$$M_{16} = M_{15} = 49.9 \text{ IN-LB/IN}$$

By CLH  
 Checked \_\_\_\_\_  
 Subject NIRO

Page \_\_\_\_\_ of \_\_\_\_\_  
 Date \_\_\_\_\_  
 Work Order 901320-2010

HEAD CAP (CONT'D)  
 ELEMENT ①



$$g = 2216.5 \text{ LB/IN./IN.}$$

$$N^{-17} = N^{+16} = 1399.1 \text{ LB/IN.}$$

$$N^{+17} = N^{-17} + .280g$$

$$= \left[ 1399.1 + .280(2216.5) \right] \frac{3.5979}{3.51845} \frac{3.51845}{3.535}$$

$$= 2522.1 \text{ LB/IN.}$$

$$M_{17} = 2216.5(.280)(3.5979 - 3.51845) \frac{3.5979}{3.51845}$$

$$- 2522.1(3.535 - 3.51845) \frac{3.535}{3.51845}$$

$$= 50.1 - 40.7$$

$$= 9.4 \text{ IN-LB/IN.}$$

By CLH  
 Checked \_\_\_\_\_  
 Subject NIRO

Page \_\_\_\_\_ of \_\_\_\_\_  
 Date \_\_\_\_\_  
 Work Order 901320-2010

HEAD CAP (CONT'D)  
 LOADS

ELEMENT ⑦

$$RVI = \frac{F}{2\pi} = \frac{\pi PR^2}{2\pi} = \frac{PR^2}{2}$$

$$R = 3.875 - 1.141 + \frac{316}{2} = 2.932 \text{ in.}$$

$$= \frac{1440(2.932)^2}{2}$$

$$= 6189.6$$

$$PH(1-3) = 1440 \cos 56^\circ 44' = 1440 (.54854) = 789.9 \text{ PSI}$$

$$PV(1-3) = -1440 \sin 56^\circ 44' = -1440 (.83613) = -1204.0 \text{ PSI}$$

ELEMENT ⑧

$$RVI = \frac{PR^2}{2} = \frac{1440(3.51895)^2}{2} = 8915.8$$

ELEMENT ⑨

$$RVI = 8915.8$$

$$PH(1-10) = -900.0$$

$$p^{-9} = \frac{2N^{-9}}{R} = \frac{2(2377)}{3.7515} = 1267.23$$

$$p^{+9} = \frac{2N^{+9}}{R} = \frac{2(17834)}{3.73645} = 957.27$$

$$PV(1) = 1267.23(-30.996) + 957.27$$

By CLH  
 Checked \_\_\_\_\_  
 Subject NIRO

Page \_\_\_\_\_ of \_\_\_\_\_  
 Date \_\_\_\_\_  
 Work Order 901320-2010

HEAD CAP (CONTD)

LOADS (CONTD)

ELEMENT ⑩

$$RVI = \frac{P^{-10} R^2}{2} = \frac{957.27 (3.73645)^2}{2} = 6682.2$$

$$PH(1-10) = -900.0$$

$$P^{-10} = P^{+9} = 957.27$$

$$P^{+10} = \frac{2N^{+10}}{R} = \frac{2(1192.9)}{3.73645} = 638.52$$

$$PV(1) + 957.27(-31.875) + 638.52$$

ELEMENT ⑪

$$RVI = \frac{P^{-11} R^2}{2} = \frac{638.52 (3.73645)^2}{2} = 4457.2$$

$$PH(1-10) = -900.0$$

$$P^{-11} = P^{+10} = 638.52$$

$$P^{+11} = \frac{2N^{+11}}{R} = \frac{2(597.4)}{3.73645} = 319.77$$

$$PV(1) + 638.52(-31.875) + 319.77$$

ELEMENT ⑫

$$RVI = \frac{P^{-12} R^2}{2} = \frac{319.77 (3.73645)^2}{2} = 2232.2$$

$$PH(1-10) = -900.0$$

$$P^{-12} = P^{+11} = 319.77$$

$$P^{+12} = \frac{2N^{+12}}{R} = \frac{2(0)}{R} = 0$$

$$PV(1) + 319.77(-31.875) + 0.0$$

|         |      |
|---------|------|
| By      | CLH  |
| Checked |      |
| Subject | NIRO |

|            |             |
|------------|-------------|
| Page       | of          |
| Date       |             |
| Work Order | 901320-2010 |

HEAD CAP (CONT'D)

LOADS (CONT'D)

ELEMENT (14)

$$RVI = 0.0$$

$$PH(1-10) = -540$$

$$P^{-14} = 0.0$$

$$P^{+14} = \frac{2N^{+14}}{R} = \frac{2(634.5)}{3.51895} = 360.62$$

$$PV(1) = 0.0 (+36.062) 360.62$$

ELEMENT (15)

$$RVI = \frac{P^{-15} R^2}{2} = \frac{360.62(3.51895)^2}{2} = 2232.8$$

$$PH(1-10) = -540$$

$$P^{-15} = P^{+14} = 360.62$$

$$P^{+15} = \frac{2N^{+15}}{R} = \frac{2(1266.8)}{3.51895} = 719.99$$

$$PV(1) = +360.62 (+35.937) + 719.99$$

ELEMENT (16)

$$RVI = \frac{P^{-16} R^2}{2} = \frac{719.99(3.51895)^2}{2} = 4457.8$$

$$PH(1-10) = -540$$

$$P^{-16} = P^{+15} = 719.99$$

$$P^{+16} = \frac{2N^{+16}}{R} = \frac{2(1899.1)}{3.51895} = 1079.36$$

$$PV(1) = 719.99 (+35.937) + 1079.36$$



|         |      |
|---------|------|
| By      | CLH  |
| Checked |      |
| Subject | NIRO |

|            |             |
|------------|-------------|
| Page       | of          |
| Date       |             |
| Work Order | 901320-2-10 |

HEAD CAP (CONT'D)

LOADS (CONT'D)

ELEMENT (17)

$$RVI = \frac{P^{-17} R^2}{2} = \frac{1079.36 (3.51895)^2}{2} = 6692.9$$

$$PH(1-10) = -540$$

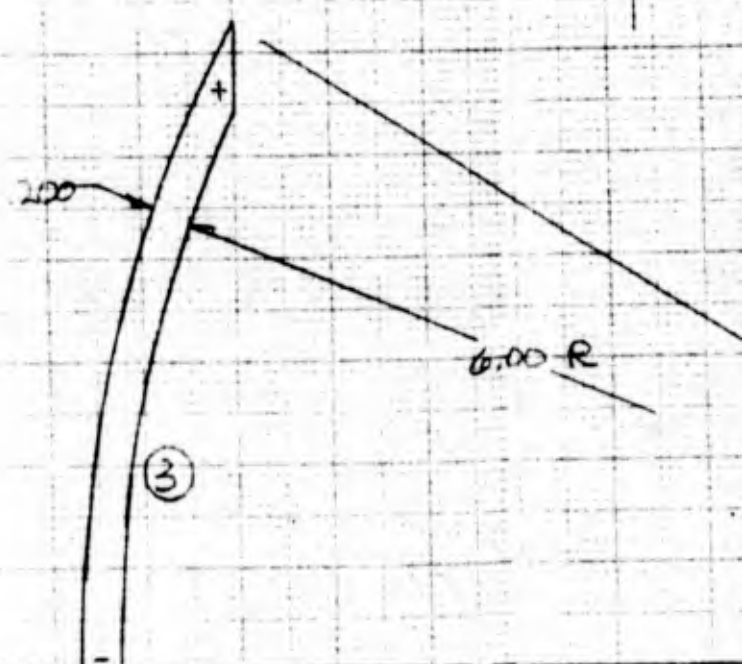
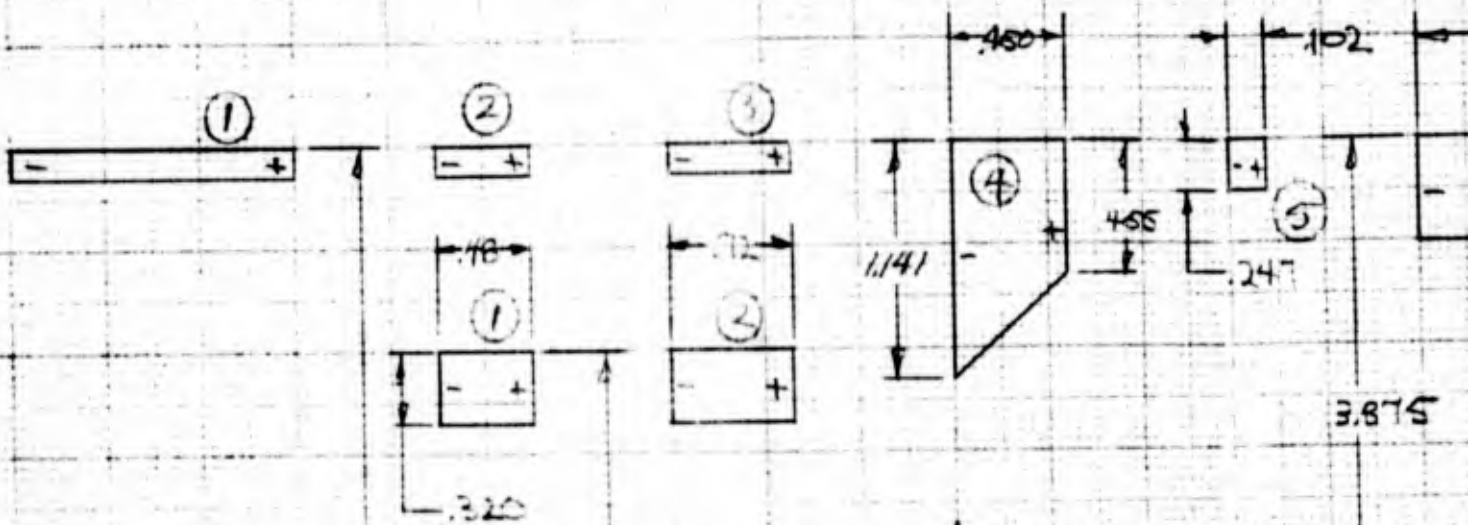
$$P^{-17} = P^{+16} = 1079.36$$

$$P^{+17} = \frac{2N^{+17}}{R} = \frac{2(2522.1)}{3.535} = 1426.93$$

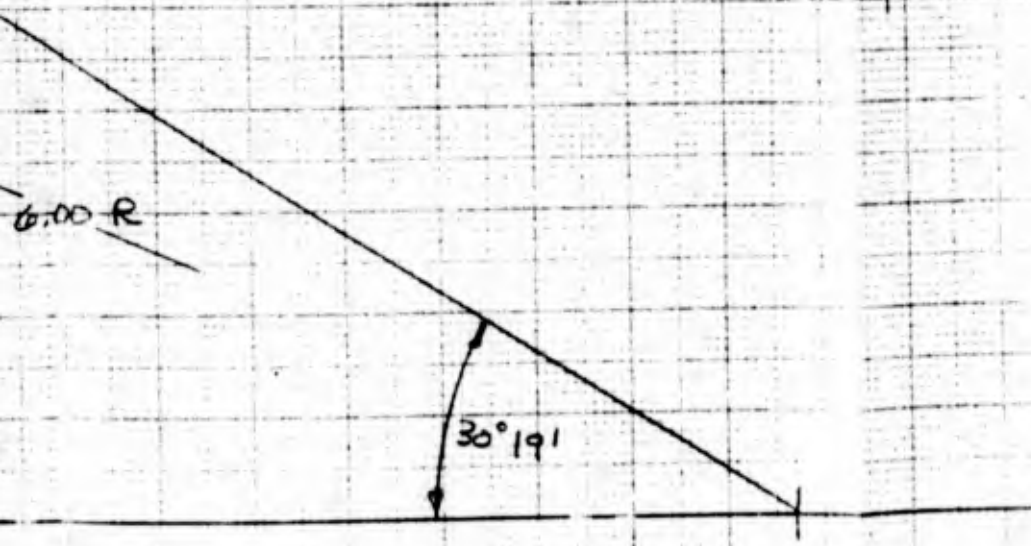
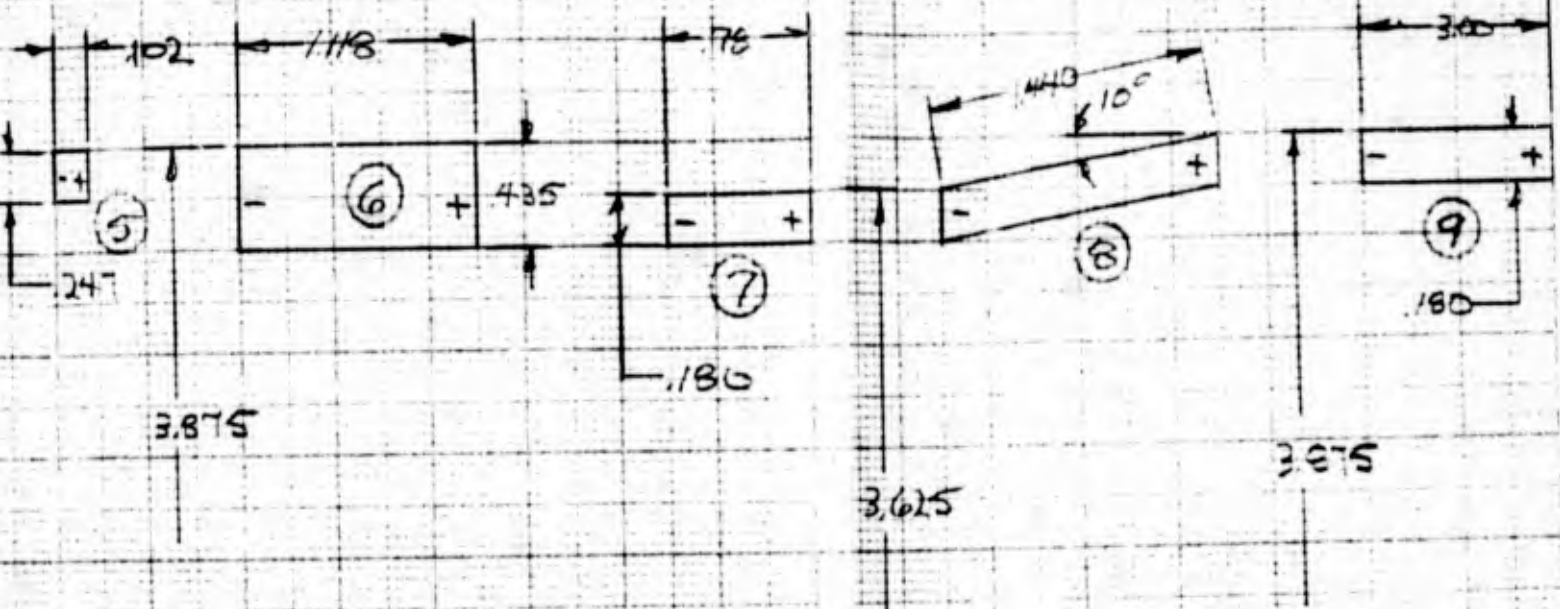
$$PV(1) = 1079.36 (+34.757) + 1426.93$$

ELEMENT (18)

$$RVI = \frac{P^{-18} R^2}{2} = \frac{1426.93 (3.535)^2}{2} = 8915.6$$



A



NIRO HEADCAP REGIONS

B

TABLE OF MACHINE PRINTOUT SYMBOLS

Machine Printout

|              |   |  |
|--------------|---|--|
| XI           | $\xi$   | Wrap distance from beginning of region           |
| K THETA      | $K_{\theta}$                                    | Curvature in $\theta$ direction                  |
| K XI         | $K_{\xi}$                                       | Curvature in $\xi$ direction                     |
| BETA         | $\beta$   | Rotation in $\xi$ direction                      |
| C            | $C = \int_h E d\zeta$                           | Membrane elastic parameter                       |
| D            | $D = \frac{1}{1-\nu^2} \int_h E \zeta^2 d\zeta$ | Bending elastic parameter                        |
| NT           | $N_T = \int_h E \bar{\alpha} T d\zeta$          | Thermal membrane force                           |
| MT           | $M_T = \int_h E \bar{\alpha} T \zeta d\zeta$    | Thermal bending moment                           |
| U            | $u$   | Deflection, radially                             |
| Q            | $Q = \int_h T \xi \zeta d\zeta$                 | Shear force                                      |
| W            | $w$   | Deflection, axially                              |
| ROS          | $R_{o.s.}$                                      | Radius of outer surface                          |
| ZOS          | $Z_{o.s.}$                                      | Axial coordinate, outer surface                  |
| STRAIN XI    | $\epsilon_{\xi}$                                | Strain in $\xi$ direction                        |
| STRAIN THETA | $\epsilon_{\theta}$                             | Strain in $\theta$ direction                     |
| A            | $a$   | Distance from outer surface to reference surface |
| (RV)         | $r V = - \int_0^{\xi} r \alpha P_v d\xi$        | Total vertical load $- 2 \pi$                    |

TABLE OF MACHINE PRINTOUT SYMBOLS (Continued)

Machine Printout

|                |   |                                    |
|----------------|---|------------------------------------|
| N(XI)          | $N_{\xi} = \int_h \sigma_{\xi} d \zeta$             | Membrane force, $\xi$ direction    |
| N(THETA)       | $N_{\theta} = \int_h \sigma_{\theta} d \zeta$       | Membrane force, $\theta$ direction |
| M(XI)          | $M_{\xi} = \int_h \sigma_{\xi} \zeta d \zeta$       | Bending moment, $\xi$ direction    |
| M(THETA)       | $M_{\theta} = \int_h \sigma_{\theta} \zeta d \zeta$ | Bending moment, $\theta$ direction |
| SIGMA XI       | $\sigma_{\xi}$                                      | Stress, $\xi$ direction            |
| SIGMA $\theta$ | $\sigma_{\theta}$                                   | Stress, $\theta$ direction         |

The stresses, SIGMA XI and SIGMA  $\theta$  are printed out at each XI interval and at each surface or layer interface. "Wrap distance" is the name given to the XI =  $\xi$  , measured along the reference surface.

INPUT DATA

```

WITHOUT
* NIFO JOINT ROTATION STUDY---HEAD GAP AND CASE
DATE 2.6.68 CASE 1.0 NREGIONS 9
ENDC(1,1) -1 4 C.0 ENDC(2,1) -1 0 0.0
ENDC(3,1) -3 5 C.0 ENDC(4,1) -3 7 0.0
ENDC(5,1) 69 4 C.0 ENDC(6,1) 59 7 0.0
JUNC(1,1) 61 -2 0 0.0 0.0 JUNC(2,1) 62 63 -4 0.0 61395.0
JUNC(3,1) 64 -5 0 0.0 0.0 JUNC(4,1) 65 -6 0 0.0 6223.4
JUNC(5,1) 66 -7 0 0.0 630d.3 JUNC(6,1) 67 -8 0 0.0 0.0
JUNC(7,1) 68 -9 0 0.0 0.0
NSTATIONS 3 DELTAXI .005 NU .3 PRINTOUT 10
RVCCNT 0 NGRV 0 KVI C.0 NLAYERS 1
GECM 1 RO 3.695 ANGLE 90.
XI 0.0(.24).48
H(1-3) .32C
P(1-3) 0.0 PCCMP 0 Y(1-3) 10.560 A(1-3) 0. T(1-3) 0.
1
NSTATIONS 3 DELTAXI .005 NU .3 PRINTOUT 10
RVCCNT 1 NGRV 0 KVI C.0 NLAYERS 1
GECM 1 RU 3.695 ANGLE 90.
XI C.0(.36C).720
1
NSTATIONS 3 DELTAXI .05 NU .3 PRINTOUT 2
RVCCNT 0 NGRV 0 RVI 0.0 NLAYERS 1
GECM 2 RCURVE 0.200 OFFSET 0.0 XIMIN 0.0
PHI 0.0(15.15833)30.31657
H(1-3) 0.200
P(1-3)-144C. PCLMP C
1
NSTATIONS 3 DELTAXI .005 NU .3 PRINTOUT 10
RVCCNT 0 NGRV 0 KVI 6189.8 NLAYERS 1
GECM 1 RG 3.875 ANGLE 90.
XI 0.0 .3C .45
H(1) 1.141 .684 .455
P(1-3) C.0 PCCMP 1 PH(1-3) 789.9 PV(1-3) -1204.0
1
NSTATIONS 3 DELTAXI .001 NU .3 PRINTOUT 10
RVCCNT C NGRV 0 KVI 8915.8 NLAYERS 1
GECM 1 RO 3.875 ANGLE 90.C
XI C.0(.051).102
H(1-3) .247
P(1-3)-1440. PCLMP C
1

```



INSTATIUNS 3 DELTAXI .01 NU .3 PRINTCUT 10  
RVCCNT 1 NGRV C RVI 0.0 NLAYERS 1  
GEM 1 RO 3.875 ANGLE 90.  
XI 0.0(.559)1.118  
H(1-3) .435  
P(1-3) -144G. PCCMP 0

1  
INSTATIUNS 3 DELTAXI .008 NU .3 PRINTCUT 5  
RVCCNT 0 NGRV 0 RVI 8915.6 NLAYERS 1  
GEM 1 RO 3.625 ANGLE 90.  
XI 0.0(.39) .78  
H(1-3) .180

1  
INSTATIUNS 3 DELTAXI .015 NU .3 PRINTCUT 10  
RVCCNT 1 NGRV 0 RVI 0.0 NLAYERS 1  
GEM 1 RO 3.625 ANGLE 80.  
XI 0.0(.720)1.440

1  
INSTATIUNS 3 DELTAXI .03 NU .3 PRINTCUT 10  
RVCCNT 1 NGRV C RVI 0.0 NLAYERS 1  
GEM 1 RO 3.875 ANGLE 90.  
XI 0.0(1.513) .00

1  
E

NIPC JOINT ROTATION STUDY---HEAD CAP AND CASE

WITHOUT MERIDIONAL LOAD EFFECT  
CASE 1.00

STRESS CALCULATIONS FOR SHELLS OF REVOLUTION  
DATE 2.07.62

REGION 1 OF 9 REGIONS

GEOMETRY IS PRESCRIBED BY A CONE OR CYLINDER EQUATION

| XI     | K         | THETA      | K XI       | BETA      | C         | D  | NT | NT | U          | V       |
|--------|-----------|------------|------------|-----------|-----------|----|----|----|------------|---------|
| 0.     | 1.477E-11 | -3.842E-06 | -2.002E-03 | 3.256E 06 | 3.091E 04 | 0. | 0. | 0. | 0.434E-04  | 0.      |
| C.0500 | 1.477E-11 | -8.967E-06 | -2.002E-03 | 3.256E 06 | 3.091E 04 | 0. | 0. | 0. | 7.433E-04  | -1.045E |
| 0.1000 | 1.478E-11 | -3.362E-05 | -2.005E-03 | 3.256E 06 | 3.091E 04 | 0. | 0. | 0. | 0.431E-04  | -1.700E |
| 0.1500 | 1.480E-11 | -7.204E-05 | -2.006E-03 | 3.256E 06 | 3.091E 04 | 0. | 0. | 0. | 5.429E-04  | -2.743E |
| 0.2000 | 1.483E-11 | -1.220E-04 | -2.011E-03 | 3.256E 06 | 3.091E 04 | 0. | 0. | 0. | 4.425E-04  | -3.352E |
| C.2500 | 1.489E-11 | -1.814E-04 | -2.018E-03 | 3.256E 06 | 3.091E 04 | 0. | 0. | 0. | 3.418E-04  | -3.710E |
| 0.3000 | 1.497E-11 | -2.481E-04 | -2.029E-03 | 3.256E 06 | 3.091E 04 | 0. | 0. | 0. | 2.407E-04  | -4.254E |
| 0.3500 | 1.507E-11 | -3.195E-04 | -2.043E-03 | 3.256E 06 | 3.091E 04 | 0. | 0. | 0. | 1.369E-04  | -4.544E |
| 0.4000 | 1.520E-11 | -3.947E-04 | -2.061E-03 | 3.256E 06 | 3.091E 04 | 0. | 0. | 0. | 3.632E-03  | -4.660E |
| 0.4500 | 1.536E-11 | -4.702E-04 | -2.083E-03 | 3.256E 06 | 3.091E 04 | 0. | 0. | 0. | -6.725E-05 | -4.639E |
| 0.4750 | 1.545E-11 | -5.076E-04 | -2.095E-03 | 3.256E 06 | 3.091E 04 | 0. | 0. | 0. | -1.195E-04 | -4.578E |
| C.4800 | 1.547E-11 | -5.150E-04 | -2.097E-03 | 3.256E 06 | 3.091E 04 | 0. | 0. | 0. | -1.299E-04 | -4.561E |





NIRG JOINT RUINATION STUDY---REAL GAP AND CASE

STRESS CALCULATIONS FOR SHELLS OF REVOLUTION  
 DATE 2.27.62  
 REGION 2 OF 9 REGIONS  
 GEOMETRY IS PRESCRIBED BY A CONE OR CYLINDER EQUATION  
 STRAIN XI STRAIN THETA A

| XI     | RCS       | ZCS        | STRAIN XI | STRAIN THETA | A         | (RV) | N(XI)      | M(THETA)   | M(XI)   |
|--------|-----------|------------|-----------|--------------|-----------|------|------------|------------|---------|
| 0.0500 | 3.695E 00 | 0.000E-02  | 1.103E-05 | -3.676E-05   | 1.600E-01 | 0.   | -1.190E-06 | -1.212E 02 | -1.592E |
| 0.1000 | 3.695E 00 | 5.000E-02  | 1.598E-05 | -6.661E-05   | 1.600E-01 | 0.   | -1.127E-06 | -2.196E 02 | -1.815E |
| 0.1500 | 3.695E 00 | 10.000E-02 | 2.907E-05 | -9.689E-05   | 1.600E-01 | 0.   | -1.027E-06 | -3.193E 02 | -2.022E |
| 0.2000 | 3.695E 00 | 1.500E-01  | 3.829E-05 | -1.276E-04   | 1.600E-01 | 0.   | -8.710E-07 | -4.206E 02 | -2.208E |
| 0.2500 | 3.695E 00 | 2.000E-01  | 4.766E-05 | -1.589E-04   | 1.600E-01 | 0.   | -7.169E-07 | -5.236E 02 | -2.363E |
| 0.3000 | 3.695E 00 | 2.500E-01  | 5.719E-05 | -1.908E-04   | 1.600E-01 | 0.   | -5.045E-07 | -6.283E 02 | -2.481E |
| 0.3500 | 3.695E 00 | 3.000E-01  | 6.689E-05 | -2.230E-04   | 1.600E-01 | 0.   | -2.991E-07 | -7.349E 02 | -2.555E |
| 0.4000 | 3.695E 00 | 3.500E-01  | 7.677E-05 | -2.559E-04   | 1.600E-01 | 0.   | 3.769E-07  | -8.435E 02 | -2.576E |
| 0.4500 | 3.695E 00 | 4.000E-01  | 8.683E-05 | -2.894E-04   | 1.600E-01 | 0.   | 3.693E-07  | -9.539E 02 | -2.539E |
| 0.5000 | 3.695E 00 | 4.500E-01  | 9.706E-05 | -3.235E-04   | 1.600E-01 | 0.   | 7.418E-07  | -1.060E 03 | -2.433E |
| 0.5500 | 3.695E 00 | 5.000E-01  | 1.075E-04 | -3.582E-04   | 1.600E-01 | 0.   | 1.195E-06  | -1.181E 03 | -2.253E |
| 0.6000 | 3.695E 00 | 5.500E-01  | 1.180E-04 | -3.933E-04   | 1.600E-01 | 0.   | 1.613E-06  | -1.296E 03 | -1.989E |
| 0.6500 | 3.695E 00 | 6.000E-01  | 1.287E-04 | -4.290E-04   | 1.600E-01 | 0.   | 2.113E-06  | -1.414E 03 | -1.633E |
| 0.7000 | 3.695E 00 | 6.500E-01  | 1.395E-04 | -4.650E-04   | 1.600E-01 | 0.   | 2.656E-06  | -1.533E 03 | -1.177E |
| 0.7150 | 3.695E 00 | 7.000E-01  | 1.504E-04 | -5.012E-04   | 1.600E-01 | 0.   | 3.243E-06  | -1.652E 03 | -6.129E |
| 0.7200 | 3.695E 00 | 7.200E-01  | 1.547E-04 | -5.175E-04   | 1.600E-01 | 0.   | 3.428E-06  | -1.688E 03 | -4.213E |
|        |           |            |           |              |           |      | 3.491E-06  | -1.700E 03 | -3.557E |

WITHOUT PERIODICAL LOAD EFFECT  
 CASE 1.00

NIRG JOINT ROTATION STUDY---HEAD CAP AND CASE

| STRESS CALCULATIONS FOR SHELLS OF REVOLUTION |              |            |           |           |    |            |         |    |      |
|--|--------------|------------|-----------|-----------|----|------------|---------|----|------|
| LATE 2.07.62                                 |              |            |           |           |    |            |         |    |      |
| CASE 1.00                                    |              |            |           |           |    |            |         |    |      |
| WITHOUT ADDITIONAL LOAD EFFECT               |              |            |           |           |    |            |         |    |      |
| REGION 3                                     | OF 9 REGIONS | LATE       | 2.07.62   | NT        | MT | U          | D       | C  | BETA |
| GEOMETRY IS PRESCRIBED BY A SPHERE OR TORUS  | ELLIPSOID    |            |           |           |    |            |         |    |      |
| XI   | K THETA      | K XI       | BETA      |           |    |            |         |    |      |
| 0.1009                                       | -1.570E-03   | -1.000E-04 | 2.060E 06 | 7.546E 03 | 0. | 1.642E-13  | 0.      | 0. | 0.   |
| 0.2017                                       | -1.612E-03   | -1.000E-04 | 2.060E 06 | 7.546E 03 | 0. | 1.655E-04  | -7.248E | 0. | 0.   |
| 0.3026                                       | -1.720E-03   | -3.271E-04 | 2.060E 06 | 7.546E 03 | 0. | 3.304E-04  | -1.443E | 0. | 0.   |
| 0.4035                                       | -1.859E-03   | -5.087E-04 | 2.060E 06 | 7.546E 03 | 0. | 4.940E-04  | -2.148E | 0. | 0.   |
| 0.5043                                       | -2.148E-03   | -7.120E-04 | 2.060E 06 | 7.546E 03 | 0. | 6.557E-04  | -2.350E | 0. | 0.   |
| 0.6052                                       | -2.463E-03   | -9.437E-04 | 2.060E 06 | 7.546E 03 | 0. | 8.145E-04  | -3.482E | 0. | 0.   |
| 0.7061                                       | -2.841E-03   | -1.210E-03 | 2.060E 06 | 7.546E 03 | 0. | 9.694E-04  | -4.093E | 0. | 0.   |
| 0.8069                                       | -3.275E-03   | -1.518E-03 | 2.060E 06 | 7.546E 03 | 0. | 1.119E-03  | -4.805E | 0. | 0.   |
| 0.9078                                       | -3.761E-03   | -1.872E-03 | 2.060E 06 | 7.546E 03 | 0. | 1.262E-03  | -5.142E | 0. | 0.   |
| 1.0086                                       | -4.288E-03   | -2.278E-03 | 2.060E 06 | 7.546E 03 | 0. | 1.397E-03  | -5.550E | 0. | 0.   |
| 1.1095                                       | -4.847E-03   | -2.738E-03 | 2.060E 06 | 7.546E 03 | 0. | 1.520E-03  | -5.857E | 0. | 0.   |
| 1.2104                                       | -5.426E-03   | -3.256E-03 | 2.060E 06 | 7.546E 03 | 0. | 1.631E-03  | -6.042E | 0. | 0.   |
| 1.3112                                       | -6.008E-03   | -3.833E-03 | 2.060E 06 | 7.546E 03 | 0. | 1.726E-03  | -6.002E | 0. | 0.   |
| 1.4121                                       | -6.576E-03   | -4.468E-03 | 2.060E 06 | 7.546E 03 | 0. | 1.803E-03  | -5.950E | 0. | 0.   |
| 1.5130                                       | -7.109E-03   | -5.159E-03 | 2.060E 06 | 7.546E 03 | 0. | 1.857E-03  | -5.617E | 0. | 0.   |
| 1.6138                                       | -7.582E-03   | -5.901E-03 | 2.060E 06 | 7.546E 03 | 0. | 1.886E-03  | -5.051E | 0. | 0.   |
| 1.7147                                       | -8.046E-03   | -6.686E-03 | 2.060E 06 | 7.546E 03 | 0. | 1.886E-03  | -4.220E | 0. | 0.   |
| 1.8156                                       | -8.261E-03   | -7.505E-03 | 2.060E 06 | 7.546E 03 | 0. | 1.854E-03  | -3.087E | 0. | 0.   |
| 1.9164                                       | -8.458E-03   | -8.335E-03 | 2.060E 06 | 7.546E 03 | 0. | 1.787E-03  | -1.801E | 0. | 0.   |
| 2.0173                                       | -8.632E-03   | -9.181E-03 | 2.060E 06 | 7.546E 03 | 0. | 1.681E-03  | 2.322E  | 0. | 0.   |
| 2.1182                                       | -8.774E-03   | -9.999E-03 | 2.060E 06 | 7.546E 03 | 0. | 1.534E-03  | 2.493E  | 0. | 0.   |
| 2.2190                                       | -8.878E-03   | -1.077E-02 | 2.060E 06 | 7.546E 03 | 0. | 1.345E-03  | 3.203E  | 0. | 0.   |
| 2.3199                                       | -8.933E-03   | -1.146E-02 | 2.060E 06 | 7.546E 03 | 0. | 1.114E-03  | 3.952E  | 0. | 0.   |
| 2.4207                                       | -8.932E-03   | -1.203E-02 | 2.060E 06 | 7.546E 03 | 0. | 8.424E-04  | 4.710E  | 0. | 0.   |
| 2.5216                                       | -8.864E-03   | -1.243E-02 | 2.060E 06 | 7.546E 03 | 0. | 5.330E-04  | 5.533E  | 0. | 0.   |
| 2.6225                                       | -8.720E-03   | -1.263E-02 | 2.060E 06 | 7.546E 03 | 0. | 1.920E-04  | 6.444E  | 0. | 0.   |
| 2.7233                                       | -8.489E-03   | -1.256E-02 | 2.060E 06 | 7.546E 03 | 0. | -1.717E-04 | 7.444E  | 0. | 0.   |
| 2.8242                                       | -8.162E-03   | -1.215E-02 | 2.060E 06 | 7.546E 03 | 0. | -5.456E-04 | 8.586E  | 0. | 0.   |
| 2.9251                                       | -7.727E-03   | -1.135E-02 | 2.060E 06 | 7.546E 03 | 0. | -9.130E-04 | 9.868E  | 0. | 0.   |
| 3.0259                                       | -7.174E-03   | -1.007E-02 | 2.060E 06 | 7.546E 03 | 0. | -1.253E-03 | 1.122E  | 0. | 0.   |
| 3.1268                                       | -6.455E-03   | -8.256E-03 | 2.060E 06 | 7.546E 03 | 0. | -1.537E-03 | 1.522E  | 0. | 0.   |
| 3.2277                                       | -5.680E-03   | -5.766E-03 | 2.060E 06 | 7.546E 03 | 0. | -1.734E-03 | 1.922E  | 0. | 0.   |
|  | -4.680E-03   | -4.260E-03 | 2.060E 06 | 7.546E 03 | 0. | -1.787E-03 | 2.403E  | 0. | 0.   |
|  | -3.219E-03   | -2.573E-03 | 2.060E 06 | 7.546E 03 | 0. | -1.823E-03 | 2.906E  | 0. | 0.   |



NIFC JOINT ROTATION STUDY--HEAD CAP AND CASE

STRESS CALCULATIONS FOR SMELLS OF REVOLUTION  
 DATE 2.07.02  
 REGION 3 OF 9 REGIONS  
 GEOMETRY IS PRESCRIBED BY A SPHERE OR TORUS EQUATION

CASE 1.00  
 WITHOUT RESIDUAL LOAD EFFECT

| XI     | RUS       | ZUS       | STRAIN XI  | STRAIN THETA | A          | (RV)      | N(XI)     | N(THETA)   | A(XI)   |
|--------|-----------|-----------|------------|--------------|------------|-----------|-----------|------------|---------|
| 0.     | 1.000E-10 | 3.073E-C8 | 1.642E-03  | 1.642E-03    | 10.000E-02 | 0.        | 4.831E 03 | 4.831E 03  | -1.540E |
| 0.1009 | 1.025E-01 | 8.476E-C4 | 1.642E-03  | 1.641E-03    | 10.000E-02 | 7.324E 00 | 4.530E 03 | 4.829E 03  | -1.576E |
| 0.2017 | 2.050E-01 | 3.390E-03 | 1.641E-03  | 1.635E-03    | 10.000E-02 | 2.929E 01 | 4.526E 03 | 4.823E 03  | -1.580E |
| 0.3026 | 3.074E-01 | 7.627E-03 | 1.641E-03  | 1.633E-03    | 10.000E-02 | 6.567E 01 | 4.822E 03 | 4.812E 03  | -1.815E |
| 0.4035 | 4.098E-01 | 1.356E-C2 | 1.641E-03  | 1.625E-03    | 10.000E-02 | 1.170E 02 | 4.819E 03 | 4.795E 03  | -2.020E |
| 0.5043 | 5.120E-01 | 2.118E-02 | 1.641E-03  | 1.617E-03    | 10.000E-02 | 1.827E 02 | 4.812E 03 | 4.774E 03  | -2.281E |
| 0.6052 | 6.141E-01 | 3.049E-02 | 1.640E-03  | 1.604E-03    | 10.000E-02 | 2.628E 02 | 4.803E 03 | 4.748E 03  | -2.595E |
| 0.7061 | 7.160E-01 | 4.148E-02 | 1.640E-03  | 1.589E-03    | 10.000E-02 | 3.573E 02 | 4.792E 03 | 4.710E 03  | -2.950E |
| 0.8069 | 8.178E-01 | 5.417E-02 | 1.640E-03  | 1.569E-03    | 10.000E-02 | 4.661E 02 | 4.772E 03 | 4.665E 03  | -3.360E |
| 0.9078 | 9.193E-01 | 6.853E-02 | 1.640E-03  | 1.544E-03    | 10.000E-02 | 5.889E 02 | 4.762E 03 | 4.610E 03  | -3.800E |
| 1.0086 | 1.021E 00 | 8.456E-02 | 1.641E-03  | 1.514E-03    | 1.000E-01  | 7.258E 02 | 4.743E 03 | 4.542E 03  | -4.267E |
| 1.1095 | 1.121E 00 | 1.023E-01 | 1.642E-03  | 1.478E-03    | 1.000E-01  | 8.766E 02 | 4.728E 03 | 4.482E 03  | -4.751E |
| 1.2104 | 1.222E 00 | 1.217E-01 | 1.643E-03  | 1.436E-03    | 1.000E-01  | 1.041E 03 | 4.694E 03 | 4.366E 03  | -5.241E |
| 1.3112 | 1.322E 00 | 1.427E-01 | 1.645E-03  | 1.385E-03    | 1.000E-01  | 1.219E 03 | 4.664E 03 | 4.253E 03  | -5.722E |
| 1.4121 | 1.422E 00 | 1.654E-01 | 1.647E-03  | 1.327E-03    | 1.000E-01  | 1.410E 03 | 4.630E 03 | 4.123E 03  | -6.177E |
| 1.5130 | 1.522E 00 | 1.897E-01 | 1.650E-03  | 1.260E-03    | 1.000E-01  | 1.615E 03 | 4.591E 03 | 3.972E 03  | -6.550E |
| 1.6138 | 1.621E 00 | 2.157E-01 | 1.654E-03  | 1.183E-03    | 1.000E-01  | 1.832E 03 | 4.548E 03 | 3.801E 03  | -6.927E |
| 1.7147 | 1.720E 00 | 2.433E-01 | 1.659E-03  | 1.098E-03    | 1.000E-01  | 2.062E 03 | 4.499E 03 | 3.607E 03  | -7.174E |
| 1.8156 | 1.818E 00 | 2.726E-01 | 1.664E-03  | 9.988E-04    | 1.000E-01  | 2.304E 03 | 4.445E 03 | 3.391E 03  | -7.299E |
| 1.9164 | 1.916E 00 | 3.035E-01 | 1.669E-03  | 8.916E-04    | 1.000E-01  | 2.558E 03 | 4.385E 03 | 3.152E 03  | -7.047E |
| 2.0173 | 2.013E 00 | 3.360E-01 | 1.676E-03  | 7.745E-04    | 1.000E-01  | 2.825E 03 | 4.319E 03 | 2.891E 03  | -6.590E |
| 2.1182 | 2.110E 00 | 3.700E-01 | 1.682E-03  | 6.481E-04    | 1.000E-01  | 3.103E 03 | 4.248E 03 | 2.610E 03  | -5.990E |
| 2.2190 | 2.206E 00 | 4.057E-01 | 1.689E-03  | 5.134E-04    | 1.000E-01  | 3.392E 03 | 4.171E 03 | 2.309E 03  | -5.803E |
| 2.3199 | 2.301E 00 | 4.430E-01 | 1.695E-03  | 3.720E-04    | 1.000E-01  | 3.692E 03 | 4.094E 03 | 1.993E 03  | -4.817E |
| 2.4207 | 2.356E 00 | 4.818E-01 | 1.700E-03  | 2.200E-04    | 1.000E-01  | 4.002E 03 | 4.002E 03 | 1.666E 03  | -3.406E |
| 2.5216 | 2.491E 00 | 5.222E-01 | 1.704E-03  | 7.834E-05    | 10.000E-02 | 4.323E 03 | 3.911E 03 | 1.335E 03  | -1.580E |
| 2.6225 | 2.584E 00 | 5.642E-01 | 1.706E-03  | -5.754E-05   | 10.000E-02 | 4.654E 03 | 3.815E 03 | 1.005E 03  | 7.099E  |
| 2.7233 | 2.677E 00 | 6.077E-01 | 1.704E-03  | -2.072E-04   | 10.000E-02 | 4.994E 03 | 3.717E 03 | 6.854E 02  | 5.513E  |
| 2.8242 | 2.769E 00 | 6.527E-01 | 1.698E-03  | -3.351E-C4   | 10.000E-02 | 5.344E 03 | 3.617E 03 | 5.947E 02  | 0.875E  |
| 2.9251 | 2.860E 00 | 6.993E-01 | 1.687E-03  | -4.451E-04   | 10.000E-02 | 5.702E 03 | 3.517E 03 | 1.382E 02  | 1.084E  |
| 3.0259 | 2.951E 00 | 7.473E-01 | 1.669E-03  | -5.294E-04   | 10.000E-02 | 6.069E 03 | 3.418E 03 | -6.534E 01 | 1.545E  |
| 3.1268 | 3.041E 00 | 7.968E-01 | 1.641E-03  | -5.796E-04   | 10.000E-02 | 6.444E 03 | 3.322E 03 | -1.974E 02 | 2.072E  |
| 3.1772 | 3.085E 00 | 8.222E-01 | 1.6024E-03 | -5.888E-04   | 10.000E-02 | 6.834E 03 | 3.275E 03 | -2.302E 02 | 2.561E  |
| 3.2277 | 3.130E 00 | 8.479E-01 | 1.6005E-03 | -5.921E-04   | 10.000E-02 | 6.826E 03 | 3.231E 03 | -2.504E 02 | 2.660E  |

NIRC JOINT ROTATION STUDY---HEAD CAP AND CASE

WITHOUT MERIDIONAL LOAD EFFECT  
CASE 1.00

STRESS CALCULATIONS FOR SHELLS OF REVOLUTION  
DATE 2.07.02

REGION 4  
OF 9 REGIONS

| GEOMETRY<br>X1 | K         | THETA     | K         | X1         | DELTA     | C         | D  | NT | MT | J          |
|----------------|-----------|-----------|-----------|------------|-----------|-----------|----|----|----|------------|
| 0.0500         | 2.031E-11 | 1.958E-11 | 1.185E-03 | -2.573E-03 | 1.175E 07 | 1.401E 09 | 0. | 0. | 0. | -1.823E-03 |
| 0.1000         | 1.881E-11 | 1.545E-11 | 1.340E-03 | -2.510E-03 | 1.097E 07 | 1.150E 06 | 0. | 0. | 0. | -1.960E-03 |
| 0.1500         | 1.796E-11 | 1.796E-11 | 1.822E-03 | -2.355E-03 | 9.400E 06 | 7.393E 05 | 0. | 0. | 0. | -2.095E-03 |
| 0.2000         | 1.701E-11 | 1.701E-11 | 2.212E-03 | -2.254E-03 | 8.610E 06 | 5.655E 05 | 0. | 0. | 0. | -2.226E-03 |
| 0.2500         | 1.590E-11 | 1.590E-11 | 2.778E-03 | -2.130E-03 | 7.831E 06 | 4.227E 05 | 0. | 0. | 0. | -2.352E-03 |
| 0.3000         | 1.455E-11 | 1.455E-11 | 3.637E-03 | -1.972E-03 | 7.045E 06 | 3.018E 05 | 0. | 0. | 0. | -2.472E-03 |
| 0.3500         | 1.284E-11 | 1.284E-11 | 4.987E-03 | -1.759E-03 | 6.259E 06 | 2.059E 05 | 0. | 0. | 0. | -2.584E-03 |
| 0.4000         | 1.055E-11 | 1.055E-11 | 7.129E-03 | -1.460E-03 | 5.473E 06 | 1.349E 05 | 0. | 0. | 0. | -2.685E-03 |
| 0.4450         | 7.733E-12 | 7.733E-12 | 9.827E-03 | -1.081E-03 | 4.765E 06 | 9.233E 04 | 0. | 0. | 0. | -2.774E-03 |
| 0.4500         | 7.368E-12 | 7.368E-12 | 1.015E-02 | -1.031E-03 | 4.686E 06 | 8.885E 04 | 0. | 0. | 0. | -2.841E-03 |

NIRC JOINT ROTATION STUDY---HEAD CAP AND CASE

STRESS CALCULATIONS FOR SHELLS OF REVOLUTION  
 WITHOUT REGIONAL LOAD EFFECT  
 CASE 1.00

DATE 2.07.92

REGION 4 OF 9 REGIONS

GEOMETRY IS PRESCRIBED BY A CCNE UK CYLINDER EQUATION

| XI     | RCS       | ZCS        | STRAIN XI | STRAIN THETA | A         | (RV)      | R(KI)     | A(THETA)   | M(KI)  |
|--------|-----------|------------|-----------|--------------|-----------|-----------|-----------|------------|--------|
| 0.     | 3.875E 00 | 0.         | 3.106E-04 | -9.518E-04   | 5.705E-01 | 6.190E 03 | 1.575E 03 | -9.923E 03 | 1.060E |
| 0.050C | 3.875E 00 | 5.000E-02  | 3.345E-04 | -5.005E-04   | 5.325E-01 | 6.390E 03 | 1.912E 03 | -9.859E 03 | 1.549E |
| C.1000 | 3.875E 00 | 10.000E-02 | 3.601E-04 | -0.197E-04   | 4.944E-01 | 6.592E 03 | 1.950E 03 | -9.727E 03 | 1.444E |
| C.1500 | 3.875E 00 | 1.500E-01  | 3.678E-04 | -6.511E-04   | 4.563E-01 | 6.797E 03 | 1.988E 03 | -9.525E 03 | 1.347E |
| 0.2000 | 3.875E 00 | 2.000E-01  | 4.181E-04 | -6.805E-04   | 4.182E-01 | 7.004E 03 | 2.020E 03 | -9.255E 03 | 1.257E |
| 0.2500 | 3.875E 00 | 2.500E-01  | 4.521E-04 | -7.074E-04   | 3.801E-01 | 7.213E 03 | 2.004E 03 | -4.920E 03 | 1.174E |
| C.3000 | 3.875E 00 | 3.000E-01  | 4.909E-04 | -7.314E-04   | 3.420E-01 | 7.424E 03 | 2.101E 03 | -4.523E 03 | 1.098E |
| C.3500 | 3.875E 00 | 3.500E-01  | 5.366E-04 | -7.520E-04   | 3.039E-01 | 7.638E 03 | 2.139E 03 | -4.005E 03 | 1.027E |
| C.4000 | 3.875E 00 | 4.000E-01  | 5.924E-04 | -7.685E-04   | 2.657E-01 | 7.854E 03 | 2.170E 03 | -3.553E 03 | 9.617E |
| 0.445C | 3.875E 00 | 4.450E-01  | 6.559E-04 | -7.798E-04   | 2.313E-01 | 8.051E 03 | 2.210E 03 | -3.053E 03 | 9.075E |
| C.450C | 3.875E 00 | 4.500E-01  | 6.609E-04 | -7.703E-04   | 2.275E-01 | 8.073E 03 | 2.213E 03 | -2.946E 03 | 9.016E |

NIRC JOINT ROTATION STUDY---HEAD CAP AND CASE

| STRESS CALCULATIONS FOR SHELLS OF REVOLUTION           |            |       |           |            |           |            |    |    |    |            |
|--|------------|-------|-----------|------------|-----------|------------|----|----|----|------------|
| WITHOUT MERIDIONAL LOAD EFFECT                         |            |       |           |            |           |            |    |    |    |            |
| CASE 1.00  |            |       |           |            |           |            |    |    |    |            |
| REGION   | OF         | 9     | REGIONS   | DATE       | 2.07.62   | REVOLUTION | D  | NT | MT | U          |
| GECOMETRY IS PRESCRIBED BY A CONE OR CYLINDER EQUATION |            |       |           |            |           |            |    |    |    |            |
| XI   | K          | THETA | K         | XI         | BETA      | C          | D  | NT | MT | U          |
| 0.   | 7.164E-12  |       | 6.343E-02 | -1.031E-03 | 2.544E 06 | 1.421E 04  | 0. | 0. | 0. | -2.810E-03 |
| 0.0100   | 2.782E-12  |       | 6.263E-02 | -4.003E-04 | 2.544E 06 | 1.421E 04  | 0. | 0. | 0. | -2.813E-03 |
| 0.0200   | -1.543E-12 |       | 6.183E-02 | 2.220E-04  | 2.544E 06 | 1.421E 04  | 0. | 0. | 0. | -2.809E-03 |
| 0.0300   | -5.814E-12 |       | 6.105E-02 | 8.364E-04  | 2.544E 06 | 1.421E 04  | 0. | 0. | 0. | -2.800E-03 |
| 0.0400   | -1.003E-11 |       | 6.028E-02 | 1.443E-03  | 2.544E 06 | 1.421E 04  | 0. | 0. | 0. | -2.784E-03 |
| 0.0500   | -1.419E-11 |       | 5.953E-02 | 2.042E-03  | 2.544E 06 | 1.421E 04  | 0. | 0. | 0. | -2.763E-03 |
| 0.0600   | -1.831E-11 |       | 5.878E-02 | 2.634E-03  | 2.544E 06 | 1.421E 04  | 0. | 0. | 0. | -2.736E-03 |
| 0.0700   | -2.247E-11 |       | 5.805E-02 | 3.218E-03  | 2.544E 06 | 1.421E 04  | 0. | 0. | 0. | -2.703E-03 |
| 0.0800   | -2.668E-11 |       | 5.734E-02 | 3.795E-03  | 2.544E 06 | 1.421E 04  | 0. | 0. | 0. | -2.665E-03 |
| 0.0900   | -3.084E-11 |       | 5.663E-02 | 4.365E-03  | 2.544E 06 | 1.421E 04  | 0. | 0. | 0. | -2.621E-03 |
| 0.1000   | -3.425E-11 |       | 5.594E-02 | 4.927E-03  | 2.544E 06 | 1.421E 04  | 0. | 0. | 0. | -2.571E-03 |
| 0.1010   | -3.464E-11 |       | 5.587E-02 | 4.983E-03  | 2.544E 06 | 1.421E 04  | 0. | 0. | 0. | -2.566E-03 |
| 0.1020   | -3.503E-11 |       | 5.580E-02 | 5.039E-03  | 2.544E 06 | 1.421E 04  | 0. | 0. | 0. | -2.561E-03 |



NIFC JJUNT ROTATION STUDY---HEAD GAP AND CASE

WITHOUT RESIDUAL LOAD EFFECT  
CASE 1.00

STRESS CALCULATIONS FOR SHELLS OF REVOLUTION  
DATE 2.07.62

| REGION 6<br>OF 9 REGIONS<br>IS DESCRIBED BY A CURVE OR CYLINDER EQUATION | K          | THETA | K XI      | BETA      | C         | J         | NT | MT | U          | V       |
|--|------------|-------|-----------|-----------|-----------|-----------|----|----|------------|---------|
| 0.0  | -3.593E-11 |       | 7.338E-03 | 5.039E-03 | 4.480E 06 | 7.764E 04 | 0. | 0. | -2.561E-03 | -9.762E |
| C.1C07   | -4.078E-11 |       | 6.206E-03 | 5.719E-03 | 4.430E 06 | 7.764E 04 | 0. | 0. | -2.018E-03 | -7.742E |
| 0.2014   | -4.450E-11 |       | 5.323E-03 | 6.298E-03 | 4.480E 06 | 7.764E 04 | 0. | 0. | -1.412E-03 | -5.913E |
| 0.3C22   | -4.847E-11 |       | 4.663E-03 | 6.799E-03 | 4.480E 06 | 7.764E 04 | 0. | 0. | -7.518E-04 | -4.298E |
| 0.4029   | -5.164E-11 |       | 4.157E-03 | 7.243E-03 | 4.480E 06 | 7.764E 04 | 0. | 0. | -7.428E-05 | -2.913E |
| 0.5036   | -5.454E-11 |       | 3.856E-03 | 7.650E-03 | 4.480E 06 | 7.764E 04 | 0. | 0. | 7.060E-04  | -1.774E |
| 0.6043   | -5.727E-11 |       | 3.726E-03 | 8.033E-03 | 4.480E 06 | 7.764E 04 | 0. | 0. | 1.496E-03  | -3.958E |
| 0.7C50   | -5.991E-11 |       | 3.652E-03 | 8.403E-03 | 4.480E 06 | 7.764E 04 | 0. | 0. | 2.324E-03  | -2.900E |
| C.8C58   | -6.253E-11 |       | 3.638E-03 | 8.770E-03 | 4.480E 06 | 7.764E 04 | 0. | 0. | 3.189E-03  | 3.029E  |
| 0.9C65   | -6.515E-11 |       | 3.647E-03 | 9.137E-03 | 4.480E 06 | 7.764E 04 | 0. | 0. | 4.090E-03  | 5.257E  |
| 1.0C72   | -6.776E-11 |       | 3.638E-03 | 9.504E-03 | 4.480E 06 | 7.764E 04 | 0. | 0. | 5.029E-03  | -2.358E |
| 1.1C75   | -7.036E-11 |       | 3.571E-03 | 9.868E-03 | 4.480E 06 | 7.764E 04 | 0. | 0. | 6.005E-03  | -8.467E |
| 1.118C   | -7.061E-11 |       | 3.566E-03 | 9.904E-03 | 4.480E 06 | 7.764E 04 | 0. | 0. | 6.104E-03  | -9.251E |



NIFC JOINT ROTATION STUDY---HEAD CAP AND CASE

| REGION 6   |           | STRESS CALCULATIONS FOR SHELLS OF REVOLUTION |            | DATE 2.07.02 |           | WITHOUT MERIDIONAL LOAD EFFECT |           | CASE 1.00  |           |            |        |          |        |
|--|-----------|--|------------|--------------|-----------|--------------------------------|-----------|------------|-----------|------------|--------|----------|--------|
| GECOMETRY IS PRESCRIBED BY A CONE OR CYLINDER EQUATION |           | STRAIN XI STRAIN THETA                       |            | A            |           | (KV)                           |           | M(XI)      |           | M(THETA)   |        | M(XI)    |        |
| XI   | HOS       | ZCS  | STRAIN XI  | STRAIN THETA | A         | (KV)                           | M(XI)     | M(THETA)   | M(XI)     | M(THETA)   | M(XI)  | M(THETA) | M(XI)  |
| 0.   | 3.875E 00 | 0.   | 7.052E-04  | -7.002E-04   | 2.175E-01 | 8.916E 03                      | 2.438E 03 | -2.406E 03 | 2.438E 03 | -2.406E 03 | 5.697E | 03       | 5.697E |
| C.1007   | 3.875E 00 | 1.007E-01                                    | 0.000E-04  | -5.517E-04   | 2.175E-01 | 8.916E 03                      | 2.438E 03 | -1.741E 03 | 2.438E 03 | -1.741E 03 | 4.818E | 03       | 4.818E |
| 0.2014   | 3.875E 00 | 2.014E-01                                    | 0.109E-04  | -3.860E-04   | 2.175E-01 | 8.916E 03                      | 2.438E 03 | -9.983E 02 | 2.438E 03 | -9.983E 02 | 4.132E | 02       | 4.132E |
| 0.3022   | 3.875E 00 | 3.022E-01                                    | 5.500E-04  | -2.056E-04   | 2.175E-01 | 8.916E 03                      | 2.438E 03 | -1.897E 02 | 2.438E 03 | -1.897E 02 | 3.820E | 02       | 3.820E |
| 0.4029   | 3.875E 00 | 4.029E-01                                    | 4.987E-04  | -1.211E-05   | 2.175E-01 | 8.916E 03                      | 2.438E 03 | 0.771E 02  | 2.438E 03 | 0.771E 02  | 3.259E | 02       | 3.259E |
| 0.5036   | 3.875E 00 | 5.036E-01                                    | 4.372E-04  | 1.930E-04    | 2.175E-01 | 8.916E 03                      | 2.438E 03 | 1.596E 03  | 2.438E 03 | 1.596E 03  | 3.025E | 03       | 3.025E |
| 0.6043   | 3.875E 00 | 6.043E-01                                    | 3.724E-04  | 4.090E-04    | 2.175E-01 | 8.916E 03                      | 2.438E 03 | 2.564E 03  | 2.438E 03 | 2.564E 03  | 2.893E | 03       | 2.893E |
| 0.7050   | 3.875E 00 | 7.050E-01                                    | 3.045E-04  | 6.353E-04    | 2.175E-01 | 8.916E 03                      | 2.438E 03 | 3.578E 03  | 2.438E 03 | 3.578E 03  | 2.835E | 03       | 2.835E |
| 0.8058   | 3.875E 00 | 8.058E-01                                    | 2.336E-04  | 8.718E-04    | 2.175E-01 | 8.916E 03                      | 2.438E 03 | 4.537E 03  | 2.438E 03 | 4.537E 03  | 2.825E | 03       | 2.825E |
| 0.9065   | 3.875E 00 | 9.065E-01                                    | 1.596E-04  | 1.118E-03    | 2.175E-01 | 8.916E 03                      | 2.438E 03 | 5.742E 03  | 2.438E 03 | 5.742E 03  | 2.831E | 03       | 2.831E |
| 1.0072   | 3.875E 00 | 1.007E 00                                    | 8.259E-05  | 1.375E-03    | 2.175E-01 | 8.916E 03                      | 2.438E 03 | 8.892E 03  | 2.438E 03 | 8.892E 03  | 2.825E | 03       | 2.825E |
| 1.1079   | 3.875E 00 | 1.108E 00                                    | 2.561E-06  | 1.642E-03    | 2.175E-01 | 8.916E 03                      | 2.438E 03 | 9.067E 03  | 2.438E 03 | 9.067E 03  | 2.773E | 03       | 2.773E |
| 1.1180   | 3.875E 00 | 1.118E 00                                    | -5.591E-06 | 1.669E-03    | 2.175E-01 | 8.916E 03                      | 2.438E 03 | 9.209E 03  | 2.438E 03 | 9.209E 03  | 2.764E | 03       | 2.764E |

NIRC JOINT ROTATION STUDY---HEAD CAP AND CASE  
 WITHOUT PERIODICAL LOAD EFFECT

| REGION 7 OF 5 REGIONS                                  |            | STRESS CALCULATIONS FOR SHELLS OF REVOLUTION |           | CASE 1.00 |         |
|--|------------|--|-----------|-----------|---------|
| GECOMETRY IS PRESCRIBED BY A CONE OR CYLINDER EQUATION |            | DATE   | 2.07.62   | NT        | MT      |
| XI   | K THETA    | K XI   | BETA      | U         | W       |
| 0.0402   | -7.306E-11 | -5.902E-03                                   | 9.904E-03 | 0.104E-03 | -9.261E |
| 0.0804   | -7.121E-11 | -6.533E-03                                   | 9.624E-03 | 0.497E-03 | -9.040E |
| 0.1206   | -6.919E-11 | -7.089E-03                                   | 9.380E-03 | 0.880E-03 | -7.152E |
| 0.1608   | -6.701E-11 | -7.584E-03                                   | 9.084E-03 | 0.251E-03 | -6.643E |
| 0.2010   | -6.470E-11 | -8.035E-03                                   | 8.770E-03 | 0.510E-03 | -5.942E |
| 0.2412   | -6.225E-11 | -8.458E-03                                   | 8.439E-03 | 0.750E-03 | -5.057E |
| 0.2814   | -5.968E-11 | -8.867E-03                                   | 8.090E-03 | 0.259E-03 | -5.573E |
| 0.3216   | -5.659E-11 | -9.278E-03                                   | 7.726E-03 | 0.607E-03 | -5.654E |
| 0.3619   | -5.418E-11 | -9.703E-03                                   | 7.344E-03 | 0.510E-03 | -5.950E |
| 0.4021   | -5.123E-11 | -1.016E-02                                   | 6.945E-03 | 0.197E-03 | -6.453E |
| 0.4423   | -4.815E-11 | -1.065E-02                                   | 6.527E-03 | 0.408E-03 | -7.091E |
| 0.4825   | -4.451E-11 | -1.120E-02                                   | 6.088E-03 | 0.721E-03 | -7.558E |
| 0.5227   | -4.150E-11 | -1.181E-02                                   | 5.626E-03 | 0.957E-03 | -8.028E |
| 0.5629   | -3.790E-11 | -1.249E-02                                   | 5.138E-03 | 1.017E-02 | -9.464E |
| 0.6031   | -3.408E-11 | -1.326E-02                                   | 4.620E-03 | 1.037E-02 | -1.110E |
| 0.6433   | -2.970E-11 | -1.412E-02                                   | 4.070E-03 | 1.054E-02 | -1.241E |
| 0.6835   | -2.570E-11 | -1.507E-02                                   | 3.484E-03 | 1.070E-02 | -1.382E |
| 0.7237   | -2.107E-11 | -1.614E-02                                   | 2.857E-03 | 1.082E-02 | -1.531E |
| 0.7639   | -1.612E-11 | -1.731E-02                                   | 2.185E-03 | 1.093E-02 | -1.687E |
| 0.7720   | -1.079E-11 | -1.861E-02                                   | 1.403E-03 | 1.100E-02 | -1.848E |
| 0.7800   | -9.680E-12 | -1.888E-02                                   | 1.312E-03 | 1.101E-02 | -1.881E |
|  | -8.552E-12 | -1.915E-02                                   | 1.159E-03 | 1.102E-02 | -1.914E |

NIRC JUNIT ROTATION STUDY---HEAD CAP AND CASE

STRESS CALCULATIONS FOR SHELLS OF REVOLUTION  
 DATE 2.07.62

| GECMETRY IS DESCRIBED BY A CONE UR CYLINDER EQUATION |              | STRAIN XI STRAIN THETA |                       | CASE 1.00 |           | WITHOUT REGIONAL LOAD EFFECT |          |
|--|--------------|------------------------|-----------------------|-----------|-----------|------------------------------|----------|
| REGION 7   | OF 9 REGIONS | ZOS                    | STRAN XI STRAIN THETA | (RV)      | (X1)      | (X1)                         | (X1)     |
| 0.0  | 3.625E 00    | 0.                     | 7.199E-04             | 8.916E 03 | 2.522E 03 | 3.958E 03                    | -3.247E  |
| 0.0402   | 3.625E 00    | 4.021E-02              | 6.805E-04             | 8.916E 03 | 2.522E 03 | 4.164E 03                    | -3.594E  |
| 0.0804   | 3.625E 00    | 6.041E-02              | 6.540E-04             | 8.916E 03 | 2.522E 03 | 4.305E 03                    | -3.899E  |
| 0.1206   | 3.625E 00    | 1.206E-01              | 6.225E-04             | 8.916E 03 | 2.522E 03 | 4.500E 03                    | -4.172E  |
| 0.1608   | 3.625E 00    | 1.608E-01              | 5.921E-04             | 8.916E 03 | 2.522E 03 | 4.748E 03                    | -4.420E  |
| 0.2010   | 3.625E 00    | 2.010E-01              | 5.627E-04             | 8.916E 03 | 2.522E 03 | 4.929E 03                    | -4.653E  |
| 0.2412   | 3.625E 00    | 2.412E-01              | 5.345E-04             | 8.916E 03 | 2.522E 03 | 5.104E 03                    | -4.878E  |
| 0.2814   | 3.625E 00    | 2.814E-01              | 5.075E-04             | 8.916E 03 | 2.522E 03 | 5.271E 03                    | -5.104E  |
| 0.3216   | 3.625E 00    | 3.216E-01              | 4.818E-04             | 8.916E 03 | 2.522E 03 | 5.429E 03                    | -5.337E  |
| 0.3619   | 3.625E 00    | 3.619E-01              | 4.574E-04             | 8.916E 03 | 2.522E 03 | 5.580E 03                    | -5.537E  |
| 0.4021   | 3.625E 00    | 4.021E-01              | 4.344E-04             | 8.916E 03 | 2.522E 03 | 5.722E 03                    | -5.759E  |
| 0.4423   | 3.625E 00    | 4.423E-01              | 4.129E-04             | 8.916E 03 | 2.522E 03 | 5.855E 03                    | -5.9159E |
| 0.4825   | 3.625E 00    | 4.825E-01              | 3.929E-04             | 8.916E 03 | 2.522E 03 | 5.979E 03                    | -6.0495E |
| 0.5227   | 3.625E 00    | 5.227E-01              | 3.745E-04             | 8.916E 03 | 2.522E 03 | 6.092E 03                    | -6.1871E |
| 0.5629   | 3.625E 00    | 5.629E-01              | 3.579E-04             | 8.916E 03 | 2.522E 03 | 6.195E 03                    | -7.293E  |
| 0.6031   | 3.625E 00    | 6.031E-01              | 3.431E-04             | 8.916E 03 | 2.522E 03 | 6.287E 03                    | -7.765E  |
| 0.6433   | 3.625E 00    | 6.433E-01              | 3.302E-04             | 8.916E 03 | 2.522E 03 | 6.367E 03                    | -8.292E  |
| 0.6835   | 3.625E 00    | 6.835E-01              | 3.193E-04             | 8.916E 03 | 2.522E 03 | 6.434E 03                    | -8.878E  |
| 0.7237   | 3.625E 00    | 7.237E-01              | 3.107E-04             | 8.916E 03 | 2.522E 03 | 6.487E 03                    | -9.525E  |
| 0.7639   | 3.625E 00    | 7.639E-01              | 3.045E-04             | 8.916E 03 | 2.522E 03 | 6.525E 03                    | -1.024E  |
| 0.7720   | 3.625E 00    | 7.720E-01              | 3.035E-04             | 8.916E 03 | 2.522E 03 | 6.531E 03                    | -1.039E  |
| 0.7800   | 3.625E 00    | 7.800E-01              | 3.026E-04             | 8.916E 03 | 2.522E 03 | 6.537E 03                    | -1.054E  |

NIRC JOINT ROTATION STUDY---HEAD CAP AND CASE

STRESS CALCULATIONS FOR SHELLS OF REVOLUTION  
DATE 2.07.62

WITHOUT MERIDIONAL LOAD EFFECT  
CASE 1.00

| REGION 8<br>OF 9 REGIONS | UF         | K XI       | BETA       | C         | U         | NT | MT | V         |
|--------------------------|------------|------------|------------|-----------|-----------|----|----|-----------|
| 0.                       | 5.693E-05  | -1.917E-02 | 1.159E-03  | 1.854E 06 | 5.501E 03 | 0. | 0. | 1.102E-02 |
| 0.150C                   | -6.033E-05 | -1.305E-02 | -1.238E-03 | 1.854E 06 | 5.501E 03 | 0. | 0. | 1.101E-02 |
| 0.300C                   | -1.371E-04 | -8.446E-03 | -2.832E-03 | 1.854E 06 | 5.501E 03 | 0. | 0. | 1.071E-02 |
| 0.450C                   | -1.841E-04 | -5.076E-03 | -3.833E-03 | 1.854E 06 | 5.501E 03 | 0. | 0. | 1.022E-02 |
| 0.600C                   | -2.058E-04 | -2.560E-03 | -4.358E-03 | 1.854E 06 | 5.501E 03 | 0. | 0. | 9.621E-03 |
| 0.750C                   | -2.190E-04 | -4.886E-04 | -4.624E-03 | 1.854E 06 | 5.501E 03 | 0. | 0. | 8.955E-03 |
| 0.900C                   | -2.137E-04 | 1.598E-03  | -4.544E-03 | 1.854E 06 | 5.501E 03 | 0. | 0. | 8.299E-03 |
| 1.050C                   | -1.925E-04 | 4.124E-03  | -4.123E-03 | 1.854E 06 | 5.501E 03 | 0. | 0. | 7.672E-03 |
| 1.200C                   | -1.514E-04 | 7.482E-03  | -3.265E-03 | 1.854E 06 | 5.501E 03 | 0. | 0. | 7.139E-03 |
| 1.350C                   | -8.385E-05 | 1.200E-02  | -1.821E-03 | 1.854E 06 | 5.501E 03 | 0. | 0. | 6.775E-03 |
| 1.4250                   | -3.761E-05 | 1.477E-02  | -8.150E-04 | 1.854E 06 | 5.501E 03 | 0. | 0. | 6.687E-03 |
| 1.440C                   | -2.723E-05 | 1.536E-02  | -5.937E-04 | 1.854E 06 | 5.501E 03 | 0. | 0. | 5.677E-03 |



NIRC JOINT ROTATION STUDY---HEAD CAP AND CASE

| REGION 9  |            | STRESS CALCULATIONS FOR SHELLS OF REVOLUTION |            | DATE 2.07.02 |           | WITHOUT MERIDIONAL LOAD EFFECT |         |
|---|------------|--|------------|--------------|-----------|--------------------------------|---------|
| GECMETFY IS PRESCRIBED BY A CONE OR CYLINDER EQUATION |            | DATE   |            | CASE 1.00    |           | NT MT                          |         |
| XI  | K THETA    | K XI   | BETA       | C            | D         | U                              | W       |
| 0.  | 4.090E-12  | 1.535E-02                                    | -5.937E-04 | 1.854E 06    | 5.501E 03 | 6.677E-03                      | -2.470E |
| 0.3000  | -1.574E-11 | 4.787E-03                                    | 2.285E-03  | 1.854E 06    | 5.501E 03 | 7.015E-03                      | -1.430E |
| 0.6000  | -1.921E-11 | -6.821E-04                                   | 2.789E-03  | 1.854E 06    | 5.501E 03 | 7.817E-03                      | -6.274E |
| 0.9000  | -1.531E-11 | -2.639E-03                                   | 2.223E-03  | 1.854E 06    | 5.501E 03 | 8.583E-03                      | -1.390E |
| 1.2000  | -9.603E-12 | -2.675E-03                                   | 1.394E-03  | 1.854E 06    | 5.501E 03 | 9.128E-03                      | 9.168E  |
| 1.5000  | -4.772E-12 | -1.937E-03                                   | 6.927E-04  | 1.854E 06    | 5.501E 03 | 9.433E-03                      | 1.553E  |
| 1.8000  | -1.661E-12 | -1.088E-03                                   | 2.411E-04  | 1.854E 06    | 5.501E 03 | 9.557E-03                      | 1.437E  |
| 2.1000  | -1.428E-13 | -4.240E-04                                   | 2.073E-05  | 1.854E 06    | 5.501E 03 | 9.601E-03                      | 9.779E  |
| 2.4000  | 2.761E-13  | -2.772E-05                                   | -4.008E-05 | 1.854E 06    | 5.501E 03 | 9.595E-03                      | 4.794E  |
| 2.7000  | 1.506E-13  | 1.067E-04                                    | -2.185E-05 | 1.854E 06    | 5.501E 03 | 9.585E-03                      | 2.010E- |
| 2.9700  | 2.091E-15  | 2.023E-05                                    | -3.034E-07 | 1.854E 06    | 5.501E 03 | 9.582E-03                      | -3.709E |
| 3.0000  | 0.         | -5.457E-12                                   | -0.        | 1.854E 06    | 5.501E 03 | 9.582E-03                      | -4.141E |



NIRC JOINT ROTATION STUDY---HEAD CAP AND CASE

STRESS CALCULATIONS FOR SHELLS OF REVOLUTION  
 DATE 2.27.62  
 CASE 1.00  
 WITHOUT RESIDUAL LOAD EFFECT

| REGION 9<br>OF 9 REGIONS | ZCS       | STRAIN XI | STRAIN XI | THETA     | (RV)      | M(XI)     | M(THETA)  | M(XI)   |
|--------------------------|-----------|-----------|-----------|-----------|-----------|-----------|-----------|---------|
| C.3000                   | 0.        | 7.979E-04 | 1.764E-03 | 9.000E-02 | 1.023E 04 | 2.704E 03 | 4.082E 03 | 6.443E  |
| C.6000                   | 3.000E-01 | 7.711E-04 | 1.853E-03 | 9.000E-02 | 1.023E 04 | 2.704E 03 | 4.247E 03 | 2.633E  |
| C.9000                   | 6.000E-01 | 7.076E-04 | 2.065E-03 | 9.000E-02 | 1.023E 04 | 2.704E 03 | 4.640E 03 | -3.752E |
| 1.2000                   | 9.000E-01 | 6.468E-04 | 2.268E-03 | 9.000E-02 | 1.023E 04 | 2.704E 03 | 5.015E 03 | -1.452E |
| 1.5000                   | 1.200E 00 | 6.036E-04 | 2.411E-03 | 9.000E-02 | 1.023E 04 | 2.704E 03 | 5.281E 03 | -1.472E |
| 1.8000                   | 1.500E 00 | 5.795E-04 | 2.492E-03 | 9.000E-02 | 1.023E 04 | 2.704E 03 | 5.452E 03 | -1.066E |
| 2.1000                   | 1.800E 00 | 5.669E-04 | 2.525E-03 | 9.000E-02 | 1.023E 04 | 2.704E 03 | 5.497E 03 | -5.986E |
| 2.4000                   | 2.100E 00 | 5.001E-04 | 2.537E-03 | 9.000E-02 | 1.023E 04 | 2.704E 03 | 5.514E 03 | -2.332E |
| 2.7000                   | 2.400E 00 | 5.000E-04 | 2.535E-03 | 9.000E-02 | 1.023E 04 | 2.704E 03 | 5.511E 03 | -1.525E |
| 2.9700                   | 2.700E 00 | 5.574E-04 | 2.532E-03 | 9.000E-02 | 1.023E 04 | 2.704E 03 | 5.506E 03 | 5.867E  |
| 3.0000                   | 3.000E 00 | 5.676E-04 | 2.532E-03 | 9.000E-02 | 1.023E 04 | 2.704E 03 | 5.505E 03 | 1.113E  |
|                          |           | 5.575E-04 | 2.532E-03 | 9.000E-02 | 1.023E 04 | 2.704E 03 | 5.505E 03 | -5.002E |

STRESSES REGION 1

GEOMETRY IS PRESCRIBED BY A CONE OR CYLINDER EQUATION  
 STRESSES ARE PRINTED AS FOLLOWS LINE 1 SIGMA XI LINE 2 SIGMA THETA OUTER SURFACE... INTERFACES... I

XI = 0.  
 SIGMA F1E SIGMA H1- SIGMA H2- SIGMA H3E SIGMA H4E  
 6.95648E-02 -6.55648E-02  
 2.45738E 03 2.45734E C3

XI = 0.05000  
 SIGMA F1E SIGMA H1- SIGMA H2- SIGMA H3E SIGMA H4E  
 1.62389E 01 -1.62389E C1  
 2.17055E 03 2.16080E C3

XI = 0.10000  
 SIGMA F1E SIGMA H1- SIGMA H2- SIGMA H3E SIGMA H4E  
 6.08921E 01 -6.08921E C1  
 1.85219E 03 1.85565E C3

XI = 0.15000  
 SIGMA F1E SIGMA H1- SIGMA H2- SIGMA H3E SIGMA H4E  
 1.30470E 02 -1.30470E C2  
 1.62106E 03 1.54276E C3

XI = 0.20000  
 SIGMA F1E SIGMA H1- SIGMA H2- SIGMA H3E SIGMA H4E  
 2.20957E 02 -2.20957E C2  
 1.35568E 03 1.22311E C3

XI = 0.25000  
 SIGMA F1E SIGMA H1- SIGMA H2- SIGMA H3E SIGMA H4E  
 3.28542E 02 -3.28542E C2  
 1.09455E 03 8.57420E C2

XI = 0.30000  
 SIGMA F1E SIGMA H1- SIGMA H2- SIGMA H3E SIGMA H4E  
 4.45341E 02 -4.45341E C2  
 6.36048E 02 5.66444E C2

XI = 0.35000  
 SIGMA F1E SIGMA H1- SIGMA H2- SIGMA H3E SIGMA H4E  
 5.79342E 02 -5.79342E C2  
 5.78452E 02 2.30888E C2

XI = 0.40000

0  
 0  
 0  
 0  
 0

SIGMA F16  
7.14782E 02  
3.20247E C2

SIGMA H26

SIGMA H2-

SIGMA F36

SIGMA F3-

SIGMA H46

XI= 0.45000  
SIGMA F16  
8.51577E C2  
5.95268E C1

SIGMA F26

SIGMA H2-

SIGMA F36

SIGMA F3-

SIGMA H46

XI= 0.47500  
SIGMA F16  
9.19279E 02  
-7.22885E C1

SIGMA H26

SIGMA H2-

SIGMA F36

SIGMA F3-

SIGMA H46

XI= 0.48000  
SIGMA F16  
9.32715E 02  
-5.87738E 01

SIGMA H26

SIGMA H2-

SIGMA H36

SIGMA F3-

SIGMA H46

STRESSES REGION 2

GEOMETRY IS PRESCRIBED BY A CONE OR CYLINDER EQUATION  
 STRESSES ARE PRINTED AS FOLLOWS LINE 1 SIGMA XI LINE 2 SIGMA THETA OUTER SURFACE... INTERFACES... IN

|              |              |           |           |           |           |
|--------------|--------------|-----------|-----------|-----------|-----------|
| XI = 0.      | SIGMA H1-    | SIGMA H2- | SIGMA H3E | SIGMA H3- | SIGMA H4E |
| SIGMA F1E    | -5.32659E 02 |           |           |           |           |
|              | -5.8E175E 01 |           |           |           |           |
| XI = 0.05000 | SIGMA H1-    | SIGMA H2- | SIGMA H3E | SIGMA H3- | SIGMA H4E |
| SIGMA F1E    | -1.06342E 03 |           |           |           |           |
|              | -3.671C7E 02 |           |           |           |           |
| XI = 0.10000 | SIGMA H1-    | SIGMA H2- | SIGMA H3E | SIGMA H3- | SIGMA H4E |
| SIGMA F1E    | -1.18501E 03 |           |           |           |           |
|              | -6.42419E 02 |           |           |           |           |
| XI = 0.15000 | SIGMA H1-    | SIGMA H2- | SIGMA H3E | SIGMA H3- | SIGMA H4E |
| SIGMA F1E    | -1.29348E 03 |           |           |           |           |
|              | -9.26416E 02 |           |           |           |           |
| XI = 0.20000 | SIGMA H1-    | SIGMA H2- | SIGMA H3E | SIGMA H3- | SIGMA H4E |
| SIGMA F1E    | -1.38437E 03 |           |           |           |           |
|              | -1.22090E 03 |           |           |           |           |
| XI = 0.25000 | SIGMA H1-    | SIGMA H2- | SIGMA H3E | SIGMA H3- | SIGMA H4E |
| SIGMA F1E    | -1.45361E 03 |           |           |           |           |
|              | -1.52744E 03 |           |           |           |           |
| XI = 0.30000 | SIGMA H1-    | SIGMA H2- | SIGMA H3E | SIGMA H3- | SIGMA H4E |
| SIGMA F1E    | -1.45687E 03 |           |           |           |           |
|              | -1.84762E 03 |           |           |           |           |
| XI = 0.35000 | SIGMA H1-    | SIGMA H2- | SIGMA H3E | SIGMA H3- | SIGMA H4E |
| SIGMA F1E    | -1.50960E 03 |           |           |           |           |
|              | -2.18297E 03 |           |           |           |           |
| XI = 0.40000 |              |           |           |           |           |

SIGMA F16  
1.48747E 03  
-2.53484E 03

XI = 0.45000  
SIGMA F16  
1.42578E 03  
-2.90456E 03

XI = 0.50000  
SIGMA F16  
1.31957E 03  
-3.29325E 03

XI = 0.55000  
SIGMA F16  
1.16524E 03  
-3.70153E 03

XI = 0.60000  
SIGMA F16  
5.56738E 02  
-4.1314CE 03

XI = 0.65000  
SIGMA F16  
6.85710E 02  
-4.58229E 03

XI = 0.70000  
SIGMA F16  
3.55144E 02  
-5.0550CE 03

XI = 0.71500  
SIGMA F16  
2.46868E 02  
-5.20109E 03

XI = 0.72000  
SIGMA F16  
2.08401E 02  
-5.25012E 03

SIGMA H1-  
-1.48747E C3  
-3.42732E C3

SIGMA H1-  
-1.42578E C3  
-3.70003E C3

SIGMA H1-  
-1.31957E C3  
-4.08523E C3

SIGMA H1-  
-1.16524E C3  
-4.40107E C3

SIGMA H1-  
-9.56738E C2  
-4.70544E C3

SIGMA H1-  
-6.89710E C2  
-4.99611E C3

SIGMA H1-  
-3.55144E C2  
-5.27048E C3

SIGMA H1-  
-2.46868E C2  
-5.34921E C3

SIGMA H1-  
-2.08401E C2  
-5.37516E C3

SIGMA H46

SIGMA H36

SIGMA H26

SIGMA H16

SIGMA H06

SIGMA H46

SIGMA H36

SIGMA H26

SIGMA H16

SIGMA H06

SIGMA H46

SIGMA H36

SIGMA H26

SIGMA H16

SIGMA H06

SIGMA H46

SIGMA H36

SIGMA H26

SIGMA H16

SIGMA H06

SIGMA H46

SIGMA H36

SIGMA H26

SIGMA H16

SIGMA H06

SIGMA H46

SIGMA H36

SIGMA H26

SIGMA H16

SIGMA H06

SIGMA H46

SIGMA H36

SIGMA H26

SIGMA H16

SIGMA H06

SIGMA H46

SIGMA H36

SIGMA H26

SIGMA H16

SIGMA H06

SIGMA H46

SIGMA H36

SIGMA H26

SIGMA H16

SIGMA H06

STRESSES REGION 3

GEOMETRY IS PRESCRIBED BY A SPHERE OR TORUS EQUATION  
 STRESSES ARE PRINTED AS FOLLOWS LINE 1 SIGMA XI LINE 2 SIGMA THETA LUTER SURFACE...INTERFACES... I

XI= 0.  
 SIGMA F16 SIGMA H1- SIGMA H2E SIGMA H2- SIGMA H3E SIGMA H3- SIGMA H4E  
 2.04676E 04 2.18409E 04  
 2.64676E 04 2.18469E 04

XI= 0.10086  
 SIGMA F16 SIGMA H1- SIGMA H2E SIGMA H2- SIGMA H3E SIGMA H3- SIGMA H4E  
 2.65145E 04 2.17878E 04  
 2.64862E 04 2.18007E 04

XI= 0.20173  
 SIGMA F16 SIGMA H1- SIGMA H2E SIGMA H2- SIGMA H3E SIGMA H3- SIGMA H4E  
 2.66377E 04 2.16438E 04  
 2.65313E 04 2.16939E 04

XI= 0.30259  
 SIGMA F16 SIGMA H1- SIGMA H2E SIGMA H2- SIGMA H3E SIGMA H3- SIGMA H4E  
 2.68424E 04 2.14026E 04  
 2.66050E 04 2.15126E 04

XI= 0.40346  
 SIGMA F16 SIGMA H1- SIGMA H2E SIGMA H2- SIGMA H3E SIGMA H3- SIGMA H4E  
 2.71253E 04 2.10666E 04  
 2.67033E 04 2.12558E 04

XI= 0.50432  
 SIGMA F16 SIGMA H1- SIGMA H2E SIGMA H2- SIGMA H3E SIGMA H3- SIGMA H4E  
 2.74823E 04 2.06389E 04  
 2.68210E 04 2.09221E 04

XI= 0.60519  
 SIGMA F16 SIGMA H1- SIGMA H2E SIGMA H2- SIGMA H3E SIGMA H3- SIGMA H4E  
 2.75075E 04 2.01233E 04  
 2.65510E 04 2.05052E 04

XI= 0.70605  
 SIGMA F16 SIGMA H1- SIGMA H2E SIGMA H2- SIGMA H3E SIGMA H3- SIGMA H4E  
 2.83937E 04 1.95252E 04  
 2.70849E 04 2.00148E 04

XI= 0.80692



SIGMA F16  
2.89316E 04  
2.72128E 04

SIGMA H1-

1.88515E 04  
1.54366E 04

SIGMA H2-

SIGMA F36

SIGMA H3-

SIGMA H46

XI= 0.50778

SIGMA F16

2.95093E 04  
2.73230E 04

SIGMA H1-

1.81109E 04  
1.87724E 04

SIGMA H2-

SIGMA F36

SIGMA H3-

SIGMA H46

XI= 1.00865

SIGMA F16

3.01145E 04  
2.74022E 04

SIGMA H1-

1.73143E 04  
1.80207E 04

SIGMA H2-

SIGMA F36

SIGMA H3-

SIGMA H46

XI= 1.10951

SIGMA F16

3.07290E 04  
2.74354E 04

SIGMA H1-

1.64753E 04  
1.71803E 04

SIGMA H2-

SIGMA F36

SIGMA H3-

SIGMA H46

XI= 1.21037

SIGMA F16

3.13335E 04  
2.74062E 04

SIGMA H1-

1.56103E 04  
1.62517E 04

SIGMA H2-

SIGMA F36

SIGMA H3-

SIGMA H46

XI= 1.31124

SIGMA F16

3.15048E 04  
2.72967E 04

SIGMA H1-

1.47392E 04  
1.52363E 04

SIGMA H2-

SIGMA F36

SIGMA H3-

SIGMA H46

XI= 1.41210

SIGMA F16

3.24160E 04  
2.70815E 04

SIGMA H1-

1.38857E 04  
1.41378E 04

SIGMA H2-

SIGMA F36

SIGMA H3-

SIGMA H46

XI= 1.51297

SIGMA F16

3.28360E 04  
2.67582E 04

SIGMA H1-

1.30776E 04  
1.29621E 04

SIGMA H2-

SIGMA F36

SIGMA H3-

SIGMA H46

XI= 1.61383

SIGMA F16

3.31293E 04  
2.62371E 04

SIGMA H1-

1.23474E 04  
1.17181E 04

SIGMA H2-

SIGMA F36

SIGMA H3-

SIGMA H46

XI= 1.71470

SIGMA F16

SIGMA H2-

SIGMA F36

SIGMA H3-

SIGMA H46

3.32558E C4 1.17323E C4  
2.56522E 04 1.C4180E C4

XI= 1.81556 SIGMA H1- SIGMA H2E SIGMA H2- SIGMA H3E SIGMA H3- SIGMA H4E

3.31707E 04 1.12749E 04  
2.48213E 04 5.C7831E C3

XI= 1.51643 SIGMA H1- SIGMA H2E SIGMA H2- SIGMA H3E SIGMA H3- SIGMA H4E

3.28244E 04 1.10232E C4  
2.38C22E 04 7.71592E C3

XI= 2.01729 SIGMA H1- SIGMA H2E SIGMA H2- SIGMA H3E SIGMA H3- SIGMA H4E

3.21623E 04 1.10305E C4  
2.2544CE 04 6.26514E C3

XI= 2.11816 SIGMA H1- SIGMA H2E SIGMA H2- SIGMA H3E SIGMA H3- SIGMA H4E

3.11257E 04 1.13557E C4  
2.1C370E C4 5.C5819E C3

XI= 2.21902 SIGMA H1- SIGMA H2E SIGMA H2- SIGMA H3E SIGMA H3- SIGMA H4E

2.96513E 04 1.20627E C4  
1.92645E 04 3.82588E C3

XI= 2.31986 SIGMA H1- SIGMA H2E SIGMA H2- SIGMA H3E SIGMA H3- SIGMA H4E

2.76726E 04 1.32204E 04  
1.72131E C4 2.71820E C3

XI= 2.42075 SIGMA H1- SIGMA H2E SIGMA H2- SIGMA H3E SIGMA H3- SIGMA H4E

2.51202E 04 1.49018E C4  
1.48742E 04 1.78897E C3

XI= 2.52161 SIGMA H1- SIGMA H2E SIGMA H2- SIGMA H3E SIGMA H3- SIGMA H4E

2.19233E 04 1.71827E C4  
1.22453E C4 1.10C23E C3

XI= 2.62248 SIGMA H1- SIGMA H2E SIGMA H2- SIGMA H3E SIGMA H3- SIGMA H4E

1.80113E 04 2.01410E C4

9.33155E C3 7.22776E C2

XI = 2.72334  
SIGMA F16 SIGMA H1-  
1.33154E 04 2.38540E 04  
6.14728E 03 7.36338E C2

SIGMA H36 SIGMA H3-

SIGMA H46

XI = 2.82421  
SIGMA F16 SIGMA H1-  
7.77108E 03 2.83993E C4  
2.71782E 03 1.22565E C3

SIGMA H36 SIGMA H3-

SIGMA H46

XI = 2.92507  
SIGMA F16 SIGMA H1-  
1.32085E 03 3.38404E 04  
-9.18442E 02 2.30045E C3

SIGMA H36 SIGMA H3-

SIGMA H46

XI = 3.02594  
SIGMA F16 SIGMA H1-  
-6.08241E 03 4.02592E C4  
-4.70825E 03 4.05488E C3

SIGMA H36 SIGMA H3-

SIGMA H46

XI = 3.12680  
SIGMA F16 SIGMA H1-  
-1.44716E 04 4.76898E C4  
-8.58109E 03 6.60656E C3

SIGMA H36 SIGMA H3-

SIGMA H46

XI = 3.17723  
SIGMA F16 SIGMA H1-  
-1.90412E 04 5.17989E C4  
-1.05214E 04 8.21556E C3

SIGMA H36 SIGMA H3-

SIGMA H46

XI = 3.22767  
SIGMA F16 SIGMA H1-  
-2.37380E 04 5.60514E C4  
-1.24775E 04 9.97324E C3

SIGMA H36 SIGMA H3-

SIGMA H46

STRESSES REGION 4

GEOMETRY IS PRESCRIBED BY A CONE OR CYLINDER EQUATION  
 STRESSES ARE PRINTED AS FOLLOWS LINE 1 SIGMA XI LINE 2 SIGMA THETA OUTER SURFACE... INTERFACES... IN

|              |              |          |           |          |          |
|--------------|--------------|----------|-----------|----------|----------|
| XI = 0.      | SIGMA H1-    | SIGMA H2 | SIGMA H2- | SIGMA F3 | SIGMA H4 |
| SIGMA F1     | 9.29395E 03  |          |           |          |          |
| -6.01072E 03 | -2.89506E 03 |          |           |          |          |
| -7.48646E 03 |              |          |           |          |          |
| XI = 0.05000 | SIGMA H1-    | SIGMA H2 | SIGMA H2- | SIGMA H3 | SIGMA H4 |
| SIGMA F1     | 9.87200E 03  |          |           |          |          |
| -6.28184E 03 | -3.07911E 03 |          |           |          |          |
| -7.92526E 03 |              |          |           |          |          |
| XI = 0.10000 | SIGMA H1-    | SIGMA H2 | SIGMA H2- | SIGMA H3 | SIGMA H4 |
| SIGMA F1     | 1.06166E 04  |          |           |          |          |
| -6.67256E 03 | -3.15832E 03 |          |           |          |          |
| -8.38507E 03 |              |          |           |          |          |
| XI = 0.15000 | SIGMA H1-    | SIGMA H2 | SIGMA H2- | SIGMA H3 | SIGMA H4 |
| SIGMA F1     | 1.15917E 04  |          |           |          |          |
| -7.23501E 03 | -3.22930E 03 |          |           |          |          |
| -8.87733E 03 |              |          |           |          |          |
| XI = 0.20000 | SIGMA H1-    | SIGMA H2 | SIGMA H2- | SIGMA H3 | SIGMA H4 |
| SIGMA F1     | 1.28926E 04  |          |           |          |          |
| -8.04821E 03 | -3.14109E 03 |          |           |          |          |
| -9.42336E 03 |              |          |           |          |          |
| XI = 0.25000 | SIGMA H1-    | SIGMA H2 | SIGMA H2- | SIGMA H3 | SIGMA H4 |
| SIGMA F1     | 1.40678E 04  |          |           |          |          |
| -9.23850E 03 | -2.88579E 03 |          |           |          |          |
| -1.00577E 04 |              |          |           |          |          |
| XI = 0.30000 | SIGMA H1-    | SIGMA H2 | SIGMA H2- | SIGMA H3 | SIGMA H4 |
| SIGMA F1     | 1.71495E 04  |          |           |          |          |
| -1.10049E 04 | -2.38903E 03 |          |           |          |          |
| -1.08353E 04 |              |          |           |          |          |
| XI = 0.35000 | SIGMA H1-    | SIGMA H2 | SIGMA H2- | SIGMA H3 | SIGMA H4 |
| SIGMA F1     | 2.06724E 04  |          |           |          |          |
| -1.36331E 04 | -1.54370E 03 |          |           |          |          |
| -1.16354E 04 |              |          |           |          |          |

SIGMA F1G  
-1.73431E 04  
-1.3118E 04

SIGMA H1-

SIGMA H2G

SIGMA H3G

SIGMA H4G

XI= 0.44500

SIGMA F1G

-2.09550E 04

-1.4218E 04

SIGMA H1-

3.05070E 04

1.12055E 03

SIGMA H2G

SIGMA H3G

SIGMA H4G

XI= 0.45000

SIGMA F1G

-2.12697E 04

-1.42153E 04

SIGMA H1-

3.05982E 04

1.36509E 03

SIGMA H2G

SIGMA H3G

SIGMA H4G





|              |             |           |           |           |
|--------------|-------------|-----------|-----------|-----------|
| SIGMA F16    | SIGMA H1-   | SIGMA H26 | SIGMA H36 | SIGMA H46 |
| -7.05270E 04 | 8.97777E 04 |           |           |           |
| -2.84748E 04 | 1.56145E 04 |           |           |           |
| XI = 0.09000 |             |           |           |           |
| SIGMA F16    | SIGMA H1-   | SIGMA H26 | SIGMA H36 | SIGMA H46 |
| -6.95411E 04 | 8.87848E 04 |           |           |           |
| -2.80582E 04 | 1.94395E 04 |           |           |           |
| XI = 0.10000 |             |           |           |           |
| SIGMA F16    | SIGMA H1-   | SIGMA H26 | SIGMA H36 | SIGMA H46 |
| -6.85724E 04 | 8.78161E 04 |           |           |           |
| -2.76318E 04 | 1.92847E 04 |           |           |           |
| XI = 0.10100 |             |           |           |           |
| SIGMA F16    | SIGMA H1-   | SIGMA H26 | SIGMA H36 | SIGMA H46 |
| -6.84764E 04 | 8.77201E 04 |           |           |           |
| -2.75867E 04 | 1.92703E 04 |           |           |           |
| XI = 0.10200 |             |           |           |           |
| SIGMA F16    | SIGMA H1-   | SIGMA H26 | SIGMA H36 | SIGMA H46 |
| -6.83806E 04 | 8.76243E 04 |           |           |           |
| -2.75456E 04 | 1.92559E 04 |           |           |           |

STRESSES REGION 6

GEOMETRY IS PRESCRIBED BY A CONE OR CYLINDER EQUATION  
 STRESSES ARE PRINTED AS FOLLOWS LINE 1 SIGMA XI LINE 2 SIGMA THETA OUTER SURFACE... INTERFACES... IF

| XI =         | SIGMA H1-    | SIGMA H2- | SIGMA H3- | SIGMA H4- |
|--------------|--------------|-----------|-----------|-----------|
| 0.           |              |           |           |           |
| SIGMA F16    |              |           |           |           |
| -1.24617E 04 | 2.36694E C4  |           |           |           |
| -1.09556E 04 | -1.11268E C2 |           |           |           |
| XI = 0.10072 |              |           |           |           |
| SIGMA F16    |              |           |           |           |
| -9.67436E 03 | 2.08821E C4  |           |           |           |
| -8.58483E C3 | 5.82055E C2  |           |           |           |
| XI = 0.20144 |              |           |           |           |
| SIGMA F16    |              |           |           |           |
| -7.49922E 03 | 1.87069E C4  |           |           |           |
| -6.22556E 03 | 1.63588E C3  |           |           |           |
| XI = 0.30216 |              |           |           |           |
| SIGMA F16    |              |           |           |           |
| -5.87469E 03 | 1.70824E C4  |           |           |           |
| -3.87568E 03 | 2.00745E C3  |           |           |           |
| XI = 0.40288 |              |           |           |           |
| SIGMA F16    |              |           |           |           |
| -4.72958E 03 | 1.59373E C4  |           |           |           |
| -1.54357E C3 | 4.65649E C3  |           |           |           |
| XI = 0.50360 |              |           |           |           |
| SIGMA F16    |              |           |           |           |
| -3.98772E 03 | 1.51954E C4  |           |           |           |
| 7.91668E 02  | 6.54681E C3  |           |           |           |
| XI = 0.60432 |              |           |           |           |
| SIGMA F16    |              |           |           |           |
| -3.56830E 03 | 1.47760E C4  |           |           |           |
| 3.14218E C3  | 8.64547E C3  |           |           |           |
| XI = 0.70505 |              |           |           |           |
| SIGMA F16    |              |           |           |           |
| -3.38620E 03 | 1.45939E C4  |           |           |           |
| 5.52758E 03  | 1.09220E C4  |           |           |           |

SIGMA F16  
-3.35235E 03  
7.97377E 03  
SIGMA H1-  
1.45601E 04  
1.33475E 04  
SIGMA H26  
SIGMA H2-  
SIGMA F36  
SIGMA F3-

XI = 0.90649  
SIGMA F16  
-3.37360E 03  
1.0507CE 04  
SIGMA H1-  
1.45613E 04  
1.58535E 04  
SIGMA H26  
SIGMA H2-  
SIGMA H36  
SIGMA F3-

XI = 1.00721  
SIGMA F16  
-3.35263E 03  
1.31571E 04  
SIGMA H1-  
1.45603E 04  
1.85310E 04  
SIGMA H26  
SIGMA H2-  
SIGMA H36  
SIGMA F3-

XI = 1.10793  
SIGMA F16  
-3.18848E 03  
1.55539E 04  
SIGMA H1-  
1.43562E 04  
2.12293E 04  
SIGMA H26  
SIGMA H2-  
SIGMA H36  
SIGMA F3-

XI = 1.11800  
SIGMA F16  
-3.16137E 03  
1.62419E 04  
SIGMA H1-  
1.43691E 04  
2.15010E 04  
SIGMA H26  
SIGMA H2-  
SIGMA H36  
SIGMA F3-

STRESSES REGION 7

GEOMETRY IS PRESCRIBED BY A CONE OR CYLINDER EQUATION  
 STRESSES ARE PRINTED AS FOLLOWS LINE 1 SIGMA XI LINE 2 SIGMA THETA OUTER SURFACE... INTERFACES... IM

XI= 0.  
 SIGMA F16 SIGMA H1- SIGMA H26 SIGMA H2- SIGMA H36 SIGMA H3- SIGMA H46  
 2.00240E 04 7.99225E 03  
 2.37922E 04 2.01858E C4

XI= 0.04021  
 SIGMA F16 SIGMA H1- SIGMA H26 SIGMA H2- SIGMA H36 SIGMA H3- SIGMA H46  
 2.06660E 04 7.35664E 03  
 2.51313E 04 2.11383E C4

XI= 0.08041  
 SIGMA F16 SIGMA H1- SIGMA H26 SIGMA H2- SIGMA H36 SIGMA H3- SIGMA H46  
 2.12327E 04 6.79056E C3  
 2.64162E 04 2.20835E C4

XI= 0.12062  
 SIGMA F16 SIGMA H1- SIGMA H26 SIGMA H2- SIGMA H36 SIGMA H3- SIGMA H46  
 2.17373E 04 6.28595E 03  
 2.76453E 04 2.30139E C4

XI= 0.16082  
 SIGMA F16 SIGMA H1- SIGMA H26 SIGMA H2- SIGMA H36 SIGMA H3- SIGMA H46  
 2.21970E 04 5.82630E C3  
 2.88232E 04 2.35220E C4

XI= 0.20103  
 SIGMA F16 SIGMA H1- SIGMA H26 SIGMA H2- SIGMA H36 SIGMA H3- SIGMA H46  
 2.26276E 04 5.39564E C3  
 2.95705E 04 2.48009E C4

XI= 0.24124  
 SIGMA F16 SIGMA H1- SIGMA H26 SIGMA H2- SIGMA H36 SIGMA H3- SIGMA H46  
 2.30445E 04 4.97871E C3  
 3.10629E 04 2.56442E C4

XI= 0.28144  
 SIGMA F16 SIGMA H1- SIGMA H26 SIGMA H2- SIGMA H36 SIGMA H3- SIGMA H46  
 2.34026E 04 4.56060E C3  
 3.21159E 04 2.64453E C4

XI= 0.32165

|              |              |           |           |           |           |           |
|--------------|--------------|-----------|-----------|-----------|-----------|-----------|
| SIGMA F16    | SIGMA H1-    | SIGMA H26 | SIGMA H2- | SIGMA F36 | SIGMA F3- | SIGMA H46 |
| 2.38958E 04  | 4.12742E C3  |           |           |           |           |           |
| 3.31288E 04  | 2.71582E C4  |           |           |           |           |           |
| XI = 0.36186 |              |           |           |           |           |           |
| SIGMA F16    | SIGMA H1-    | SIGMA H26 | SIGMA H2- | SIGMA F36 | SIGMA F3- | SIGMA H46 |
| 2.43577E 04  | 3.66552E C3  |           |           |           |           |           |
| 3.41045E 04  | 2.78588E C4  |           |           |           |           |           |
| XI = 0.40206 |              |           |           |           |           |           |
| SIGMA F16    | SIGMA H1-    | SIGMA H26 | SIGMA H2- | SIGMA F36 | SIGMA F3- | SIGMA H46 |
| 2.48610E 04  | 3.16223E C3  |           |           |           |           |           |
| 3.56448E 04  | 2.85351E C4  |           |           |           |           |           |
| XI = 0.44227 |              |           |           |           |           |           |
| SIGMA F16    | SIGMA H1-    | SIGMA H26 | SIGMA H2- | SIGMA F36 | SIGMA F3- | SIGMA H46 |
| 2.54178E 04  | 2.60551E C3  |           |           |           |           |           |
| 3.55509E 04  | 2.91072E C4  |           |           |           |           |           |
| XI = 0.48247 |              |           |           |           |           |           |
| SIGMA F16    | SIGMA H1-    | SIGMA H26 | SIGMA H2- | SIGMA F36 | SIGMA F3- | SIGMA H46 |
| 2.60392E 04  | 1.58409E C3  |           |           |           |           |           |
| 3.68237E 04  | 2.56071E C4  |           |           |           |           |           |
| XI = 0.52268 |              |           |           |           |           |           |
| SIGMA F16    | SIGMA H1-    | SIGMA H26 | SIGMA H2- | SIGMA F36 | SIGMA F3- | SIGMA H46 |
| 2.67357E 04  | 1.28753E C3  |           |           |           |           |           |
| 3.76633E 04  | 3.00289E C4  |           |           |           |           |           |
| XI = 0.56289 |              |           |           |           |           |           |
| SIGMA F16    | SIGMA H1-    | SIGMA H26 | SIGMA H2- | SIGMA F36 | SIGMA F3- | SIGMA H46 |
| 2.75171E 04  | 5.06154E C2  |           |           |           |           |           |
| 3.84656E 04  | 2.03663E C4  |           |           |           |           |           |
| XI = 0.60309 |              |           |           |           |           |           |
| SIGMA F16    | SIGMA H1-    | SIGMA H26 | SIGMA H2- | SIGMA F36 | SIGMA F3- | SIGMA H46 |
| 2.82919E 04  | -2.88664E C2 |           |           |           |           |           |
| 3.92414E 04  | 3.06132E C4  |           |           |           |           |           |
| XI = 0.64330 |              |           |           |           |           |           |
| SIGMA F16    | SIGMA H1-    | SIGMA H26 | SIGMA H2- | SIGMA F36 | SIGMA F3- | SIGMA H46 |
| 2.93680E 04  | -1.34477E C3 |           |           |           |           |           |
| 3.95770E 04  | 3.07632E C4  |           |           |           |           |           |
| XI = 0.68351 |              |           |           |           |           |           |
| SIGMA F16    | SIGMA H1-    | SIGMA H26 | SIGMA H2- | SIGMA F36 | SIGMA F3- | SIGMA H46 |
|              |              |           |           |           |           |           |

3.04521E 04 -2.42882E 03  
4.06740E 04 3.08058E 04

XI= C.72371

SIGMA F16

SIGMA H1-

SIGMA H26

SIGMA H2-

SIGMA H36

SIGMA H3-

SIGMA H46

3.16458E 04 -3.62654E 03  
4.13251E 04 3.07462E 04

XI= 0.76392

SIGMA F16

SIGMA H1-

SIGMA H26

SIGMA H2-

SIGMA H36

SIGMA H3-

SIGMA H46

3.25657E 04 -4.94241E 03  
4.15375E 04 3.05655E 04

XI= 0.77196

SIGMA F16

SIGMA H1-

SIGMA H26

SIGMA H2-

SIGMA H36

SIGMA H3-

SIGMA H46

3.32433E 04 -5.22007E 03  
4.20537E 04 3.05147E 04

XI= 0.78000

SIGMA F16

SIGMA H1-

SIGMA H26

SIGMA H2-

SIGMA H36

SIGMA H3-

SIGMA H46

3.35234E 04 -5.50017E 03  
4.21685E 04 3.04614E 04



STRESSES REGION 8

GEOMETRY IS PRESCRIBED BY A CONE OR CYLINDER EQUATION  
 STRESSES ARE PRINTED AS FOLLOWS LINE 1 SIGMA XI LINE 2 SIGMA THETA  
 OUTER SURFACE... INTERFACES...

|              |              |          |          |          |
|--------------|--------------|----------|----------|----------|
| XI = 0.      | SIGMA H1-    | SIGMA H2 | SIGMA H3 | SIGMA H4 |
| SIGMA F1     | -5.53375E C3 |          |          |          |
| 3.34858E 04  | 3.04517E C4  |          |          |          |
| 4.20532E 04  |              |          |          |          |
| XI = 0.15000 | SIGMA H1-    | SIGMA H2 | SIGMA H3 | SIGMA H4 |
| SIGMA F1     | 8.24650E C2  |          |          |          |
| 2.74574E 04  | 3.20240E C4  |          |          |          |
| 4.01257E 04  |              |          |          |          |
| XI = 0.30000 | SIGMA H1-    | SIGMA H2 | SIGMA H3 | SIGMA H4 |
| SIGMA F1     | 5.65070E C3  |          |          |          |
| 2.29420E 04  | 3.23084E C4  |          |          |          |
| 3.77501E 04  |              |          |          |          |
| XI = 0.45000 | SIGMA H1-    | SIGMA H2 | SIGMA H3 | SIGMA H4 |
| SIGMA F1     | 9.21329E C3  |          |          |          |
| 1.96684E 04  | 3.17211E C4  |          |          |          |
| 3.51951E 04  |              |          |          |          |
| XI = 0.60000 | SIGMA H1-    | SIGMA H2 | SIGMA H3 | SIGMA H4 |
| SIGMA F1     | 1.18921E C4  |          |          |          |
| 1.72467E 04  | 3.05938E C4  |          |          |          |
| 3.25857E 04  |              |          |          |          |
| XI = 0.75000 | SIGMA H1-    | SIGMA H2 | SIGMA H3 | SIGMA H4 |
| SIGMA F1     | 1.41195E 04  |          |          |          |
| 1.52489E 04  | 2.52162E C4  |          |          |          |
| 2.95611E 04  |              |          |          |          |
| XI = 0.90000 | SIGMA H1-    | SIGMA H2 | SIGMA H3 | SIGMA H4 |
| SIGMA F1     | 1.63451E C4  |          |          |          |
| 1.32194E 04  | 2.78552E C4  |          |          |          |
| 2.73136E 04  |              |          |          |          |
| XI = 1.05000 | SIGMA H1-    | SIGMA H2 | SIGMA H3 | SIGMA H4 |
| SIGMA F1     | 1.90077E C4  |          |          |          |
| 1.07227E 04  | 2.67736E C4  |          |          |          |
| 2.46451E 04  |              |          |          |          |
| XI = 1.20000 |              |          |          |          |

|              |             |           |           |           |           |           |
|--------------|-------------|-----------|-----------|-----------|-----------|-----------|
| SIGMA F16    | SIGMA F1-   | SIGMA H2E | SIGMA H2- | SIGMA H3E | SIGMA H3- | SIGMA H4E |
| 7.35923E 03  | 2.25105E C4 |           |           |           |           |           |
| 2.15E40E 04  | 2.62487E C4 |           |           |           |           |           |
| XI= 1.35000  | SIGMA H1-   | SIGMA H2E | SIGMA H2- | SIGMA H3E | SIGMA H3- | SIGMA H4E |
| SIGMA F1E    | 2.71911E 04 |           |           |           |           |           |
| 2.75711E 03  | 2.65E58E C4 |           |           |           |           |           |
| 1.94231E 04  |             |           |           |           |           |           |
| XI= 1.42500  | SIGMA H1-   | SIGMA H2E | SIGMA H2- | SIGMA H3E | SIGMA H3- | SIGMA H4E |
| SIGMA F1E    | 3.00520E C4 |           |           |           |           |           |
| -9.81812E 00 | 2.71826E C4 |           |           |           |           |           |
| 1.82337E 04  |             |           |           |           |           |           |
| XI= 1.44000  | SIGMA H1-   | SIGMA H2E | SIGMA H2- | SIGMA H3E | SIGMA H3- | SIGMA H4E |
| SIGMA F1E    | 3.06611E C4 |           |           |           |           |           |
| -6.08363E 02 | 2.73351E C4 |           |           |           |           |           |
| 1.80047E 04  |             |           |           |           |           |           |

STRESSES REGION 9

GEOMETRY IS PRESCRIBED BY A CONE OR CYLINDER EQUATION  
 STRESSES ARE PRINTED AS FOLLOWS LINE 1 SIGMA XI LINE 2 SIGMA THETA  
 OUTER SURFACE...INTERFACES...

|              |             |           |           |           |
|--------------|-------------|-----------|-----------|-----------|
| XI = 0.      | SIGMA H1-   | SIGMA H2- | SIGMA H3- | SIGMA H4- |
| SIGMA F1-    | 3.0656CE C4 |           |           |           |
| -6.13490E 02 | 2.73656E C4 |           |           |           |
| 1.79847E 04  |             |           |           |           |
| XI = 0.30000 | SIGMA H1-   | SIGMA H2- | SIGMA H3- | SIGMA H4- |
| SIGMA F1-    | 1.98976E C4 |           |           |           |
| 1.01450E 04  | 2.50661E C4 |           |           |           |
| 2.21343E 04  |             |           |           |           |
| XI = 0.60000 | SIGMA H1-   | SIGMA H2- | SIGMA H3- | SIGMA H4- |
| SIGMA F1-    | 1.43264E C4 |           |           |           |
| 1.57161E 04  | 2.55696E C4 |           |           |           |
| 2.55865E 04  |             |           |           |           |
| XI = 0.90000 | SIGMA H1-   | SIGMA H2- | SIGMA H3- | SIGMA H4- |
| SIGMA F1-    | 1.23227E C4 |           |           |           |
| 1.77058E 04  | 2.70562E C4 |           |           |           |
| 2.86653E 04  |             |           |           |           |
| XI = 1.20000 | SIGMA H1-   | SIGMA H2- | SIGMA H3- | SIGMA H4- |
| SIGMA F1-    | 1.22962E C4 |           |           |           |
| 1.77464E 04  | 2.85218E C4 |           |           |           |
| 3.01565E 04  |             |           |           |           |
| XI = 1.50000 | SIGMA H1-   | SIGMA H2- | SIGMA H3- | SIGMA H4- |
| SIGMA F1-    | 1.30477E C4 |           |           |           |
| 1.65948E 04  | 2.55838E C4 |           |           |           |
| 3.07679E 04  |             |           |           |           |
| XI = 1.80000 | SIGMA H1-   | SIGMA H2- | SIGMA H3- | SIGMA H4- |
| SIGMA F1-    | 1.39127E C4 |           |           |           |
| 1.61298E 04  | 3.02072E C4 |           |           |           |
| 3.08723E 04  |             |           |           |           |
| XI = 2.10000 | SIGMA H1-   | SIGMA H2- | SIGMA H3- | SIGMA H4- |
| SIGMA F1-    | 1.42894E C4 |           |           |           |
| 1.54531E 04  | 3.05036E C4 |           |           |           |
| 3.07628E 04  |             |           |           |           |
| XI = 2.40000 |             |           |           |           |

|             |             |           |           |           |           |           |
|-------------|-------------|-----------|-----------|-----------|-----------|-----------|
| SIGMA F16   | SIGMA H1-   | SIGMA H26 | SIGMA H2- | SIGMA H36 | SIGMA H3- | SIGMA H46 |
| 1.50495E 04 | 1.49930E C4 |           |           |           |           |           |
| 3.06255E C4 | 3.06088E C4 |           |           |           |           |           |
| XI= 2.70000 |             |           |           |           |           |           |
| SIGMA F16   | SIGMA H1-   | SIGMA H26 | SIGMA H2- | SIGMA H36 | SIGMA H3- | SIGMA H46 |
| 1.49126E 04 | 1.51259E C4 |           |           |           |           |           |
| 3.05567E 04 | 3.06215E C4 |           |           |           |           |           |
| XI= 2.97000 |             |           |           |           |           |           |
| SIGMA F16   | SIGMA H1-   | SIGMA H26 | SIGMA H2- | SIGMA H36 | SIGMA H3- | SIGMA H46 |
| 1.50006E 04 | 1.50419E C4 |           |           |           |           |           |
| 3.05764E 04 | 3.05888E C4 |           |           |           |           |           |
| XI= 3.00000 |             |           |           |           |           |           |
| SIGMA F16   | SIGMA H1-   | SIGMA H26 | SIGMA H2- | SIGMA H36 | SIGMA H3- | SIGMA H46 |
| 1.50213E 04 | 1.50213E C4 |           |           |           |           |           |
| 3.05826E 04 | 3.05826E C4 |           |           |           |           |           |

INPUT DATA

```

WITHJUT
# WRC JOINT RELATION STUDY---SYSTEM RECOVERY HOUSING
DATE 1.24.00  CASE 1.0  NREGIONS 3
ENDC(1,1) -1 4 0.0  ENDC(2,1) -1 7 0.0
ENDC(3,1) 23 4 0.0  ENDC(4,1) 23 6 0.0
JUNC(1,1) 21 -2 0 0.0 0.0  NU .3  JUNC(2,1) 22 -3 0 -1.0 0.0
INSTATIONS 3  DELTAXI .03  NLAYEFS 1
RVCUNT 0  NURV 0  KVI 0.0
GEOM 1  RO 3.875  ANGLE 90.
XI 0.0 1.5 3.0
P(1-3) 0.0  PCLAP 0  Y(1-3) 10.300  A(1-3) 0.  T(1-3) 0.
m(1-3)0.180

1  INSTATIONS 3  DELTAXI .005  NU .3  PRINTOUT 10
RVCUNT 1  NURV 0  KVI 0.0  NLAYERS 1
GEOM 1  RO 3.875  ANGLE 90.
XI 0.0 .24 .40

1  INSTATIONS 3  DELTAXI .005  NU .3  PRINTOUT 10
RVCUNT 1  NURV 0  KVI 0.0  NLAYERS 1
GEOM 1  RO 3.875  ANGLE 90.
XI 0.0 .3055 .711
1
E

```

NIKO JOINT ROTATION STUDY---SYSTEM RECOVERY HOUSING

WITHOUT MERIDIONAL LOAD EFFECT

CASE 1.00

DATE 1.25.62

STRESS CALCULATIONS FOR SHELLS OF REVOLUTION

GEOMETRY IS DESCRIBED BY A CONE OR CYLINDER EQUATION

REGION 1 OF 3 REGIONS

BETA

DATE

DATE

DATE

| XI     | K          | THETA      | K XI       | BETA      | C         | J  | NT | MT | U          | Q          |
|--------|------------|------------|------------|-----------|-----------|----|----|----|------------|------------|
| 0.     | 1.039E-20  | -8.006E-12 | -1.508E-12 | 1.854E 06 | 5.501E 03 | 0. | 0. | 0. | 7.998E-08  | 6.408E-03  |
| 0.0900 | -3.056E-17 | 9.637E-09  | 4.436E-09  | 1.854E 06 | 5.501E 03 | 0. | 0. | 0. | 8.013E-08  | 5.476E-03  |
| 0.1800 | -1.167E-16 | 1.763E-07  | 1.894E-08  | 1.854E 06 | 5.501E 03 | 0. | 0. | 0. | 8.104E-08  | 4.539E-03  |
| 0.2700 | -2.448E-16 | 2.448E-07  | 3.612E-08  | 1.854E 06 | 5.501E 03 | 0. | 0. | 0. | 8.339E-08  | 3.583E-03  |
| 0.3600 | -4.173E-16 | 2.953E-07  | 6.057E-08  | 1.854E 06 | 5.501E 03 | 0. | 0. | 0. | 8.771E-08  | 2.589E-03  |
| 0.4500 | -6.120E-16 | 3.292E-07  | 8.883E-08  | 1.854E 06 | 5.501E 03 | 0. | 0. | 0. | 9.442E-08  | 1.532E-03  |
| 0.5400 | -8.222E-16 | 3.445E-07  | 1.192E-07  | 1.854E 06 | 5.501E 03 | 0. | 0. | 0. | 1.038E-07  | 3.810E-04  |
| 0.6300 | -1.036E-15 | 3.409E-07  | 1.504E-07  | 1.854E 06 | 5.501E 03 | 0. | 0. | 0. | 1.159E-07  | -8.951E-04 |
| 0.7200 | -1.241E-15 | 3.147E-07  | 1.801E-07  | 1.854E 06 | 5.501E 03 | 0. | 0. | 0. | 1.308E-07  | -2.329E-03 |
| 0.8100 | -1.422E-15 | 2.636E-07  | 2.064E-07  | 1.854E 06 | 5.501E 03 | 0. | 0. | 0. | 1.482E-07  | -3.951E-03 |
| 0.9000 | -1.563E-15 | 1.842E-07  | 2.265E-07  | 1.854E 06 | 5.501E 03 | 0. | 0. | 0. | 1.678E-07  | -5.789E-03 |
| 0.9500 | -1.644E-15 | 7.282E-08  | 2.387E-07  | 1.854E 06 | 5.501E 03 | 0. | 0. | 0. | 1.888E-07  | -7.864E-03 |
| 1.0800 | -1.646E-15 | -7.455E-08 | 2.390E-07  | 1.854E 06 | 5.501E 03 | 0. | 0. | 0. | 2.104E-07  | -1.019E-02 |
| 1.1700 | -1.545E-15 | -2.620E-07 | 2.242E-07  | 1.854E 06 | 5.501E 03 | 0. | 0. | 0. | 2.313E-07  | -1.276E-02 |
| 1.2600 | -1.313E-15 | -4.935E-07 | 1.906E-07  | 1.854E 06 | 5.501E 03 | 0. | 0. | 0. | 2.501E-07  | -1.557E-02 |
| 1.3500 | -5.239E-16 | -7.726E-07 | 1.341E-07  | 1.854E 06 | 5.501E 03 | 0. | 0. | 0. | 2.649E-07  | -1.857E-02 |
| 1.4400 | -3.459E-16 | -1.102E-06 | 5.021E-08  | 1.854E 06 | 5.501E 03 | 0. | 0. | 0. | 2.734E-07  | -2.172E-02 |
| 1.5300 | 4.524E-16  | -1.484E-06 | -6.567E-08 | 1.854E 06 | 5.501E 03 | 0. | 0. | 0. | 2.729E-07  | -2.491E-02 |
| 1.6200 | 1.503E-15  | -1.917E-06 | -2.182E-07 | 1.854E 06 | 5.501E 03 | 0. | 0. | 0. | 2.604E-07  | -2.803E-02 |
| 1.7100 | 2.839E-15  | -2.400E-06 | -4.120E-07 | 1.854E 06 | 5.501E 03 | 0. | 0. | 0. | 2.323E-07  | -3.093E-02 |
| 1.8000 | 4.487E-15  | -2.926E-06 | -6.513E-07 | 1.854E 06 | 5.501E 03 | 0. | 0. | 0. | 1.848E-07  | -3.338E-02 |
| 1.8900 | 6.474E-15  | -3.488E-06 | -9.357E-07 | 1.854E 06 | 5.501E 03 | 0. | 0. | 0. | 1.136E-07  | -3.515E-02 |
| 1.9800 | 8.817E-15  | -4.071E-06 | -1.280E-06 | 1.854E 06 | 5.501E 03 | 0. | 0. | 0. | 1.403E-08  | -3.593E-02 |
| 2.0700 | 1.152E-14  | -4.656E-06 | -1.673E-06 | 1.854E 06 | 5.501E 03 | 0. | 0. | 0. | -1.185E-07 | -3.536E-02 |
| 2.1600 | 1.459E-14  | -5.218E-06 | -2.117E-06 | 1.854E 06 | 5.501E 03 | 0. | 0. | 0. | -2.887E-07 | -3.304E-02 |
| 2.2500 | 1.798E-14  | -5.724E-06 | -2.610E-06 | 1.854E 06 | 5.501E 03 | 0. | 0. | 0. | -5.011E-07 | -2.849E-02 |
| 2.3400 | 2.167E-14  | -6.134E-06 | -3.145E-06 | 1.854E 06 | 5.501E 03 | 0. | 0. | 0. | -7.598E-07 | -2.121E-02 |
| 2.4300 | 2.566E-14  | -6.399E-06 | -3.711E-06 | 1.854E 06 | 5.501E 03 | 0. | 0. | 0. | -1.068E-06 | -1.062E-02 |
| 2.5200 | 2.957E-14  | -6.459E-06 | -4.291E-06 | 1.854E 06 | 5.501E 03 | 0. | 0. | 0. | -1.428E-06 | 3.856E-03  |
| 2.6100 | 3.352E-14  | -6.247E-06 | -4.866E-06 | 1.854E 06 | 5.501E 03 | 0. | 0. | 0. | -1.840E-06 | 2.283E-02  |
| 2.7000 | 3.725E-14  | -5.683E-06 | -5.406E-06 | 1.854E 06 | 5.501E 03 | 0. | 0. | 0. | -2.303E-06 | 4.690E-02  |
| 2.7900 | 4.049E-14  | -4.680E-06 | -5.877E-06 | 1.854E 06 | 5.501E 03 | 0. | 0. | 0. | -2.811E-06 | 7.664E-02  |
| 2.8800 | 4.295E-14  | -3.140E-06 | -6.234E-06 | 1.854E 06 | 5.501E 03 | 0. | 0. | 0. | -3.357E-06 | 1.125E-01  |
| 2.9700 | 4.427E-14  | -9.602E-07 | -6.425E-06 | 1.854E 06 | 5.501E 03 | 0. | 0. | 0. | -3.928E-06 | 1.549E-01  |
| 3.0600 | 4.438E-14  | -1.153E-07 | -6.441E-06 | 1.854E 06 | 5.501E 03 | 0. | 0. | 0. | -4.121E-06 | 1.706E-01  |



STRESS CALCULATIONS FOR SHELLS OF REVOLUTION  
 OF 3 REGIONS DATE 1.25.62  
 WITHOUT MERIDIONAL LOAD EFFECT  
 CASE 1.00

| REGION 1 | RUS       | ZOS       | STRAIN XI  | THETA      | A         | (RV) | N(XI)      | M(THETA)   | M(XI)      |
|----------|-----------|-----------|------------|------------|-----------|------|------------|------------|------------|
| C.       | 3.875E 00 | 0.        | -6.339E-C9 | 2.113E-08  | 9.000E-02 | 0.   | 1.671E-10  | 3.918E-02  | -4.404E-08 |
| 0.0500   | 3.875E 00 | 9.000E-C2 | -6.351E-C9 | 2.117E-08  | 9.000E-02 | 0.   | 1.426E-10  | 3.925E-02  | 5.301E-04  |
| 0.1800   | 3.875E 00 | 1.800E-C1 | -6.424E-09 | 2.141E-08  | 9.000E-02 | 0.   | 1.184E-10  | 3.970E-02  | 9.808E-04  |
| 0.2700   | 3.875E 00 | 2.700E-C1 | -6.610E-09 | 2.203E-08  | 9.000E-02 | 0.   | 9.344E-11  | 4.085E-02  | 1.347E-03  |
| 0.3600   | 3.875E 00 | 3.600E-C1 | -6.952E-09 | 2.317E-08  | 9.000E-02 | 0.   | 6.753E-11  | 4.296E-02  | 1.625E-03  |
| 0.4500   | 3.875E 00 | 4.500E-C1 | -7.483E-09 | 2.494E-08  | 9.000E-02 | 0.   | 3.995E-11  | 4.625E-02  | 1.811E-03  |
| 0.5400   | 3.875E 00 | 5.400E-C1 | -8.225E-09 | 2.742E-08  | 9.000E-02 | 0.   | 9.934E-12  | 5.083E-02  | 1.897E-03  |
| 0.6300   | 3.875E 00 | 6.300E-C1 | -9.187E-09 | 3.062E-08  | 9.000E-02 | 0.   | -2.334E-11 | 5.678E-02  | 1.875E-03  |
| 0.7200   | 3.875E 00 | 7.200E-C1 | -1.037E-08 | 3.456E-08  | 9.000E-02 | 0.   | -6.073E-11 | 6.407E-02  | 1.731E-03  |
| 0.8100   | 3.875E 00 | 8.100E-C1 | -1.175E-08 | 3.916E-08  | 9.000E-02 | 0.   | -1.030E-10 | 7.261E-02  | 1.450E-03  |
| 0.9000   | 3.875E 00 | 9.000E-C1 | -1.330E-08 | 4.432E-08  | 9.000E-02 | 0.   | -2.051E-10 | 8.218E-02  | 1.013E-03  |
| 0.9900   | 3.875E 00 | 9.900E-C1 | -1.496E-08 | 4.988E-08  | 9.000E-02 | 0.   | -2.657E-10 | 9.247E-02  | 4.006E-04  |
| 1.0800   | 3.875E 00 | 1.080E 00 | -1.667E-08 | 5.558E-08  | 9.000E-02 | 0.   | -3.328E-10 | 1.030E-01  | -4.101E-04 |
| 1.1700   | 3.875E 00 | 1.170E 00 | -1.833E-08 | 6.111E-08  | 9.000E-02 | 0.   | -4.060E-10 | 1.133E-01  | -1.441E-03 |
| 1.2600   | 3.875E 00 | 1.260E 00 | -1.982E-08 | 6.608E-08  | 9.000E-02 | 0.   | -4.844E-10 | 1.225E-01  | -2.715E-03 |
| 1.3500   | 3.875E 00 | 1.350E 00 | -2.100E-08 | 6.999E-08  | 9.000E-02 | 0.   | -5.664E-10 | 1.298E-01  | -4.250E-03 |
| 1.4400   | 3.875E 00 | 1.440E 00 | -2.167E-08 | 7.223E-08  | 9.000E-02 | 0.   | -6.496E-10 | 1.339E-01  | -6.063E-03 |
| 1.5300   | 3.875E 00 | 1.530E 00 | -2.163E-08 | 7.211E-08  | 9.000E-02 | 0.   | -7.311E-10 | 1.276E-01  | -8.161E-03 |
| 1.6200   | 3.875E 00 | 1.620E 00 | -2.004E-08 | 6.880E-08  | 9.000E-02 | 0.   | -8.064E-10 | 1.138E-01  | -1.054E-02 |
| 1.7100   | 3.875E 00 | 1.710E 00 | -1.842E-08 | 6.139E-08  | 9.000E-02 | 0.   | -8.705E-10 | 9.052E-02  | -1.610E-02 |
| 1.8000   | 3.875E 00 | 1.800E 00 | -1.465E-08 | 4.883E-08  | 9.000E-02 | 0.   | -9.166E-10 | 5.562E-02  | -1.919E-02 |
| 1.8900   | 3.875E 00 | 1.890E 00 | -9.000E-09 | 3.000E-08  | 9.000E-02 | 0.   | -9.369E-10 | 6.871E-03  | -2.239E-02 |
| 1.9800   | 3.875E 00 | 1.980E 00 | -1.112E-09 | 3.706E-09  | 9.000E-02 | 0.   | -9.221E-10 | -5.803E-02 | -2.561E-02 |
| 2.0700   | 3.875E 00 | 2.070E 00 | 9.390E-09  | -3.130E-08 | 9.000E-02 | 0.   | -8.615E-10 | -1.414E-01 | -2.870E-02 |
| 2.1600   | 3.875E 00 | 2.160E 00 | 2.286E-08  | -7.627E-08 | 9.000E-02 | 0.   | -7.430E-10 | -2.455E-01 | -3.149E-02 |
| 2.2500   | 3.875E 00 | 2.250E 00 | 3.972E-08  | -1.324E-07 | 9.000E-02 | 0.   | -5.530E-10 | -3.722E-01 | -3.374E-02 |
| 2.3400   | 3.875E 00 | 2.340E 00 | 6.022E-08  | -2.007E-07 | 9.000E-02 | 0.   | -2.769E-10 | -5.232E-01 | -3.520E-02 |
| 2.4300   | 3.875E 00 | 2.430E 00 | 8.466E-08  | -2.822E-07 | 9.000E-02 | 0.   | 1.006E-10  | -6.996E-01 | -3.553E-02 |
| 2.5200   | 3.875E 00 | 2.520E 00 | 1.132E-07  | -3.773E-07 | 9.000E-02 | 0.   | 5.953E-10  | -9.015E-01 | -3.436E-02 |
| 2.6100   | 3.875E 00 | 2.610E 00 | 1.459E-07  | -4.852E-07 | 9.000E-02 | 0.   | 1.223E-09  | -1.128E 00 | -3.126E-02 |
| 2.7000   | 3.875E 00 | 2.700E 00 | 1.825E-07  | -6.085E-07 | 9.000E-02 | 0.   | 1.998E-09  | -1.377E 00 | -2.574E-02 |
| 2.7900   | 3.875E 00 | 2.790E 00 | 2.228E-07  | -7.428E-07 | 9.000E-02 | 0.   | 2.934E-09  | -1.645E 00 | -1.727E-02 |
| 2.8800   | 3.875E 00 | 2.880E 00 | 2.661E-07  | -8.870E-07 | 9.000E-02 | 0.   | 4.040E-09  | -1.924E 00 | -5.282E-03 |
| 2.9700   | 3.875E 00 | 2.970E 00 | 3.114E-07  | -1.038E-06 | 9.000E-02 | 0.   | 4.448E-09  | -2.019E 00 | -6.341E-04 |
| 3.0600   | 3.875E 00 | 3.060E 00 | 3.266E-07  | -1.089E-06 | 9.000E-02 | 0.   |            |            |            |

NIRO JOINT ROTATION STUDY---SYSTEM RECOVERY HOUSING

| REGION 2<br>OF 3 REGIONS                              |           | STRESS CALCULATIONS FOR SHELLS OF REVOLUTION |            | DATE 1.25.62 |           | WITHOUT MERIDIONAL LOAD EFFECT |    |            |           |
|---|-----------|--|------------|--------------|-----------|--------------------------------|----|------------|-----------|
| GEOMETRY IS PRESCRIBED BY A CONE OR CYLINDER EQUATION |           | C  |            | D            |           | CASE 1.00                      |    |            |           |
| XI  | K THETA   | K XI   | BETA       | C            | D         | NT                             | MT | U          | Q         |
| 0.  | 4.438E-14 | -1.153E-07                                   | -6.441E-06 | 1.854E 06    | 5.501E 03 | 0.                             | 0. | -4.121E-06 | 1.706E-01 |
| 0.0500  | 4.414E-14 | 1.560E-06                                    | -6.406E-06 | 1.854E 06    | 5.501E 03 | 0.                             | 0. | -4.443E-06 | 1.983E-01 |
| 0.1000  | 4.327E-14 | 3.496E-06                                    | -6.281E-06 | 1.854E 06    | 5.501E 03 | 0.                             | 0. | -4.760E-06 | 2.280E-01 |
| 0.1500  | 4.170E-14 | 5.711E-06                                    | -6.052E-06 | 1.854E 06    | 5.501E 03 | 0.                             | 0. | -5.069E-06 | 2.599E-01 |
| 0.2000  | 3.931E-14 | 8.224E-06                                    | -5.705E-06 | 1.854E 06    | 5.501E 03 | 0.                             | 0. | -5.364E-06 | 2.936E-01 |
| 0.2500  | 3.600E-14 | 1.105E-05                                    | -5.225E-06 | 1.854E 06    | 5.501E 03 | 0.                             | 0. | -5.638E-06 | 3.292E-01 |
| 0.3000  | 3.165E-14 | 1.421E-05                                    | -4.594E-06 | 1.854E 06    | 5.501E 03 | 0.                             | 0. | -5.884E-06 | 3.665E-01 |
| 0.3500  | 2.616E-14 | 1.772E-05                                    | -3.797E-06 | 1.854E 06    | 5.501E 03 | 0.                             | 0. | -6.095E-06 | 4.053E-01 |
| 0.4000  | 1.940E-14 | 2.159E-05                                    | -2.816E-06 | 1.854E 06    | 5.501E 03 | 0.                             | 0. | -6.261E-06 | 4.453E-01 |
| 0.4500  | 1.125E-14 | 2.582E-05                                    | -1.633E-06 | 1.854E 06    | 5.501E 03 | 0.                             | 0. | -6.373E-06 | 4.862E-01 |
| 0.4750  | 6.610E-15 | 2.807E-05                                    | -9.594E-07 | 1.854E 06    | 5.501E 03 | 0.                             | 0. | -6.406E-06 | 5.069E-01 |
| 0.4800  | 5.635E-15 | 2.854E-05                                    | -6.179E-07 | 1.854E 06    | 5.501E 03 | 0.                             | 0. | -6.411E-06 | 5.110E-01 |

NIRC JOINT ROTATION STUDY---SYSTEM RECOVERY HOUSING

STRESS CALCULATIONS FOR SHELLS OF REVOLUTION  
 OF 3 REGIONS DATE 1.25.62  
 GEOMETRY IS PRESCRIBED BY A CONE OR CYLINDER EQUATION

| REGION 2 | ROD       | ZOS        | STRAIN XI | STRAIN THETA | A         | (RV) | CASE | WITHOUT MERIDIONAL LOAD EFFECT | N(XI)      | N(THETA)   | M(XI) |
|----------|-----------|------------|-----------|--------------|-----------|------|------|--------------------------------|------------|------------|-------|
| 0.0500   | 3.875E 00 | 0.         | 3.266E-07 | -1.089E-06   | 9.000E-02 | 0.   | 1.00 | 4.448E-09                      | -2.019E 00 | -6.341E-04 |       |
| 0.1000   | 3.875E 00 | 5.000E-02  | 3.521E-07 | -1.174E-06   | 9.000E-02 | 0.   |      | 5.170E-09                      | -2.176E 00 | 8.582E-03  |       |
| 0.1500   | 3.875E 00 | 10.000E-02 | 3.773E-07 | -1.258E-06   | 9.000E-02 | 0.   |      | 5.947E-09                      | -2.332E 00 | 1.923E-02  |       |
| 0.2000   | 3.875E 00 | 1.500E-01  | 4.018E-07 | -1.339E-06   | 9.000E-02 | 0.   |      | 6.776E-09                      | -2.483E 00 | 3.142E-02  |       |
| 0.2500   | 3.875E 00 | 2.000E-01  | 4.252E-07 | -1.417E-06   | 9.000E-02 | 0.   |      | 7.657E-09                      | -2.627E 00 | 4.524E-02  |       |
| 0.3000   | 3.875E 00 | 2.500E-01  | 4.469E-07 | -1.490E-06   | 9.000E-02 | 0.   |      | 8.585E-09                      | -2.762E 00 | 6.080E-02  |       |
| 0.3500   | 3.875E 00 | 3.000E-01  | 4.664E-07 | -1.555E-06   | 9.000E-02 | 0.   |      | 9.558E-09                      | -2.882E 00 | 7.819E-02  |       |
| 0.4000   | 3.875E 00 | 3.500E-01  | 4.831E-07 | -1.610E-06   | 9.000E-02 | 0.   |      | 1.057E-08                      | -2.985E 00 | 9.748E-02  |       |
| 0.4500   | 3.875E 00 | 4.000E-01  | 4.985E-07 | -1.654E-06   | 9.000E-02 | 0.   |      | 1.161E-08                      | -3.067E 00 | 1.187E-01  |       |
| 0.4750   | 3.875E 00 | 4.500E-01  | 5.052E-07 | -1.684E-06   | 9.000E-02 | 0.   |      | 1.268E-08                      | -3.122E 00 | 1.420E-01  |       |
| 0.4800   | 3.875E 00 | 4.750E-01  | 5.077E-07 | -1.692E-06   | 9.000E-02 | 0.   |      | 1.322E-08                      | -3.138E 00 | 1.544E-01  |       |
| 0.4800   | 3.875E 00 | 4.800E-01  | 5.081E-07 | -1.694E-06   | 9.000E-02 | 0.   |      | 1.333E-08                      | -3.140E 00 | 1.570E-01  |       |

NIRC JOINT ROTATION STUDY---SYSTEM RECOVERY HOUSING

| STRESS CALCULATIONS FOR SHELLS OF REVOLUTION          |            |       |           |            |           |           |    |    |    | WITHOUT MERIDIONAL LOAD EFFECT |            |  |
|---|------------|-------|-----------|------------|-----------|-----------|----|----|----|--------------------------------|------------|--|
| DATE 1.25.62  |            |       |           |            |           |           |    |    |    | CASE 1.00                      |            |  |
| REGION 3  |            |       |           |            |           |           |    |    |    | NT                             |            |  |
| UF 3 REGIONS  |            |       |           |            |           |           |    |    |    | MT                             |            |  |
| GECMETRY IS PRESCRIBED BY A CONE OR CYLINDER EQUATION |            |       |           |            |           |           |    |    |    | Q                              |            |  |
| XI  | K          | THETA | K         | XI         | BETA      | C         | D  | NT | MT | Q                              | U          |  |
| 0.  | 5.635E-15  |       | 2.854E-05 | -8.179E-07 | 1.854E 06 | 5.501E 03 | 0. | 0. | 0. | -6.411E-06                     | -4.890E-01 |  |
| 0.0501  | -3.463E-15 |       | 2.428E-05 | 5.027E-07  | 1.854E 06 | 5.501E 03 | 0. | 0. | 0. | -6.417E-06                     | -4.474E-01 |  |
| 0.1001  | -1.116E-14 |       | 2.039E-05 | 1.619E-06  | 1.854E 06 | 5.501E 03 | 0. | 0. | 0. | -6.363E-06                     | -4.059E-01 |  |
| 0.1502  | -1.758E-14 |       | 1.688E-05 | 2.551E-06  | 1.854E 06 | 5.501E 03 | 0. | 0. | 0. | -6.258E-06                     | -3.650E-01 |  |
| 0.2003  | -2.285E-14 |       | 1.375E-05 | 3.316E-06  | 1.854E 06 | 5.501E 03 | 0. | 0. | 0. | -6.110E-06                     | -3.249E-01 |  |
| 0.2504  | -2.710E-14 |       | 1.097E-05 | 3.933E-06  | 1.854E 06 | 5.501E 03 | 0. | 0. | 0. | -5.928E-06                     | -2.859E-01 |  |
| 0.3004  | -3.045E-14 |       | 8.538E-06 | 4.420E-06  | 1.854E 06 | 5.501E 03 | 0. | 0. | 0. | -5.718E-06                     | -2.482E-01 |  |
| 0.3505  | -3.303E-14 |       | 6.445E-06 | 4.794E-06  | 1.854E 06 | 5.501E 03 | 0. | 0. | 0. | -5.487E-06                     | -2.118E-01 |  |
| 0.4006  | -3.494E-14 |       | 4.677E-06 | 5.071E-06  | 1.854E 06 | 5.501E 03 | 0. | 0. | 0. | -5.239E-06                     | -1.771E-01 |  |
| 0.4506  | -3.629E-14 |       | 3.217E-06 | 5.267E-06  | 1.854E 06 | 5.501E 03 | 0. | 0. | 0. | -4.980E-06                     | -1.440E-01 |  |
| 0.5007  | -3.719E-14 |       | 2.051E-06 | 5.398E-06  | 1.854E 06 | 5.501E 03 | 0. | 0. | 0. | -4.713E-06                     | -1.126E-01 |  |
| 0.5508  | -3.774E-14 |       | 1.163E-06 | 5.477E-06  | 1.854E 06 | 5.501E 03 | 0. | 0. | 0. | -4.440E-06                     | -8.291E-02 |  |
| 0.6008  | -3.802E-14 |       | 5.370E-07 | 5.519E-06  | 1.854E 06 | 5.501E 03 | 0. | 0. | 0. | -4.165E-06                     | -5.503E-02 |  |
| 0.6509  | -3.814E-14 |       | 1.565E-07 | 5.535E-06  | 1.854E 06 | 5.501E 03 | 0. | 0. | 0. | -3.888E-06                     | -2.894E-02 |  |
| 0.7010  | -3.816E-14 |       | 5.165E-09 | 5.538E-06  | 1.854E 06 | 5.501E 03 | 0. | 0. | 0. | -3.611E-06                     | -4.643E-03 |  |
| 0.7509  | -3.816E-14 |       | 2.061E-09 | 5.538E-06  | 1.854E 06 | 5.501E 03 | 0. | 0. | 0. | -3.583E-06                     | -2.313E-03 |  |
| 0.7711  | -3.816E-14 |       | 2.274E-13 | 5.538E-06  | 1.854E 06 | 5.501E 03 | 0. | 0. | 0. | -3.555E-06                     | -0.        |  |

NIRC JOINT ROTATION STUDY---SYSTEM RECOVERY HOUSING

| REGION 3  |           | STRESS CALCULATIONS FOR SHELLS OF REVOLUTION |           | DATE 1.25.62 |           | WITHOUT MERIDIONAL LOAD EFFECT |            |            |           |
|---|-----------|--|-----------|--------------|-----------|--------------------------------|------------|------------|-----------|
| GEGMETRY IS PRESCRIBED BY A CONE OR CYLINDER EQUATION |           | OF 3 REGIONS                                 |           | DATE 1.25.62 |           | CASE 1.00                      |            |            |           |
| XI  | ROS       | ZUS  | STRAIN XI | THETA        | A         | (RV)                           | N(XI)      | N(THETA)   | M(XI)     |
| 0.  | 3.875E 00 | 0.   | 5.081E-07 | -1.694E-06   | 9.000E-02 | 0.                             | -1.275E-08 | -3.140E 00 | 1.570E-01 |
| 0.0501  | 3.875E 00 | 5.007E-02                                    | 5.086E-07 | -1.695E-06   | 9.000E-02 | 0.                             | -1.167E-08 | -3.143E 00 | 1.335E-01 |
| 0.1001  | 3.875E 00 | 1.001E-01                                    | 5.043E-07 | -1.691E-06   | 9.000E-02 | 0.                             | -1.059E-08 | -3.117E 00 | 1.122E-01 |
| 0.1502  | 3.875E 00 | 1.502E-01                                    | 4.960E-07 | -1.653E-06   | 9.000E-02 | 0.                             | -9.519E-09 | -3.065E 00 | 9.288E-02 |
| 0.2003  | 3.875E 00 | 2.003E-01                                    | 4.843E-07 | -1.614E-06   | 9.000E-02 | 0.                             | -8.473E-09 | -2.993E 00 | 7.561E-02 |
| 0.2504  | 3.875E 00 | 2.504E-01                                    | 4.698E-07 | -1.568E-06   | 9.000E-02 | 0.                             | -7.456E-09 | -2.904E 00 | 6.033E-02 |
| 0.3004  | 3.875E 00 | 3.004E-01                                    | 4.532E-07 | -1.511E-06   | 9.000E-02 | 0.                             | -6.471E-09 | -2.801E 00 | 4.696E-02 |
| 0.3505  | 3.875E 00 | 3.505E-01                                    | 4.349E-07 | -1.450E-06   | 9.000E-02 | 0.                             | -5.524E-09 | -2.688E 00 | 3.146E-02 |
| 0.4006  | 3.875E 00 | 4.006E-01                                    | 4.153E-07 | -1.384E-06   | 9.000E-02 | 0.                             | -4.618E-09 | -2.566E 00 | 2.173E-02 |
| 0.4506  | 3.875E 00 | 4.506E-01                                    | 3.947E-07 | -1.316E-06   | 9.000E-02 | 0.                             | -3.754E-09 | -2.439E 00 | 1.770E-02 |
| 0.5007  | 3.875E 00 | 5.007E-01                                    | 3.735E-07 | -1.245E-06   | 9.000E-02 | 0.                             | -2.935E-09 | -2.308E 00 | 1.128E-02 |
| 0.5508  | 3.875E 00 | 5.508E-01                                    | 3.519E-07 | -1.173E-06   | 9.000E-02 | 0.                             | -2.162E-09 | -2.175E 00 | 6.398E-03 |
| 0.6008  | 3.875E 00 | 6.008E-01                                    | 3.301E-07 | -1.100E-06   | 9.000E-02 | 0.                             | -1.435E-09 | -2.040E 00 | 2.954E-03 |
| 0.6509  | 3.875E 00 | 6.509E-01                                    | 3.082E-07 | -1.027E-06   | 9.000E-02 | 0.                             | -7.546E-10 | -1.904E 00 | 8.606E-04 |
| 0.7010  | 3.875E 00 | 7.010E-01                                    | 2.862E-07 | -9.540E-07   | 9.000E-02 | 0.                             | -1.211E-10 | -1.769E 00 | 2.841E-05 |
| 0.7500  | 3.875E 00 | 7.500E-01                                    | 2.640E-07 | -9.466E-07   | 9.000E-02 | 0.                             | -6.031E-11 | -1.755E 00 | 1.133E-05 |
| 0.7110  | 3.875E 00 | 7.110E-01                                    | 2.618E-07 | -9.393E-07   | 9.000E-02 | 0.                             | -0.        | -1.741E 00 | 1.188E-09 |

STRESSES REGION 1

GEOMETRY IS PRESCRIBED BY A CONE OR CYLINDER EQUATION  
 STRESSES ARE PRINTED AS FOLLOWS LINE 1 SIGMA XI LINE 2 SIGMA THETA OUTER SURFACE...INTERFACES...

XI= 0.  
 SIGMA F16 SIGMA H1- SIGMA H26 SIGMA H2- SIGMA H36 SIGMA H3- SIGMA H46  
 8.15053E-00 -8.15468E-00  
 2.17657E-01 2.17652E-01

XI= 0.09000  
 SIGMA F16 SIGMA H1- SIGMA H26 SIGMA H2- SIGMA H36 SIGMA H3- SIGMA H46  
 -9.81007E-02 9.81607E-02  
 1.00009E-01 2.47509E-01

XI= 0.18000  
 SIGMA F16 SIGMA H1- SIGMA H26 SIGMA H2- SIGMA H36 SIGMA H3- SIGMA H46  
 -1.81635E-01 1.81638E-01  
 1.00051E-01 2.75034E-01

XI= 0.27000  
 SIGMA F16 SIGMA H1- SIGMA H26 SIGMA H2- SIGMA H36 SIGMA H3- SIGMA H46  
 -2.49350E-01 2.49356E-01  
 1.52124E-01 3.01738E-01

XI= 0.36000  
 SIGMA F16 SIGMA H1- SIGMA H26 SIGMA H2- SIGMA H36 SIGMA H3- SIGMA H46  
 -3.00858E-01 3.00858E-01  
 1.48431E-01 3.28947E-01

XI= 0.45000  
 SIGMA F16 SIGMA H1- SIGMA H26 SIGMA H2- SIGMA H36 SIGMA H3- SIGMA H46  
 -3.52000E-01 3.52000E-01  
 1.50340E-01 3.57520E-01

XI= 0.54000  
 SIGMA F16 SIGMA H1- SIGMA H26 SIGMA H2- SIGMA H36 SIGMA H3- SIGMA H46  
 -3.91375E-01 3.91375E-01  
 1.70959E-01 3.87009E-01

XI= 0.63000  
 SIGMA F16 SIGMA H1- SIGMA H26 SIGMA H2- SIGMA H36 SIGMA H3- SIGMA H46  
 -3.47200E-01 3.47265E-01  
 2.11259E-01 4.17613E-01

XI= 0.72000



|              |              |           |           |           |           |
|--------------|--------------|-----------|-----------|-----------|-----------|
| SIGMA F16    | SIGMA H1-    | SIGMA H26 | SIGMA H36 | SIGMA H3- | SIGMA H46 |
| -3.20019E-01 | 3.20615E-01  |           |           |           |           |
| 2.59785E-01  | 4.52134E-01  |           |           |           |           |
| XI= 0.91000  |              |           |           |           |           |
| SIGMA F16    | SIGMA H1-    | SIGMA H26 | SIGMA H36 | SIGMA H3- | SIGMA H46 |
| -2.68530E-01 | 2.68530E-01  |           |           |           |           |
| 3.22801E-01  | 4.63523E-01  |           |           |           |           |
| XI= 0.90000  |              |           |           |           |           |
| SIGMA F16    | SIGMA H1-    | SIGMA H26 | SIGMA H36 | SIGMA H3- | SIGMA H46 |
| -1.87854E-01 | 1.87654E-01  |           |           |           |           |
| 4.00243E-01  | 5.12335E-01  |           |           |           |           |
| XI= 0.99000  |              |           |           |           |           |
| SIGMA F16    | SIGMA H1-    | SIGMA H26 | SIGMA H36 | SIGMA H3- | SIGMA H46 |
| -7.41822E-02 | 7.41832E-02  |           |           |           |           |
| 4.51489E-01  | 5.35975E-01  |           |           |           |           |
| XI= 1.03000  |              |           |           |           |           |
| SIGMA F16    | SIGMA H1-    | SIGMA H26 | SIGMA H36 | SIGMA H3- | SIGMA H46 |
| 7.55420E-02  | -7.55420E-02 |           |           |           |           |
| 5.95234E-01  | 5.45674E-01  |           |           |           |           |
| XI= 1.17000  |              |           |           |           |           |
| SIGMA F16    | SIGMA H1-    | SIGMA H26 | SIGMA H36 | SIGMA H3- | SIGMA H46 |
| 2.66854E-01  | -2.66894E-01 |           |           |           |           |
| 7.09548E-01  | 5.49411E-01  |           |           |           |           |
| XI= 1.26000  |              |           |           |           |           |
| SIGMA F16    | SIGMA H1-    | SIGMA H26 | SIGMA H36 | SIGMA H3- | SIGMA H46 |
| 5.02719E-01  | -5.02719E-01 |           |           |           |           |
| 6.31472E-01  | 5.25840E-01  |           |           |           |           |
| XI= 1.35000  |              |           |           |           |           |
| SIGMA F16    | SIGMA H1-    | SIGMA H26 | SIGMA H36 | SIGMA H3- | SIGMA H46 |
| 7.57041E-01  | -7.57041E-01 |           |           |           |           |
| 5.52989E-01  | 4.84789E-01  |           |           |           |           |
| XI= 1.44000  |              |           |           |           |           |
| SIGMA F16    | SIGMA H1-    | SIGMA H26 | SIGMA H36 | SIGMA H3- | SIGMA H46 |
| 1.12273E 00  | -1.12270E 00 |           |           |           |           |
| 1.08019E 00  | 4.07176E-01  |           |           |           |           |
| XI= 1.5      |              |           |           |           |           |
| SIGMA F16    | SIGMA H1-    | SIGMA H26 | SIGMA H36 | SIGMA H3- | SIGMA H46 |
|              |              |           |           |           |           |

|             |              |           |           |           |           |           |           |           |           |
|-------------|--------------|-----------|-----------|-----------|-----------|-----------|-----------|-----------|-----------|
| 1.01129E 00 | -1.51129E 00 |           |           |           |           |           |           |           |           |
| 1.15610E 00 | 2.89327E-C1  |           |           |           |           |           |           |           |           |
| XI= 1.02000 |              |           |           |           |           |           |           |           |           |
| SIGMA F16   | SIGMA H1-    | SIGMA H2G | SIGMA H2- | SIGMA H3G | SIGMA H3- | SIGMA H4G | SIGMA H4- | SIGMA H4G | SIGMA H4- |
| 1.75270E 00 | -1.95270E 00 |           |           |           |           |           |           |           |           |
| 1.25447E 00 | 1.22849E-C1  |           |           |           |           |           |           |           |           |
| XI= 1.71000 |              |           |           |           |           |           |           |           |           |
| SIGMA F16   | SIGMA H1-    | SIGMA H2G | SIGMA H2- | SIGMA H3G | SIGMA H3- | SIGMA H4G | SIGMA H4- | SIGMA H4G | SIGMA H4- |
| 2.44444E 00 | -2.44444E 00 |           |           |           |           |           |           |           |           |
| 1.36500E 00 | -1.01061E-C1 |           |           |           |           |           |           |           |           |
| XI= 1.80000 |              |           |           |           |           |           |           |           |           |
| SIGMA F16   | SIGMA H1-    | SIGMA H2G | SIGMA H2- | SIGMA H3G | SIGMA H3- | SIGMA H4G | SIGMA H4- | SIGMA H4G | SIGMA H4- |
| 2.98100E 00 | -2.98100E 00 |           |           |           |           |           |           |           |           |
| 1.39721E 00 | -3.91289E-C1 |           |           |           |           |           |           |           |           |
| XI= 1.87000 |              |           |           |           |           |           |           |           |           |
| SIGMA F16   | SIGMA H1-    | SIGMA H2G | SIGMA H2- | SIGMA H3G | SIGMA H3- | SIGMA H4G | SIGMA H4- | SIGMA H4G | SIGMA H4- |
| 2.55309E 00 | -3.55309E 00 |           |           |           |           |           |           |           |           |
| 1.37493E 00 | -7.56529E-C1 |           |           |           |           |           |           |           |           |
| XI= 1.93000 |              |           |           |           |           |           |           |           |           |
| SIGMA F16   | SIGMA H1-    | SIGMA H2G | SIGMA H2- | SIGMA H3G | SIGMA H3- | SIGMA H4G | SIGMA H4- | SIGMA H4G | SIGMA H4- |
| 4.14682E 00 | -4.14682E 00 |           |           |           |           |           |           |           |           |
| 1.28222E 00 | -1.20588E 00 |           |           |           |           |           |           |           |           |
| XI= 2.07000 |              |           |           |           |           |           |           |           |           |
| SIGMA F16   | SIGMA H1-    | SIGMA H2G | SIGMA H2- | SIGMA H3G | SIGMA H3- | SIGMA H4G | SIGMA H4- | SIGMA H4G | SIGMA H4- |
| 4.74280E 00 | -4.74280E 00 |           |           |           |           |           |           |           |           |
| 1.10049E 00 | -1.74924E 00 |           |           |           |           |           |           |           |           |
| XI= 2.10000 |              |           |           |           |           |           |           |           |           |
| SIGMA F16   | SIGMA H1-    | SIGMA H2G | SIGMA H2- | SIGMA H3G | SIGMA H3- | SIGMA H4G | SIGMA H4- | SIGMA H4G | SIGMA H4- |
| 5.31025E 00 | -5.31529E 00 |           |           |           |           |           |           |           |           |
| 8.09028E-01 | -2.38012E 00 |           |           |           |           |           |           |           |           |
| XI= 2.25000 |              |           |           |           |           |           |           |           |           |
| SIGMA F16   | SIGMA H1-    | SIGMA H2G | SIGMA H2- | SIGMA H3G | SIGMA H3- | SIGMA H4G | SIGMA H4- | SIGMA H4G | SIGMA H4- |
| 5.93109E 00 | -5.83105E 00 |           |           |           |           |           |           |           |           |
| 3.85064E-C1 | -3.11294E 00 |           |           |           |           |           |           |           |           |
| XI= 2.30000 |              |           |           |           |           |           |           |           |           |
| SIGMA F16   | SIGMA H1-    | SIGMA H2G | SIGMA H2- | SIGMA H3G | SIGMA H3- | SIGMA H4G | SIGMA H4- | SIGMA H4G | SIGMA H4- |
| 8.24491E 00 | -8.24891E 00 |           |           |           |           |           |           |           |           |

-1.95035E-01 -3.54229E 00

XI= 2.073000  
SIGMA F16 SIGMA H1-  
6.51657E 00 -6.51657E 00  
-5.51211E-01 -4.66235E 00

SIGMA H3-

SIGMA H36

SIGMA H2-

SIGMA H26

SIGMA H1-

SIGMA F16

SIGMA H46

XI= 2.52000  
SIGMA F16 SIGMA H1-  
6.55012E 00 -6.55012E 00  
-1.91255E 00 -5.85061E 00

SIGMA H3-

SIGMA H36

SIGMA H2-

SIGMA H26

SIGMA H1-

SIGMA F16

SIGMA H46

XI= 2.61000  
SIGMA F16 SIGMA H1-  
6.56368E 00 -6.56368E 00  
-3.09719E 00 -6.51740E 00

SIGMA H3-

SIGMA H36

SIGMA H2-

SIGMA H26

SIGMA H1-

SIGMA F16

SIGMA H46

XI= 2.70000  
SIGMA F16 SIGMA H1-  
5.78925E 00 -5.78925E 00  
-4.03026E 00 -6.00372E 00

SIGMA H3-

SIGMA H36

SIGMA H2-

SIGMA H26

SIGMA H1-

SIGMA F16

SIGMA H46

XI= 2.79000  
SIGMA F16 SIGMA H1-  
4.76711E 00 -4.76711E 00  
-6.22041E 00 -5.08067E 00

SIGMA H3-

SIGMA H36

SIGMA H2-

SIGMA H26

SIGMA H1-

SIGMA F16

SIGMA H46

XI= 1.93000  
SIGMA F16 SIGMA H1-  
3.19667E 00 -3.19667E 00  
-5.17662E 00 -1.00958E 01

SIGMA H3-

SIGMA H36

SIGMA H2-

SIGMA H26

SIGMA H1-

SIGMA F16

SIGMA H46

XI= 2.97000  
SIGMA F16 SIGMA H1-  
3.78195E-01 -3.78195E-01  
-1.05768E 01 -1.05823E 01

SIGMA H3-

SIGMA H36

SIGMA H2-

SIGMA H26

SIGMA H1-

SIGMA F16

SIGMA H46

XI= 2.00000  
SIGMA F16 SIGMA H1-  
1.17430E-01 -1.17430E-01  
-1.11768E 01 -1.12499E 01

SIGMA H3-

SIGMA H36

SIGMA H2-

SIGMA H26

SIGMA H1-

SIGMA F16

SIGMA H46



|              |              |           |           |           |           |
|--------------|--------------|-----------|-----------|-----------|-----------|
| SIGMA H16    | SIGMA H16    | SIGMA H26 | SIGMA H36 | SIGMA H36 | SIGMA H46 |
| -2.17607E 01 | 2.19685E 01  |           |           |           |           |
| -2.50348E 01 | -1.04417E 01 |           |           |           |           |
| XI = 0.45000 |              |           |           |           |           |
| SIGMA H16    | SIGMA H16    | SIGMA H26 | SIGMA H36 | SIGMA H36 | SIGMA H46 |
| -2.03004E 01 | 2.53004E 01  |           |           |           |           |
| -2.52339E 01 | -9.45372E 00 |           |           |           |           |
| XI = 0.47500 |              |           |           |           |           |
| SIGMA H16    | SIGMA H16    | SIGMA H26 | SIGMA H36 | SIGMA H36 | SIGMA H46 |
| -2.85991E 01 | 2.85991E 01  |           |           |           |           |
| -2.00123E 01 | -8.65287E 00 |           |           |           |           |
| XI = 0.40000 |              |           |           |           |           |
| SIGMA H16    | SIGMA H16    | SIGMA H26 | SIGMA H36 | SIGMA H36 | SIGMA H46 |
| -2.90850E 01 | 2.90850E 01  |           |           |           |           |
| -2.51003E 01 | -8.72518E 00 |           |           |           |           |

SIGMA F16 SIGMA H1- SIGMA H26 SIGMA H2- SIGMA H36 SIGMA H3- SIGMA H46  
-4.76413E 00 4.76413E 00  
-1.26869E 01 -1.26264E 01

XI= 0.42063  
SIGMA F16 SIGMA H1- SIGMA H26 SIGMA H2- SIGMA H36 SIGMA H3- SIGMA H46  
-3.27720E 00 3.27720E 00  
-1.45354E 01 -1.25651E 01

XI= 0.50070  
SIGMA F16 SIGMA H1- SIGMA H26 SIGMA H2- SIGMA H36 SIGMA H3- SIGMA H46  
-2.00944E 00 2.00944E 00  
-1.34517E 01 -1.21580E 01

XI= 0.55077  
SIGMA F16 SIGMA H1- SIGMA H26 SIGMA H2- SIGMA H36 SIGMA H3- SIGMA H46  
-1.18483E 00 1.18483E 00  
-1.24388E 01 -1.17279E 01

XI= 0.60035  
SIGMA F16 SIGMA H1- SIGMA H26 SIGMA H2- SIGMA H36 SIGMA H3- SIGMA H46  
-5.47008E-01 5.47008E-01  
-1.14970E 01 -1.11696E 01

XI= 0.65032  
SIGMA F16 SIGMA H1- SIGMA H26 SIGMA H2- SIGMA H36 SIGMA H3- SIGMA H46  
-1.59374E-01 1.59374E-01  
-1.06282E 01 -1.05325E 01

XI= 0.70059  
SIGMA F16 SIGMA H1- SIGMA H26 SIGMA H2- SIGMA H36 SIGMA H3- SIGMA H46  
-5.26190E-03 5.26190E-03  
-9.32742E 00 -9.62420E 00

XI= 0.70599  
SIGMA F16 SIGMA H1- SIGMA H26 SIGMA H2- SIGMA H36 SIGMA H3- SIGMA H46  
-2.35900E-03 2.09900E-03  
-5.75101E 00 -5.74575E 00

XI= 0.71100  
SIGMA F16 SIGMA H1- SIGMA H26 SIGMA H2- SIGMA H36 SIGMA H3- SIGMA H46  
-2.19900E-07 2.19960E-07  
-5.67491E 00 -5.67451E 00



